CLONING AND HETEROLOGOUS EXPRESSION OF GENES INVOLVED IN AZO DYE DECOLORIZATION AND METABOLIC ENGINEERING FOR EFFICIENT BIOREMEDIATION

A THESIS SUBMITTED TO

THE MAHARAJA SAYAJIRAO UNIVERSITY OF BARODA

FOR THE DEGREE OF

DOCTOR OF PHILOSOPHY IN MICROBIOLOGY

BY

RATHOD JAGAT VIRENDRABHAI

DEPARTMENT OF MICROBIOLOGY

FACULTY OF SCIENCE

THE MAHARAJA SAYAJIRAO UNIVERSITY OF BARODA

VADODARA – 390 002, GUJARAT, INDIA

OCTOBER 2013

STATEMENT UNDER O. Ph.D. 8/ (iii) OF

THE M. S. UNIVERSITY OF BARODA, VADODARA

This is to certify that the work presented in this thesis is original and was obtained from the studies undertaken by me under the supervision of **Dr. G. Archana**

Vadodara **JAGAT RATHOD**

Date: Candidate

This is to certify that the work presented in the form of a thesis in fulfilment of the requirement for the award of the Ph. D. degree of The M. S. University of Baroda by **Mr. Jagat Rathod** is his original work. The entire research work and the thesis have been built up under my supervision.

Dr. G. ARCHANA
Research Supervisor
Department of Microbiology
Faculty of Science
The M. S. University of Baroda
Vadodara- 390 002.

Dedicated to my beloved Family....

ACKNOWLEDGEMENTS

With the grace of the One who is the most kind, I take this opportunity to put on record the gratitude I have felt towards one & all who have unambiguously or implicitly assisted me in completion of my PhD. It gives me immense pleasure to not only acknowledge their views, actions and continuous help, but also thank them for moulding my thought process towards wisdom and truth. I have certainly realized that for success of any project, it is very essential to imbibe true knowledge and hard work should associate with real passion.

First of all I am indebted to my guide, Prof. G. Archana (Archana madam) for accepting me as a Ph.D. student under her guidance. I strongly cherish her scientific insight and attitude. Her vision towards applying newer techniques and approaches to resolve the scientific problem was always big help to me. She really provided best research environment to my first and forward step in research endeavour as per the continuous advancing science and also redefined the word "Patience" to me. I can't even change the paragraph to mention Prof. G. Naresh Kumar (Real Cool Prof.); he is the one who gave me virtue of "objectivity", keeping always calm and wise enough to give least to the issues, which are actually minor. He has inspired me to set higher goal and work towards without getting distracted by local oscillations. His vision and school of thoughts always taught me the need of deep fundamental knowledge allows correlating, able think out of the box and being passionate to own ideas. I have always found Archana mam and NK Sir on the same page shaping the holistic approach to any questions.

I cherish and felt privileged to be an intermediate to Dr. J. Manjrekar's master students working on Yeast prions, thanks for giving me an opportunity to understand this misfolding phenomenon of proteins and lovely friends like Anil, Dominic and Sharad.

I express my deep sense of gratitude to Prof. T. Bagchi (Present Head, Department of Microbiology), I must learn to lateral thinking from your experience. I strongly extend my deep respect to former Heads, Prof. H. S. Chhatpar and Prof. Anjana Desai, for providing me excellent research facilities. I strongly appreciate the vision of Prof. Anjana Desai to develop department infrastructure and advanced instrument facility for strengthening the research and always helping nature towards students.

I sincerely thank Prof. B. B. Chattoo for all the continuous support and scientifically enriching experiences. I am really thankful to all the members of department whose contributions made a very positive and encouraging environment for research. I extend my thanks to Dr. Pranav Vyas, for spiritual knowledge. I also thank Dr. A. S. Nerurkar, Dr. Sanjay Ingle and Dr. Nandita Baxi for readily extending help when required.

I would like to thank my senior mates Arif, Kuldeep, Ruchi, Priyamam, Marpe, Vikas and Anil for their enormous support whenever required without any hesitation.I cordially thank other research

colleagues Ketan, Murli, Darshan, Aparna, Sandip, Harishbhai and Nandan for their help. Working in old RL-1 was fun and long-lasting memory that I will always cherish. I also thank Subbu, Parul, Anoop, and Krushi. It was fun to grab tea and run to University office for our scholarship issues with Akhilesh. I also wish new PhD students Sneha, Gosai, Sweta, Siddhi, Janki, Jigar and others of this department all the success.

I thank Pradeep, KC, Hemendra, Gopit, Chirayu, Aditi, Divya and Modi for continuous encouragement and support. I am especially thankful to Pradeep for all the help and knowledge sharing on protein expression and structure; it is also very warm and homely relations. I also cherish fun trip with GRCmates and thankful to all the research support you guys gave me. It was a stress buster jamming with you people over tea sessions.

Special thanks to all my hostelmates and roommates, who really made my PhD stay smooth and memorable. No words to thank Hemanta and Anindita for gala time we spent and kind support. I honestly thank Hashim, Hiral and Abhik for amazing homely food and time. I am very thankful to CP, Riyaz, Mande, Hardik and Akhil for bearing with all my continuous nonsense pranks and bangs. Similarly, it was great to have friends like Jignesh, Bhaumik, Shrukhal, Yash, Payal, Sunil, Shaili, Jesal, Indrajeet, Kunal, Tilak, Harsh, Vipul, Nilay and Yash during ups n downs of PhD. And others whose names are not mentioned…. Thank you guys!!!

I am grateful to Shirish bhai who helped me in all official as well as personal aspects whenever required. I also thank and remember Khatribhai for support; Talatibhai for issuing chemicals and plastic ware. I thank Praveenbhai for providing glass ware and Seema madam for distilled water during its shortage. My special thanks to Mandvekarbhai, Aparnamam, Seemamam, Thomasmam, Nairbhai, Varghesebhai and Niteshbhai who willingly extended their help every time I required. I am thankful to Babukaka for his help whenever required. I also thank Nileshbhai, Pradeepbhai and Jayeshbhai for their help and cooperation.

How can I forgot all my master dissertation students who have not only work with me in RL-1 but actually made me what I have able to achieve during my PhD tenure. I clearly remember each and every episode of struggle and success with them. I thank Deval, Sweta, Niraj, Shivani, Kasturi, Ketan and Shubhangi for all work hard party harder moments.

Words would be less for rock solid support from my family and friends. Everyone needs some special core persons in life whose endless support makes the life living and great experience. I am grateful to God for giving me wonderful parents and family members, without whom it was not possible for me to do anything in life. I take this opportunity to thank my Bhai, Ba, Maa, Papa, Ruchi, Jiju and other family members. Especially calls from Tapanbhai used to make things lighter at end of the day.

I am very thankful to the scientific community for sending me the required articles, bacterial strain and plasmid. I acknowledge financial support by Department of Biotechnology (DBT), Ministry of

Science and Technology, New Delhi, India. I am also thankful to University Grants Commission, New Delhi, India for Research Fellowship in Sciences for Meritorious Students (UGC-RFSMS). Dr. Stephanie Bringer-Meyer for generous gift of pT7 fdh gene cassette source. I also thank Prof. Victor de Lorenzo for continuous support to my scientific ventures for advance carriers.

Ahead of all these, I stand with folded hands before the One who is omniscient. I thank Him for providing strength in my arms and will in my mind, with the vigour of which I could venture towards the completion of the project. I consider the accomplishment of the project as an achievement which could not have been possible without His authority.

Jagat Rathod

PREFACE

Azo dyes are the largest and versatile group of dyes having wide range of applications in the textile, paper, food, leather, cosmetics and pharmaceutical industries. They are xenobiotic and toxic, and have high recalcitrance and stability in environment as a result create aesthetic and environmental problems. Conventional treatment of colored effluents by physical or chemical procedures suffers from formation of hazardous by-products, high cost and intensive energy requirements. Several microorganisms including algae, yeast, filamentous fungi and bacteria are reported to bring about azo dye decolorization and degradation.

Various pure bacterial strains, mix cultures and acclimatized consortia have been isolated or enriched from diverse environments, although bacterial strains reported have not been limited to any specific taxa or niche. Azo dye decolorization and subsequent degradation require different biochemical and enzymatic machinery for breaking the azo bond and ring cleavage activity resulting in the complete mineralization of the dye molecule. Two steps bioprocess for dye removal from effluent include the reductive breakage of the azo bond under anaerobic/anoxic conditions followed by aerobic degradation of the aromatic amines. Often mixed cultures or microbial consortia are found to play efficient role in dealing with the azo dye bioremediation strategy. Dye decolorization depends not only on the dye structure and properties but also on several nutritional factors under which the microbial decolorization is carried out. Acclimatized microbial consortia enrichment techniques have been largely performed by repeated transfers of the microbial population in dye containing media for adaptation with time. However systematic studies on enrichment procedure with respect to the sample type, medium composition and incubation conditions are lacking.

Decolorization of dyes can be brought about by specifically isolated microbes by enzymatic mechanisms. There are two major groups of enzymes used by bacteria in the degradation of azo dyes: reductive or oxidative enzymes. Laccases, lignin and manganese peroxidases, tyrosinase form the oxidative enzyme systems and are largely found in fungi whereas reductive enzymes are azoreductases which are classified as flavin dependent (FMN) or flavin independent, and could use NADH or NADPH or both as a cofactor are found in diverse groups of bacteria. The

necessity to isolate, identify and characterize new genes from different environment sources is vital as azo dyes with diverse structures are synthesized every year. Thus it is important to develop novel enzymatic clean-up operations as these can be used as tools for elimination of low molecular weight aromatics which are highly carcinogenic at a very low concentration.

As azoreductases have high K_m values for NADH as compared to the NADH peroxidase and other NADH: Quinone reductase systems, thus overall rate of dye decolorization may be impeded by this factor. To overcome this problem, a plausible strategy may be to increase in the overall NADH pool inside the cell by NADH regeneration system.

Physiological function of azoreductases in bacteria is thought to be different than azo dye reduction. Azoreductases basically belong to quinone reductase family. It was shown that *azoR* is essential for the maintenance of cellular reduced glutathione (GSH) levels after addition of 2-hydroxy quinone, catechol, and menadione. Thus, *azoR* seems to be involved in resistance to thiol specific stress. This implicates the role of azoreductases under conditions of stress.

Based on this background, the objectives of this work involved,

1) Bacterial diversity and biodecolorization studies of Reactive violet 5R (RV5R) by microbial consortia
2) Azoreductase (*azoA*) from *Enterococcus* sp. L2: cloning, heterologous expression and physiological role.
3) Metabolic engineering for efficient azo dye decolorization by NADH regeneration system

Present study showed both pristine and dye contaminated samples could be used to enrich acclimatized bacterial consortia for decolorization of the azo dye reactive violet 5R (RV5R). Acclimatized consortia showed significant diversity profiles in their communities as analyzed by amplified rDNA restriction analysis (ARDRA) and denaturing gradient gel electrophoresis (DGGE). It may be concluded that the composition of the consortia is governed by nature of the sample, enrichment media composition and incubation conditions. The phylogenetic diversity in the consortia was correlated with different dye

decolorization/degradation end products as revealed by Fourier transformed Infrared spectroscopy (FTIR) and GC- Mass spectroscopy analysis.

Enterococcus sp. L2 was isolated as an efficient azo dye decolorizing strain during these studies. Further, enterococcal *azoA* gene was isolated, cloned and expressed in gram negative and positive host systems for enhanced azo dye decolorization. To justify the cofactor (NADH) requirement of AzoA, metabolic engineering approach was used to construct NADH regeneration system by NAD^+ dependent formate dehydrogenase from *Mycobacterium vaccae* N10. We were able to develop FDH-AzoA dual enzyme system for dye decolorization. At the same time, we showed the overexpression of *azoA* in enterococcal host lead to enhanced survival under oxidative stress by inhibiting the free radical formation and increased heavy metal resistance.

Table of Contents

LIST OF FIGURES

LIST OF TABLES

LIST OF APPENDICES

LISTS OF ABBREVIATIONS

Amp	Ampicillin
APS	Ammonium per sulphate
ARDRA	Amplified ribosomal DNA restriction analysis
ATCC	American type culture collection
ATP	Adenosine triphosphate
azoA	Enterococcal azoreductase gene
BLAST	Basic local alignment search tool
bp	base pair (s)
BYGT	Brain Heart Infusion broth Yeast extract Glycerol Tris-Cl
CI	Color index
CTAB	Cetyl trimethylammonium bromide
DCW	Dry cell weight
DGGE	Denaturing Gradient Gel Electrophoresis
DNA	Deoxyribonucleic acid
DTT	1, 4-Dithiothreitol
ED	Electron donor
EDTA	Ethylene diamine tetra acetic acid
ETC	Electron transport chain
FDH	Formate dehydrogenase
FMN	Flavin mononucleotide
FRE-I	Ferric reductase I
FTIR	Fourier transformed Infrared Spectroscopy

GC-MS	Gas Chromatography Mass spectrometer
Gen	Gentamycin
H´ index	Shannon-Weaver diversity Index
IPTG	Isopropyl β-D-1-thiogalactopyranoside
Kan (Km)	Kanamycin
LiP	Lignin peroxidase
MnP	Manganese peroxidase
NAD(P)	Nicotinamide adenine dinucleotide (phosphate)
NADH	Nicotinamide adenine dinucleotide (reduced)
NADPH	Nicotinamide adenine dinucleotide phosphate reduced
O.D.	Optical Density
Ori	Origin of replication
pBBR1MCS2	Gram negative broad host strain expression vector
PCR	Polymerase chain reaction
PEG	Polyethylene glycol
pMGS100	Gram positive *Enterococcus* based expression system
PQQ	Pyrolloquinoline quinone
RE	Restriction enzyme
RM	Redox mediator
rpm	Revolutions per minute
RV5R	Reactive violet 5R
SDS PAGE	Sodium dodecyl sulphate polyacrylamide gel electrophoresis
SOD	Superoxide dismutase

TEMED	N,N,N′,N′ - tetramethylenediamine
THB	Todd Hewitt Broth
Tris	Tris (hydroxymethyl) aminomethane buffer
TTN	Total turnover number
VC	Vector control
WT	Wild type
X-Gal	5-Bromo-4-chloro-3-indolyl-β-D galactopyranoside

LIST OF SYMBOLS

%	Percentage
µl	microlitre
µM	micromolar
^{0}C	Degree Celsius
e^{-}	Electron
E'^{0}	Standard reduction potential
g/L	Gram/Litre
kb	kilobase (s)
k_{cat}	Catalytic constant
kDa	Kilodalton
K_m	Michaelis -Menten constant
ng	Nanogram
nm	Nanometer

t	tonne
V	Volt
α	Alpha
β	Beta
γ	Gamma
Δ	Delta (mutant)
Ɛ	Molar extinction coefficient

1 Introduction

With the boom in the worldwide textile industry in recent years, there has been a commensurate increase in the use of various dyes, and this has been accompanied by increase in the discharge of coloured wastewater from dye-manufacturing and dyeing units. It is estimated that 280,000 t of textile dyes effluent are discharged annually worldwide (Jin et al., 2007). Azo dyes make up approximately 70% of all dyestuffs (Zollinger, 2004), making them the largest group of synthetic colorants and the most common synthetic dyes released into the environment (Chang et al., 2001; Zhao & Hardin, 2007). Many azo dyes, dye precursors and their amine constituents produced through biotransformation are carcinogenic in nature. Effluents containing dyes have the ability to impart colour in to large volume of natural aquatic sources and create a serious environmental problem and public health concern. Efficient colour removal and degradation process, specifically from textile industry effluents, has become great concern over the last few decades. The current physicochemical technologies for the treatment of wastewaters containing dyes include adsorption, precipitation, chemical oxidation, photo-degradation, or membrane filtration (Yeh & Thomas, 1995). These have serious restrictions as economically feasible methods for decolorizing textile wastewaters (such as high cost, formation of hazardous by-products or intensive energy requirements). According to one study in mid 90s, in India, dyestuff industry produces around 60,000 t of dyes, which is approximately 6.6% of total world output (Shenai, 1995).

Biodegradation as eco-friendly and cost effective green process is the best alternative for the azo dye effluents treatment. Most of the synthetic dyes are recalcitrant and usually resist biodegradation in conventional sewage-treatment plants (Shaul et al., 1991). Various specialised biological systems able to decolorize and metabolize azo dyes into less toxic compounds have been reported (Stolz, 2001) and this has tremendously fortified the biodegradation efforts. An important aspect of azo dye degradation is the reductive cleavage of the azo bond which results in dye decolorization and is considered as the bottle neck step in the degradation pathway. This work deals with the study of azo bond reduction by bacterial enzyme systems. Azo dye decolourization was studied in natural bacterial isolates and enriched

acclimatized microbial consortia. The dye decolorization process improvement was attempted by cloning and overexpression of the azoreductase gene along with cofactor regeneration system.

The review of literature describes the important features of azo dyes, microbial systems known to carry out dye decolorization and degradation, the enzymatic machinery in microbial systems for azo dye decolorization with particular emphasis on the azoreductase enzyme and factors affecting its catalytic activity.

1.1. Azo dyes

Dyes are classified as anionic (direct, acid, and reactive dyes), cationic (basic dyes), and non-ionic (disperse dyes) (Chen, 2006). Anionic and non-ionic dyes mostly contain azo or anthraquinone type of chromophores. Azo dyes form a major class of chemically related compounds that are ubiquitously used in several industries. Azo dyes are the largest and most versatile class of dyes, and account for more than half of the annually produced amount of dyes (Stolz, 2001). They constitute the largest class of synthetic dyes used in commercial applications (Zollinger, 2004).

Azo dyes are characterized by one or more R1-N=N-R2 (Azo or diimide) bonds, in which R1 and R2 can be either aryl or alkyl groups. The azo group of azo dyes links two sp2 hybridized carbon atoms. Often these carbons are part of aromatic systems but this is not always the case. Diethyldiazene is an aliphatic azo compound. Mainly aromatic side groups around the azo bond help to stabilize the -N=N- group by making it part of an extended delocalized system.

Unlike most organic compounds, dyes possess colour because they 1) absorb light in the visible spectrum (400–700 nm), 2) have at least one chromophore (color –bearing group), 3) have a conjugated system, i.e., a structure with alternating double and single bonds, and 4) exhibit resonance of electrons, which is a stabilizing force in organic compounds. When any one of these features is lacking from the molecular structure the colour is lost. Azo dyes have the capacity to absorb light of specific intensity and thus are capable to give bright, high intensity colours. They have fair to good fastness properties, but not better than as the carbonyl and phthalocyanine classes. Their biggest advantage it their cost-effectiveness, which is due to the ease in the processes involved in their synthesis.

1.2. Structures of azo dyes

The color index (CI) number, developed by the *Society of Dyers and Colourists* (UK) and by the *American association of Textile Chemists and Colourists* (USA) is used for dye classification. The first word is the dye classification and the second word is the hue or shade of the dye. For example, CI Acid Yellow 36 (CI 13065) is a yellow dye of the acid type (Christie, 2001). Azo dyes are subdivided according to the number of azo bonds they possess i.e. mono-azo, di-azo, tri-azo & poly-azo (more than three azo bonds) (Chacko and Subramaniam, 2011). Structures of representative examples of members of different classes of azo dyes are shown in Table 1.1.

By making a series of reactions and couplings it is possible to build up more than one azo group into a dye molecule, these structures are called poly-azo dyes. This concept is the basis for the manufacture of the main leather colours of brown and black. Normally, more the azo chromophores present, the more the colour tends towards brown or black, as the individual red, yellow, blue, etc. chromophores start to work together. Many of the major brown and black dyes for application to leather are polyazo compounds. Azo dye structures directly play significant role in determining its toxicity and biodegradation rate (Puvaneswari et al., 2006). Addition of different sulphonate, amide, amine and hydroxyl groups to the aryl rings alters its ability to cross biological membranes based on its polar nature. Reductive cleavage of azo dyes sometimes leads to even higher toxic aromatic amines. These aromatic amines are characterized for their carcinogenic properties and oxidative damage to the cellular machinery. Tan et al., (2005) have shown that sulphonated aromatic amines, one of the major types of amines released after the reductive cleavage of azo dyes, are mainly degraded under aerobic conditions. Although the biodecolorization process widely considered as an anoxic or anaerobic process due to its oxygen sensitivity.

Dyes owe much of their character to the presence of aromatic rings such as benzene and naphthalene. These aromatic rings usually have chloride, hydroxyl, sulphate or nitro groups attached to increase solubility in water and enhance interactions with the substrate. Various metals such as copper form a coordinates with different dye structures and delivers dyes higher stability. Thus different metal ions (electron poor, Cu^{+2}ions) interact with electron donating nitrogen, oxygen groups or ligands to generate co-ordination complexes.

Table 1.1Structures of representative azo dyes

Class	Examples	Structure
Mono azo dyes	Reactive violet 5R	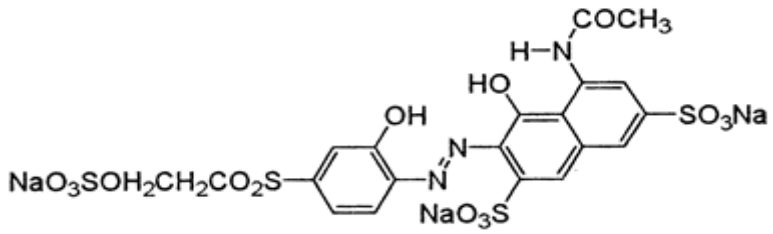
	Methyl red CI 13020	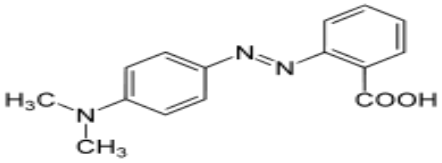
Di-azo dyes	Sudan III	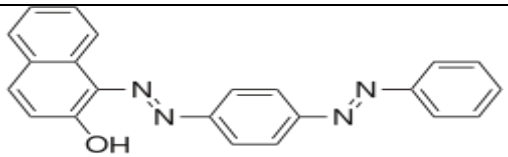
	Direct blue 1	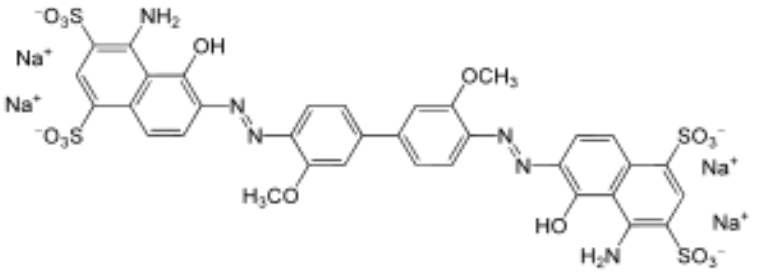
Tri-azo dyes	Direct green 6	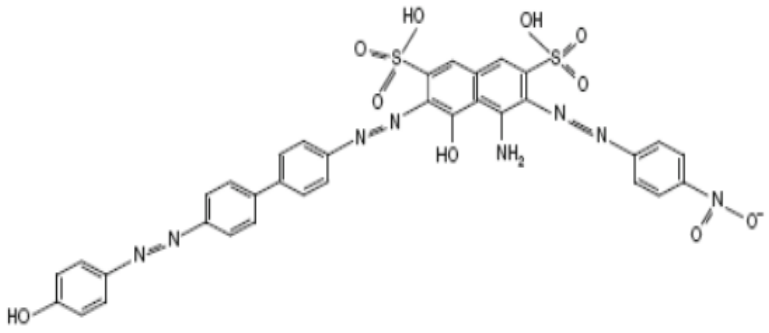

1.3. Dye removal techniques

Several methods for the reduction of azo dyes from textile effluents to achieve decolourization are depicted in Figure 1.1. Physical and chemical dye removal methods have the inherent drawbacks of being economically unfeasible (as they require more energy and chemicals), being unable to completely remove the recalcitrant azo dyes and/or their organic metabolites, generating a significant amount of sludge that may cause secondary pollution problems, and involving complicated procedures. Advantages and disadvantages of various methods are listed in Table 1.2.

1.4. Microbial degradation of azo dyes

The use of microbial or enzymatic treatment method for the complete decolorization and degradation of such dyes from textile effluent has the following advantages: (1) being environmentally-friendly, (2) being cost-competitive, (3) producing less sludge, (4) yielding end products that are non-toxic or have complete mineralization; and (5) requiring less water consumption compared to physicochemical methods. Bioremediation, or the use of microbial techniques to deal with pollution, is a key research area in the environmental sciences. In such approaches microbes acclimatize themselves to the toxic wastes and new resistant strains develop naturally, which then transform various toxic chemicals into less harmful forms. The mechanism behind the biodegradation of recalcitrant compounds in the microbial system is based on the action of the biotransformation enzymes.

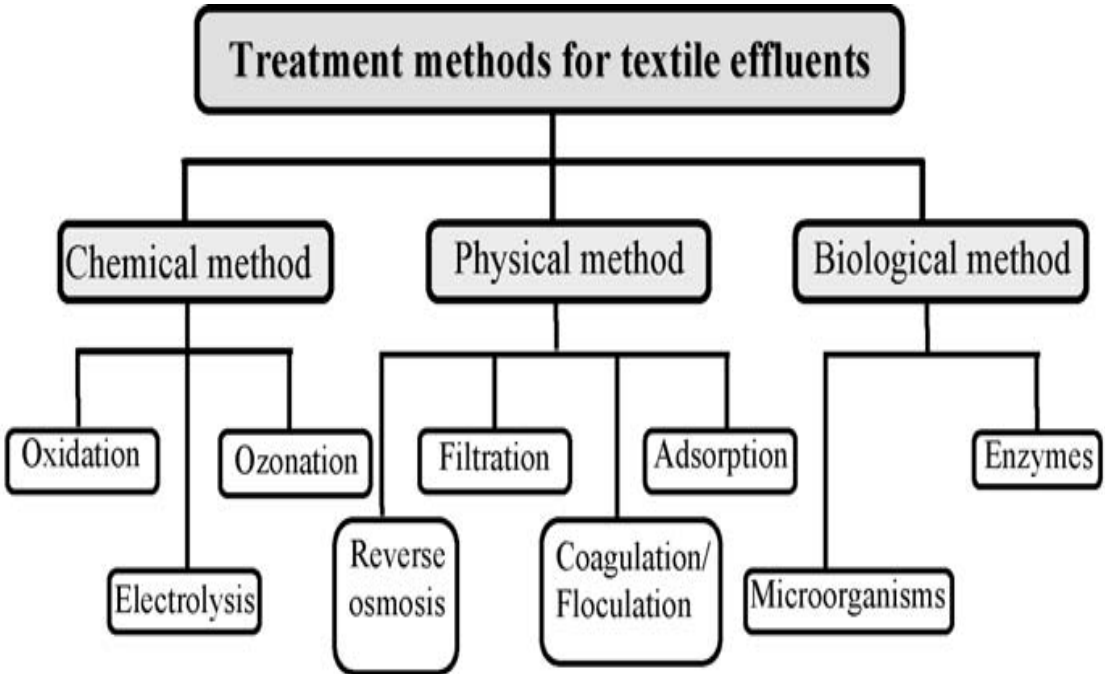

(Saratale et al., 2011)

Figure 1.1 Different methods for removal of dyes from textile effluents

Shaul et al. (1991) studied the efficacy of dye removal by conventional biological treatment systems. They spiked the raw wastewater influent with various commercial dyes in concentrations of either 1 or 5 mg l^{-1} and conducted dye analyses on the wastewater effluent and activated sludge. Data obtained from this study demonstrated that 11 of 18 dyes passed through an activated sludge process untreated, 4 adsorbed onto the activated sludge and 3 underwent biodegradation (Shaul et al., 1991). Different dye classes showed different grades of adsorption, which seems to depend on the dyes' solubility. For example, acid dyes with more sulphonic groups (higher solubility) tend to adsorb to a lesser degree (Shaul et al., 1991). Thus, the effectiveness of microbial decolorization depends on the adaptability and the activity of the microorganisms and specially selected strains need to be used in the process.

A variety of microorganisms are capable of decolorizing of a wide range of dyes including; bacteria, fungi, yeasts, actinomycetes, algae (Saratale et al., 2011). The oxidoreductive enzymes, such as lignin peroxidase, laccases, tyrosinase, azoreductase, riboflavin reductase, NADH DCIP reductase and aminopyrine N-demethylase, have been mainly utilized in the microbial decolorization/degradationof azo dyes (Stolz, 2001; Chen, 2006; Saratale et al., 2011; Solís et al., 2012; Chengalroyen and Dabbs, 2013).

Table 1.2Advantages and disadvantages of current methods of dye removal techniques.

(Chacko et al., 2011 & Huber et al., 2012).

Methods	**Advantages**	**Disadvantages**
Non-destructive methods		
Adsorption	Good removal of wide variety of dyes	Very expensive Exchanger needs to be regenerated
Membrane filtration	Removes all dye types	Concentrated sludge production
Electrochemical coagulation	Economically feasible	High sludge production
Destructive methods		
Electrochemical destruction	Breakdown compounds are non -hazardous	High cost of electricity
Fenton's reagent	Effective decolorization of both soluble and insoluble dyes	Sludge generation
Ozonation	Applied in gaseous state : no alteration of volume	Short half –life (20 min)
Photochemical	No sludge production	Formation of by-products
Irradiation	Effective oxidation at lab scale	Requires a lot of dissolved oxygen

There are two major groups of enzymes used by microorganisms in the degradation of azo dyes: reductive or oxidative enzymes (Saratale et al., 2011). Examples of the oxidative enzyme activities reported are lignin and manganese peroxidase, laccase and tyrosinase (Saratale et al., 2011). Very few studies have reported activity of oxidative enzymes in bacteria, e.g. *Streptomyces* (Dos Santos, 2007) and *Sphingomonas* which produce an extracellular enzyme peroxidase (Stolz, 2001). The lignolytic enzyme system is found in the white-rot fungi. The reductive enzymes,

azoreductases are found in bacterial systems. Azoreductases carry out reductive cleavage of the azo bond(s) leading to production of aromatic amines concurrent with dye decolorization. These oxidoreductive enzymes possess the ability to accept azo compounds as substrates at catalytic site and are responsible for biotransformation. Electron withdrawing groups such as $–NH_2$ and –OH decrease the electron density around the –N=N– bond and facilitate the reduction of the azo group with a simultaneous release of an aromatic amine. Also, placing an electron donor substitute in an ortho position in relation to the azo group increases tendency for reductive cleavage of the azo bond. A similar effect is observed for water-soluble dyes i.e., those with groups such as $–SO_3Na$ and –COOH in their structure (Chen, 2006).

Microbial decolorization of azo dyes may occur under conventional anaerobic, facultative anaerobic and aerobic conditions by different groups of organisms. Some consideration of microbes and their enzymatic activities in the bioremediation treatment process is due to their sensitivity to impurities such as heavy metal and organic solvents and salts.

1.4.1. Degradation of azo dyes by filamentous fungi and yeasts

White rot fungi can degrade many complex compounds by producing extracellular hydrolytic enzymes. It has been shown that *Phanerochaete chrysosporium, Geotrichum candium, Trametes modesta, Bjerkandera adusta, Penicillium* spp., *Pleurotus ostreatus*, *Pycnoporus cinnabarinus,* and *Pyricularia oryzae* are able to degrade complex azo dyes. Most of the azo dye degrading enzymes are **oxidases and peroxidases** with a very high oxidative capacity. It has been suggested that these enzymes could oxidize the azo dyes to form compounds of lower molecular weights. Among these enzymes, **manganese peroxidase (MnP), lignin peroxidase (LiP), and laccase** are most frequently applied to azo dye degradation.

Lignin peroxidase (LiP) is an H_2O_2-dependent enzyme which contains a heme prosthetic group, and was demonstrated to oxidize a range of lignin model compounds. LiPs are able to oxidize nonphenolic aromatic compounds.

Manganese peroxidases (MnP) preferentially oxidize Mn^{2+} to Mn^{3+} and the Mn^{3+} is responsible for the oxidation of many phenolic compounds. LiPs and MnPs show a similar reaction mechanism through initiating free-radical production which oxidizes

other chemicals including azo dyes. These enzymes are considered to be the core of the lignin-degrading system of white rot fungi. Both LiP and MnP are produced by *Phanerochaete, Bjerkandera,* and *Trametes* species and some other white rot fungi. *Trametes versicolor* showed the best biodegradation performance among these fungi.

Laccase is a multicopper enzyme which catalyses the oxidation of phenolic and non-phenolic compounds. Electrons received from the substrate are subsequently transferred to oxygen, which is reduced to water. Laccase is able to decolorize several textile azo dyes. The decolorization efficiency can be improved remarkably in the presence of mediators.

Several ascomycetes yeast strains display similar decolorizing behaviours. In *Saccharomyces cerevisiae,* the ferric reductase system participates in the extracellular reduction of azo dyes. The **ferric reductase I** (FRE1) deleted *Saccharomyces cerevisiae* mutant strain showed much-reduced decolorizing capabilities(Dias et al., 2010).

Although white rot fungi are able to stably decolorize azo dyes, currently there are several problems which interfere with the utilization of lignolytic fungi for the treatment of dye-containing wastewaters:

- Wastewater treatment plants are not the natural habitat of lignolytic fungi and therefore special care has to be taken to establish these fungi in a wastewater treatment system.
- The lignolytic enzymes of the white rot fungi are thought to be expressed in most cases only during secondary metabolism following growth when carbon and/or nitrogen sources become limiting. Neither lignin nor any of the pollutants degraded by the enzymes has been shown to be utilized as a carbon or energy source, and a separate carbon source is required for the cultivation of the organisms.
- The observed degradation rates are usually rather low. In typical experiments about 50–150 mg of the dyes per liter were decolorized within 5–10 days
- Lignin peroxidases are very unspecific for the oxidation of aromatic and xenobiotic compounds. Therefore, in the presence of complex substrate mixtures such as those observed in industrial sewage-treatment systems some will remain unattacked, also other substrates will be oxidized by lignin peroxidases.

- Lignin peroxidases exhibit a pH-optimum at pH 4.5–5. Therefore a rather acid pH of the wastewater treatment system is required, which may inhibit the growth of several other useful microorganisms (Swamy and Ramsay, 1999; Stolz, 2001; Salame et al., 2010).

Primary decolorization is further degraded via different ring cleavage pathways, wherein initial substitution reactions proceed by dehalogenation and hydroxylation to allow the aromatic amines to enter in various degradation pathways. Aromatic rings with substituents such as hydroxyl, amino, acetamido, or nitro functions were mineralized to greater extent than unsubstituted rings in case of *Phanerochaete chrysosporium* (Spadaro et al., 1992).White-rot fungus *Pyricularia oryzae* is reported to degrade phenolic azo dyes without the formation of aromatic amines (Chivukula and Renganathan, 1995).

1.4.2. Bacterial decolorization and degradation of azo dyes

Bacterial decolorization of azo dyes is normally faster compared to fungal systems with regard to the decolorization and mineralization kinetics. The mechanism of microbial degradation of azo dyes involves the reductive cleavage of azo bonds or direct ring cleavage pathway. Similar to the oxidoreductive enzymes of fungal systems, different bacterial origin lignin peroxidase, laccases, tyrosinase, azoreductase, riboflavin reductase, NADH-DCIP reductase and aminopyrine N-demethylase (Kagalkar et al., 2009; Kalyani et al., 2009; Olukanni et al., 2013), have been mainly utilized in the bacterial decolorization and degradation of azo dyes. Azo dyes undergo initial reductive cleavage which results in the decolorization of the dye molecule forming corresponding aromatic amines. Subsequently, aerobic organisms like *Pseudomonas, Rhodococcus* and *Sphingomonas* degrade aromatic amines by introducing hydroxyl groups on the benzene, naphthalene and anthracene structure to allow it to undergo gentisic pathway or β-ketoadipate pathway for complete mineralization of azo dyes. The bacterial decolorization and degradation of azo dyes has been of considerable interest since it can achieve a higher degree and broad spectrum of biodegradation and mineralization, is cost-effective and environmentally-friendly, and produces less sludge (Khehra et al., 2005; Rai et al., 2005; Saratale et al., 2009b). Both pure cultures as well as mixed cultures have been reported for decolorization of azo dyes.

1.4.2.1. *Azo dye decolorizing bacteria*

Continuous efforts to isolate pure bacterial cultures able of degrading azo dyes started in the1970s with reports of *Aeromonas hydrophila* and *Bacillus* (Mechsner and Wuhrmann, 1982; Olukanni et al., 2013). Pure culture system ensures reproducible data, and thus interpretation of experimental observations becomes easier with various analytical and biological investigations on the mode of dye breakage mechanisms. Statistical optimization for azo dye degradation/ decolorization possible as shown by *Pseudomonas oleovorans* PAMD_1 possessing a defined enzyme system (azoreductase) (Aranganathan et al., 2013). It becomes easier to determine the bacterial strategy for biodegradation using the tools of biochemistry and molecular biology, and this information could be utilized to regulate the enzyme system in order to produce genetically modified strains with enhanced activities. It is also feasible to analyze and model the kinetics of azo dye decolorization by a particular pure bacterial culture (Chang and Kuo, 2000). Azo dyes decolorization and azoreductase activity has been reported primarily from prokaryotes although they are also present in lower eukaryotes, plants and animals including humans. Bacteria decolorizing azo dyes belong to different phyla of *Eubacteria* such as *Proteobacteria*, *Firmicutes*, *Actinobacteria*, mycoplasmas and *Cyanobacteria* (Puvaneswari et al., 2006). National Center for Biotechnology Information (NCBI) data bank possesses total 1077 genes entries for putative and annotated azoreductases, which is an important determinant for the biological decolorization of azo dyes. Figure 1.2.shows the taxonomic distribution and abundance (number of entries) for azoreductase genes in diverse taxa of biological systems (1061 entries for bacteria and 16 for eukaryotes). Bacterial pure cultures studied for azo dye decolorization and degradation are mentioned in Table 1.3.

Table 1.3 Dye decolorizing bacterial strains and mixed culture studies.

Name of strain	Name of the dye and concentration	Conditions (pH, temp (^{o}C), agitation conditions)	Time (h)	Decolorization (%)	Mechanism	References
***Pseudomonas* sp.**	Reactive Blue 13, (200mg/L)	7.0, 35, static	70	83.2	NA	Lin et al., 2010
***Micrococcus glutamicus* NCIM 2168**	Reactive Green 19 A; (50mg/L)	6.8, 37, static	42	100	Oxidoreductase	Saratale et al., 2009a
***Enterobacter* EC3**	Reactive Black, (1g/L)	7.0, 37, anaerobic	36	92.56	NA	Wang et al., 2009a; Wang et al., 2009b; Wang et al., 2009c
Mutant *Bacillus* sp. ACT2	Congo Red; (3 g /L)	7.0, 37, static	37–48	12–30	Reductive	Gopinath et al., 2009
Lactobacillus acidophilus* and *Lactobacillus fermentum	Water and oil soluble azo dyes; (6mg/L)	NA, 37, anaerobic	36	86–100	NA	Chen et al., 2009b
***Geobacillus stearothermophilus* (UCP 986)**	Orange II; (0.050mM)	5–6, 50, aeration (150 rpm)	24	96–98	NA	Evangelista-Barreto et al., 2009
Aeromonas hydrophila	Reactive Red 198, Reactive Black 5, Reactive Red 141, Reactive Blue 171, Reactive Yellow 84	7.5, 30, agitation (125 rpm)	60.2; 80.9; 66.5;36.0; 33.7[a]	-	Reductive	Hsueh et al., 2009

	(300mg/L)					
Aeromonas hydrophila	Reactive Red 141; (3.8 g/ l)	7.0, 30, 200 rpm, Chemostat pulse technique	48	100	NA	Chen et al., 2009a
***Bacillus* sp. VUS**	Navy Blue 2GL; (50mg/L)	7.0, 40, static	18	94	Oxidative and reductive	Dawkar et al., 2009
***Citrobacter* sp. CK3**	Reactive Red 180; (200mg/L)	7.0, 32, anaerobic	36	96	NA	Wang et al., 2009a; Wang et al., 2009b; Wang et al., 2009c
***Acinetobacter calcoaceticus* NCIM-2890**	Direct Brown MR; (50mg/L)	7.0, 30, static	48	91.3	Oxidative and reductive	Ghodake et al., 2009
***Bacillus* sp.**	C.I. Reactive Orange 16; (100mg/L)	7–8, 30, static	24	88	Reductive	Telke et al., 2009
Pseudomonas aeruginosa	Remazol Orange; (200mg/L)	7.0, 30, static	24	94	Reductive	Sarayu & Sandhya, 2010
***Pseudomonas* sp. SUK1**	Reactive Red 2; (5 g/L)	6.2–7.5, 30, static	6	96	Oxidative and reductive	Kalyani et al., 2009
Enterococcus gallinarum	Direct Black 38; (100mg/L)	NA, NA, static	20 days	100	Reductive	Bafana et al., 2009
***Pseudomonas* sp. SU-EBT**	Congo red; (1 g /L)	8.0, 40, static	12	97	Oxidative	Telke et al., 2009
***Brevibacillus laterosporus* MTCC 2298**	Golden Yellow HER; (50mg/L)	7.0, 30, static	48	87	Oxidative and reductive	Gomare & Govindwar, 2009

***Rhizobium radiobacter* MTCC 8161**	Reactive Red 141; (50mg/L)	7.0, 30, static	48	90	Oxidative and reductive	Telke et al., 2008
***Comamonas* sp. UVS**	Direct Red 5B; (1.1 g/L)	6.5, 40, static	13	100	Oxidative	Jadhav et al., 2008)
***Exiguobacterium* sp. RD3**	Navy Blue HE2R; (50mg/L)	7.0, 30, static	48	91	Oxidative and reductive	Dhanve et al., 2008
Proteus mirabilis	RED RBN; (1 g/L)	6.5–7.5, 30–35, static	20	95	Reductive followed by biosorption	Chen et al., 1999
Aeromonas hydrophila	Red RBN;(3000mg/L)	5.5–10.0, 20–35, NA	8	90	NA	Chen et al., 2003
***Pseudomonas aeruginosa* NBAR12**	Reactive Blue 172; (500mg/L)	7.0–8.0, 40, static	42	83	Oxidative and reductive	Bhatt et al., 2005
***Bacillus* sp.**	Congo Red; (100–300mg/L)	7.0, 37, NA	24–27[b] 12[c]	100[b] 100[c]	Effect of sonication	Gopinath et al., 2009
***Klebsiella pneumoniae* R5-13**	Methy1 Red; (100mg/L)	6.0–8.0, 30, 200rpm	168	100	Reductive	Wong & Yuen, 1996
***Rhodopseudomonas palustris* AS1.2352**	Reactive Brilliant Red; X-3B; (50mg/L)	8, 30–35, anaerobic	24	90	Reductive	Liu et al., 2006
***Shewanella decolorationis* S12**	Acid Red GR; (150mM)	NA, 30	68[d]	100[d]	Reductive	Xu et al., 2007
***Paenibacillus azoreducens* sp. nov.**	Remazol Black B; (0.1 g/L)	NA, 37, static	24	98	NA	Meehan et al., 2001
Bacteroides fragilis	Amaranth, Orange II and Tartrazine;	8, 35, static	NA	95	NA	Bragger et al., 1997

	(0.1mM)					
Desulfovibrio desulfuricans	Reactive Orange 96 and Reactive Red 120	NA, 28, Anaerobic	2	95	Reductive	Yoo et al., 2001
Bacillus fusiformis **KMK5**	Disperse Blue 79 and Acid Orange 10; (1.5 g/L each)	9, 37, anoxic	48	100	Reductive	Kolekar et al., 2008
Alishewanella **sp. strain KMK6**	mixture of textile dyes (0.5–2.0 g/L)	Anoxic and subsequently shaking condition	8h	>90	Azoreductase	Kolekar et al., 2013
Aeromonas hydrophila **var 24 B**	Various azo dyes; (10–100mg/L)	NA	24	50–90	Reductive	Idaka et al., 1978
Sphingomonas **sp. BN6**	Acid azo dyes, Direct azo dyes and Amaranth; (0.1mM)	NA	NA	NA	Flavin Reductase	Russ et al., 2000

NA: Information not available. [a]: Decolorization mg/L/h/ODU, [b]: Without sonication pretreatment, [c]: With sonication pretreatment,

[d]: Anaerobic condition.

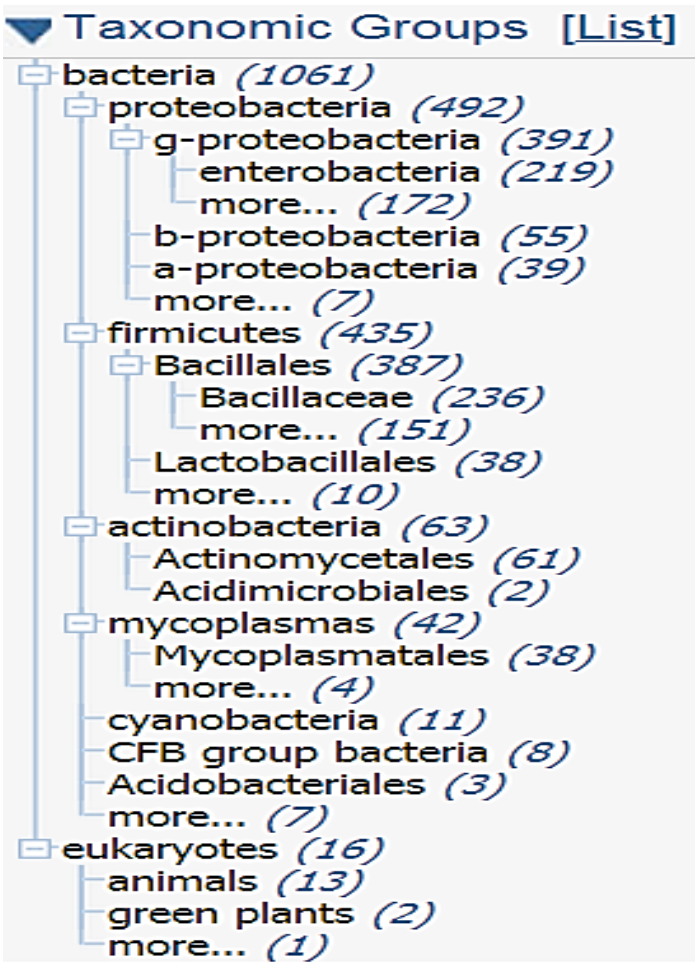

Figure 1.2 Presence of azoreductase genes in different biological systems.

(Bracket number denotes the total numbers of entries at particular taxonomic unit) (http://www.ncbi.nlm.nih.gov/gene/?term=azoreductase on 9th September, 2013)

1.4.3. Azo dye decolorization by bacteria under anaerobic condition

Decolorization of azo dyes under anaerobic conditions is thought to be a relatively simple and non-specific process. Azo dyes act as an oxidising agent for the reduced flavin nucleotides of the microbial electron chain and are reduced and decolorised concurrently with oxidation of the reduced flavin nucleotides. Additional carbon source such as glucose, acetate, starch, ethanol, etc. is required in order for decolorisation to proceed at a viable rate. This additional carbon is converted to methane and carbon dioxide, releasing electrons. Anaerobic degradation of textile dyes yields only azo reduction, in most of the cases mineralisation does not occur (Santos et al., 2007).

It has been reported that under anaerobic conditions a low redox potential (≤50 mV) forms which causes the effective decolorization of the azo dyes (Knapp et al., 2000). It was observed that the presence of oxygen usually inhibits the azo bond reduction activity, since aerobic respiration may dominate utilization of NADH, thus impeding the electron transfer from NADH to azo bonds (Chang et al., 2001). It was also reported that anaerobic azo dye decolorization is a fortuitous process, where azo dye might act as an electron acceptor supplied by the carriers of the electron transport chain (Knapp et al., 2000; Stolz, 2001; Chen, Xu, et al., 2010). Species of *Bacillus, Pseudomonas, Aeromonas, Proteus, Micrococcus* and purple non-sulphur photosynthetic bacteria were found to be effective in the anaerobic degradation of a number of azo dyes, and although many of these cultures were able to grow aerobically, decolorization was achieved only under anaerobic or anoxic conditions (Stolz, 2001).

Alternatively, decolorization might be attributed to nonspecific extracellular reactions occurring between reduced compounds generated by the anaerobic biomass. It was also reported that in anaerobic conditions the permeation of the azo dyes through biological membrane into the microbial cells acts as the principal rate-limiting factor for the decolorization (Soojhawon et al., 2005). It was suggested that reduction of these dyes could occur through mechanisms that are not dependent on their transport into the cell. There are now many reports on the role of redox mediators in azo bond reduction by bacteria under anaerobic conditions. Figure 1.3 represents the different mechanisms of anaerobic azo dyes reduction.

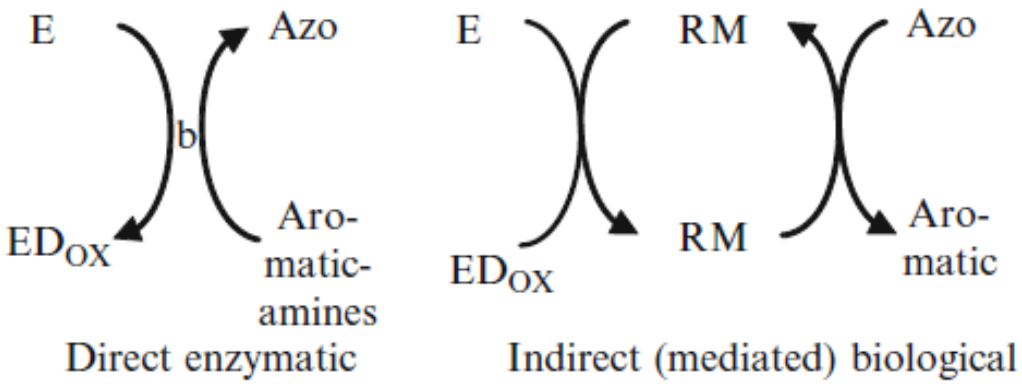

Figure 1.3 Mechanism of anaerobic azo dye reduction.

RM redox mediator; ED electron donor; b bacteria (enzyme)

Azo dye reduction by *Shewanella* strains is coupled to the oxidation of electron donors and linked to the electron transport and energy conservation in the cell membrane (Hong and Gu, 2010). Under anaerobic conditions the bacterium tends to utilize unconventional electron acceptors such as azo dyes, which lead to the decolorization phenotype by *Shewanella*. Various components of electron transport chains are involved for the transport the electrons up to the azo compounds via redox mediators or directly by membrane bound reductases as depicted in Fig. 1.4.

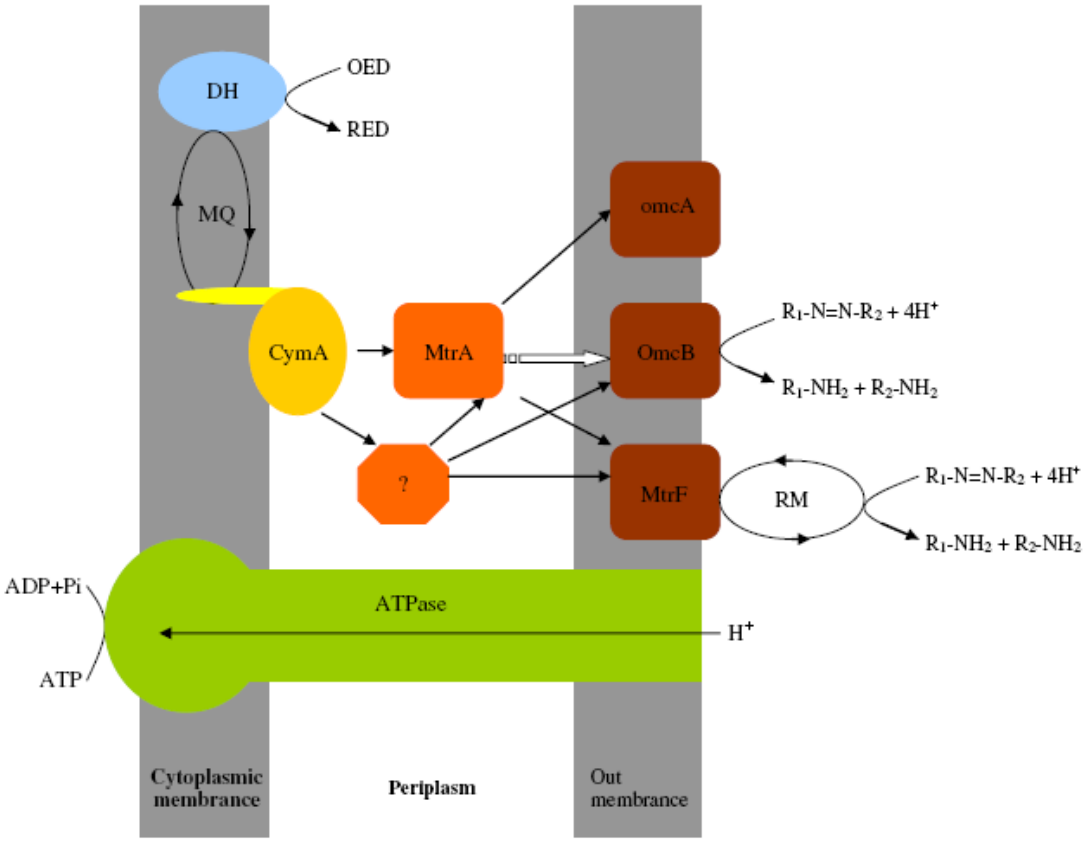

Figure 1.4 Chemiosmotic model of the azorespiration electron transport chain in *Shewanella decolorationis* S12.

(Chen et al., 2010)

1.4.3.1. *Role of redox mediators in azo dye decolorization*

Redox mediators are compounds that accelerate the electron transfer from a primary electron donor to a terminal electron acceptor, which may increase the reaction rates by one to several orders of magnitude. Flavin-based compounds like FAD, FMN and riboflavin, as well as quinone- based compounds like anthraquinone sulphonate (AQS), anthraquinone 2,6 disulphonate (AQDS) and lawsone, have been extensively reported

as redox mediators during azo dye reduction (Keck et al., 2002; Stolz, 2002; dos Santos et al., 2003; Albuquerque et al., 2005; Van der Zee and Cervantes, 2009). Reductive decolorisation of azo dyes in the presence of redox mediators occurs in two distinct steps, the first step being a non-specific enzymatic mediator reduction, and the second step being a chemical reoxidation of the mediator by the azo dyes. Theoretically, feasible redox mediators for biological azo dye reduction must have redox potentials between the half reactions of the azo dye and the primary electron donor. Figure 1.5 shows the E'_0 values for both quinone-based and non-quinone-based redox mediators.

1.4.4. Azo dye decolorization under aerobic condition

Under aerobic conditions, the enzymes mono- and di-oxygenase catalyse the incorporation of oxygen from O_2 into the aromatic ring of organic compounds prior to ring fission (Madigan, M.T., Martinko, J.M., Parker, 2003). In most monooxygenases, the electron donor is NADH or NAD(P)H, even though the direct coupling to O_2 is through a flavin that is reduced by the NADH or NAD(P)H donor. The substituents of azo dyes, mainly nitro and sulfonic groups, are recalcitrant to aerobic bacterial degradation (Claus et al., 2002). This fact is probably related either to the electron-withdrawing nature of the azo bond and their resistance to oxygenases attack, or because oxygen is a more effective electron acceptor, therefore having more preference for reducing equivalents than the azo dye (Hans-Joachim Knackmuss, 1996; Keck et al., 1997).

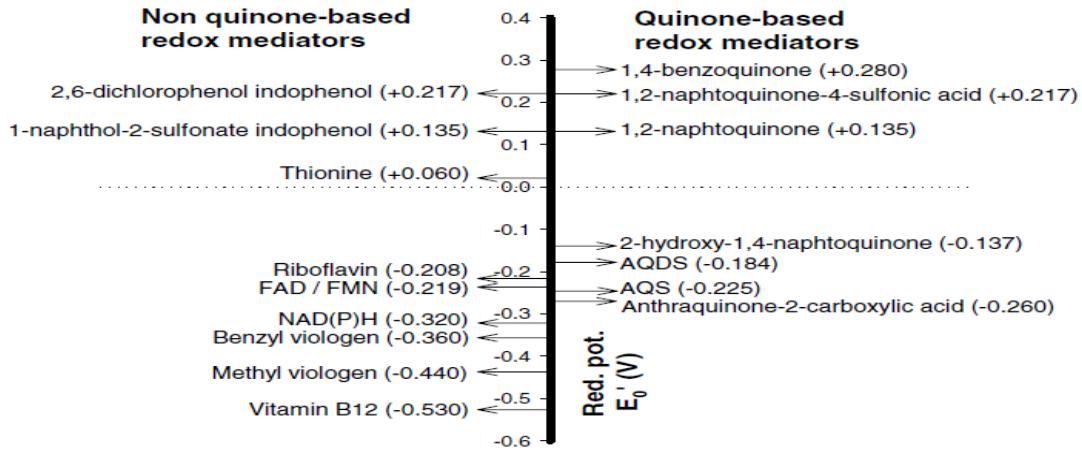

Figure 1.5E'0 values both for quinone-based redox mediators and non-quinone-based redox mediators.

(Santos et al., 2007)

P. kullae K24 was first described to contain oxygen-insensitive flavin free azoreductase. This soil bacterium was isolated by long-term adaptation in the chemostat for growth on Orange I as the sole source of carbon and energy .(Zimmermann et al., 1984). In the presence of specific oxygen-tolerant enzymes **azoreductases**, some aerobic bacteria are able to reduce azo compounds and produce aromatic amines (Stolz, 2001). The aerobic azo reductases are able to use both NAD(P)H and NADH as cofactors and reductively cleave not only the carboxylated growth substrates of the bacteria, but also the sulfonated structural analogues. This type of azoreductase activity was found in *Xenophilus* species strains K22 and KF46. These bacteria cannot utilize azo dye as the growth substrate, and require additional organic carbon sources (Stolz, 2001). Moreover, there are few bacteria that are able to grow on azo compounds as the sole carbon source. These bacteria cleave azo (–N=N–) bonds reductively and utilize amines as the source of carbon and energy for their growth. Such organisms are specific towards their substrate. Examples of bacterial strains with this trait are *Xenophilus azovorans* KF 46 (previously *Pseudomonas* sp. KF46) and *Pigmentiphaga kullae* K24 (previously *Pseudomonas* sp. K24), which can grow aerobically on carboxy orange I and carboxy orange II, respectively (McMullan et al., 2001).

1.5. Factors affecting azo dye degradation

In biological treatment processes, various physicochemical operational parameters, such as the level of agitation, oxygen, temperature, pH, dye structure, dye concentration, supplementation of different carbon and nitrogen sources, electron donor and redox mediator, directly influence the bacterial decolorization performance of azo dyes. Apart from this, availability of NADH is an important limiting factor which will determine the overall rate of dye decolorization. Table 1.4 describes different azo dye degradation studies and analytical methods used to identify the end products of the biodegradation. Most of the biodegradation and decolorization studies analysed their end products by Uv-visible, Fourier transformed Infrared spectroscopy (FTIR), Gas-Chromatography Mass spectroscopy (GC-MS), Liquid-Chromatography Mass spectroscopy (LC-MS), H^1-NMR (Nuclear magnetic resonance) and High pressure liquid chromatography (HPLC).

1.6. Bacterial azoreductases

Azoreductases are the enzymes which catalyze the reductive cleavage of azo bonds to produce colorless aromatic amine products (Chang et al., 2001). They are cytoplasmic enzymes and belong to quinone reductase family. Based on function, azoreductases are categorized as either **flavin-dependent azoreductases** (Nakanishi et al., 2001; Chen et al., 2005) or **flavin-independent azoreductases** (Stolz, 2003). The flavin-dependent azoreductases are further organized into three groups: NADH-preferring flavin reductases (FRD), NADPH-preferring flavin reductases (FRP), and general flavin reductases (FRG). Azoreductases belonging to all three groups (FRD, FRP, and FRG) have been found in bacteria. Azoreductases can broadly be divided into two groups depending on oxygen tolerance. Those from *Enterococcus faecalis* (Chen et al., 2004), *P. kullae* K24 (Stolz, 2003), *Rhodobacter sphaeroides* (Bin, 2004), *X. azovorans* KF46 (Knackmuss and Stolz, 2002), *Bacillus* sp. *OY1-2* (Suzuki et al., 2001), *Escherichia coli* (Nakanishi et al., 2001)and rat liver (Elliott, 1984) have been shown to decolorize azo dyes in the presence of oxygen. Azoreductase from yeast have been shown to possess weak activity under oxic conditions (Liger et al., 2004).However, enzymes from *Pseudomonas luteola* (Chang et al., 2001), rat caecum (Elliott, 1984), etc., work only under anoxic conditions. Oxygen-insensitive azoreductases include monomeric flavin-free enzymes containing a putative NAD(P)H binding motif and the polymeric flavin-dependent enzymes (Chen, 2006).

Genes encoding azoreductase activity have been reported from different genera of bacterial kingdom and they are mainly annotated as *azo* with suffix letters describing its origin (Table.1.5). Gene coding for other biological functions metal or flavin reductase, ACP phosphor diesterase and triphenylmethane reductase are now characterized for

Table 1.4 Analytical methods used to identify the degradation products by various azo dyes degradation studies by pure bacterial cultures or consortia.

(Saratale et al., 2011)

Name of azodye	Name of dye degrader	Analytical techniques used	Identified metabolites
Reactive Orange 16	*Bacillus* sp. ADR	UV–vis, TLC, FTIR and GCMS	6-Nitroso naphthol and dihydroperoxy benzene
Reactive Red 2	*Pseudomonas* sp. SUK1	UV, HPLC, FTIR and GCMS	2-Naphthol
Reactive Green 19A	*Micrococcus glutamicus* NCIM 2168	UV–vis TLC, HPLC, GCMS	Naphthanlene
Navy Blue 2GL	*Bacillus* sp. VUS	UV–vis, HPLC, FTIR and GCMS	4-Amino-3-(2-bromo-4,6-dinitro-phenylazo)-phenol and acetic acid 2-(-acetoxy-ethylamino)-ethyl ester
Direct Brown MR	*Actinobacter calcoaceticus*	UV, TLC, FTIR and GCMS	Biphenyl amine, 2-amino 6-hydroxybenzoic acid and naphthanlene
Scarlet R	Consortium-GR	UV–vis, TLC, HPLC, FTIR and GCMS	1,4-Benzenediamine
Reactive dyes (RP2B, V2RP, Red 22)	*Pseudomonas luteola*	FTIR	Sulfonic acid
Direct Black 22	Bacterial consortium DMC	UV–vis, HPTLC	1-Naphthol
Reactive Violet 5	Bacterial consortium RVM 11.1	UV–vis, HPTLC	ND
Reactive Blue 172	*Pseudomonas aeruginosa* NBAR12	UV–vis, HPTLC	Aromatic amines
Methyl Red	*Vibrio logei* and *Pseudomonas nitroreducens*	^{1}H NMR	2 amino benzoic acid and N-N, dimethyl 1-4-phenylenediamine
Acid Red 88	*Stenotrophomonas* sp., *Pseudomonas* sp., and *Bacillus* sp.	UV, TLC and ^{1}H NMR	6 amino naphthalene sulfonic acid
Reactive Red 22	*Pseudomonas luteola*	HPLC, MS	3-Amino-4-methoxyphenyl-sulfone sulfonic acid ester
Orange II	*Bjerkandera* sp. BOS55	UV, NMR, ESI-MS, HPLC	4 hydroxy benzenesulphonate and 1 diazo 2-naphthol
Sudan azo dyes	Human Intestinal Microflora	HPLC–LCMS	Aniline, 2,4-dimethylaniline, *o*-toluidine, and 4-nitroaniline

their azoreductase activity. There are several examples for differentially annotated genes have shown to code for azoreductase activity (Table. 1.5). For example, gene *acp*D denotes ACP phospho diesterase, however it has been shown to possess more prominent azoreductase activity thus it was subsequently annotated as azoR in *E. coli*.

Based on the primary amino acid sequence the classification of azoreductases is found to be difficult, hence a classification based on the secondary and tertiary structure has been developed (Abraham & John, 2007). In reported classification a web based program Deep View/Swiss Pdb Viewer was used to predict secondary and tertiary structure based on its amino acid sequence and detect structural similarities and

differences between species, wherein azoreductases from six bacterial species [*Rhodobacter sphaeroides* (AY150311), *Bacillus subtilis* (AB071366), *B. anthracis* (AE016879), *B. stearothermophilus* (AB071367), *Bacillus* sp. (AB032601)and *Enterococcus faecalis* (AY422207)] were analyzed for secondary and tertiary protein structures. It was determined that *Enterococcus faecalis* was very distinct and different from the others. The others showed very similar 3D protein structural images indicating that these azoreductase enzymes belonged to the same family.

However based on the structural elucidation studies on *E. coli* AzoR, it acts in a homodimeric state forming the two identical catalytic sites to which both monomers contribute. The structure revealed that each monomer of AzoR has a flavodoxin-like structure, without the explicit overall amino acid sequence homology. Superposition of the structures from the two different crystal forms revealed the conformational change and suggested a mechanism for accommodating substrates of different size. Furthermore, comparison of the active site structure with that of NQO1 complexed with substrates provides clues to the possible substrate-binding mechanism of AzoR (Ito et al., 2006). Similarly, Liu et al. (2007) elucidated FMN bound AzoA from *E. faecalis* showing its overall structure and architecture of the active site was similar to the azo reductase from *E. coli* and human NQO1, there are significant differences in the active site environment implicating different substrate specificities and kinetic properties.

Moreover, substrate specificity of the azoreductase has been studied by using synthetic model substrates based on disodium-(R)-benzyl-azo-2,7-dihydroxy-3,6-disulfonyl-naphthalene (Maier et al., 2004). Chen (2004) reported an aerobic FMN-dependent azoreductase from *Enterococcus faecalis* with broad spectrum specificity and *Pseudomonas aeruginosa* shows oxygen-insensitive azoreductase activity towards several azo dyes (Nachiyar and Rajakumar, 2005).

Table 1.5 Various azoreductase genes involved in dye decolorization by bacteria

Gene	Source organism	Protein characteristics	Reference
*azoR*1	*Pseudomonas. aeruginosa*	Ligand bound crystal structure and role in drug metabolism	Wang et al., 2007
Azo	*Rhodobacter sphaeroides* AS1.1737	18.7 kDa, NADH utilizing oxygen sensitive azoreductase, optimum conditions pH 8.0 and temp. 50°C	Bin, 2004
Azo	*Bacillus subtilis and Geobacillus stearothermophilus*	174amino acids long 18kDa protein, NADP(H)dependent activity.	Sugiura et al., 2006
azoA	*Enterococcus faecalis*	Homodimer with a molecular weight of 43 kDa, probably containing one molecule of FMN per dimer. AzoA required FMN and NADH, but not NADPH. Km values for both NADH and Methyl red substrates were 0.14 and 0.024mM.	Chen et al., 2004
azoB	*Xenophilus azovorans* KF46F	Flavin-free oxygen-tolerant azoreductase with an ordered bireactant reaction mechanism and preference for rather simple monosulfonated mono azo dyes with a hydroxyl-group in orthoposition to the azo bond.	Bürger and Stolz, 2010
azoB	*Pigmentiphaga kullae* K24	22kDa size, flavin-free NADPH preferred azoreductase, The pH and temperature optima are pH 6.0 and between 37 and 45°C.	Chen et al., 2010
azo1 and azoII	*Shigella dysenteriae*	28 kDa (AzoI, homodimer) and 11 kDa (AzoII) FMN dependent FMN NAD(P)H activity at pH 7.0 and 7.2 respectively. Optimum temp. 45°C for both.	Ghosh et al., 1992
Azo	*Bacillus* sp. OY1-2	19kDa protein, NADPH dependent activity and optimum temperature 70°C.	Suzuki et al., 2001

azoC	*Clostridium perfringens*	22.6kDa, Highest activity in presence of NADH and FAD, Optimum pH of 9 and at room temperature, and in an anaerobic environment.	Morrison et al., 2012
Azo	*Bacillus* strain SF	NADH-dependent azoreductase, molecular mass of 61.6 kDa and an isoelectric point at pH 5.3, Optimum pH for activity 8 to 9 and temp. 80°C.	Kandelbauer et al., 2004
*azo*1	*Staphylococcus aureus* ATCC 25923	20kDa NADPH-flavin azoreductase (Azo1), constitutively expressed in *S. aureus* , FMN dependent tetrameric protein	Chen et al., 2005
ppazoR	*Pseudomonas putida* MET94	FMN-dependent homodimer with a molecular mass around 40 kDa NADPH preferred over NADH.	Mendes et al., 2011
ACP Phosphodiesterase Gene (acpD)	*E.coli* JM109	FMN-dependent NADH-azoreductase, 23-kDa, ping-pong mechanism, showed similarity to NAD(P)H:quinone acceptor oxidoreductase	Nakanishi et al., 2001
triphenylmethane reductase gene	*Citrobacter* sp. strain KCTC18061P	Mutational analysis of NADH-binding residues, protein of molecular mass of 30,954 Da and maximal enzyme activity occurred at pH 9.0 and 60°C.	Jang et al., 2007
Fre	*E.coli*	Overexpression of flavin reductase (naturally part of the ribonucleotide reductase complex of *E.coli*) in *E.coli* and *Sphingomonas* sp. strain BN6 under anaerobic conditions.	Rau et al., 2000
putative azoreductase gene	*Shewanella oneidensis*	Putative flavin mononucleotidedependent azoreductase, Response to heavy metal stress.	Mugerfeld et al., 2009

Recently, *E. coli* strains have been characterized for azoreductase (*azoR*) and nitroreductase (NfsA/NfsB) activity and oxygen availability was considered as essential parameter for regulations of these reductases during growth (Mercier et al., 2013).Nonspecific enzymes catalyzing azo bond reduction have been isolated from aerobically grown cultures of *Shigella dysenteriae* (Ghosh et al., 1992), *E. coli* (Nakanishi et al.,2001), *Bacillus* sp. (Maier et al., 2004b), *Staphylococcus aureus* (Chen et al., 2005) and *Pseudomonas aeruginosa* (Nachiyar and Rajkumar, 2005); where characterized, these enzymes have been shown to be flavoproteins as azoreductases.

As nucleotide sequence of azoreductase from various biological systems shows change in the length and sequences, whereas amino acids sequence showed limited homology. To analyze closely, the protein sequences of azoreductases from different organisms were aligned and analyzed by different methods to find out their phylogenetic relationships. With an increase in the number of the completed bacterial genome sequences, it was found that genes encoding putative proteins similar to the protein sequences of NAD(P)H flavin azoreductases and their phylogenetic relationship is depicted in Fig. 1.6.

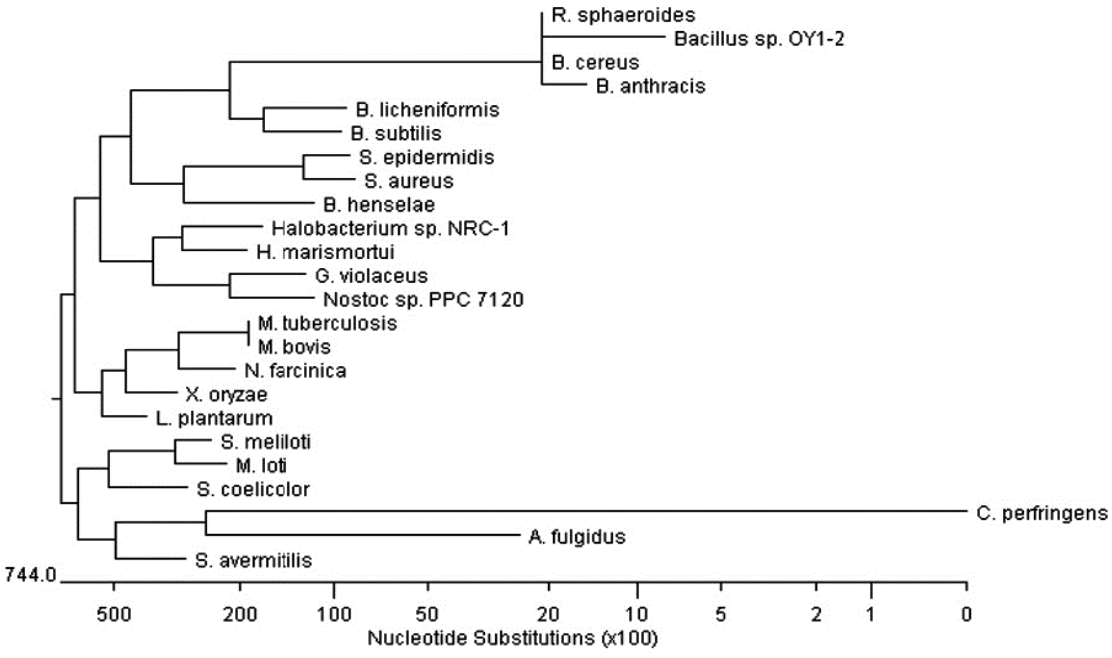

Figure 1.6 Unrooted phylogenetic tree of NADPH-flavin azoreductases.

(Chen, 2006)

Recently, Chen et al. (2010) have reported phylogenetic analysis of azoreductases with the NAD(P)H binding domain information. The tree (Fig. 1.7) shows three distinct groups for the 30 azoreductases or hypothetic azoreductases. The polymeric flavin-dependent enzymes were further divided into two groups, NADPH-dependent and NADH-dependent azoreductases, respectively. The third group contains several monomeric flavin-free NADPH-preferred azoreductases, such as AzoA from strain *P. kullae* K24 (Chen et al., 2010).

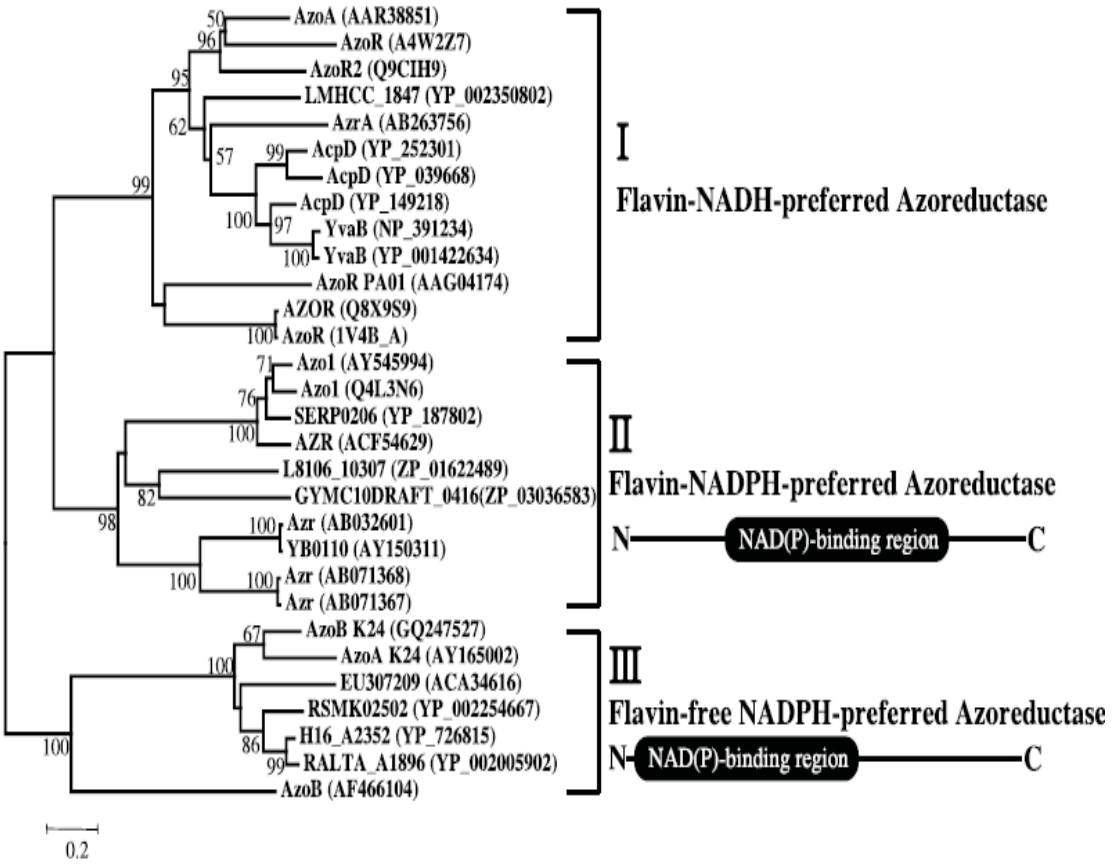

Figure 1.7 Conserved dinucleotide binding domain sequences based grouping ofAzoreductase

Based on codon usage and conserved motif analysis by MEME program, azoreductase from yeast is positioned surprisingly with prokaryotic sequences, mainly *Firmicutes* and *Rhodobacter sphaeroides* and *Bacillus* sp. OY1-2 appear together on the codon usage tree, indicating lateral transfer of this gene (Fig. 1.8) (Bafana and Chakrabarti, 2008a). Similarly, *E. coli* and *Enterococcus feacalis* showed similar lateral gene transfer indications.

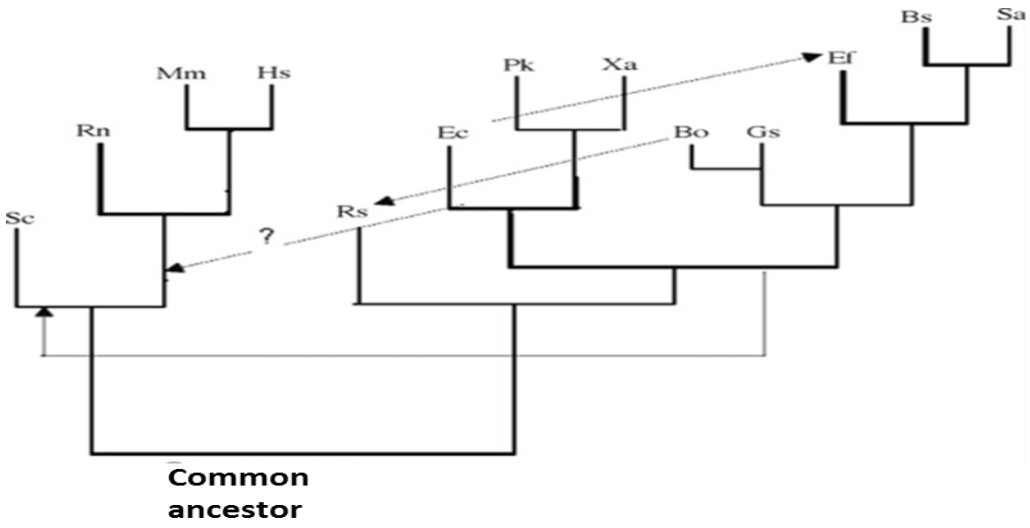

Figure 1.8 Scheme for evolution of azoreductase gene, shown within the frame of SSU rRNA-based phylogeny of organisms.

Solid lines indicate the SSU rRNA-based phylogeny of organisms, while dotted arrows indicate the lateral transfer of azoreductase gene

(Abbreviations: Gs—*G. stearothermophilus*; Bs—*B. subtilis*; Sa—*S. aureus*; Ef—*E. faecalis*; Pk—*P. kullae*; Rs—*R. sphaeroides*; Xa—*X. azovorans*; Bo—*Bacillus* sp. OY1-2; Ec—E. coli; Hs—H. *sapiens* (human); Cp—*C. porcellus* (guinea pig); Mm—*M. musculus* (mouse); Rn—*R. norvegicus* (rat); Sc—*S. cerevisiae* (yeast))

Putative azoreductase gene sequences for which azoreductase activity has been experimentally demonstrated are very few (Table 1.6).Various biochemical properties of azoreductases are summarized in Table 1.7. Azoreductases are found to be monomeric to multimeric forms. They usually are mesophilic for enzyme temperature optima, except azoreductases from *Bacillus* sp. OY 1-2 and SF strains for which enzyme temperature optima was found to be 70 and 80°C. An organism may possess more than one azoreductase enzyme. To function efficiently in dye effluent containing various organic solvents, recently an efficient catalytic and organic solvent-tolerant azoreductase has been reported by Yang et al. (2013a).

Table 1.6 Azoreductase sequences for which azoreductase activity has been experimentally demonstrated.

(Bafana & Chakrabarti, 2008)

Organism	Azoreductase		
	GenBank accession no.	PDB ID	Length (amino acids)
Geobacillus stearothermophilus IFO13737	AB071367		174
Bacillus subtilis ISW1214	AB071368	1nni	174
Staphylococcus aureus	AY545994		188
Enterococcus faecalis ATCC 19433	AY422207		208
Pigmentiphaga kullae K24	AY165002		200
Rhodobacter sphaeroides AS1.1737	AY150311		178
Xenophilus azovorans KF46F	AF466104		281
Bacillus sp. *OY1-2*	AB032601		178
E. coli	BAB35437	1v4b	201
Homo sapiens (Human)	NM_000903	1qbg	274
Cavia porcellus (guinea pig)	Q8CHK7		275
Mus musculus (mouse)	Q64669	1dxq	274
Rattus norvegicus (rat)	P05982	1qrd	274
Saccharomyces cerevisiae (yeast)	Z73183	1t0i	191

1.7. Physiological role of azoreductases

The introduction of azo compounds into the environment is a human activity, thus reduction of azo dyes may not be the primary role of azoreductases. *E. coli* azoreductase encoded by *azo*R is capable of reducing several benzo-, naphtho-, and anthraquinone compounds, which were found to be better substrates for *azoR* than the model azo substrate methyl red (Liu et al., 2009). AQDS was the best substrate for AzoR among the quinones examined, as these quinones have higher *k*cat/*Km* values than methyl red. Quinones are found widely in nature and are metabolites or products of different organisms (Deller et al., 2008). They can participate in deleterious redox cycling, which leads to the accumulation of reactive oxygen species that are deleterious to the cells (Patridge and Ferry, 2006). Liu et al., (2008) expressed *Rhodobacter spheroides* azoreductase AZR gene in *E. coli* and characterized the purified protein as quinone reductase. AZR overexpressing strain showed significantly higher survival rate than the control strain exposed to the oxidative stressors such as H_2O_2 and menadione. Thus azoreductase (AZR) is involved in quinone detoxification and oxidative stress resistance. Quinones can undergo reduction via one electron transfer or two electron transfer leading to either semi-

quinone radicals or hydro-quinone respectively (Fig. 1.9). Semi-quinone radical is readily oxidized back to quinone in the presence of oxygen resulting in generation of superoxide anion, thus generating oxidative stress. Semi reduced quinones lead to depletion of cellular reduced glutathione, resulting in thiol stress. Azoreductases carry out two electron transfer not allowing semiquinone formation thus preventing oxidative stress caused by quinones (Liu et al., 2008).Corroborating this, mutational inactivation of *azoR* was found to impair the growth of *E. coli* cells when exposed to different electrophilic quinones (Liu et al., 2009).

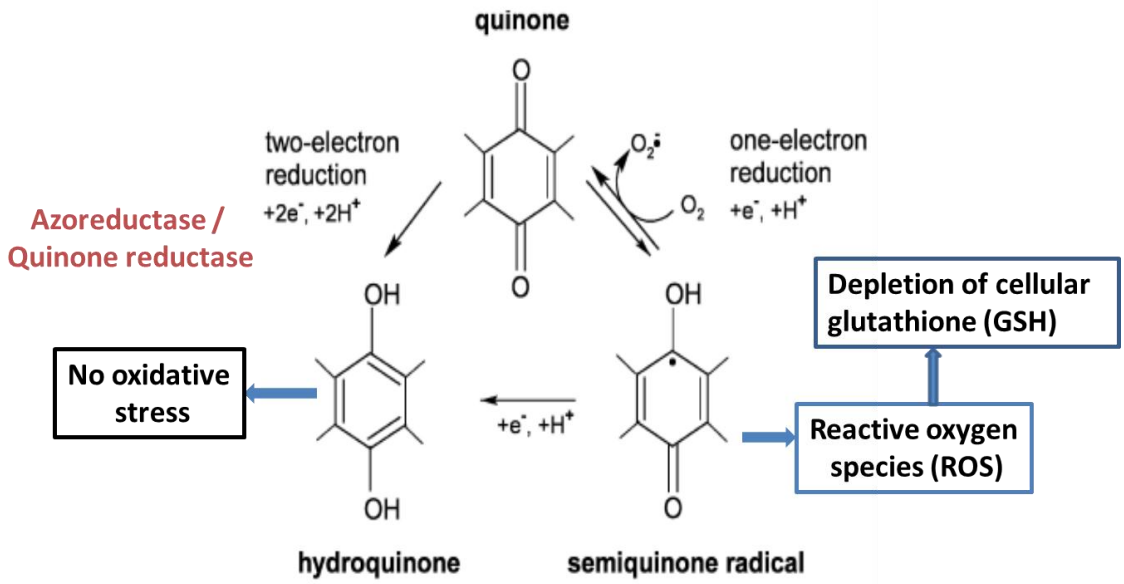

Figure 1.9 Reduction mechanism of quinones.

(Figure was modified from Deller et al. 2008)

Electrophilic quinones can form *S*-adducts through covalent bonds with cellular thiols, lead to depletion of cellular free thiols and causes thiol-specific stress in cells (Liebeke et al., 2008). Glutathione (GSH) is the major low-molecular-weight thiol and can interact with toxic dicarbonyl compounds, such as methylglyoxal and *N*-ethylmaleimide, resulting in the formation of GSH-*S*-adduct as a mechanism for detoxification (GSH-dependent detoxification) (Ferguson et al., 2000; Li et al., 2003). In conclusion, the well-studied azoreductase AzoR is actually a quinone reductase playing a role in protection against thiol-specific stress (Liu et al., 2009). Further, this study demonstrated that the transcription of azoR was induced by different quinones.

A catalytic pocket about 40 to 50 amino acids involved in the binding of substrates and flavin cofactors was found to be conserved in the amino acid sequences of AzoR and other quinone reductases (Ito et al., 2008). Quinone reductases (QRs) from *Bacillus* spp. (YhdA), *Enterococcus faecalis* (AzoA) and *E. coli* (AcpD) possess an amino acid sequence typical for the a flavodoxin-like fold consisting of 5 α-helical layers sandwiching a five-stranded parallel β sheet in the center (Deller et al., 2008).

Table 1.7 Biochemical properties of azoreductases from representative bacteria

Species	**Molecular mass**	**Cofactor**	**Electron donor**	**pH optima**	**Temperature Optima (°C)**
Xenophilus azovorans KF46	30 kDa (Monomer)	NR	NAD(P)H	6.5	45
Pigmentiphaga kullae K24	21 kDa (Monomer)	NR	NAD(P)H	6.2	41
Shigella dysenteriae	28 kDa (AzoI, homodimer) 11 kDa (AzoII)	FMN FMN	NAD(P)H NAD(P)H	7.0 7.2	45 45
Escherichia coli K12	28 kDa (AzoI, homodimer) 12 kDa (AzoII)	FMN FMN	NAD(P)H NAD(P)H	7.0 7.0	45 45
Bacillus sp. OY1-2	19 kDa	NA	NADPH	NA	70
Escherichia coli	46 kDa (Homodimer)	FMN	NADH	NA	NA
Enterobacter agglomerans	28 kDa (Monomer)	NA	NADH	7.0	35
Enterococcus faecalis	46 kDa (Homodimer)	FMN	NADH	6.6-7.0	35-40
Rhodobacter sphaeroides	19 kDa	NA	NADH	8.0	50
Staphylococcus aureus	85 kDa (Homotetramer)	FMN	NADPH	6.0-6.6	35-40
Bacillus sp. strain SF	62 kDa (Monomer)[a]	NA	NADH	8-9	80
Bacillus sp.BTI1	N.A.	FMN	NADPH	Dye specific	35

NR: Not Required, NA: Information not available, [a]: Oxygen sensitive

Different bacterial proteins having quinone reductase possess an adventitious activity and apart from quinones, non-cognate substrates were shown to be accepted. Matin and coworkers (Gonzalez et al., 2005) demonstrated quinones are physiologically relevant substrates for chromate reductase (ChrR) with an involvement of the enzyme in the oxygen stress response.

1.8. Cloning and mutagenesis of azo dye decolorization genetic determinants

The gene encoding the FMN-dependent NADH azoreductase AzrG from thermophilic *Geobacillus stearothermophilus* was cloned and overexpressed in *E. coli*; the purified enzyme efficiently decolorizes methyl red at 30°C and exhibits a wide-range of degrading activities for different recalcitrant azo dyes, e.g. Acid Red 88, Orange I and Congo Red (Sugiura et al., 2006). An *E. coli* strain co-expressing the genes *ppazoR* (azoreductase from *P. putida* MET94) and *cotA* (encoding laccase enzyme from *Bacillus subtilis*, which does not require redox mediators for decoloration) was generated in which the sequential action of the PpAzoR and CotA enzymes could be fine-tuned by the presence or absence of oxygen. The resulting genetically engineered *E. coli* strain LOM529 significantly decolorized and detoxified the three model wastewaters tested. The decolorization and detoxification property of the strain was considered as cumulative effects of host strains and overexpressed proteins (Mendes et al. 2011). A *Bacillus* sp. mutant obtained by random mutagenesis lead to increase in the decolorization of congo red. As compared with the wild type which decolorized 1000ppm dye, the mutant showed decolorization up to 3000 ppm along with the reduction in the incubation time and enhanced growth parameters (Gopinath e t al. 2009). Cytoplasmic azoreductase (AzoA) from *Enterococcus faecalis* was expressed in *E. coli*, and AzoA-expressing cells showed enhanced rate of methyl red, ponceau BS and orange II reduction, with increase of 2- to 4-fold compared to non-induced cells (Chen et al., 2004). The azoreductase gene from *B. latrosporus* RRK1 was cloned into *E. coli* DH5α, and the resulting recombinant strain *E. coli* SS125 was able to decolorize remazol red, while the original host strain had no color removal activity (Sandhya et al., 2008). Azoreductase gene from *Rhodobacter sphaeroides* was expressed in *E. coli* JM109, and the recombinant strain was tested in anaerobic sequential batch reactors. The decoloration kinetics of acid red GR in the presence of recombinant strains was found to be faster as compared to the vector control strain

(Liu et al., 2007). The advantage of utilizing whole cells include improved enzymatic activity towards the degradation of azo dyes with the overcome of costs associated with enzyme purification and cofactor addition.

1.9. Recent advances and challenges in biotechnological applications of microorganism for dye decolorization/degradation

Efficient treatment of textile wastewater containing various azo dyes has become an important challenge over the past few decades, and until now there are no viable end point solutions to the effluent treatment for the removal of color of the dye and toxic compounds as well. Although biological treatment of colored effluents is recognized to be ecofriendly and economically attractive alternative to the conventional treatment methods, it encounters continuous different issues towards the effective decolorization and detoxification process. In today's scenario dye mineralization along with decolorization is the most essential need of any dye bioremediation strategies. As both the processes may be supported by different oxygen levels and may require the application of different groups of microorganisms, recently research has been focused on the combination of anaerobic-aerobic alternate processes such as combined two stage anaerobic–aerobic system and advanced oxidation process (AOPs) (Saratale et al. 2011, Solís et al., 2012). The use of microbial fuel cells (MFCs) to mineralize dyes and produce energy is explored in high interest as it could be solution to energy catastrophe (Solís et al., 2012).

Other primary challenge in azo dye bioremediation is the repertoire of azo dye structures for the finer color differences with higher stability and surface interactions. More than 100,000 commercial dyes exist of which azo dyes account for more than few thousand. Thus degradation and decolorization machineries of the biological systems constantly come across the modified dye structures and they need to evolve diverse structures to be able to recognize and act on the novel azo dyes. There is a clear correlation between structure, cofactor requirement, and substrate specificity in azoreductases. Structural characteristics at active site determine the spectrum of substrates enzyme can catalyze. Based on the earlier studies by Blumel and Stolz (2003) it was shown that AzoB is only able to degrade Orange I. Similarly other monomeric flavin-free azoreductases have showed very narrow substrate specificity (Chen et al., 2010). On the other hand, polymeric flavin-dependent azoreductase

families could act on a broad substrate spectrum (both chemical nature and size) (Chen, 2004). Dimeric AzoA from *E. faecalis* has two separate active sites located at the interfaces between the two monomers, and FMN lies inside each active site, creating room for different substrates (Liu et al., 2007). Thus, this enzyme is not only able to decolorize methyl red, but is also able to convert sulfonated azo dyes Orange II, Amaranth, Ponceau BS, and Ponceau S. AzoB has a relatively small substrate binding site, which simultaneously accepts both the nicotinamide ring of NADPH and the substrate in the catalytic cycle. Moreover, monomeric azoreductases demands for successful direct hydride transfer between the two substrates which requires a more sophisticated binding mode, thus reduces the number of substrates catalyzed. Thus, enzyme characteristics of the bacterial consortium or bioremediation strains are important factors which need to be taken into the consideration.

Azoreductases catalyzing the reductive cleavage of azo bond of the dye carry out two electron transfers at a time collectively which requires reduction power from redox equivalents (NAD(P)H or $FADH_2$). These enzymes also compete with other cellular oxidoreductases for NAD(P)H in cytosolic soup based on their affinities. In any physiological state a fixed pool of reducing equivalents is available in cytoplasm and its oscillations are driven by metabolism and environmental conditions. Various systems have been developed by conjugating azoreductase (azo dye decolorization) and NADH reductase (leuco dye decolorization) and with a reducing equivalent regenerative enzymes such as glucose dehydrogenase (Yang et al., 2013b) and formate dehydrogenase (Bozic et al., 2010). However these systems are *in vitro* constituted dual enzyme preparations which are externally supplied with the respective electron donor such as glucose or formate. At same time development of whole cell *in vivo* systems with coupled enzyme expression need to be validated for their functionality for azo dye decolorization. Heterologous overexpression of azoreductase in *E. coli* host systems has been shown to enhance the azo dye reductions, however decolorization was found to be limited.

Feng et al. (2010) provided the evidence for significantly enhancing reduction of azo dyes in *E. coli* by intact cells expressing cytoplasmic azoreductase (AzoA) of *Enterococcus faecalis* externally supplied with NADH, as azoreductases have high Km values for NADH as compared to the NADH peroxidase and other

NADH:quinone reductase systems, thus limiting the overall rate of dye decolorization. To overcome this problem, a plausible strategy may be to increase in the overall NADH pool inside the cell by NADH regeneration system.

1.10. Rationale

Current literature on the dye decolorizing/degrading microorganisms mainly describes the isolation of different microbial systems and characterization of their dye decolorizing phenotype. Thus a vast amount of information exists about bacterial strains that are effective for particular dye removal. However there is void in terms of the knowledge on dye decolorization and degradation vis-à-vis microbial physiology and diversity. So far, most of the studies have been focused upon the direct enrichment process for azo dye decolorizing acclimatized bacterial strains or consortia. However, a systematic approach with media composition, incubation conditions and nature of the environment sample is needed to develop a strategic approach to enrichment process. The niche specificity to the azo dye decolorizing bacterial populations is not clearly understood. Continuous need to isolate newer potential strains and genes is essential for the construction of an efficient bioremediation strain/consortium.

Cloning of azoreductase for azo dye decolorization by overexpression studies has been largely done in standard strains such as *E. coli* however there are no reports on the heterologous expression studies in other host strains. *Pseudomonas* spp. have been extensively characterized for the biodegradation of aromatic compounds and azo dyes however no study was done to increase its ability to decolorize azo dyes. Azoreductase being cofactor dependent enzyme, may face limitation of cofactor for efficient dye decolorization. So far no work has been done on this aspect.

Azoreductases are found and well characterized from prokaryotic to eukaryotic kingdoms. There are different research studies on the overexpression of azoreductases from different microbial systems, however very few studies have been focused on the physiological role of the azoreductase in bacteria. Till date only one direct knock out study has been reported with respect to the *azoR* from *E. coli*, showing AzoR associated with thiol stress responses and oxidative stress management. There is a lacuna of knowledge on the basic native physiological role of azoreductases in other bacterial systems.

The present work was aimed at the enrichment of azo-dye decolorizing microbial consortia from various dye contaminated and pristine environment and their community fingerprinting. Reactive violet 5R (RV5R) was used as model azo dye for all the decolorization and degradation due to its complex structure having sulphonated one benzene and one naphthalene ring attached by mono azo bond (Table 1.1), additionally Cu forms a coordinate with dye electron donating moieties. Also it was found that RV5R color properties were not modified due to pH differences. Further work was focused on the isolation of dye decolorizing strains, cloning of *azoA* gene from an efficient strain in to various hosts and studying role of azoreductase in bacterial physiology. The importance of reducing equivalents for efficient dye decolorization was studied by constructing NADH regeneration system.

1.11. Objectives

1. Bacterial diversity and biodecolorization studies of Reactive violet 5R (RV5R) decolorizing microbial consortia

a) **Enrichment and maintenance of RV5R decolorizing microbial consortia from contaminated and pristine niches.**
b) **Study of azo dye decolorization/degradation characteristics of the consortia and their diversity by culture dependent and independent methods.**
c) **Characterization of pure cultures from the consortia for dye decolorization characteristics**

2. Azoreductase (*azoA*) from *Enterococcus* sp. L2: cloning, heterologous expression and physiological role.

a) **RV5R decolorization by *azoA* over-expressing bacterial transformants**
b) **Construction and characterization of *azoA* knockout**

3. Metabolic engineering for efficient azo dye decolorization by NADH regeneration system.

a) **Cloning and heterologous expression of NAD^+ dependent formate dehydrogenase (*fdh)* gene in broad host range expression systems**
b) **Study of azo dye decolorization of *fdh* over-expressing strains**

2 MATERIALS AND METHODS

2.1. Bacterial strains and plasmids used in this study

Laboratory isolates and standard strains of bacteria used in this study are listed in Table 2.1. *P. fluorescens* PfO-1 was generous gift from Dr. M. Silby, Center for Adaptation Genetics and Drug Resistance, Department of Molecular Biology and Microbiology, Tufts University School of Medicine. All the cultures were maintained in Luria Bertani (LB) medium.

Plasmids used in this study are listed in Table 2.2. The plasmid vector pBBR1MCS-2 was obtained from Dr. M.Kovach, Department of Microbiology and Immunology, Louisiana State University Medical Center-Shreveport, Shreveport, LA 71130-3932, USA. pBBR1MCS-2 myc*fdh* clone with pT7 at *Spe*I site in opposite orientation to p*lac* was generous gift fromDr. S. Bringer-Meyer, Institut für Biotechnologie 1, Forschungszentrum Jülich GmbH, Germany. pMGS 100 was generous gift from Dr. S. Fujimoto, Department of Microbiology, School of Medicine, Gunma University, Japan.pBS KS(+) is a high copy number (*E. coli*) generalized cloning vector having blue-white selection strategy for screening of putative clone (Fig. 2.1). pJET1.2 is a blunt end cloning vector having self-ligation inhibitory suicidal strategy from Fermentas, Canada make, which allows only transformants with ligated products to survive (Fig. 2.2). pBBR1MCS2 is a broad host range gram negative expression vector having kanamycin resistance gene, blue-white selection and p*lac* driven expression assembly (Fig. 2.3). pMGS100 is a *Enterococcus-E. coli* shuttle vector having p*bac*A along with the Ribosomal bindng site (RBS) to drive the constitutive expression in *Enterococcus* host (Fig. 2.4). pTEX5501ts has a temperature sensitive mode of replication containing counter selection of chloramphenicol and gentamycin antibiotic resistance marker genes for knock-out construction in *Enterococcus*spp.(Fig. 2.5).

Table 2.1 Bacterial strains used in the study

BacterialStrains	**Remarks**	**Usedas**	**Source**
Escherichia coli DH5α	Standard strain	Host for expression of *azoA* and *fdh*	Sambrook et al. 2001
Escherichia coli BL21	Standard strain	Host for expression of *azoA* and *fdh*	Sambrook et al. 2001
Pseudomonas fluorescens PfO-1	Standard strain	Host for expression of *azoA* and *fdh*	Kim et al., 2009
Citrobacter sp. A3	RV5R decolorizing	Host for expression of *azoA* and *fdh*	This study
Providencia sp.C1	RV5R decolorizing	Host for expression of *azoA* and *fdh*	This study
Klebsiella sp.E2	RV5R decolorizing	Host for expression of *azoA* and *fdh*	This study
Providencia sp. G1	RV5R decolorizing	Host for expression of *azoA* and *fdh*	This study
Klebsiella sp. K1	RV5R decolorizing	Host for expression of *azoA* and *fdh*	This study
Acinetobacter sp. L1	RV5R decolorizing	Host for expression of *azoA* and *fdh*	This study
Enterococcus sp. L2	RV5R decolorizing	Cloning of *azoA*, as host for expression of *azoA* and *fdh*, construction of Δ*azoA* mutant	This study

Table 2.2 Plasmids used in this study

Plasmid	Characteristics	Source/Reference	Map
pBS KS(+)	*E. coli* cloning vector, Amp^r	Sambrook et al. 2001	Fig. 2.1
pJET1.2	*E. coli* cloning vector, Amp^r	Fermentas, Canada	Fig. 2.2
pBBR1MCS2	Broad host range gram negative expression vector, Kan^r	Kovach et al. 1995	Fig. 2.3
pBBR1MCS2 myc*fdh*	pBBR1MCS2 carrying *Mycobacterium vaccaefdh* under p*T7* promoter, Kan^r	Ernst et al., 2005	Fig. 2.8 (pT7 myc*fdh* fragment)
pMGS100	*E. coli-Enterococcus* shuttle vector, Cm^r	Fujimoto, 2001	Fig. 2.4
pTEX5501ts	Temperature sensitive plasmid for knock out construction in *Enterococcus*, Cm^r, Gen^r	Nallapareddy et al., 2006	Fig. 2.5
pBBR1MCS2*azoA*	pBBR1MCS2 carrying *Enterococcus* sp. L2 *azoA* under p*lac* promoter	This study	Fig. 2.7
pMGS100*azoA*	pMGS100 carrying *Enterococcus* sp. L2 *azoA* under p*bac* promoter	This study	Fig. 2.12
pBBR1MCS2*fdh*	pBBR1MCS2 carrying *Mycobacteriumvaccaefdh* under p*lac* and p*T7* promoters	This study	Fig. 2.9
pBBR1MCS2*fdh-azoA*	pBBR1MCS2 carrying *fdh and azoA* under p*lac* and p*T7* promoters (transcription fusion)		Fig. 2.10
pMGS100*fdh*	pMGS100 carrying *fdh* under p*bac* promoter	This study	Fig. 2.11
pTEX5501ts updown*azoA*	pTEX5501ts carrying up and down region of *azoA* gene	This study	Fig. 2.14

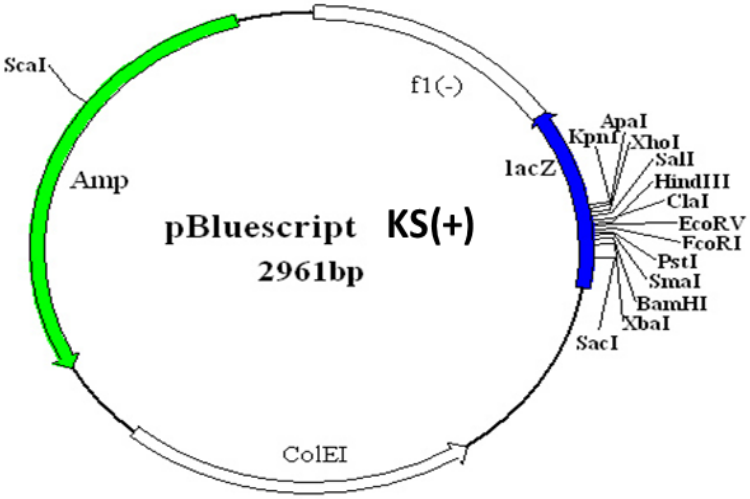

Figure 2.1Feature map of pBS KS(+)

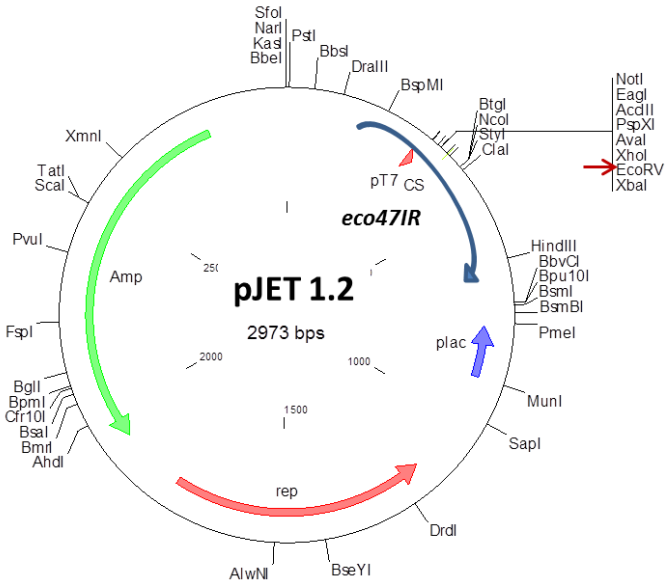

CS- Blunt end Cloning site

Figure 2.2Feature map of pJET1.2

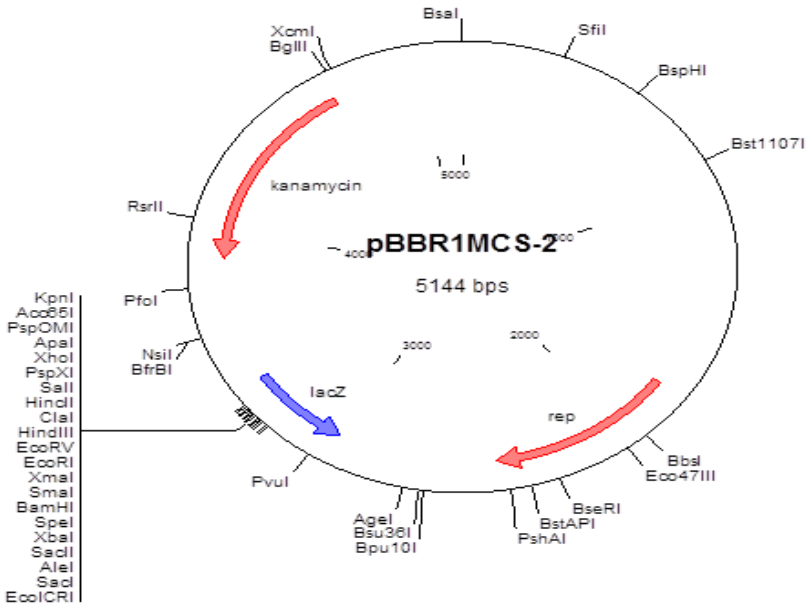

Figure 2.3Feature map of pBBR1MCS-2

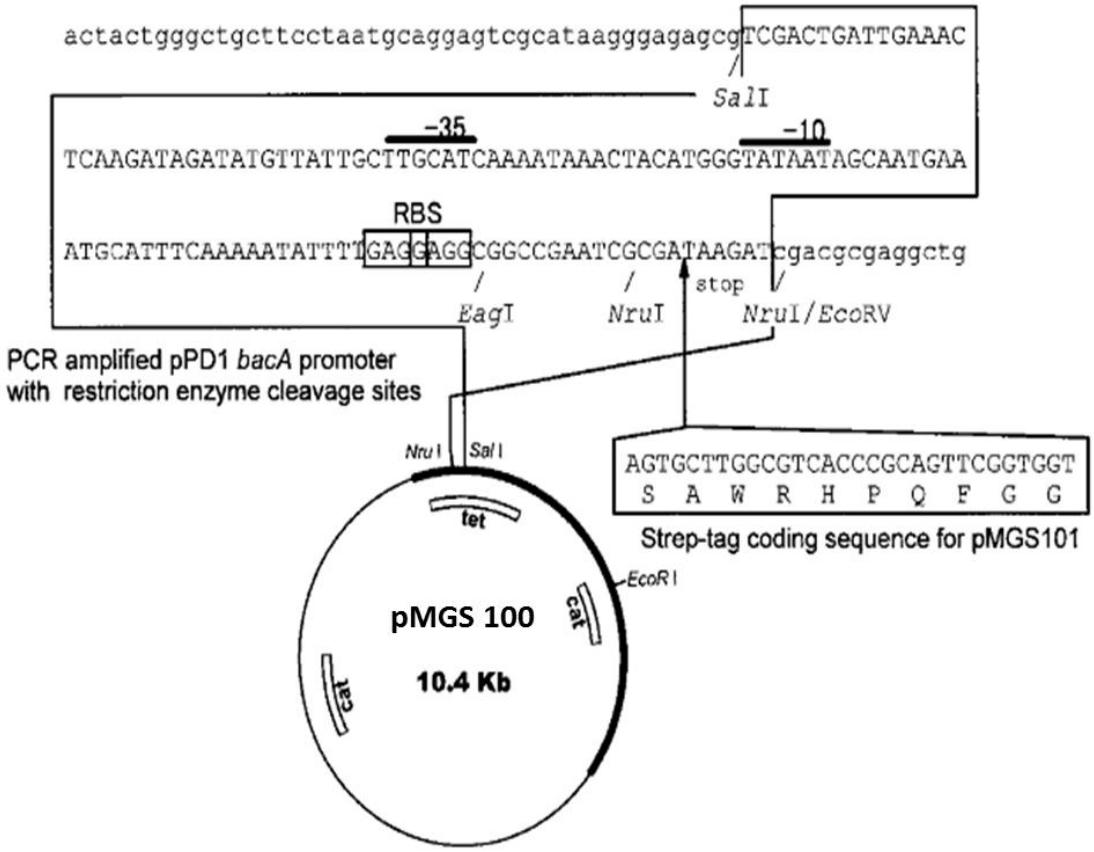

Figure 2.4Feature map of pMGS100

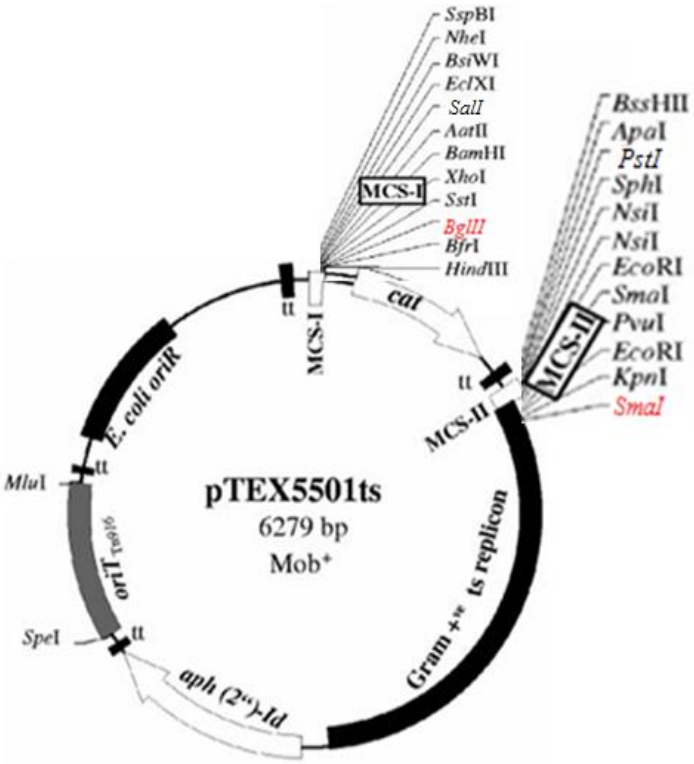

Figure 2.5 Feature map of pTEX5501ts

2.2. Enrichment and development of RV5R decolorizing microbial consortia

Enrichment of Reactive violet 5R decolorizing and degrading microbial communities was carried out by acclimatization through continuous sub-culturing method. Different media compositions and incubation conditions were applied to each environmental sample. All the samples were initially inoculated andpassaged in different media, however only certain combinations ofsamples and media which showed efficient and stable RV5R decolorization were further sub-cultured and maintained.

Samples of soil, sand, water and effluents from pristine and contaminated areas located at different geographic regions of Gujarat, India (Table 2.3,Fig. 2.6), were collected in sterile containers and processed within 24h for enrichment in the laboratory. Marine samples were from coastal areas of western India located near Bhavanagar, Gujarat and were considered as pristine samples as the probability of exposure to dye was low. Hydrocarbon contaminated soil sample was taken from area surrounding petroleum refinery, Vadodara, Gujarat; aeration tank sample was from a common effluent treatment plant, Green Environment Ltd. and effluent sample was from Meghmani Dyes and Intermediates Pvt. Ltd. (dye manufacture industry),

situated at Vatva, Gujarat; petroleum industry effluent sample was from petroleum refinery, Vadodara, Gujarat; and sample from canal for disposal of treated industrial effluent was collected at Amalakhadi, Gujarat. The GIDCaeration tank sample from Green Environment Ltd. Vatva, Ahmedabad, receives the treated industrial effluents from Naroda, Vatva and Odhav industrial estates. Amlakhadi canal effluent sample was collected at (N21038′, E72053′) in the province of Ankleshwar, receives the treated industrial effluents from Ankleshwar, Panoli and Jagadia industrial estates which constitute the major petro-chemical, dye and paint industries.

The ready-made Bushnell Haas Medium (BHM) [Composition (g/L): $MgSO_4$, 0.2; K_2HPO_4, 1.0; $CaCl_2$, 0.02; $FeCl_3$, 0.05; NH_4NO_3, 1.0] and media additives used in this study were from HiMedia Laboratories, India. RV5R was obtained from Meghmani Dyes and Intermediates Pvt. Ltd, GIDC Vatva, Ahmedabad, India. Samples were suspended or diluted in phosphate buffered saline (PBS; 8 g NaCl, 0.2 g KCl, 1.44 g Na_2HPO_4, 0.25 g KH_2PO_4 for 1000 ml, pH 7.4) at 10% w/v or 10% v/v, mixed thoroughly and resulting suspension was used as inocula (5%v/v) in to the different media and incubated under static or shaking (80 rpm) conditions at 30°C. Considering the sample location, following different media were used for acclimatizing the dye decolorizing consortia: Medium A: BHM with glucose (0.5% w/v) and yeast extract (0.5% w/v); Medium B: BHM with glycerol (0.5% v/v) and yeast extract (0.5% w/v); Medium C: Peptone 2 % w/v, K_2HPO_4 0.15% w/v, $MgS0_4$ 0.15% w/v, glycerol 1% (v/v) and Medium D: Tryptone 1.5% w/v, Soya peptone 0.5% w/v, NaCl 0.5 % w/v. All the media were amended with filter sterilized RV5R solution to give a final concentration of 100 mg/L. Visual colour change of the medium from violet to colorless was used as an indication of dye decolorization. After decolorization was obtained, the enrichment culture was re-inoculated (5% v/v) in to fresh medium and in this manner several successive passages were given.

Various azo dyes used in this study are listed in Table 2.4.

Table 2.3 Locations and characteristics of sampling sites for enrichment of RV5R decolorizing microbial consortia

Serial no.	**Sampling location**	**Sample type**	**Probability of exposure to azodye**
1	Bhavnagar, India	Marine water	Low
2	Bhavnagar, India	Marine sand	Low
3	Bhavnagar, India	Marine intertidal zone sand	Low
4	Bhavnagar, India	Marine beach sand	Low
5	Vadodara, India	Hydrocarbon contaminated soil	Low
6	Vadodara, India	Petroleum industry effluent	Low
7	Gujarat ….. (GIDC), Vatva, Ahmedabad, India	Aeration tank effluent, Green Environment Ltd.	High (Colored sample)
8	GIDC, Vatva, Ahmedabad, India	Dye industry effluent, Meghmani Dyes and Intermediates Pvt. Ltd	High (Colored sample)
9	Amalakhadi effluent Canal, Ankleshwar, India	Treated effluent from various industries	High (Colored sample)

1- Marine samples from Bhavnagar
2- Dye contaminated soil and effluent samples from Vatva (GIDC)
3- Hydrocarbon and petroleum contaminated samples , Vadodara
4- Amalakhadi effluent canal samples, Ankleshwar
***Blue line indicate the industrial golden corridor of Gujarat, India**

Figure 2.6Sampling sites located on the geographic map of Gujarat, India.

Table 2.4Different azo dyes used in this study, their structures and absorption maxima (λ_{max})

AZO DYE	Structure	λ_{max}
Reactive violet 5R	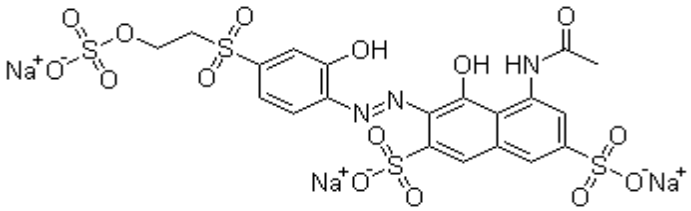	558nm
Reactive Red 97 (Acid)	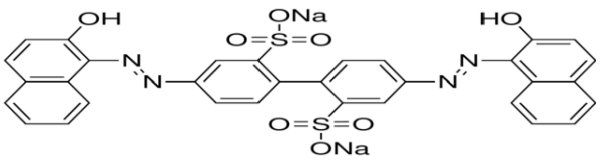	495nm
Acid red 119	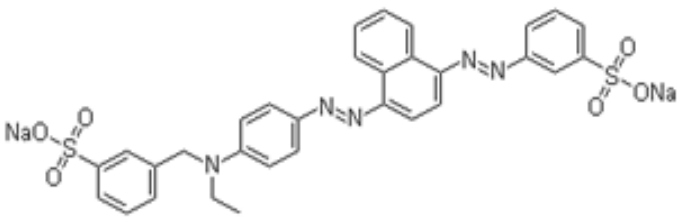	530nm

Reactive Blue 3R	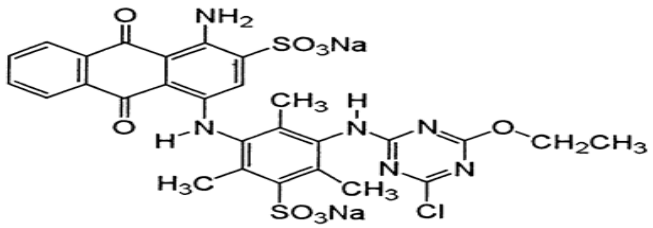	572nm
Reactive Orange 122	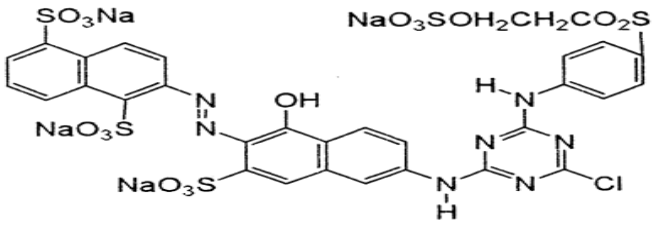	490nm
Reactive Blue 222	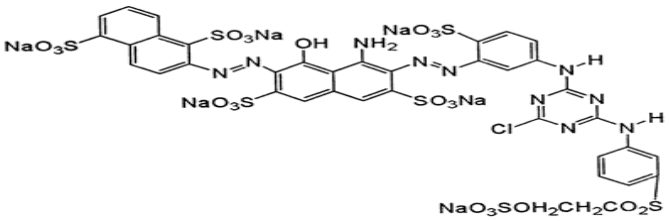	614nm
Mordant Blue 13	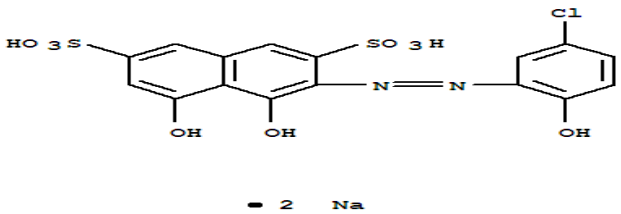	528nm
Reactive Yellow 186	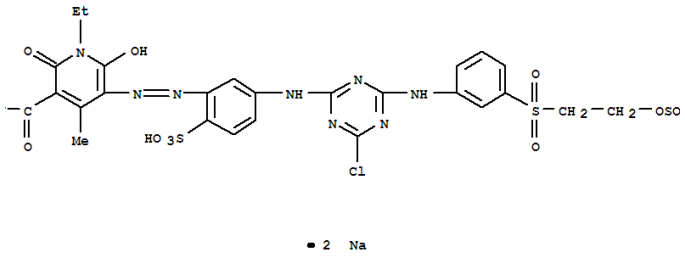	428nm
Reactive red 195	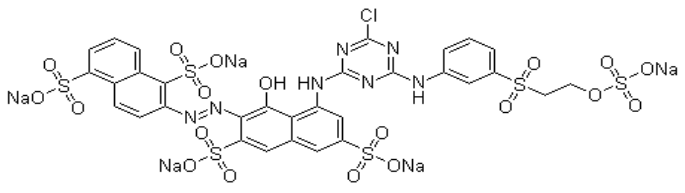	535nm

Reactive Black B5	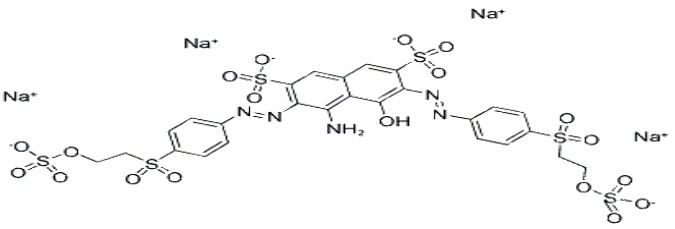	598nm

2.3. Azo dye decolorization

Aliquots (1ml) were withdrawn from the bacterial suspensions and centrifuged at 14,000 *g* for 10 min to separate the bacterial cell mass. Absorbance of the supernatant was measured at the absorbance maximum wavelength for the RV5R (λ max = 558nm) using Spectronic 20D+ (Thermo Scientific. USA) and percentage decolorization was calculated using the equation,

Decolorization (%) = [O.D. at time (t_0) - O.D. at time (t_1)] /O.D. at time (t_0) * 100

Besides RV5R, other azo dyes shown in Table 2.2 were also used for the decolorization studies and Decolorization (%) was calculated as above using the absorbance measurements at the corresponding λ_{max}.

To study the effect of heterologous expression onRV5R decolorization, transformants harbouring expression plasmids were grown in LB containing 100 mg/L RV5R along with appropriate antibiotic. IPTG (1mM) induction was given at the mid log phase culture (0.4 O.D). After different time intervals (0, 12, 24, 36h) aliquots were taken to analyzed decolorization (%) as per the mentioned protocol above.

2.4. Extraction of community DNA from RV5R decolorizing microbial consortia

Total community DNA was isolated from enriched microbial consortia by modified method of Zhou et al., (1996). The cells were harvested from 2 ml of the culture by centrifugation at14,000 *g* rpm, 4°C for 10 min. Resulting pellet was resuspended in TE25S buffer(25mM Tris-HCl pH 8.0, 25 mM EDTA pH 8.0, 0.3 M sucrose) to which 7µL lysozyme solution (100mg/ml) was added and incubated at 37°C for 1h. Sodium Dodecyl Sulphate (SDS) and proteinase K were added to it at final concentrations of 0.5% and 0.1 mg/ ml respectively, followed by incubation at 55°C for 1h. To the lysed cell solution, 0.2 volumes of 5M NaCl were added followed by

0.1 volume of 10% cetyltrimethylammonium bromide (CTAB) in 0.7M NaCl for 10min at 55°C. Resulting gelatinous mass was further treated with equal volume of chloroform: iso-amyl alcohol (24:1) for 30 min. Aqueous phase was transferred to fresh tube and 0.6 volume of isopropanol was added and centrifuged at at14,000 *g*, 4°C for 10 min. Resulting DNA pellet was washed twice with 70% ethanol and dissolved in 50 µl TE buffer (10 mMTris-HCl pH8.0, 1 mM EDTA).

2.5. PCR primers and protocols

The PCR technique has been used in this study for several applications such as PCR-DGGE, ARDRA and gene cloning using different primers mentioned in Table 2.5. Basic PCR reaction mixture for most of the PCR protocols is mentioned below in Table 2.6 and the PCR programs for the various genes are mentioned in appendices.

Table 2.5 PCR primers utilized in this study

Primer name	Gene target	Sequence detail (5'→3')
27F	Eubacterial 16S rRNA gene/fragment for ARDRA and sequencing	GAG AGT TTG ATC CTG GCT CAG
1107R		GCT CGT TGC GGG ACT TAA CC
1541R		AAG GAG GTG ATC CAG CCG C
GC-341F	Eubacterial 16S rRNA gene fragment (V3 region) for DGGE	CGC CCG CCG CGC CCC GCG CCC GGC CCG CCG CCC CCG CCC CCC TACGGG AGG CAG CAG
534R		ATT ACC GCG GCT GCT GGG
azoA F	*azoA* gene of *Enterococcus* spp.	GTA **AGG AGG** TAC ACA ATG TCA AAA TTA TTA GTT G
azoA R		CTT AGA ATG TTT TCA CGT ATT CAG TTG C
azoA ATG F		ATG TCA AAA TTA TTA GTT G
up *azoA* F	Up region of *azoA* of *Enterococcus* spp.	TAT AGT CGA CGA AAT TCG TCC TCC TCA TCA TGC GC
Up *azoA* R		ATA TAG ATC TCG CTT AAT GTT TCA AAT GCT GCG CC
Down *azoA* F	*Down* region of *azoA Enterococcus* spp.	TAT ACT GCA GGG ACC AAA ACC TCT AAC AAG TGG
Down *azoA* R		ATA TCC CGG GTC ACG TGT CTG GAG TAT TAT CGG

*fdh*F	NAD^+-Formate dehydrogenase of *Mycobacterium vaccae* N10	ATG CA A GGA GAT GGC GCC CAA CAG TC
fdhR		TAC CTT CGG ATC CTC AGA CCG CCT TCT TGA
Myc*fdh* F		ATA T**GG TAC C**AT GCA AGG AGA TGG CGC CCA ACA GTC
Myc*fdh* R		TAT A**GG TAC C**TT CGG ATC CTC AGA CCG CCTT CTT GA
MGS100 *fdh* F		ATG GCA AAG GTC CTG TGC GTT CTT TAC G
Chlr F	Chloramphenicol resistance gene of pTEX5501ts, used for screening of disruptant mutants	AAT GGT TCG GGG AAA TTG TTT CCC
Chlr R		GTC ATT AGG CCT ATC TGA CAA TTC CT
Gen F	Gentamycin resistance gene of pTEX5501ts, used for screening of disruptant mutants	AGA TAG GTT ATG CAA GAT TTT TAT ATG
Gen R		ATT CCG GAT TCT AAA AAA GGA TTG CTA

Nucleotides in bold underlined are RBS site (Nucleotides in bold are RE sites for KpnI)

Table 2.6 Basic PCR reaction mixture composition

Components	Amount per reaction	Volume (µl)
Taq or *Pfu*Buffer (15mM $MgCl_2$) (10X)	1x	2.0
dNTPs	2.5mM each	0.5
Forward Primer	5 pmole	2.0
Reverse primer	5 pmole	2.0
DNA Template	50-80 ng	0.5-2.0
Taq DNA Polymerase or *Pfu*polymerase	5U	0.3
Nuclease free deionized water	-	To make up volume to 20

2.6. Amplified ribosomal DNA restriction digestion analysis (ARDRA) of RV5R decolorizing microbial consortia

PCR amplification of 16S rRNA gene fragments was carried out using community DNA extracted from the acclimatized dye decolorizing consortia as template. PCR was performed in 50µl reaction mixtures consisting of template DNA (50-200ng), 0.3µM of each of the primers (27F and 1541R, Table 2.5), 1µL of 2.5mM dNTPs each, 1.5U of *Taq* polymerase and 5 µL 10X *Taq* polymerase buffer. The universal eubacterial16S rRNA primers were expected to give an amplicon of approximately 1.5kb (Pillai and Archana, 2008). The reactions were carried out in Applied Biosystems (USA) master cycler with a touchdown program shown in Appendix A. PCR products were analysed on 0.7% agarose gel and quantified using Nano spectrophotometer (Inkarp, U.S.A). ARDRA was performed by digesting the PCR products with the restriction enzymes HaeIII and HinfI. The digested samples were electrophoresed on 2.5% agarose gels and visualised by ethidium bromide staining under UV. ARDRA profiles were manually analyzed, binary data for presence or absence of bands were computed and the dendrogram was plotted using NTSys software (Exeter software, NY) with UPGMA method (Patel et al., 2010a).

2.7. PCR- Denaturing gradient gel electrophoresis (DGGE) of 16S rRNA gene fragments

For DGGE, PCR amplification of 16S rRNA gene was performed in 50µl reaction mixtures with consortial community DNA as template. Primer GC-341F with GC clampand 534Rwere used for targeting the V3 region of 16S rRNA gene of eubacteria (Muyzer et al.,1993, Chaturvedi and Archana, 2012). The PCR reaction mixture consisted of template DNA (50-200ng), 0.3µM of each of the primers, 1µl of 2.5mMdNTPs each, 1.5U of *Taq* polymerase and 5µL of 10X *Taq* polymerase buffer. The reactions were carried out in Applied Biosystems(USA) master cycler with PCR cycling conditions shown in Appendix B. PCR products (of ~200bp) were quantified using Nano spectrophotometer (Inkarp, U.S.A) and analysed on 2% agarose gel and. About 300 ng of PCR products were loaded on denaturing polyacrylamide gels to explore relative diversity in acclimatized consortia. DGGE was performed using the Dcode universal mutation detection system (BioRad Laboratories, Hercules, USA) with a denaturing gradient of 40-60% where in 100% denaturant solution consisted of

7M urea, 40 % formamide in 10% acrylamide/bis-acrylamide (37.5:1) and 1.0× TAE buffer (pH 8.0) prepared in milliQ water. The band patterns on the gel were visualized by silver staining according to Sambrook and Russel, 2001. The gel was photographed by AlphaEase gel documentation system (Alpha Innotech Corp., USA). Band profiles were analyzed and binary data for presence or absence of bands were computed and the dendrogram was plotted using NTSys software (Exeter software, NY) with UPGMA method. Shannon Weaver diversity index was calculated as,

Shannon Index (H') = $-\sum(n_i/N) \log (n_i/N)$

Where $n_i$is the area of the peak and N is sum of all the area covered under individual peaks of the densitometric curve of the gel banding pattern determined by AlphaEase software (Alpha Innotech Corp., USA).

2.8. Isolation and screening of efficient RV5R decolorizing bacteria from acclimatized consortia

Isolation of efficient RV5R decolorizing bacteria was done by serial dilution of RV5R decolorizing microbial consortia in PBS up to 10^{-4} to 10^{-6} and spreading on Nutrient agar (NA) plates. Plates were incubated at 30 °C up to 3 d; colonies with different morphologies were transfered at regular intervals on fresh NA plates. Each morphotype of pure culture was individually tested for RV5R decolorisation in Luria Bertani (LB) broth containing 100mg/L RV5R.

2.8.1. Identification and characterization of RV5R decolorizing bacterial isolates

RV5R decolorizing bacterial isolates were identified by 16S rRNA gene sequence analysis. The isolated were grouped on the basis of ARDRA.

2.8.1.1. *Amplified rDNA Restriction Analysis (ARDRA) and 16S rRNA gene sequence analysis*

PCR amplification of the 16S rRNA genes using universal eubacterial primers was carried out with forward primer 27F and reverse primer 1541R (Table 2.5). For template DNA preparation, bacteria were grown on LB agar plates and freshly grown colonies were suspended in 50µl of nuclease free water and placed in boiling water bath for 5min. The suspension was then centrifuged and the supernatant was used as template for PCR amplification. The PCR reaction mixture was prepared as

mentioned in section 2.4 and incubated in a thermal cycler (Applied Biosystems model 2720) under the following cycling regime: initial denaturation of 95°C for 5 min, followed by 30 cycles each consisting of denaturation at 95°C for 45 s, annealing at 58°C for 45s,extension at 72°C for 1.5min and a final extension at 72 °C for 15 min (Appendix D).

About ~450 ng of the PCR products showing single band on agarose gel electrophoresis were subjected to ARDRA, where they were separately digested by restriction endonucleases (REs) HinfI, HaeIII, and HhaI. To the PCR amplicon, 1.5 µl of 10 x Tango buffer (Fermentas) and 5 units of enzymes were addedin a total volume of 15 µL. The reactions were carried out for 12 h at 37^0C. The restriction fragments were separated by electrophoresis on 2.5% (w/v) of agarose gels supplied with ethidium bromide (0.5µg/ml) and photographed under UV light. Based on the band pattern, isolates were grouped by using NTSYSpc 2.02i program. A binary scoring system was used to generate an input matrix using major and reproducible bands of the RE pattern, which was then analyzed using the weighted paired group mean average (WPGMA) clustering. A dendrogram was generated from the matrix using the SAHN subroutine of NTSYSpc 2.02i program.

Subsequently, ARDRA was also done in order to analyze the transformants. For this, ARDRA profile of the transformant was compared with ARDRA profile of their respective Wild type isolate. The enzyme used for ARDRA was *Hinf*-I (5U) per system of 450ng -1µg PCR product digestion.

2.8.1.2. *16S rRNA gene sequence analysis*

16S rRNA gene was amplified using eubacterial universal primers 27F and 1107R and PCR program mentioned in Appendix C (Chaturvedi and Archana, 2012) (Appendix C). The PCR product was sequenced using reverse primer (1107R) at Genei Merck, India, generating an optimum sequence length for the identification. The nucleotide sequence was analysed using SeqMatch tool at the RDP database (http://rdp.cme.msu.edu/seqmatch/seqmatch_intro.jsp). The phylogenetic tree was constructed using MEGA 4.0(Tamura et al., 2007).GenBank accession numbers of the16S ribosomal RNA sequences of bacterial isolates reported in this study are JQ745287-94.

2.8.1.3. *Biochemical identification of RV5R decolorizing bacterial isolates*

Efficient dye decolorizing bacterial isolates were identified using specified biochemical test of Bergey's manual (Holt et al., 1994). According to the 16S rRNA gene sequencing results, 8 potential isolates were further characterized based on the key biochemical tests suggested for particular genera in the manual.

2.9. Analytical methods

Azo dye decolorization and degradation studies were analyzed for bacterial consortia, isolates and transformants, respectively. Azo dye decolorization and end products metabolites were analyzed via Fourier Transformed Infrared spectroscopy (FTIR) and Gaschromatography-mass spectrometry (GC-MS).

2.9.1. FTIR of dye degradation products by consortia and isolate

The culture supernatants of each consortium/ pure cultures grown in appropriate medium with RV5R till complete decolorization were subjected to end point metabolite extraction by adding equal volume of ethyl acetate and dried in SpeedVac (Thermo Electron Corporation, USA). FTIR analysis was done by mixing dried sample with HPLC grade potassium bromide (KBr) in the ratio of 5:95 and analysed at mid IR region (400–4000 cm^{-1}) using Spectrum GX spectrophotometer (PerkinElmer, USA).

2.9.2. Detection of RV5R degradation products by GC-MS

GC-MS analysis was done to investigate the metabolites formed during the RV5R biodegradation process. The degradation productswereidentified by gas chromatographyfollowed by mass spectrometry (GC-MS-QP2010, Shimadzu, Japan).GC was equipped with RTX-5 capillary column (0.25 mm by 30 m) andhelium (1.0 ml/min) was used as the carrier gas.

2.10. Biochemical protocols

Different biochemical enzyme assay for azoreductase, NAD^+ dependent formate dehydrogenase and couple Fdh-AzoA azoreductase assay were done, along with NADH estimation by $A_{340nm/280nm}$ of the cell lysate.

2.10.1. SDS-PAGE and native PAGE

To analyze protein expression in transformed cells, SDS-PAGE was done. Cells were harvested and then lysed by boiling in SDS-PAGE loading buffer for 15min except

for *Enterococcus* sp. L2 in which lysis was done by French press. A 12% resolving gel and 5% stacking gel were used for SDS-PAGE and protein molecular weight marker (97, 66, 43, 29, 20, 14kDa) (Genei, Merck, India) was used as a molecular weight standard. SDS-PAGE gels were run at 70 V for 15-20 min and then, at 100 V for 2h**.** At the end of electrophoresis, gels were visualized by staining with Coomassie brilliant blue R250 and destained as described by Laemmli(1970).For activity staining of azoreductase, native PAGE was carried out by omitting SDS from the sample loading buffer, gel running buffer and acrylamide gel and electrophoresis was carried out at 4°C.

2.10.2. Activity staining of azoreductase

Bacterial cultures were grown overnight in LB broth containing RV5R (100mg/L). Cells were harvested by centrifugation of the culture at 5000*g* at 4^0C. The cell pellet was washed with PBS and resuspended in 25mM potassium phosphate buffer (pH 7.1). Sonication was done for 3 min intermittently 9s on/ 9s off pulses using Sonics VibraCellTM sonicator, lysate was centrifuged at 14,000*g* and the supernatant was used as cell freeextract.

A preparative mini 8% resolving polyacrylamide gel was prepared according to the method by Laemmli(1970), without the addition of SDS. The whole cell lysates prepared as above were loaded. Electrophoresis was performed at 4 °C in Tris-glycine buffer, pH 8.3 at 6 mA constant current. After electrophoresis, the gel was treated with 10 μM FMN followed by 0.5mM RV5R (To allow the dye to impart color to acrylamide gel). After this the solutions were drained from the gel and 1 mM NADH or 2mM NADPH was overlaid on gel placed in the staining box. Each gel was incubated for 10- 20min at room temperature with gentle shaking to assure that solutions were evenly distributed across the gels, until decolorized bands were observed on the gel.

2.10.3. Azoreductase assay

Azoreductase activity was assayed by measuring the decrease in optical density of RV5R at 558nm using Nanophotometer (Implen,GmbH) as described by Chen et al. (2004).Bacterial cultures were grown overnight in appropriate media containing 100mg/L RV5R and suitable antibiotics for plasmid bearing transformants.IPTG (1mM) induction was given wherever necessary at the mid log phase culture (0.4

O.D). Cells were harvested by centrifugation at 5000*g* and 4^0C. The cell pellet was washed with PBS and resuspended in 25mM potassium phosphate buffer (pH 7.1). Sonication was done for 3 min intermittently 9s on/ 9s off pulses using Sonics VibraCellTM sonicator, lysate was centrifuged at 14,000*g* and the supernatant was used as cell freeextract.The reaction system used for azoreductase assay was 100µlPotassium phosphate buffer (250mM) (pH-7.1),100µl RV 5(100µM), 10µlNADH (10mM), 10µl cell extract, 10µl FMN (1mM) and 770µl D/W. One unit (U) of Azoreductase enzyme is defined as the amount of enzyme required to reduce (decolorize) 1 µM azo dye per minute. The enzyme activity was calculated by using following formula,

$$A=\text{Ɛ}CL$$

Where,

A= Absorbance at 558nm

Ɛ= Molar extinction coefficient of RV5R (30,000 $M^{-1}cm^{-1}$)

C= Concentration of RV5R

L= Path length of the cuvette (1cm)

Total protein concentration in cell extracts was measured by Bradford method using bovine serum albumin as standard. Specific activity is expressed as U/mg of total protein (Bradford, 1976).

An induction experiment was designed to observe the fold increase in azoreductase specific activity for *Enterococcus* sp. L2 activity upon exposure to different stressors. An overnight grown culture of *Enterococcus*sp. L2 wild type (WT) in LB broth was taken. It was reinoculated into LB and an A_{600} of 0.3 was obtained. Stressors were added; H_2O_2 (10mM), Azo dye RV5R (100mg/L), Menadione (20mM), Anthroquinone sulfonate (AQS) (20mM). The system was incubated at 35°C for 2 hours. Cells were pelleted and washed with PBS; subsequently azoreductase specific activity was determined by protocol mention earlier.

2.10.4. NAD^+ dependent formate dehydrogenase (FDH) assay

FDH assay was performed as described by Berraos-Rivera et al.(2002). Cell extract was prepared according to the protocol described for azoreductase activity (Section 2.13) with addition of 100mM β-mercaptoethanol in lysis buffer. For 1ml enzyme reaction mixture,100µl cell extract was added along with 1.67mM $NAD^+$and 167mMsodium formate. Assay was carried out using Nanophotometer (Implen,

GmbH) with single beam cuvette based kinetic application. The enzyme activity was assayed by measuring increase in absorbance at 340nm and using formula,

$$A=\varepsilon CL$$

Where, A= Absorbance at 340nm

Ɛ= Molar extinction coefficient of NADH (6220 $M^{-1}cm^{-1}$)

C= Concentration of NADH

L= Path length of the cuvette (1cm)

One unit (U) of FDH enzyme is defined as the amount of enzyme required to oxidize 1 µM formate per minute. Total protein concentration in cell extracts was measured by Bradford method using bovine serum albumin as standard. Specific activity is expressed as U/mg of total protein (Bradford, 1976).

2.10.5. NAD^+ Formate dehydrogenase dependent azoreductase coupled assay

In this assay, one of the substrates for azoreductase i.e. NADH was replaced by the substrate for FDH i.e., formate and NAD^+. All the transformants were grown overnight in LB medium containing appropriate antibiotic. IPTG (1mM) induction was given at the mid log phase culture (0.4 O.D). Cultures were centrifuged at the 5000g for 10min and the pellet was washed with sodium phosphate buffer (pH-7.5). Then the pellet was resuspended in 10mM sodium phosphate buffer containing 0.1M β-mercaptoethanol. Sonication was done using Sonics Vibra Cell™ for 3min followed by centrifugation at 14000g for 15min at 4^0C. Supernatant was used as cell free extract. The assay was performed using Nanophotometer (Implen, GmbH). The reaction system consisted of 100µl Sodium phosphate buffer (100mM) (pH-7.5), 100µl Sodium formate (1670mM), 10µl FMN(1mM) , 20µlRV5R (100µM), 50µl Cell extract, 20µl NAD^+(12mM) and 700µl D/W. One unit (U) of coupled azoreductase enzyme activity is defined as the amount of enzyme required to decolorize 1 µM dye per minute. Total protein concentration in cell extracts was measured by Bradford method using bovine serum albumin as standard. The enzyme activity was calculated by using formula as described in section 2.10.2**.**

2.10.6. NAD(P)H estimation

All the transformants were grown overnight in LB containing appropriate antibiotic. IPTG (1mM) induction was given at the mid log phase culture (0.4 O.D). The culture was centrifuged at 5000*g* for 10min and the pellet was washed twice with

0.01M sodium phosphate buffer (pH 7.5) and resuspended in 1ml 0.01M sodium phosphate buffer (pH 7.5) containing 0.1M β-mercaptoethanol. Sonication was done for 3 min by using Sonics Vibra Cell™. Centrifugation was done at 14,000 *g*, 4^0C for 10 min in order to remove cell debris and supernatant was used to estimate the NAD(P)H. Absorbance was taken at 340nm and 280nm using Nanophotomter (Implen, GmbH) and 340/280 nm ratio was determined.

2.11. Construction of recombinant plasmids for overexpression of *azoA* and *fdh*

Five recombinant expression plasmids, pBBR1MCS-2 *azoA*, pBBR1MCS-2 *fdh*, pBBR1MCS-2 *fdh-azoA* for gram negative host systems and pMGS100 *fdh*and pMGS100 *azoA* for gram positive host system were constructed.A summary of the cloning strategies for the plasmid construction is given in Table 2.7.

Table 2.7Strategies forconstruction of recombinant plasmids

Construct	Vector	Insert	Restriction enzyme and Restriction site	Type of ligation
pBBR1MCS2*azoA*	EcoRV linearized pBBR1MCS2	PCR amplified *azoA* from *Enterococcous* sp. L2	EcoRV 5′…GAT$^{\downarrow}$ATC…3′ 3′**…**CTA$_{\uparrow}$TAG…5′	Blunt end
pBBR1MCS2 *fdh*	EcoRV linearized pBBR1MCS2	pT7 myc*fdh* cassette	EcoRV 5′…GAT$^{\downarrow}$ATC…3′ 3′**…**CTA$_{\uparrow}$TAG…5′	Blunt end
pBS KS *fdh* (Intermediate plasmid)	EcoRV linearized pBS KS(+)	pT7 myc*fdh* cassette	EcoRV 5′…GAT$^{\downarrow}$ATC…3′ 3′**…**CTA$_{\uparrow}$TAG…5′	Blunt end
pBBR1MCS2 *fdh-azoA*	KpnI linearized pBBR1MCS2 *azoA*	KpnI digested pT7 myc*fdh* cassette from pBS KS *fdh*	KpnI 5′…GGTAC$^{\downarrow}$C…3′ 3′…C$_{\uparrow}$CATGG…5′	Sticky end
pMGS100*fdh*	NruI linearized pMGS100	Coding region of myc*fdh*	NruI 5′…TCG$^{\downarrow}$CGA…3′ 3′…AGC$_{\uparrow}$GCT…5′	Blunt end
pMGS100*azoA*	NruI linearized pMGS100	Coding region of *azoA*	NruI 5′…TCG$^{\downarrow}$CGA…3′ 3′…AGC$_{\uparrow}$GCT…5′	Blunt end

2.11.1. Basic recombinant DNA protocols

Standard protocols for plasmid isolation, RE digestion, ligation and transformation were followed (Sambrook et al., 2001) and some specific protocols are described in the sections below. All the restriction enzymes and PCR reagents were obtained from Fermentas, Canada.

2.11.1.1. *Ligation protocol*

The ligation reaction was usually done in 10µl volume containing the following constituents: Purified vector and insert DNA (volume varied depending on the respective concentrations); 10X T4 DNA Ligase buffer, 1µl; T4DNA ligase (Fermentas, Canada), 0.5-1.0U and sterile double distilled water to make up the volume. The ligation reactions were incubated at 16°C for 12-16h. The vector to insert molar ratio (molar concentrations calculated by the under mentioned formula) of 1:3 was maintained, with a total of 50-100ng of DNA in each ligation system.

Amount of insert (ng) = insert size (bp) / vector size (bp) x 3 (molar ratio of insert / vector) x amount of vector to be used (ng).

2.11.1.2. *Transformation of plasmid DNA*

2.11.1.2.1. *Chemical transformation*

Plasmid DNA was transformed in*E.coli*strains by standard $CaCl_2$ protocol as described by Sambrook et al. (2001). Transformants were selected based on their resistance to appropriate antibiotics at the concentrations mentioned in Table 2.8. For pBBR1MCS-2 and pBS KS(+) Blue-White selection was used by plating on X-gal containing media. For *P.fluorescens* PfO-1 and gram negative laboratory isolates (Strains A3, C1, E2, G1, K1, L1) transformation was done with slight modification in standard chemical transformationprotocol. For them, competent cells were prepared as follows: 20ml of overnight grown culture was centrifuged at 10,000*g* at 4^0C. Cells were resuspended in 10ml of 10mM NaCl and incubated for 10-15min on ice. Centrifugation was done at 10,000*g*and at 4^0C. Pellet was resuspended in 10ml of chilled 0.1M$CaCl_2$, incubated for 1h followed by centrifugation at 10,000*g* at 4^0C. Pellet was resuspended in 200µl 0.1M $CaCl_2$. About 1µg plasmid DNA was added to 200µl competent cells, mixed gently and stored on ice for 1h. After which heat shock was given at 42^0C for 2min. This mixture was immediately transferred to ice for 5min

and then 1ml LB was added and incubated for 1.5h at 37^0C. Suspension was spread on LB agar plate containing appropriate antibiotics as shown in Table 2.8.

2.11.1.2.2. *Electroporation*

Electroporation was done for transformation of pMGS100*azoA*,pMGS100*fdh*and pTEX5501tsupdown*azoA* in *Enterococcus* sp.L2 For electroporation, culture was grown overnight at 37^0C under static condition in Brain Heart Infusion broth Yeast extract Glycerol Tris-Cl (BYGT) medium containing 4% glycine. Then culture was diluted 1:20 in BYGT medium and incubated at 37^0C for 60-90min. Culture was chilled, centrifuged and washed with 40mlelectroporation buffer. Centrifugation was done and the pellet was resuspended in electroporation buffer (0.625M Sucrose, 0.001M MgCl2, Adjust to pH 4.0 by 1M HCl) and stored on ice for 30-60min. Cell suspension (50-100µl) and 1µg DNA was added to 0.2cm electroporation cuvette. Electroporation was performed at 2500V/cm by usingElectroporator 2510 (Eppendorf) and cells were placed on ice for 1-2 min beforeadding twice the volume of Todd Hewitt Broth (THB) medium. Incubation was done 37^0C for 90-120min. Cells were spread on THB medium containing 0.25M sucrose and 10µg/ml chloramphenicol. The compositionsof BYGT and THB media are given in Table 2.9 (Dunny et al., 1991).

Table 2.8Antibiotic concentrations used for transformant selection in different host and plasmid systems

Host	**Construct**	**Antibiotic**	**Antibiotic Conc. (µg/ml)**
Citrobacter sp. A3, *Klebsiella* sp. E2, *Providencia* sp. G1, *Klebsiella* sp. K1, *E. coli* DH5α, *E. coli* BL21 and *P. fluroscens* PfO-1	pBBR1MCS-2 myc*fdh*	Kanamycin	30
Providencia sp. C1, *Acinetobacter* sp. L1			15
Enterococcus sp. L2	pMGS 100 *fdh*	Chloramphenicol	10
Citrobacter sp. A3, *Klebsiella* sp. E2, *Providencia* sp. G1, *Klebsiella* sp. K1, *E. coli* DH5α, *E. coli* BL21 and *P. fluroscens* PfO-1	pBBR1MCS-2 *fdh-azoA*	Kanamycin	30
Providencia sp. C1, *Acinetobacter* sp. L1			15
Enterococcus sp. *L2*	pTEX5501ts and its derivatives	Chloramphenicol	10

Table 2.9Composition of BYGT and THB medium

BYGT medium		**THB (Todd Hewitt Broth)**	
Item	**Concentration (g/L)**	**Item**	**Concentration (g/L)**
Meat extract	10	Meat extract	1.5
Beef extract	10	Beef extract	1.5
Yeast extract	5	Peptone	2.0
Glucose	2	Glucose	2.0
Glycerol	4ml	NaCl	2.0
1M Tris-Cl (pH 8.0)	100ml	Na_2HPO_4	0.4
Glycine	40	Na_2CO_3	2.5
		Sucrose	8.56

2.11.1.3. *Confirmation of recombinant plasmid constructs*

PCR and RE digestion of recombinant plasmids were performed in order to confirm the clones. Different restriction enzymes used for checkingeach constructs are shown in Table 2.10 along with expected fragment sizes. PCR confirmations for all the constructs were done using gene specific primers mentioned in Table 2.5 as per their respective PCR programs.

Table 2.10Restriction enzymes used for confirmation of recombinant constructs

Clone	**Restriction enzyme**	**Expected band sizes (kb)**
pBBR1MCS-2 *fdh*	XbaI	1.2 and 5.1
pBS KS (+) *fdh*	SalI	1.2 and 2.9
pBBR1MCS-2 *fdh azoA*	SalI XbaI	1.2, 0.5 and 5.1 2.1 and 5.1
pMGS100 *fdh*	BamHI	1.2 and 10.4

2.11.2. Construction of pBBR1MCS2*azoA*

The *azoA* gene of *Enterococcus* sp. L2 was pcr amplified using primers *azoA*F and *azoA*R to yield a product of 650bp. PCR amplified *azoA* gene ORF including the optimally positioned RBS was cloned at EcoRV site in pBBR1MCS2. Clones with correct orientation of *azoA* with vector p*lac* promoter were screened by SalI digestion.

2.11.3. Construction of pBBR1MCS2*fdh*

The myc*fdh* gene along with promoter pT7 was pcr amplified from pBBR1MCS2myc*fdh*using primers Myc*fdh*F and Myc*fdh*R to give 1.5kb cassette. The PCR amplified pT7 myc*fdh* cassette was cloned into pBBR1MCS2 at EcoRV site. Clones with correct orientation of *azoA* with vector p*lac* promoter were screened by XbaI digestion.in the same orientation with plac. Fig. 2.7 shows the RE map of the p*T7* mcy*fdh* cassette.

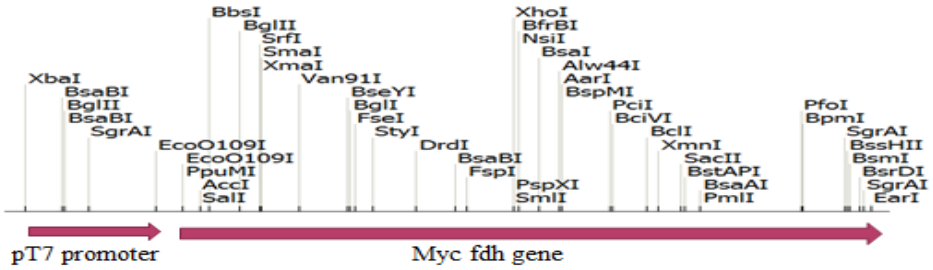

Figure 2.7Restriction map of pT7 myc *fdh*cassette

2.11.4. Construction of pBBR1MCS-2 *fdh- azoA*

The construct pBBR1MCS-2 *fdh-azoA*carries a transcription fusion in which both *fdh* and *azoA* are under the control of p*lac* and p*T7* promoters. This construct was prepared by first cloning of pT7myc*fdh* cassette into pBS KS (+) at EcoRV site to yield the intermediate plasmid pBS KS*fdh*. The transformants were selected based on blue-white selection strategy and SalI digestion. pBS KS*fdh* was subjected to KpnI digestion and resulting 1.5kb fragment was elutedusing Qiagen gel extraction kit. Then sub-cloning of eluted pT7 myc*fdh* with KpnIdigested pBBR1MCS2*azoA*was done. Orientation of the correct clone was analyzed by SalI and XbaI.

2.11.5. Construction of pMGS100*fdh*

The plasmid pMGS100*fdh* was constructed by cloning of coding region (ORF) of myc*fdh*amplified using primers MGS100*fdh*F and Myc*fdh*R into NruI site of pMGS100. Clones with correct orientation of *fdh* with constitutive promoter of bacitracin resistance gene (p*bacA*) were screened by BamHI digestion.

2.11.6. Construction of pMGS100*azoA*

The ORF of *azoA*was PCR amplified from *Enterococcus* sp. L2 using primers *azoA*ATGF and *azoA*R amplifying 627bp fragment. The plasmid pMGS100*azoA*was constructedbycloningORFof*azoA*intopMGS100 at NruI site. Clones with correct orientation of *azoA* with constitutive promoter of bacitracin resistance gene (p*bacA*) were screened by SalI digestion.

2.12.Construction of *azoA* knockout of *Enterococcus* sp. L2

Gene disruption strategy was used for construction of *azoA*knockout of *Enterococcus* sp. L2.*Enterococcus* L2 is a gram positive diplococcus.pTEX5501ts (Fig. 2.5) used as

a disruption vector is an *E.coli-Enterococcus* shuttle vector with temperature sensitive replication mode in *Enterococcus* spp. Flanking regions of the target gene to be disrupted are cloned separately at either side of chloramphenicol resistance gene in MCS-I and MCS-II in the plasmid vector. Gentamycin resistance marker (*aph-2' Id*) present on the backbone of the vector is used for counter selection of the disruptants. up*azoA*and down*azoA* were ~1.2 kb regions upstream and downstream of *azoA*gene of *Enterococcus* sp. L2. The flanking regions used for double homologous recombination for *azoA* knockout construction are shown in Fig. 2.8. These PCR amplified fragments were cloned into MCS-I and MCS-II of pTEX5501ts as pTEX5501ts updown*azoA*.

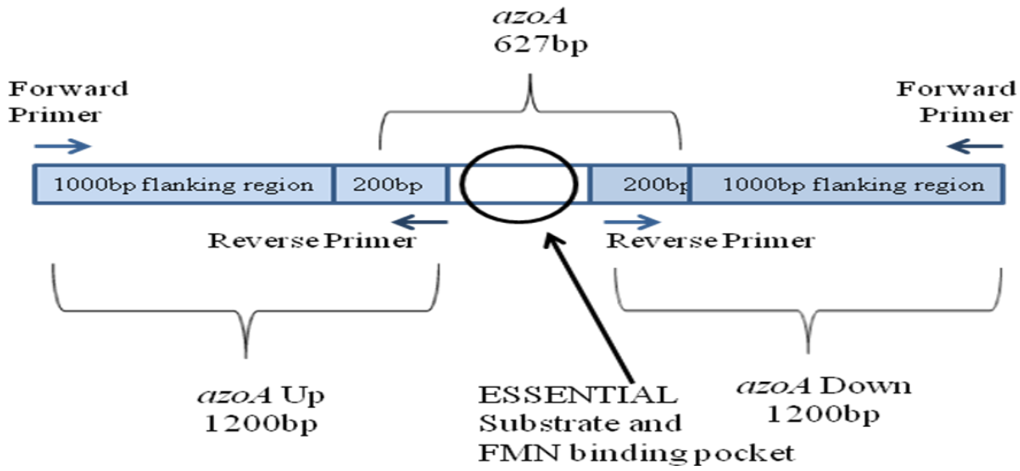

Figure 2.8*azoA* of *Enterococcus* L2 and its flanking regions used for disruption

2.12.1. Construction of Disruption Vector pTEX5501tsupdown*azoA*

The construction of the disruption vector required three intermediate steps: cloning of the *upazoA* fragment into pJET1.2, cloning of the *downazoA* fragment into pBSII KS and lastly their subsequent digestion from the respective vectors and cloning of *up azoA* in MCSI and *downazoA* in MCSII of pTEX5501ts. Commercially available pJET is in a linearized form, pBSII KS was linearized using EcoRV.*upazoA* fragment and *downazoA* fragment were PCR amplified from *Enterococcus* sp. L2 genome using primers mentioned in Table 2.5 and were cloned into pJET1.2 and pBS KS respectively using the cloning strategy mentioned in Table 2.11. pTEX5501ts was linearized at MCSI using BglII for inserting *upazoA* fragment and at MCSII using SmaI to insert the *downazoA* fragment. PCR and RE digestion of recombinant

plasmids were done to confirm the constructs. The PCR programme used is shown in appendix G.

Table 2.11Strategies forconstruction of recombinant plasmids

Construct	Vector	Insert	Restriction enzyme and its site	Type of ligation
pJET*upazo*	pJET (Linearized plasmid)	PCR amplified *upazo*	-	Blunt ended
pBS KS*down azo*	EcoRV linearized pBSII KS	PCR amplified *down azo*	EcoRV 5'...GAT↓ATC...3' 3'...CTA↑TAG...5'	Blunt ended
pTEX5501ts *up azo*	BglII linearized pTEX5501ts	*BglII* released *upazoA* from pJETup*azoA*	BglII 5'...A↓GATCT...3' 3'...TCTAG↑A...5'	Sticky end
pTEX5501ts *up down azo*	SmaI linearized pTEX5501ts *upazoA*	*PvuII* released*downazoA from pBS KS downazo*	SmaI 5'...CCC↓GGG...3' 3'...GGG↑CCC...5'	Blunt ended

2.13.Screening of *azoA* knockout

Electroporation of the disruptant construct into *Enterococcus*sp. L2 was carried out and transformants were selected bychloramphenicol or gentamycin resistance ofcolonies at 28^{O}C. The strategy followed for the generation of *azoA* knockout after electroporation is as shown in Fig. 2.9. As seen, shift in incubation temperature to 42^{O}C leads to plasmid loss and only genomic integrants would possess the antibiotic markers. Secondary recombination event upon further serial passaging at 42^{O}C would lead to the loss of the plasmid backbone creating gentamycin sensitivity and *azoA* knockout.Confirmation of chromosomal integration of disruption vector/cassette was done by PCR amplification of the chloramphenicol resistance cassette and size increase in PCR amplified *azoA* gene. Occurrence of second recombination event was confirmed by the absence of PCR amplification of gentamycin resistance gene. PCR protocols for chloramphenicol, *azoA* and Gentamycin resistance marker are as shown in Appendix H-J, respectively. Primers used for PCR amplification are mentioned in Table 2.5.

Integration into genome upon shift to42^{O}C and first recombination event

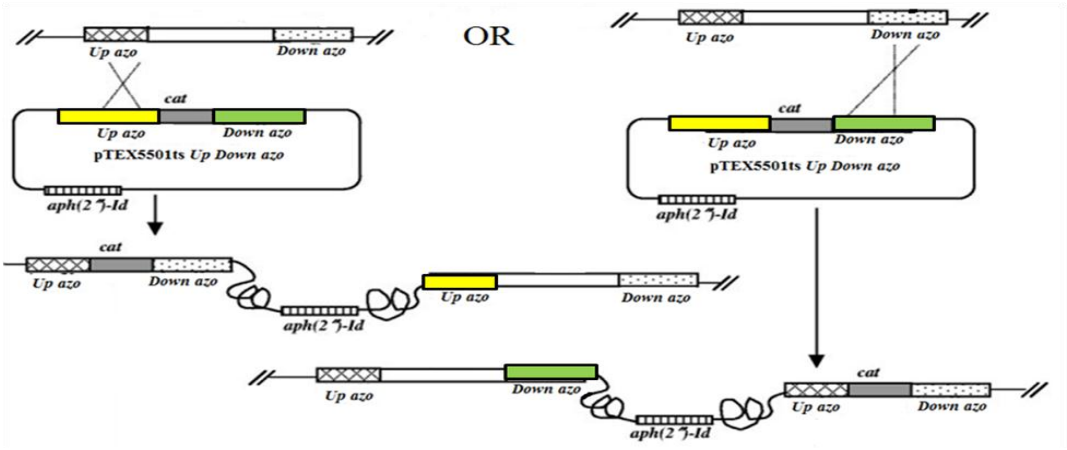

Eight serial overnight passages at 42^{O}C

Second Recombination event and loss of gentamycin resistance cassette from chromosome

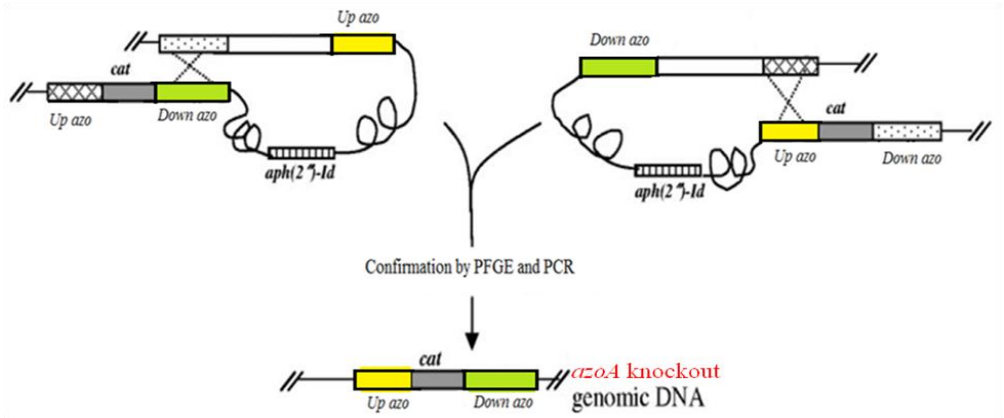

Screening for Chloramphenicol resistantand Gentamycin sensitive colonies

Figure 2.9Strategy for the generation of azo knockout

2.14.Physiological experiments

2.14.1. Growth curves

To analyze the expression of *azoA* in *Enterococcus* sp. L2 and NAD^{+} dependent *fdh* in various standard strains mentioned in Table 2.1 grows without any interruptions, growth curve experiment was performed where the growth of the transformants were compared with the empty vector clones by reading the absorbance at 600nm for 12 h. Media used for the experiment are LB, LB+ formate, Bushnell haas medium (BHM)+ 0.5%Y.E, Bushnell haas medium (BHM) + YE 0.5% (w/v) + formate (under static as well as shaking condition). For *Enterococcus* sp. L2 experiment was done under static condition at 30C.

2.14.2. Survival under oxidative stress

To study the survival of *Enterococcus* sp. L2 (pMGS100*azoA*) under oxidative stress, H_2O_2 was used at different concentrations. *Enterococcus* sp. L2 (pMGS100*azoA*) and vector control were grown up to an $O.D_{600}$ of 0.1 in LB medium with chloramphenicol, the cells were harvested by centrifugation and resuspended in PBS. Equal amount of cells were incubated with the range of H_2O_2 concentration (0-40mM) for 30 min at 37°C. Following the incubation a spot of 20 µl of each system was placed on an LB agar plate in separate demarcated areas and the plates were incubated overnight at 37°C and growth was monitored.

Time course of H_2O_2 survival was studied in a separate experiment where cells of wild type*Enterococcus* sp. L2 andstrain L2 harbouring empty vector (pMGS100) and strain harbouring pMGS100*azoA* were exposed to10mM, 15mM and 20mM H_2O_2 and were spread on LB agar plates where the contact time for H_2O_2 with the cells was varied from 0- 30 min. Percentage survival was calculated normalizing with the individual initial (0 min) reading.

2.14.3. Fluorescence microscopic analysis of Reactive Oxygen Species (ROS)

Accumulation of reactive oxygen species (ROS) inside the cells was seen using a ROS specific green fluorescent probe 2, 7-dichlorodihydrofluorescein diacetate(H_2DCFDA). Intact cells ofwild type*Enterococcus* sp. L2 andstrain L2 harbouring empty vector (pMGS100) and strain harbouring pMGS100*azoA* were incubated with H_2O_2 (0-20mM) for 5 min followed by 5 min incubation with the probe (final concentration in buffer 10 mM). This suspension was smeared on clean grease free glass slide, air dried and observed under fluorescence microscope. To quantify the fluorescence intensity in the different strains, lysates of the H_2O_2 treated cells were mixed at equal protein concentrations with the probe (final concentration in buffer 10 mM) and fluorescence intensity measured using fluorimeter at excitation wavelength 490nm and emission wavelength 519nm (Pérez et al., 2007). (H_2DCFDA dissolved in dimethyl sulfoxide)

2.14.4. Growth analysis under heavy metal stress

Oxidative stress is also induced by heavy metals. A microtitre plate experiment was performed to determine the minimal inhibitory concentration of Cu (II) and Cr (VI) on*Enterococcus* sp. L2 (pMGS100), *Enterococcus* sp. L2 (pMGS100*azoA*) and

Enterococcus sp. L2 (WT). Effect of these heavy metals on growth of the strains was monitored at 0mM, 0.3mM Cr (VI) and 3mM Cu (II) at 600nm for different time intervals up to 21h under incubation at 37°C. (Cells were harvested at an equal O.D. of 0.1 and then normalized to have equal inoculums).

3 Bacterial diversity and biodecolorization studies of Reactive violet 5R (RV5R) bymicrobial consortia

3.1. Introduction

Bioactivities on azo dyes have been reported from diverse group of organisms(Stolz, 2001) including bacteria(Pandey et al., 2007; Saratale et al., 2011a), fungi(Zhao and Hardin, 2007), yeast (Jadhav et al., 2007) and cyanobacteria(Parikh and Madamwar, 2005). Biological decolorization anddegradation of azo dyes has gained importance as a method oftreatment, as these methods are inexpensive, eco-friendly andcan be applied to wide range of dyes (Stolz, 2001). The azo bond (–N=N–), being the important chromophore group, can be reductivelycleaved resulting in aromatic amines which are colorlessin nature. However, the presence of different aromatic rings withmethyl, methoxy, nitro, and sulfo groups make dyes more resistantto microbial degradation and their residues accumulate in biota(Saratale et al., 2011). Although decolorization does not lead tocomplete degradation or detoxification, it is a rate-limiting bottleneckof the biodegradation pathway. Bacterial dye decolorization isfacilitated by enzymatic reactions or by nonspecific reduction bydifferent reduced metabolites (H_2S) or redox mediators of intraor extracellular nature (Pandey et al., 2007). Decolorization of azodyes can occur under anaerobic, anoxic or aerobic conditions bydifferent groups of microorganisms depending on the enzyme systemand microbial metabolites (Chen, 2006; Chengalroyen andDabbs, 2013; Solís et al., 2012).

Dye decolorization has been demonstrated utilizing pure culture and mix culture consortia (Banat et al., 1997; McMullan et al., 2001; Olukanni, 2006).Pure cultures of several bacteria such as *Pseudomonas, Acetobacter, Bacillus, Sphingomonas, Xanthomonas, Aeromonas, Klebsiella* etc.are reported as azo dye decolorizers (Solís et al., 2012).Different bacterial strains such as *Escherichia coli*(Nakanishi et al., 2001), *Citrobacter* sp.(An et al., 2002; Chan et al., 2012a), *Enterobacter agglomerans*(Moutaouakkil et al., 2003)**,** *Enterococcus* strain C1 (Chan et al., 2012b), *Clostridiumperfringens*(Morrison et al., 2012), *Pseudomonaseputida* MET94 (Mendes et al., 2011), *Klebsiella* sp. (Franciscon et al., 2009), *Bacillus* sp. (Bafana et al., 2008b; Dave and Dave, 2009; Kandelbauer et al., 2004; Gomare and Govindwar, 2009), *Geobacillus* sp.(Sugiura et al., 2006), *Staphylococcus* sp. (Elisangela et al.,

2009) and *Lactobacillus casei* TISTR 1500 (Seesuriyachan et al., 2007) etc. have been reported for azo dye decolorization. *Halomonas* sp. are able to decolorize azo dye under high saline conditions (up to 20% w/v) (Asad et al., 2007). Recently, bacterial community analysis at Anode of Microbial Fuel Cell(MFC) demonstrated dual role of bacterial population able to degrade dye and also generate electricity (Zhang et al., 2013).

Bacterial azo dye decolorization is efficient and fast, but individual bacterial strainsusually cannot degrade azo dyes completely, and the intermediateproducts are often carcinogenic aromatic amines, which need to befurther mineralized (Joshi et al., 2008).Recenttrend has been to use co-cultures comprising of a mixture ofwell-characterised pure cultures or acclimatized microbial consortia (Saratale et al., 2011; Solís et al.,2012). Mixed cultures have an advantage over pure cultures, sincethe mixed population attains additional co-metabolic potentialsand possesses higher degree of biodegradation and mineralization due to synergistic metabolic activities of microbial community(Banat et al., 1997; Senan and Abraham, 2004). In mixed cultures, the individual strains may attack the dye moleculeat different positions or may utilize metabolites produced bythe co-existing strains for further mineralization or have broadspectrum for dye decolorization due to variation in the enzymaticmachinery in the individual members (Chengalroyen and Dabbs, 2013). Jain et al. (2012) have shown that acclimatized consortium SB4 decolorized RV5R dyeefficiently in 18 h under static conditions which was better thanthe individual pure bacterial strains from the same consortium.

Mixed cultures that are artificially formulated by combiningindividual pure cultures have certain disadvantages such as the requirement of thorough optimization of the appropriate mixtureas well as unstable nature of the artificially mixed populationswhose proportions may vary with time.In artificially mixed cultures, it becomes very difficult to maintain the ratio of each type during application and transfer procedures. As against artificially mixed cultures, acclimatized consortia, encompassing enrichedmicrobial community derived by repeated transfers of nativemicrobial community from an appropriate sample in dye containingmedia, have several advantages. The members of the acclimatized consortia may have functional or dormant populations,both of which could be vital for the slow adaptation of the

communityto deliver stably the desired process(Dafale and Rao, 2008). Acclimatizedconsortia offer the advantages of mixed cultures but haveadditional features such as natural adaptation of the communitymembers with each other (Mikesková et al., 2012). Adaptation ofa microbial community in the presence of recalcitrant and toxicdyes improves the rate of decolorization process by acclimatized consortia(Beydilli and Pavlostathis, 2005). Community successionin bacterial adaptation results in stable consortium development(Desai et al., 2009). Additionally efficient acclimatized consortiacan be a potential source of individual efficient strains(Moosvi et al., 2005).

Dye decolorizing organisms have been isolated from contaminated as well as pristine environmental samples(Dykes et al., 1994; Mohana et al., 2007; Kolekar et al., 2008; Stingley et al., 2010).The isolation of pure cultures of dye decolorizing acclimatized consortia could be expected todepend on the original microbial community present in the environmentalsample and the enrichment medium and conditions.However, no systematic reports exist on how these factors affectconsortia development and dye degradation patterns in such differentlydeveloped enriched consortia. The enrichment culturetechnique combined with advanced molecular methods for community fingerprinting could be utilized to compare the populationsfrom different consortia.

With this in view, the objective of this chapter was to enrich dye decolorizing consortia from variouspristine and contaminated samples to develop acclimatized consortia effectively decolorizing azo dye. The acclimatized consortia were further studied for their bacterial diversityby 16S rRNA gene based molecular fingerprinting techniques suchas amplified ribosomal DNA restriction analysis (ARDRA) anddenaturing gradient gel electrophoresis (DGGE) analysis. Decolorized end-products were analyzed by FTIR and GC–MS analysis. Reactive violet 5R (RV5R), a mono azo dye having complex sulphonatedmoieties on benzene and naphthalene rings was used as themodel dye for the current study. Subsequently, efficient dye decolorizing strains were isolated from consortia and were studiedfor their ability decolorize azo dye individually and effects of various redox mediators and carbon sources on the dye decolorization phenomenon.

3.2.Results:

3.2.1. Enrichment of Reactive Violet 5R decolorizing acclimatized microbial consortia

Decolorization of azo dyes by reductive cleavage of the azo bond is an important and rate limiting step in the dye mineralization (Chengalroyan and Dabbs, 2013). Therefore, in the present study, Reactive violet 5R (RV5R) decolorizing acclimatized consortia were enriched from various samples such as effluents, sludge and soil contaminated with dyes or other organics as well as pristine environments such as marine samples from different niches as given in (Table 2.3, Chapter 2).The samples were initially inoculated and passaged in different media, however only certain combination of samples and media yielded efficient decolorizing consortia. A total of 23 acclimatized consortia which were able to decolorize 100mg/L RV5R weredeveloped in shaking and static conditions in different media.Using 5% (v/v) transfer of inoculum for every passage, 12 consortia were found to be positive in RV5R decolorization by 30 h, remaining consortia were unable to decolorize the dye efficiently (Table 3.1). During initial transfersdecolorization was slow (24-52 h) while after acclimatisation consortiawere able to decolorize within 8-24 h after which they werefound to be stable in their decolorizing proficiency. As seen in Table 3.1, hydrocarbon contaminated soil sample (HCCSV1) gave rise to 4consortia in media A–C under shaking conditions and in medium C in static conditions (Section 2.2, Chapter 2). Other samples gave efficient dye decolorizing consortia in particular medium but not in rest.The consortia reported here were stabilized for aerobic and anoxic dye decolorization after 15 passages within 40 d.

3.2.2. RV5R decolorization kinetics by microbial consortia

Out of 12 consortia that were found to decolorize RV5R, 8 decolorized RV5R in shaking and4 in static conditions (Table. 3.1). Decolorization kinetics of each acclimatized consortium was determined by decrease in O.D. at 558nm (λ_{max} of RV5R) (Fig. 3.1).Table 3.2 shows the $t_{1/2}$ as time taken to decolorize 50% of 100mg/L RV5R and the percentage dye decolorization after 30h of incubation.Except for two consortia, all the acclimatized consortia were able to decolorize >90% of

Table 3.1Details about the 12 RV5R decolorizing microbial consortia

S. No.	Microbial consortia	Sample	Mode of Incubation	Medium used for enrichment
1	ATGEV	Aeration Tank Green Env. Ltd.	static	A
2	AKW	Amalakhadi Water	static	A
3	Glc	Hydrocarbon contaminated Soil	static	A
4	ME	Meghmani Effluent	static	A
5	Gly	Hydrocarbon contaminated Soil	Shaking	B
6	PBC	Hydrocarbon contaminated Soil	Shaking	D
7	PBR	Hydrocarbon contaminated Soil	Shaking	D
8	Dalc	Petroleum industry effluent,	Shaking	D
9	MW	Marine water	Shaking	C
10	MITZ	Marine Intertidal Zone	Shaking	C
11	MBS	Marine Beach Sand	Shaking	C
12	MSS	Marine Sea Sand	Shaking	C

RV5R in 30h of incubation under shaking or static conditions. The most efficient consortia were PBC and ME under static and PBR under shaking conditions as they were able to decolorize with a $t_{1/2}$ of 3-3.5h.

In order to study decolorization efficiency of the microbial consortia at higher concentrations different concentrations of RV5R were used. Seven acclimatized consortia were found to decolorize higher concentrations up to 1000mg/L of RV5R (Fig. 3.2), thus these consortia could be utilized for highly concentrated dye effluent under aerobic conditions. Most efficient consortia PBC and PBR were able to decolorize RV5R up to 1000 mg/L.

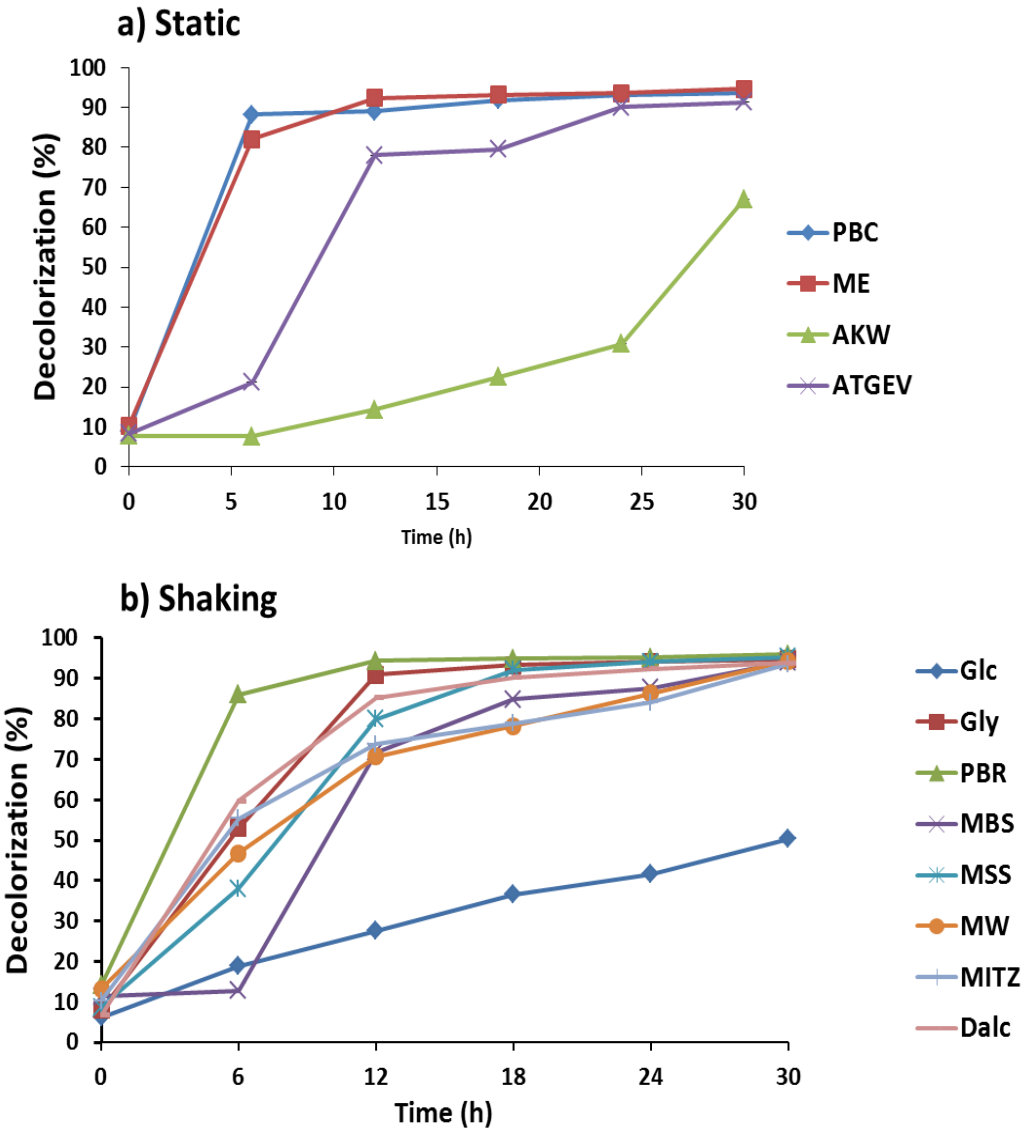

Figure 3.1Decolorization of RV5R by acclimatized microbial consortia.

(Enriched under a) Static b) Shaking conditions)

Table 3.2RV5R decolorization kinetics for microbial consortia

S. No.	Incubation conditions	Microbial consortia	$t_{1/2}$ for RV5R decolorization	Percentage decolorization at 30h (%)
1	Static	ATGEV	9	91.3
2		AKW	27	67.0
3		ME	3.5	94.6
4		PBC	3	93.6
5	Shaking	Glc	30	50.4
6		Gly	5.4	94.7
7		PBR	3	96.0
8		Dalc	4.45	94.0
9		MW	7	94.4
10		MITZ	5.15	93.6
11		MBS	9.45	94.2
12		MSS	7.45	95.3

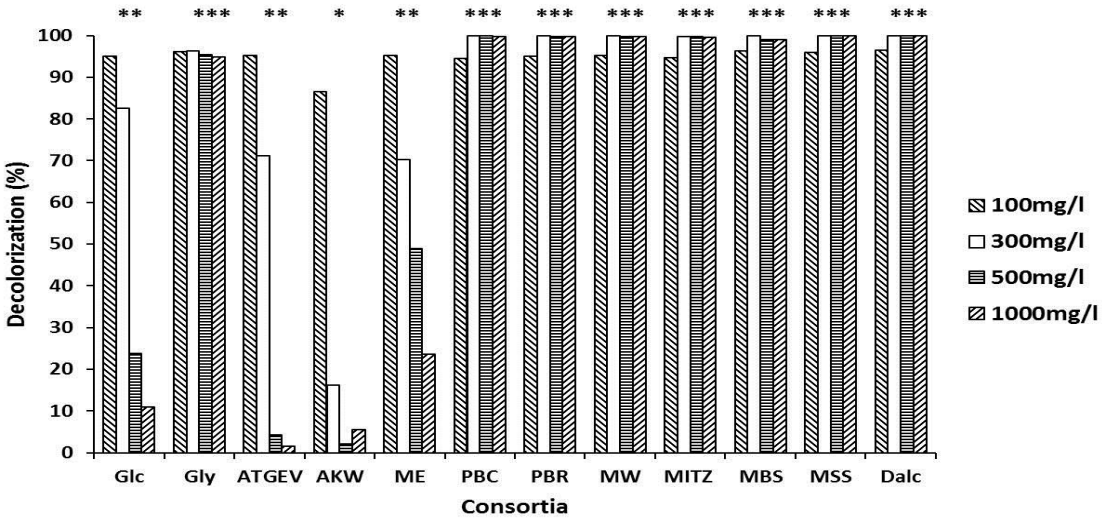

Figure 3.2RV5R decolorization up to 1000mg/L by acclimatized microbial consortia.

Asterisks indicate that the decolorization is found to be significant at 1% level using one way ANOVA analysis. Significant decolorization up to *100mg/L; ** 300mg/L; *** 500mg/L and **** 1000mg/L.

3.2.3. Bacterial community fingerprint analysis of RV5R decolorizing consortia

Bacterial community fingerprinting of dye decolorizing consortia was carried out by two techniques ARDRA and DGGE analysis, both based on 16S rRNA gene diversity. Both the techniques have been widely used for comparing the bacterial communities in diverse environments (Malik et al., 2008, Kolekar et al., 2012). HaeIII and HinfI restriction enzymes were used to digest amplified 16S rRNA gene segments of all consortia. Fig. 3.3shows thedendrogram deduced from the ARDRA patterns. The 12 consortia formed 6 clusters at 0.76 coefficient value, of which ATGEV and AKW were found to have very similar 16S rRNA digestion patterns as they clustered at highest coefficient value of 0.96. MW and MITZ samples also clustered at 0.96 coefficient value. The high similarity of the latter two consortia is not surprizing since they were obtained from the marine water and intertidal zone from the same location (Bhavnagar coastal region, Gujarat, India) and enriched in the same medium. However, acclimatized consortia ATGEV and AKW were obtained from geographically different locations (Vatva and Amalakhadi, Gujarat, India), but yet found to be highly similar. This could be because both the samples were from dye-contaminated effluents, indicating that enrichment in the same nutrient medium might lead to selection of a similar bacterial community. The 4 consortia obtained from HCCSV1 sample clustered together at 0.64 co-efficient, but were distinct, signifying the importance of the media and incubation condition for the consortia development.

Fig. 3.4 shows DGGE gel pattern of 16S rRNA gene V3 region of the microbial community in the RV5R decolorizing consortia. Different banding patterns were obtainedin each consortium indicating significant differences in the compositionof the population. Because DGGE bands indicate ribotypes/species in the sample, it could be inferred that most of the enrichedconsortia were constituted of two to four abundant species withseveral minor species. Clearly different groups of bacteria were enriched in the different consortia except for ATGEV and AKW whichappeared to be predominated by one species. Fig. 3.5 shows the corresponding dendrogram of the acclimatized consortiabasedon the binary data band of presence/absence of the band at particularposition in DGGE gel. Similar to ARDRA dendrogram, DGGE analysis also grouped the 12 consortia into 6 major clusters. However the composition of the 6 clusters was significantly different than the clusters of the ARDRA dedrogram.

Notably consortia ATGEW and AKW as well as MW and MITZ were found to similar using both techniques. The 4 consortia obtained from HCCSV1 sample were found to be dispersed in the DGGE dendrogram. Microbial diversity of the consortia depicted as Shannon index (H') (Hill et al., 2006) based on DGGE pattern is given inDGGE band pattern. The H' index for the consortia was ranging from 1.36 to 2.55 indicating differences in their species richness and abundance.

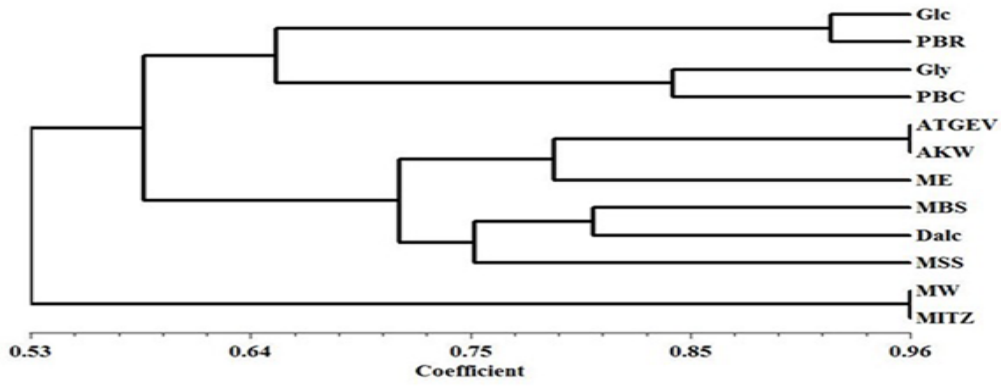

Figure 3.3 Phylogenetic clustering of the RV5R decolorizing acclimatized microbial consortia byARDRA.

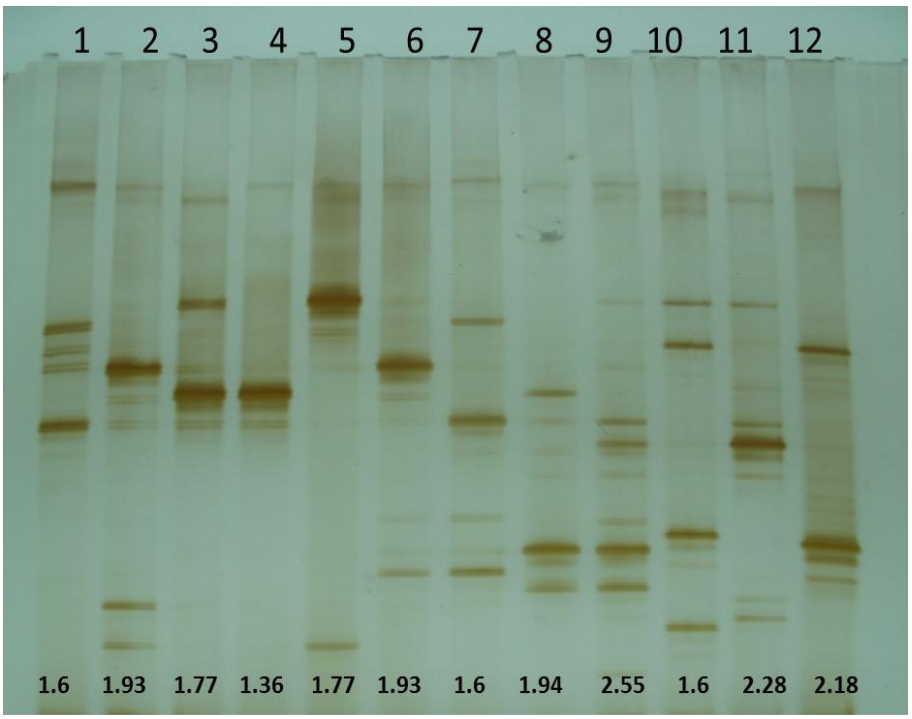

Figure 3.4 DGGE profile of V3 region of 16S rRNA genes from RV5R decolorizing acclimatizedmicrobial consortia.

(Lanes 1 to 12, Glc, Gly, ATGEV, AKW, ME, PBC, PBR, MW, MITZ, MBS, MSS and Dalc)

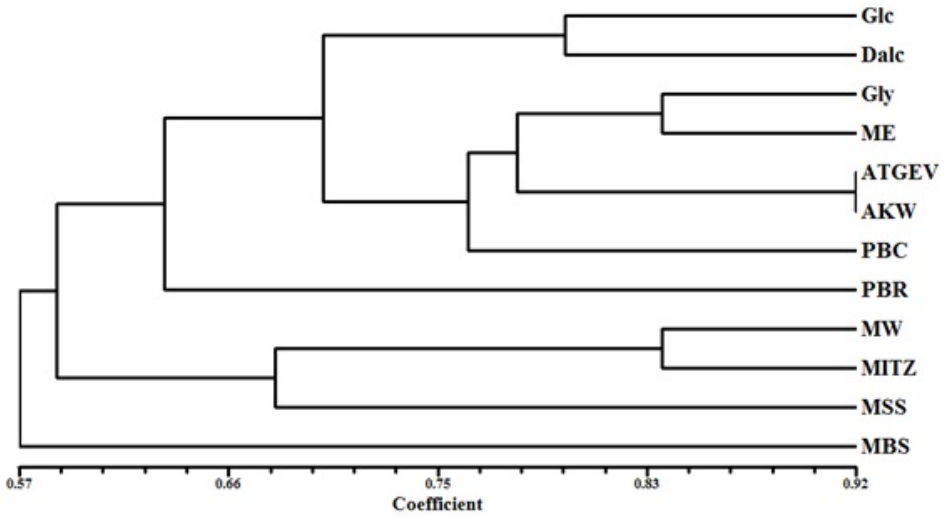

Figure 3.5Dendrogram based onDGGE profile of RV5R decolorizing acclimatized microbial consortia

3.2.4. FTIR and GC-MS analysis of the end products of RV5R decolorization by microbial consortia

Biodegradation products of azo dyes have been well characterized by various analytical methods, among which most common technique is Fourier-transform infrared (FTIR) spectroscopy determine the structural changes in the dye molecules and themetabolites of the dye degradation (Hu, 1994; Jain et al., 2012; Larrechi and Callao, 2010; Saratale, 2009b). Comparison of FTIR spectra of microbially treated samples as compared to that of the control untreated azo dye was used to discern the differences in the spectra of different dye decolorizing consortia. RV5R, a mono-azo reactive group of textile azo dye demonstrated specific azo bond (-N=N-) stretching vibration of a symmetrical trans-mono azo group peak at 1547 cm^{-1}; the disappearance of such peak in the decolorized extracts of acclimatized supernatants shows cleavage of the azo bond (Figs. 3.6 a and b). Transmission peak at 669.3 cm^{-1} signifies out of plane aromatic ring C-H bend (strong peak), SO_3H group is indicated at 1139.9cm^{-1}, all of which can be seen in the untreated control RV5R sample. All the biologically treated samples show transmission peaks between 3300-3500 cm^{-1} stretching or near 1600 cm^{-1} bending which indicate the presence of amine groups due to the reductive cleavage of azo bond. Treated fractions of consortia PBR and Dalc show the retention of 669.3cm^{-1} peak displaying the presence of aromatic rings in the decolorized supernatant.Consortium Gly found to be most effective for the degradation showing further degradation of aromatic amines, demonstrating the =C-H

bond bending of alkene nature between 675-1000cm^{-1}, 3603.14 cm^{-1} -OH group stretching and 1406.15 bending of –OH and C-O stretching along with the amine presence.

Based on the functional groups identified by FTIR spectra of the decolorized products of consortia, a binary datasheet was prepared and using the Neighbour joining method, a dendrogram was constructed to depict the similarities or differences in the FTIR spectra of the difference consortia (Fig. 3.7). As can be seen, the degradation products formed in consortia ATGEV and AKW were highly similar. However, the otherphylogenetically similar pair MW and MITZ, was functionally differenton the basis of FTIR analysis. On the other hand, consortiaME and MSS which were phylogenetically distinct showed highsimilarity in their functional groups in FTIR spectra.

In order to get obtain information of RV5R degradation end products of the most efficient consortium Gly, GC–MS analysis of degraded products from culture supernatants was performed. Based on molecular weight and chemical structure of dye we could identify two intermediary products. Two major peaks at 16.56 min with m/z of 476 and 21.2 min with m/z of 448, were found to correspond to the propanoic acid 3-hydroxy hydrazine and 1,4 epoxy naphthalene respectively (Figs. 3.7 a, b and c). These end products demonstrate the azo bond reduction and benzene ring breakage of the RV5R by Gly consortium, although the naphthalene ring was not metabolized.

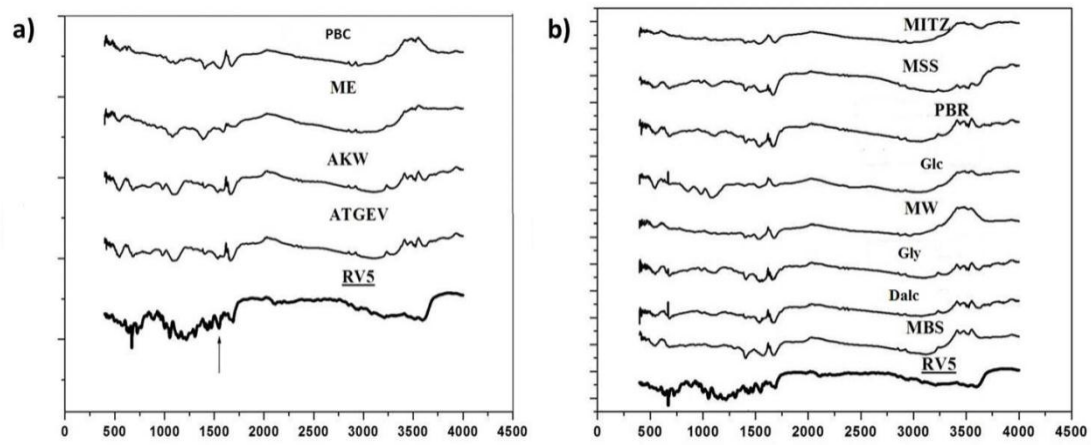

Figure 3.6 FTIR spectra of the decolorized end products of RV5R decolorizing acclimatized consortia.

[a) Static b) Shaking conditions;→, indicates the stretching vibration of a symmetrical trans-monoazo group peak]

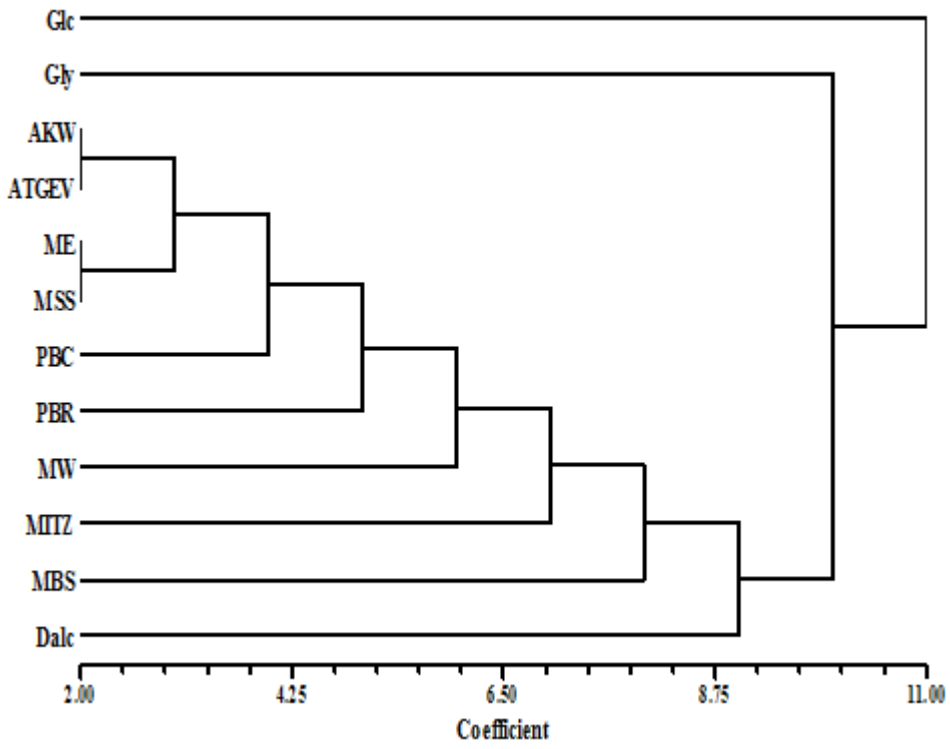

Figure 3.7 Dendrogram based on the presence of the functional groups present in treated fractions of acclimatized consortia.

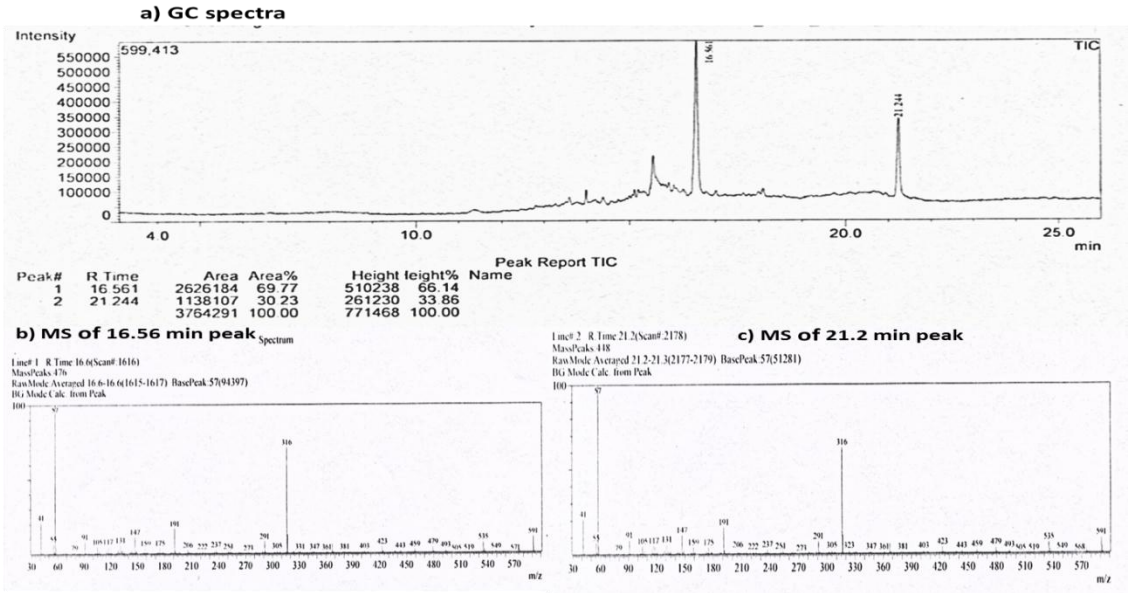

Figure 3.8 GC-MS analysis of the RV5R decolorization end products by Gly consortium.

[a) GC-MS spectra, b) RT peak at 16.56 and RT peak at 21.2]

3.2.5. RV5R decolorization by pure cultures from consortia

Different morphotypes of colonies were obtained from each consortium and were further studied for their decolorization ability in pure cultures. It was found that each consortium possessed active decolorizers as well as non-decolorizing members. Fig. 3.9 represents the decolorization ability of various isolates obtained from consortia. Isolates (name of the consortium from which the isolate was obtained is given in parenthesis) A3 (Gly), C1 (MITZ), G1 (MW), E2 (PBC), K1 (PBR), L1 (Dalc), L2 (Dalc) and ME1 (ME) were found to have efficient decolorizing ability, thus they must be the key decolorizing bacterial flora in the respective consortium. Non-decolorizing bacteria were also found to get enriched in the consortia indicating their resistance to the dye as well as perhaps active participation in the further degradation of the product of the decolorization process (Mikesková et al., 2012).Of the eight RV5R decolorizing bacterial isolates, 2 (L2, ME1) were gram positive and others were gram negative strains.

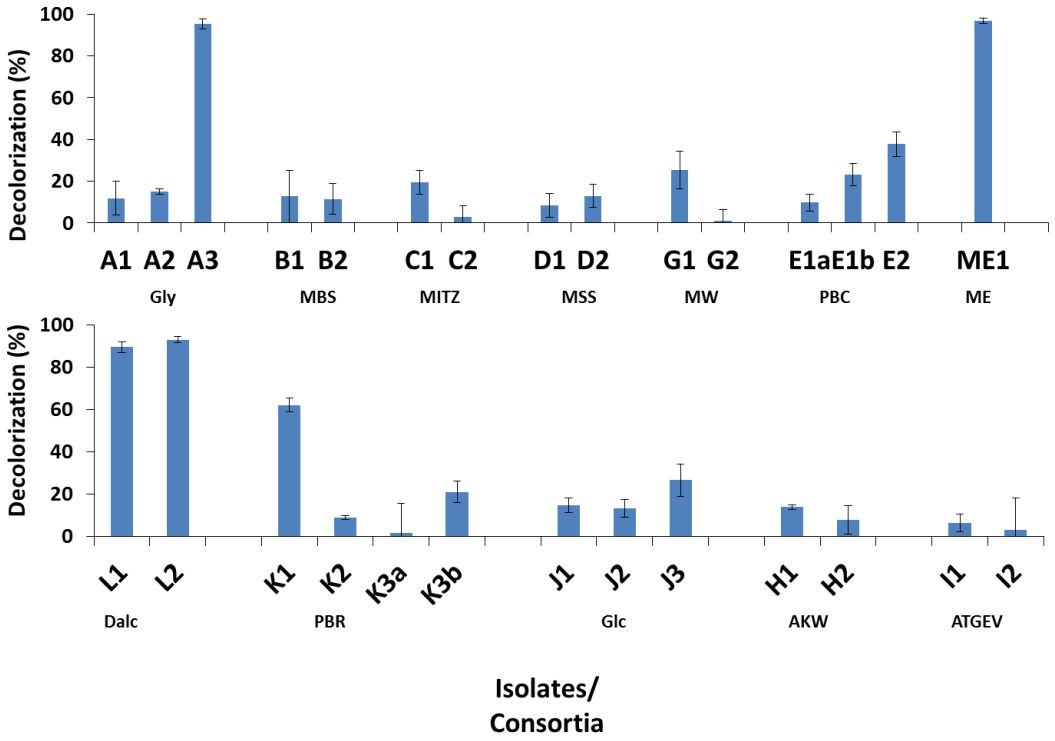

Figure 3.9Relative RV5R (100 mg/L) decolorization by bacterial pure cultures.

3.2.6. ARDRA analysis of RV5R decolorizing bacterial isolates

To understand the relationship amongst RV5R decolorizing bacterial isolates ARDRA was done. The genomic DNA of all the bacterial isolates used for the 16S rDNA

amplification by universal eubacterial primers. RE digestion was carried out by three different restriction enzymes namely HhaI, HaeIII and HinfI (Fig. 3.10).

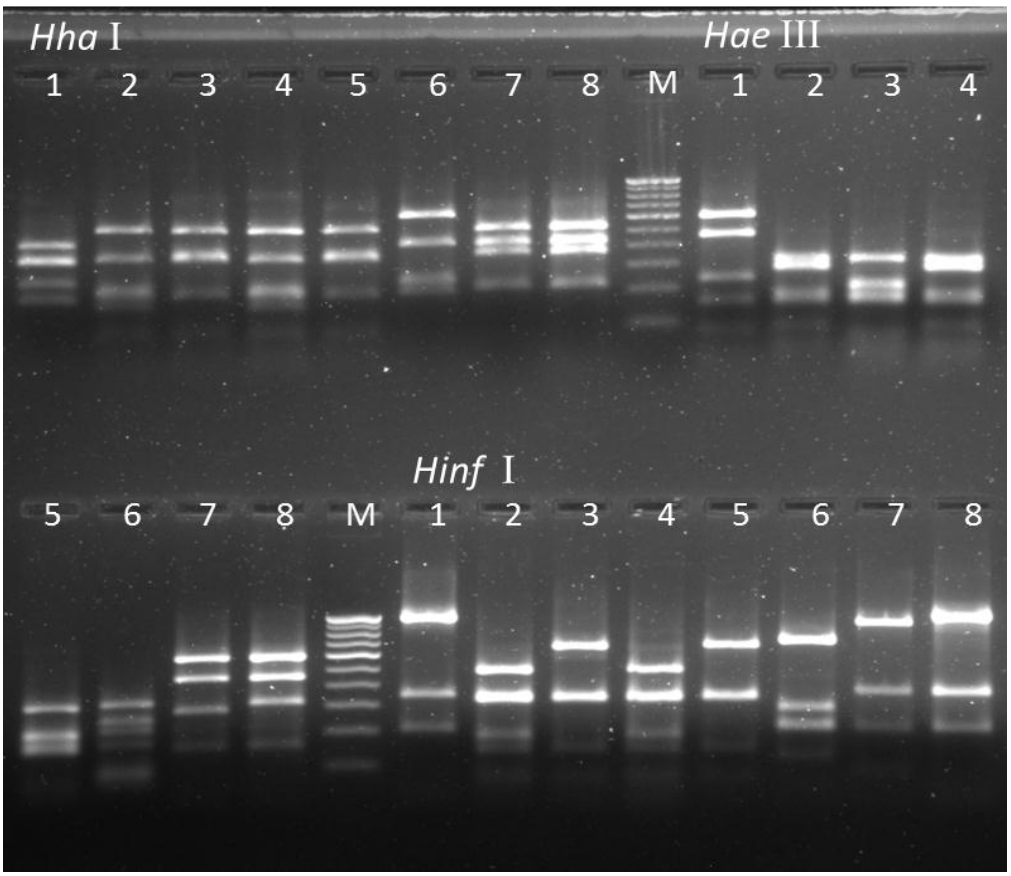

Figure 3.10ARDRA pattern of RV5R decolorizing bacterial isolates

(M- Marker 100bp) (Lanes: 1- A3, 2- C1, 3- E2, 4- G1, 5- K1, 6- L1, 7-L2, 8-ME1)

The phylogenetic tree constructed using combined band patterns of all the three enzymes (Fig. 3.11) shows that at coefficient of 3.5 four clusters were found. Isolates ME1 and L2 showed identical band patterns and clustered at highest co-efficient value.Isolates E2 and K1 clustered together so did C1 and G1.

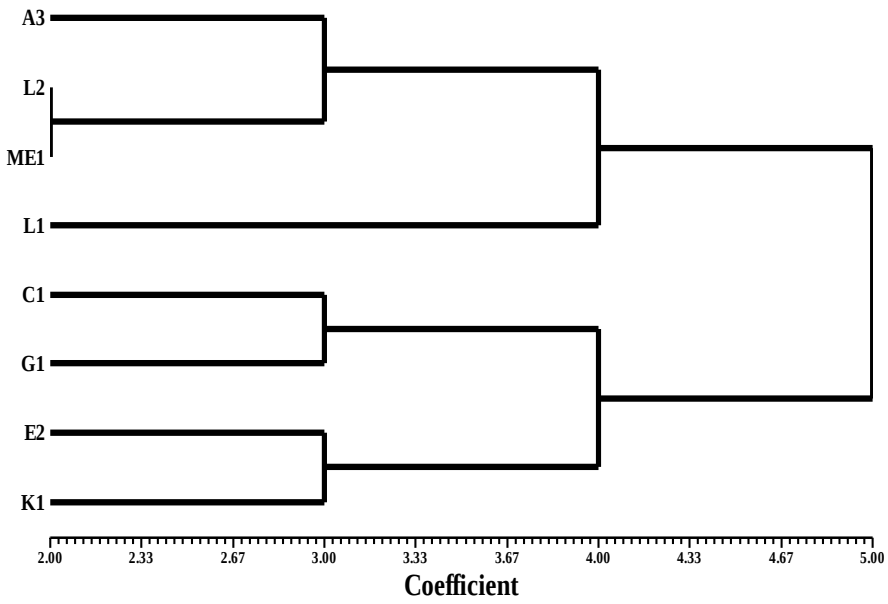

Figure 3.11Phylogenetic tree based on ARDRA analysis showing the relationship between different RV5R decolorizing bacterial isolates.

3.2.7. 16S rRNA gene sequence based identification of RV5R decolorizing isolates

Based on the 16S rRNA gene sequencing results two of the gram positive were identified as *Enterococcus*spp., whereas six of the gram negatives were found to belong to ɤ-proteobacteria. Two gram negative isolates were identified as *Providencia*spp.and two as *Klebsiella* spp.,whereas one strain of *Acinetobacter* and *Citrobacter* genus were identified (Table. 3.3).

Table 3.316s rRNA gene sequence based identification of RV5R decolorizing bacterial isolates

Isolates	GenBank Accession number	Best match with accession number	Similarity from database (%)	Isolate denoted as
A3	JQ745287	*Citrobacter*sp. S7 (HF572839)	99	*Citrobacter*sp. A3
C1	JQ745288	*Providencia vermicola* strain AR_PSBH1 (HM582881)	99	*Providencia* sp. C1
E2	JQ7452289	*Klebsiella pneumoniae* **s**train SW (AB641122)	99	*Klebsiella*sp. E2
G1	JQ7452290	*Providencia*sp. Sal2 (JN790944)	100	*Providencia* sp. G1
K1	JQ7452291	*Klebsiella pneumoniae strain ZB* (KC243315)	99	*Klebsiella*sp. K2
L1	JQ7452292	*Acinetobacter baumannii* strain DSM 30007T (HE978267)	100	*Acinetobacter* sp. L1
L2	JQ7452293	*Enterococcus faecalis* strain symbioflor 1 (HF558530)	99	*Enterococcus* sp. L2
ME1	JQ7452294	*Enterococcus casseliflavus* strain PX-EC (KC150018)	99	*Enterococcus* sp. L2

The 16S rRNA gene fragment sequences were utilized for building phylogenetic tree by MEGA 4.0. Identified isolates were phylogenetically clustered on the basis of 16S rRNA gene sequences and the phylogenetic tree shows nearest neighbouring type strains (Fig. 3.12).

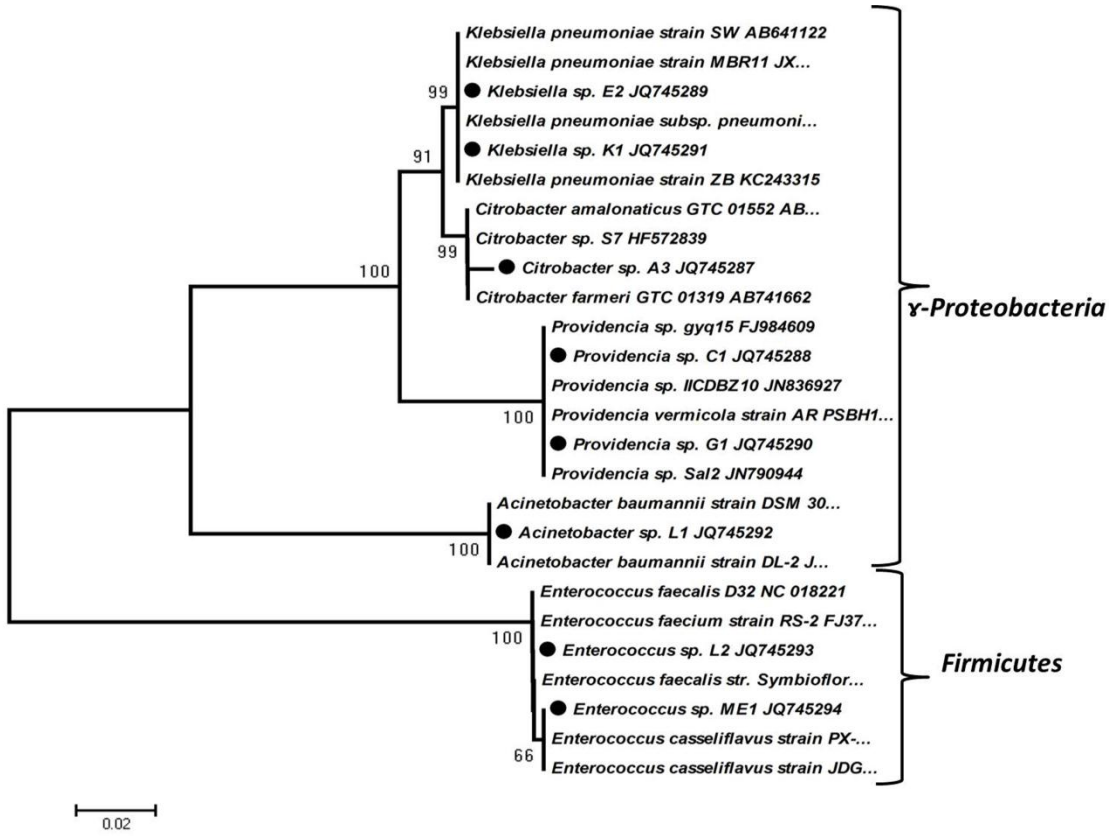

Figure 3.12Phylogenetic treeof the RV5R decolorizing bacterial isolates.

Tree was constructed based on 16S rRNA gene sequences and evolutionary history was inferred using the Neighbour-Joining method. The optimal tree with the sum of branch length = 0.37043799 is shown. The percentage of replicate trees in which the associated taxa clustered together in the bootstrap test (1000 replicates) are shown next to the branches. The tree is drawn to scale, with branch lengths in the same units as those of the evolutionary distances used to infer the phylogenetic tree. The evolutionary distances were computed using the Maximum Composite Likelihood method and are in the units of the number of base substitutions per site. All positions containing gaps and missing data were eliminated from the dataset (Complete deletion option). There were a total of 510 positions in the final dataset. Phylogenetic analyses were conducted in MEGA4 (Tamura et al., 2007). RV5R decolorizing bacterial isolates obtained from present study are indicated by dark circles.

3.2.8. Azo dye decolorization by bacterial isolates

Total eight bacterial isolates obtained from 12 microbial consortia were analyzed for decolorization of RV5R (Fig. 3.13 and 3.14).Isolates L2 and ME1 were found to decolorize RV5R more than 90% in 3 h. Isolates C1 and G1 took 30h to decolorize up to 90%. Other bacterial isolates showed slower decolorization under static and shaking conditions. Decolorization of methyl red (MR) (mono azo dye with two

benzene rings) by the bacterial isolates is shown in Fig. 3.15. As seen, 99% decolorization of MR was carried out by isolates L2 and ME1 within 5h and isolate C1 decolorized 98% of MR by 12 h (Fig. 3.15), whereas rest of the isolates took 18h to decolorize more than 90% of the dye. Decolorization of MR was relatively faster for most of the isolates than the decolorization of RV5R.

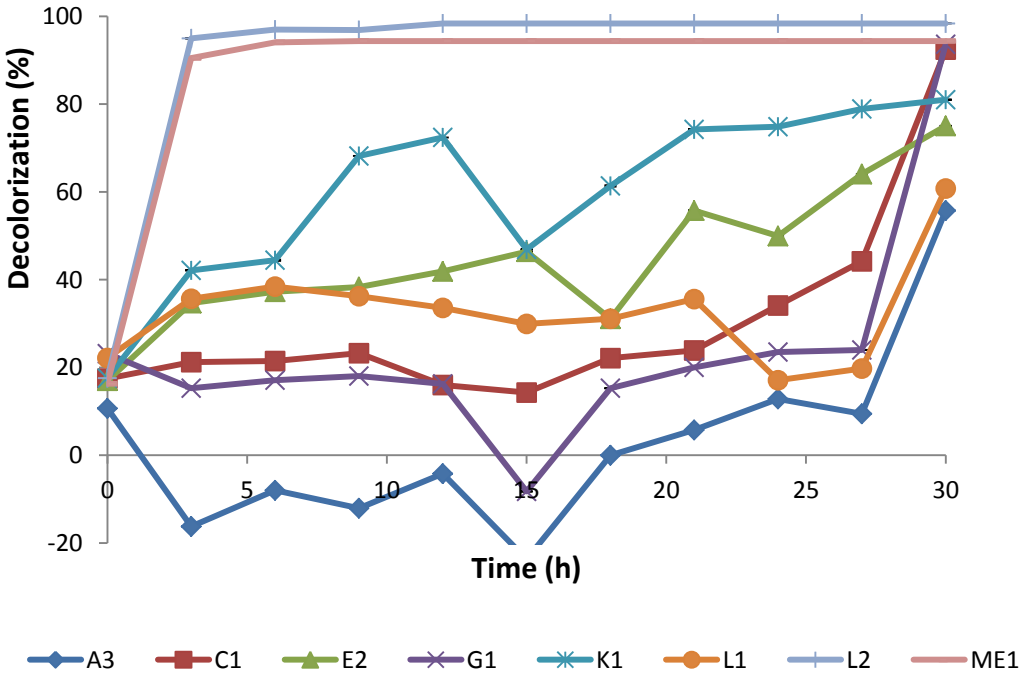

Figure 3.13 RV5R decolorization under static condition by bacterial isolates.

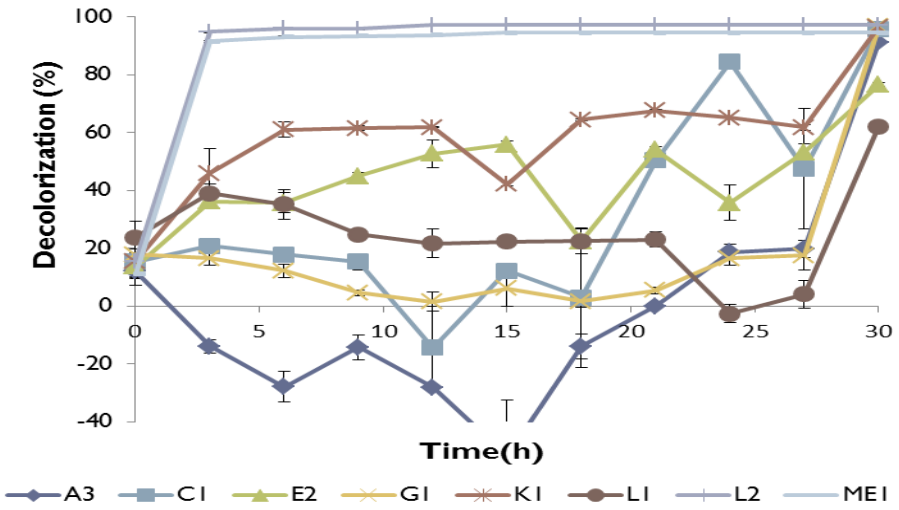

Figure 3.14 RV5R decolorization under shaking conditions by bacterial isolates.

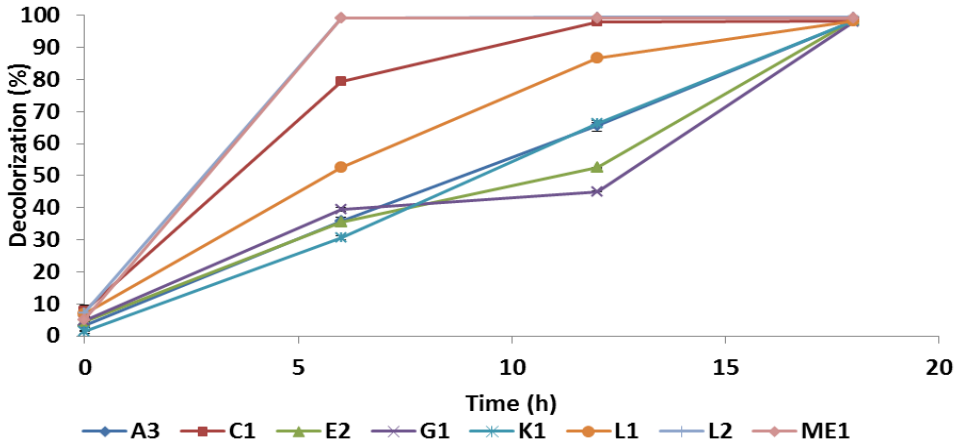

Figure 3.15 Methyl red decolorization by bacterial isolates.

3.2.9. Effect of various carbon sources on RV5R decolorization by bacterial isolates

RV5R decolorization by bacterial isolates in medium control having no C-source added (Bussnell Haas medium amended with only 0.5% w/v yeast extract) and media amended with different C-sources were compared (Fig. 3.16). Inoculation was done at similar O.D. of cells and incubated for 30h. Positive effect of C-source addition was found in case of most isolates except isolate C1 where medium without C-source added showed high decolorization. Glycerol was found to have positive effect on RV5R decolorization in case of isolates E2 and K1. Xylose enhanced RV5R decolorization in isolates G1 and L1. It is noteworthy that in all different decolorization studies, isolates L2 and ME1 were found to be the most efficient azo dye decolorizers (Fig. 3.16).

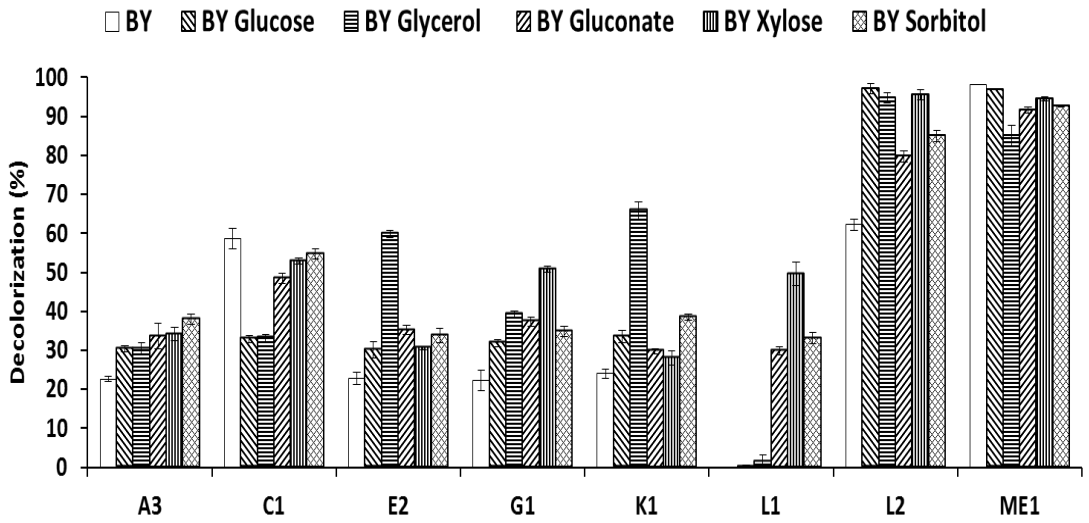

Figure 3.16Effect of different C-source on RV5R decolorization by bacterial isolates.

3.2.10. Azoreductase activity of bacterial isolates

Azoreductase activity was detected in the bacterial isolates by azoreductase assay and activity staining on native PAGE. *Enterococcus* L2 and ME1 had highest NADH- and NADPH-dependent azoreductase activities compared to the gram negative isolates (Table. 3.4). Overall NADPH dependent azoreductase activity is higher in all the isolates compared to the NADH dependent activity.

Results of activity staining showed all isolates have one or more NADH dependent azoreductases enzyme of different mobility on native PAGE (Fig. 3.17). *Providencia*spp. C1 and. G1, *Enterococcus*spp. ME1 and L2 show one NADH depdendent azoreductase band, whereas rest of the isolates *Citrobacter*sp. A3, *Klebsiella*sp. E2, *Klebsiella*sp. K1 and *Acinetobacter*sp. L1 possess up to 3 different NADH dependent azoreductases (Fig 3a). Isolates *Providencia*sp. C1 and *Providencia*sp. G1 have only one NAD(P)H dependent azoreductase, while *Klebsiella*spp. E2 and K1and *Enterococcus*sp. L2 possess two and isolate *Citrobacter*sp. A3 possesses three different NAD(P)H dependent azoreductases. Surprisingly, isolates*Acinetobacter* sp.L1 and *Enterococcus*sp. ME1 demonstrated no NAD(P)H dependent azoreductase activity band (Fig. 3.14a and b), although gave positive assay results.

Table 3.4NADH and NADPH dependent azoreductase specific activity of bacterial isolates (RV5R as substrate)

Isolate	**Azoreductase specific activity (µmole of dye reduced/min/mg of total protein)**	
	NADH	**NADPH**
*Citrobacter*sp. A3	5.79 ± 0.76(33.4%)	11.55 ± 0.9(66.6%)
*Providencia*sp. C1	5.77 ± 0.96(27.3%)	15.37±1.00(72.7%)
*Klebsiella*sp. E2	6.84 ± 1.04(31.5%)	14.88±1.16(68.5%)
*Providencia*sp. G1	5.62 ± 0.49(27.3%)	14.93± 0.8(72.7%)
*Klebsiella*sp. K1	5.07 ± 0.77(24.3%)	15.79±0.37(75.7%)
*Acinetobacter*sp. L1	5.34 ± 0.68(30.7%)	12.08±1.35(69.3%)
*Enterococuus*sp. L2	18.73 ± 1.91(38.5%)	29.87±2.14(61.5%)
*Enterococuus*sp. ME1	8.89 ± 1.23(36.5%)	15.48±0.57(63.5%)

Numbers in parenthesis indicate the percentage contribution of each type of activity (NADH and NADPH dependent).

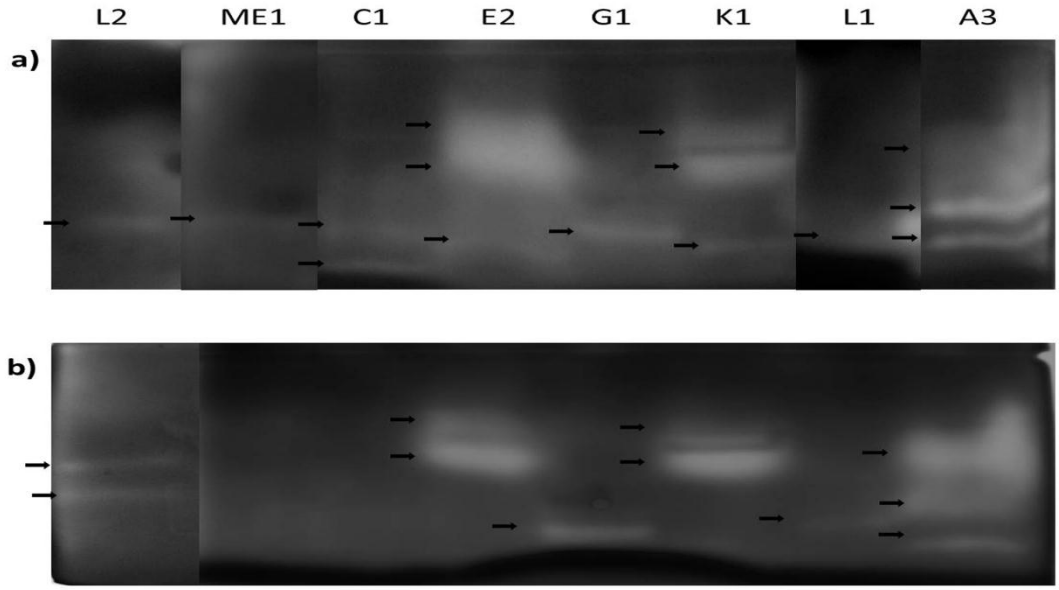

Figure 3.17NADH and NADPH dependent azoreductase activity staining.

a) NADH dependent and b) NADPH dependent azoreductases.

3.2.11. Effect of Redox mediators on RV5R decolorization by bacterial isolates

Electron shuttles or Redox mediators can help transfer electrons from electron donors to substrates (electron acceptors) and enhance reaction by increasing the activity sphere of the microbe.Quinone, indophenol, humic acid or flavin groups in nature often function as redox mediators. Azo dyes can act as electron acceptor from these redox mediators resulting in non-specific dye decolorization. Different concentrations of menadione, anthraquinone suphonate (AQS), anthraquinone 2,6 disuphonate (AQDS) and crude lawsone were used to see the effect of these redox mediators on RV5R decolorization. In the presence of 2.0 mM Menadione the bacterial isolates *Klebsiella* spp. K1 and E2 and *Acinetobacter* sp. L1 had removed approximately double the amount of the dye than the control within 15 h (Fig. 3.18a). In case of increase in the menadione concentration from 1.0 mM to 2.0 mM increase in the decolorization of the RV5R dye was seen, except *Enterococcus*spp. and*Citrobacter*sp. A3where menadione acted as an inhibitor. It was also found that isolates also decrease decolorization beyond optimum concentration of quinones (Fig. 3.18 b, c). AQS and AQDS showed an increase in the RV5R decolorization in case of all the isolates, however the increase was less than that found in case of menadione for *Klebsiella* spp. In case of *Klebsiella* strains effect of most of the redox mediators were found to be high and*Klabsiella*sp. K1 showed 1.6 fold increase in RV5R decolorization with 1% lawsone (Fig. 3.18d). Hydroxyquinone was also analyzed for its effect on decolorization, which was found negative (data not shown).

3.2.12. FTIR analysis of the RV5R decolorization/degradation end products by bacterial isolates

Shifting or dis-appearance of major absorption peaks in the Fourier transformed infrared spectroscopy (FTIR) spectrum of treated samples as compared to control dye sample demonstrates the decolorization/degradation process (Phugare et al., 2011; Jain et al., 2012b). Fig. 3.19 shows clear differences in the FTIR spectra of the bacterially decolorized products compared to the untreated dye control. The FTIR spectra of end products formed by different bacteria also varied. RV5R, a mono-azo reactive-textile azo dye demonstrated specific azo bond peak. Disappearance of this peak in the decolorized extracts of various culture supernatants shows cleavage of the azo bond (Table 3.5). The peaks corresponding to -CN asymmetric stretching at

1048.48 cm^{-1} and -SO_3H group 1139.89 and 1185.13 cm^{-1} peak disappeared in all the strains except in *Acinetobacter*sp. L1 wherein –CN asymmetric stretching was still observed indicating the presence of –NH_2 on the ring structure. Primary aromatic amines peaks were observed at 1335-1250 cm^{-1} in decolorized end products by isolated.

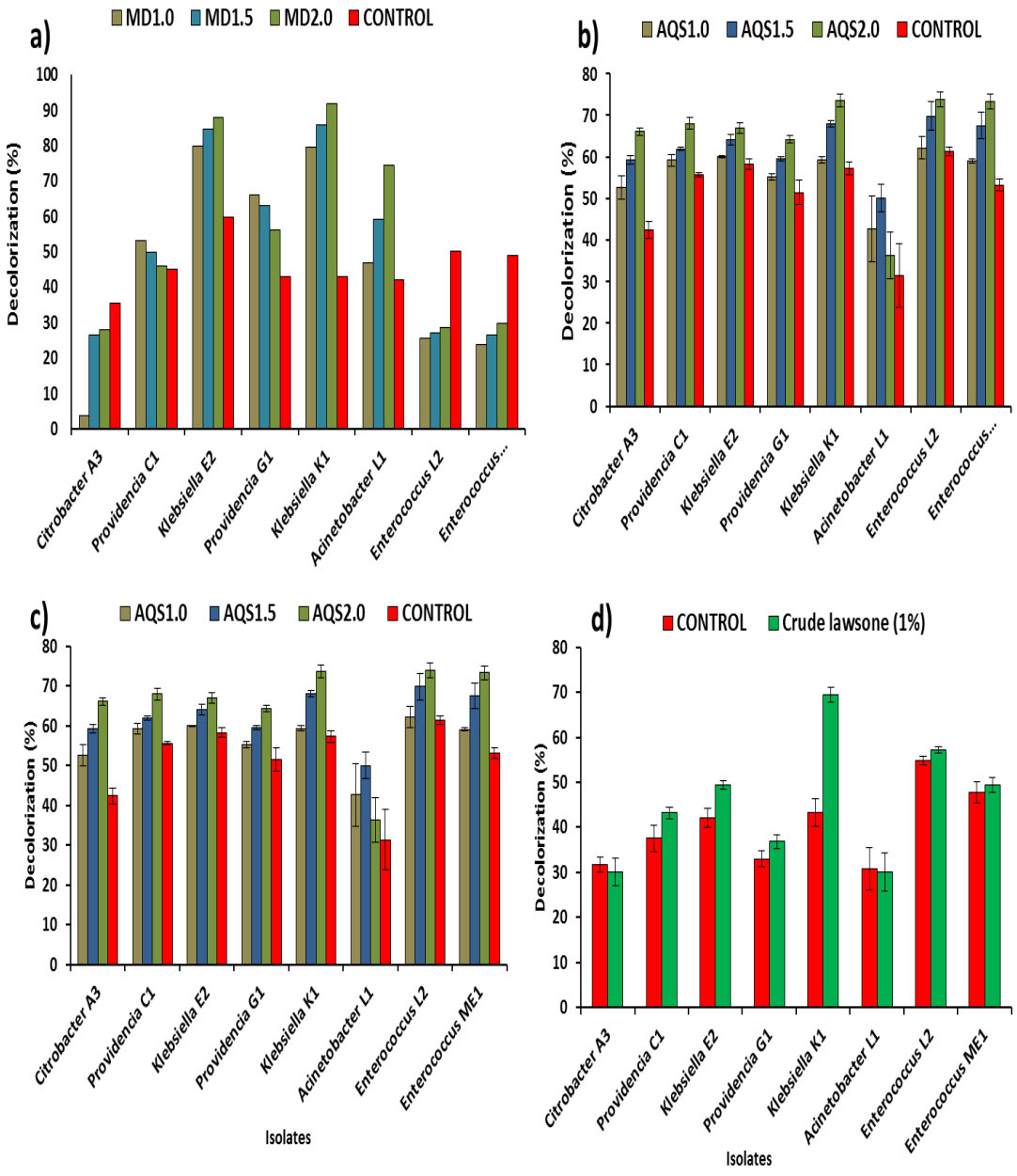

Figure 3.18Effect of redox mediators on RV5R decolorization by bacterial isolates.

a) Menadione; b) Anthraquinone-2-sulfonate (AQS); c) Anthraquinone-2,6-disulfonate (AQDS); d) 1% crude lawsone

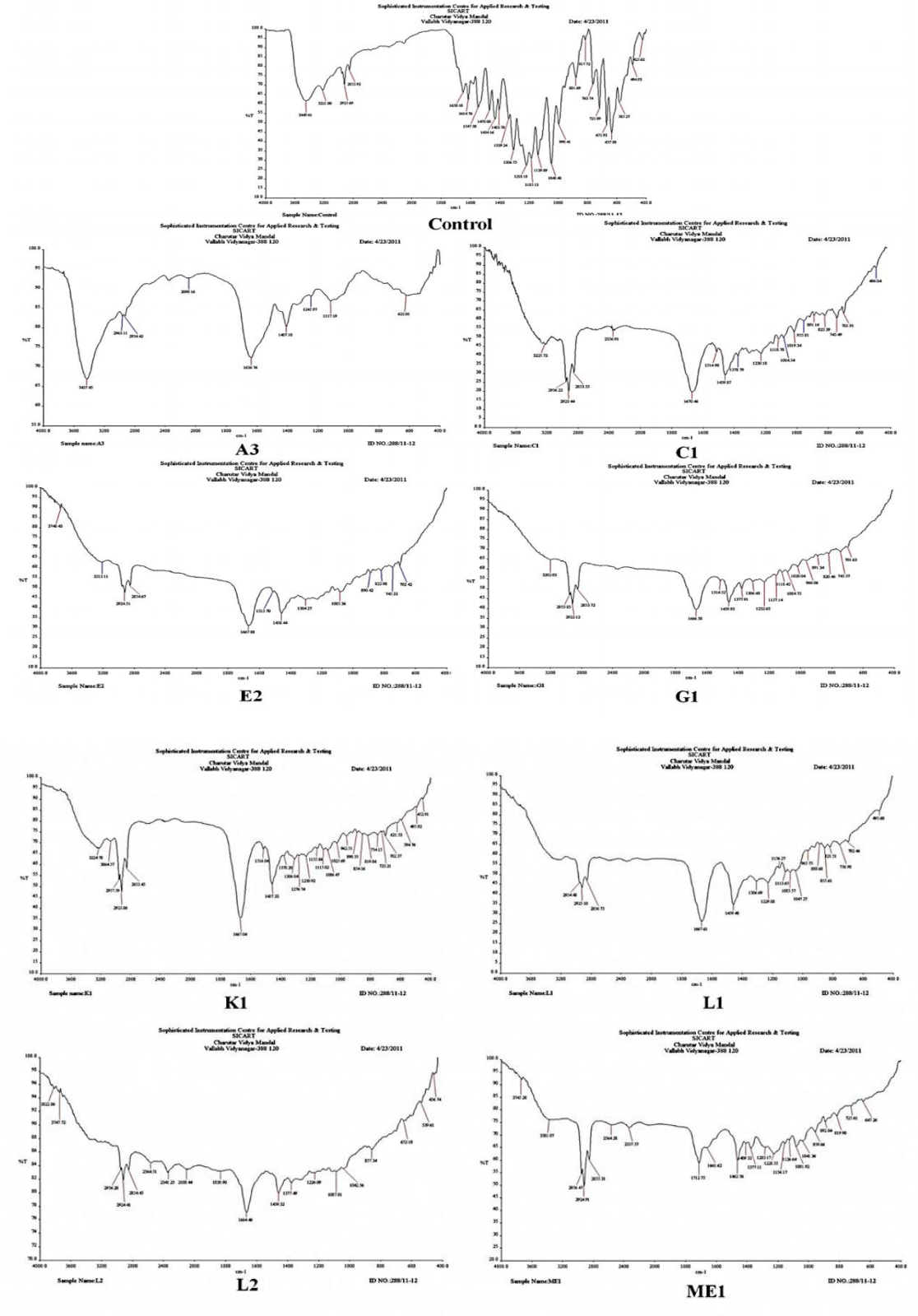

Figure 3.19FTIR spectra of RV5R decolorized/degraded end-products of bacterial isolates.

Table 3.5. Presence of key functional groups in FTIR spectra of RV5R decolorized end products

Sample	-N=N-	-CN asymmetric stretching	-SO_3H group
Control	+	+	+
*Citrobacter*sp. A3	-	-	-
*Providencia*sp. C1	-	-	-
*Klebsiella*sp. E2	-	-	-
*Providencia*sp. G1	-	-	-
*Klebsiella*sp. K1	-	-	-
*Acinetobacter*sp.L1	-	+	+
*Enterococcus*sp. L2	-	-	-
*Enterococcus*sp. ME1	-	-	-

3.2.13. Azo dye decolorization properties of *Enterococcus* sp. L2

Enterococcus sp. L2 was isolated from RV5R decolorizing bacterial consortium enriched from petroleum industry effluent sample (Vadodara, India) (16S rRNA gene sequence, GenBank accession no. JQ745293; Culture deposition accession no.MCC2124 at Microbial Culture Collection, NCCS, Pune, India).*Enterococcus*sp.L2 is a Gram positive microaerophilic diplococcus. Amongst the lab isolates it decolorizes RV5R and MR efficiently. *Enterococcus*sp. L2 was able to decolorize 97.6% of 100mg/L RV5R in 8 h under static condition. Profound acid formation was also found resulting in a decrease the medium pH 6.8 to 4.1.It is well known that *Enterococcus faecalis* grows best in the pH range of 5-8. Decolorization occurred only when carbon and nitrogen sources were available for growth, indicating that organism did not utilize dye as either carbon or energy source. In similar studies done by Sahasrabudhe et al. (2011) with *Enterococcus faecalis* strain YZ66, the strain showed complete decolorization of the selected dye (Reactive yellow 145- 50 mg/L) within 10 hours in static anoxic condition.Dye decolorization by *Enterococcus*sp. L2 was associated with growth, rather than the generally accepted view of biotransformation as a stationary phase phenomenon (Fig. 3.20). *Enterococcus*sp. L2 efficiently decolorized 500mg/L RV5R 63.9% with 29% decrease in growth compared to no dye control (Fig. 3.21).

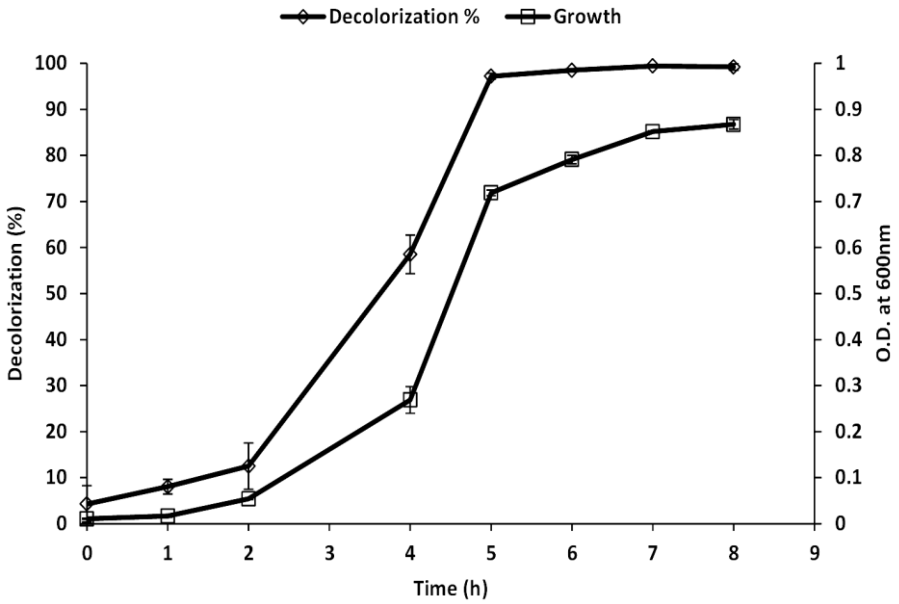

Figure 3.20Growth associated decolorization of RV5R by *Enterococcus* sp. L2

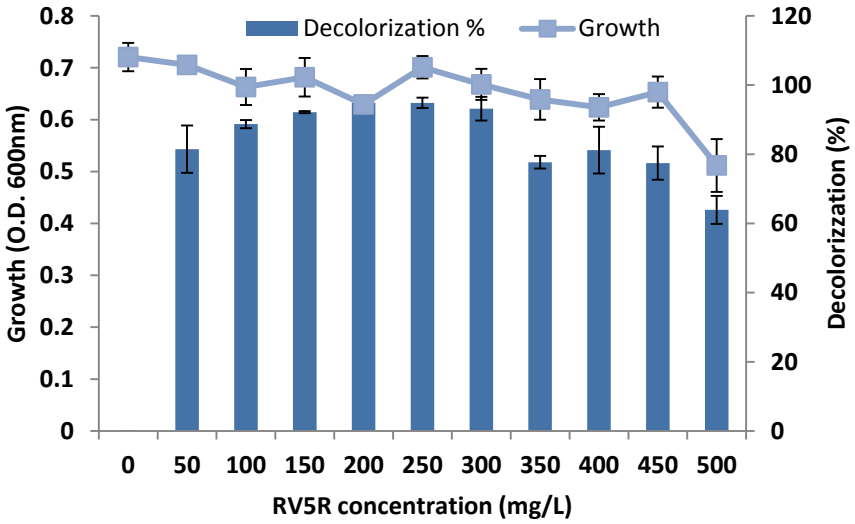

Figure 3.21 Growth and RV5R decolorization at different concentrations by *Enterococcus* sp. L2

To study the spectrum of the dye decolorized by *Enterococcus* sp. L2, different reactive group of azo dyes utilized in textile application were checked. *Enterococcus* sp. L2 was able to decolorize broad spectrum of azo dyes having complex chemical structures except Reactive yellow186 in 24h (Fig. 3.22).

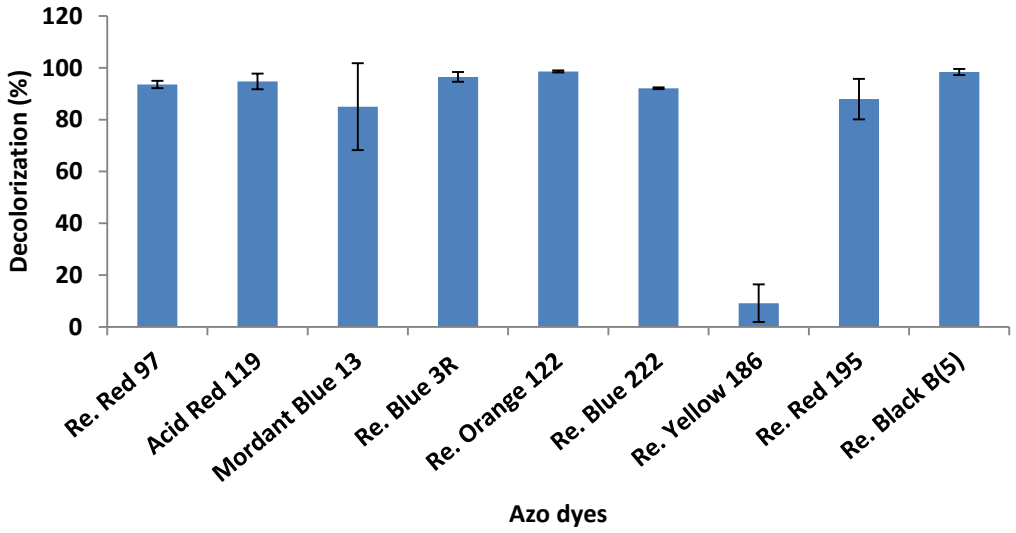

Figure 3.22Decolorization of various azo dyes by *Enterococcus* sp. L2

(Re.: Reactive)

The *Enterococcus*sp. L2 was found to decolorize RV5 dye (100mg/L) at an optimum medium pH of 7-8 and temperature 40^{o}C under static conditions (Fig 3.23 a,b).The isolate showed complete decolorization at 35 to 40^{o}C, however sharp decrease in the decolorization was observed above and below the optimum (Fig.3.23 b). Sahasrabudhe et al. (2011) reported *Enterococcus* strain to decolorize Reactive yellow at an optimum pH 5 and temperature for the decolorization at 37^{o}C. Maximum RV5R decolorization was found to be in the range of 0.5-2% NaCl (Fig. 3.23c), which is the basic survival and growth range of salinity for *Enterococcus* sp.*p.*(Fisher & Phillips, 2009).Flahaut et. al (1996) reported "flash adaptation" in *E. faecalis*, which makes this bacteria ideal for survival and growth under stress conditions under the bioremediation category.

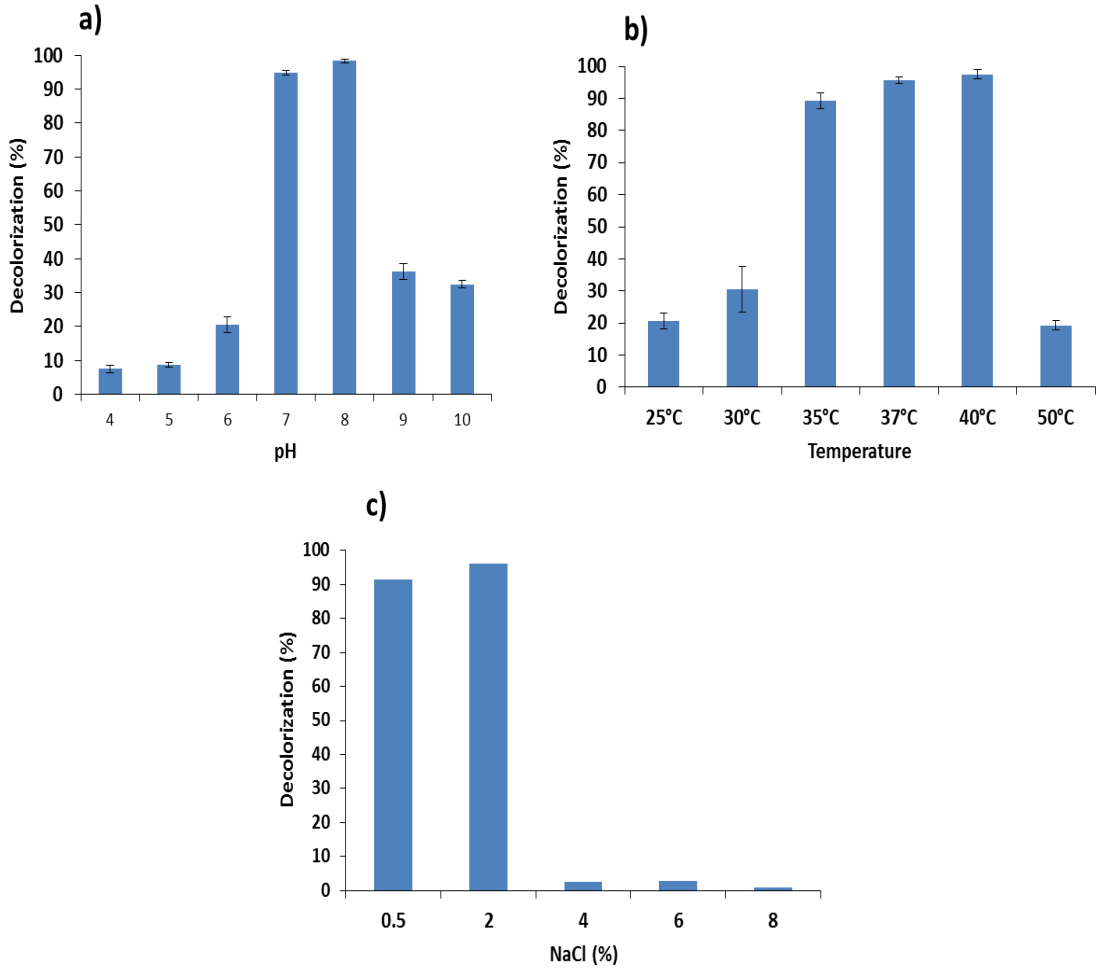

Figure 3.23 Physicochemical parameters of RV5R decolorization by *Enterococcus* sp. L2

a) pHrange b) Temperature c) Salinity as NaCl (%)

3.2.13.1. *Azoreductase activity of Enterococcus sp. L2*

The azoreductase activity of *Enterococcus* sp. L2 was found to be induced in presence of H_2O_2, quinones and azo dye (RV5R) (Table 3.6). This indicates that oxidative stress causing agents including electrophilic quinones resulted in 1.5-2.0 fold increase in azoreductase specific activity.The activity was also increased in the presence of the azo dye. Liu et al. (2009) by studying the transcription of *azoR* of *E. coli* using quantitative real time PCR showed constant basal level of *azoR* expression during different growth phases, however *azoR* expression was induced under the exposure to quinones such as2 -Methyl Hydroquinone (2-MHQ) and menadione as well as

diamide, catechol, and H_2O_2. The induction in azoreductase under oxidative stress conditions emphasizes its role in combating reactive oxygen species (ROS).

Table 3.6Inductionof azoreductase activity of *Enterococcus*sp. L2

Induction agent	Azoreductase Activity (µmole/min/mg)	Fold increase
None	21.6±3.6	
10mM H_2O_2	33.67±3.42[a]	1.56
2mM Menadione	37.26±2.98 [a]	1.72
2mM AQDS	41.65±3.25 [a]	1.93
200mg/LRV5R	39.36±2.85 [a]	1.82

[a] Values showed significant increase as compared to uninduced control at 1% level using one way ANOVA.

3.3.DISCUSSION

Microorganisms play an important role in the biodegradationof synthetic azo dyes. Reductive cleavage of the azo bond resulting in decolorization of the azo dye is the first step in dye degradation is considered as the bottleneck step in the degradation pathway. Present work was concentrated on the bacterial mode of degradation/decolorization by acclimatized microbial consortia and its indigenous members.

Bacterial acclimatized consortia have several advantages over pure or artificially mixed culture consortia. In this study, twelve acclimatized consortia wereenriched from pristine and contaminated environmental samples from the diverse locations of Gujarat, India which decolorized RV5R within 6-30h.McMullan et al., (2001) reported a requirement of the preadaptation of bacteria to decolorize and degrade carboxylated analogues of sulfonated azo compounds. In this work, it was observed that during initial transfers of the microbial consortia, decolorization was slow (50-60h), while after acclimatization the consortia were able to decolorize within 30h thereafter they were found to be stable in their decolorizing proficiency. Acclimatized consortia obtained during this investigation were found highly efficient, 10 consortia were decolorizing RV5R with a $t_{1/2}$of less than 10h while the most effective consortia had a $t_{1/2}$of only 3h. The decolorization kinetics of the consortia described here are superior to the kinetic studies reported for azo blue and azo orange with $t_{1/2}$of 14h and 10h by bacterial consortia developed from dye contaminated soil from Ngaoundere-Cameroon (Ndasi et al., 2012). Similarly, these consortia are more efficient than the one reported by Flores et al. (1997) who developed a methanogenic consortium adapted to mineralise azo dye after 200 d in a bioreactor with 99% dye removal.

Microbial community shifts are considered to play significantimpact on the bioprocess rate and these can be monitored effectivelyby 16S rRNA based diversity profiling techniques such as ARDRA, DGGE or clone sequencing(Kirk et al., 2004). Both ARDRA and DGGE techniques were used in the present study to compare the microbial diversity in the different RV5R decolorizing microbial consortia. In DGGE, the 16S rDNA PCR amplicons are directly fractionated on the basisof the differences in GC content and sequence, whereas in ARDRAthe community PCR products of 16S rRNA gene are subjected toRE digestion to reveal differences in the banding pattern

due tothe variation in occurrence of the particular RE site. Thus, the communityprofiles obtained for the same samples by the two techniquescould be expected to be dissimilar and may also showdifferences in clustering pattern in the dendrogram, as was observedin this study. Both the techniques showed the communitydifferences in 12 consortia, indicating that sample site and theenrichment conditions can result in the development of different members in the dye decolorizing consortia. In this regard, DGGEis more informative in providing insight into the members in populationand their abundances, whereas in ARDRA only overall similarityin communities is understood. Results obtained in presentstudy highlight similarities between two or more consortia as theirpopulation was found to be highly similar such as ATGEV and AKW as also the closely related MW and MITZ consortial communities. Acclimatized consortia enriched from highly contaminated niche were found to possess low H' index demonstrating reduced population diversity, indicating natural selection of resistant strains. Highest H' index was obtained for consortium MITZ which is from intertidal zone sample from a pristine marine environment while lowest H' index was found in AKW consortium obtained from highly contaminated waste water canal.

Fourier transform infrared (FTIR) spectroscopy is an important tool for rapid analysis of complex biological samples. The FTIR spectrum could be regarded as a "fingerprint" which is characteristic of the biomolecules present in the sample. It can be used as effective tool for characterization of microbial degradation products (Huang et al., 2006). Functional groups detection by FTIR analysis of the decolorized end products of each consortia demonstrated azo bond cleavage activity and further modification of the aromatic amines. The FTIR patterns of the end product functional groups were distinct for each consortium giving unique fingerprint like FTIR spectra. Based on the similarities in the groups detected the consortia could be clustered as depicted by dendrogram (Fig. 3.7). This provides a novel approach for comparing the dye degradation/decolorization end product profiles in a manner similar to the application of FTIR for rapid differentiation and classification of microbes (Naumann et al., 1991). Further, GC-MS of the metabolic end products of the most efficient consortium showed effective azo bond cleavage and benzene ring cleavage activity, although naphthalene ring was found to be intact. Benzene and naphthalene release

has been demonstrated as part of RV5R degradation, which are further degraded by gentisic acid pathway (Jain et al., 2012). A pathway for the degradation of the reactive group azo dye was proposed based on hydroxylation, carboxylation and redox reactions catalysed by different microbial enzymes (Gonza et al., 2009).

Pure cultures of RV5R decolorizing bacteria were screened from each of the consortia. Surprisingly, consortia ATGEV, AKW, MBS, MSS and Glc could not contribute effective RV5R decolorizing isolates indicating co-metabolic contribution of microbial community for RV5R decolorization. The Dalc consortium resulted in two efficient RV5R decolorizing isolates L1 and L2. In case of ME consortia only one pure culture was obtained, which was efficient RV5R decolorizing *Enterococrecus* sp. ME1, although several ribotypes were found by DGGE analysis. In every consortium both decolorizing and non-decolorizing members were obtained. Various azo dye decolorizing bacteria have been reported belonging to α- *Proteobacteria,* γ-*Proteobacteria,* cyanobacteria and *Firmicutes* (Saratale et al., 2011). In the present study RV5R decolorizing bacterial isolates were found affiliated to γ-*Proteobacteria*(6 isolates)and *Firmicutes* (2 isolates). Different samples from diverse locations were used to enrich diverse azo dye decolorizing consortia; however diverse consortia were found to possess strains of the same genus such as, *Providencia* spp. and *Klebsiella* spp. even though their enrichment media and incubation conditions were different. Activity staining of azoreductases of RV5R decolorizing isolates showed them to possess unique azoreductase profiles having NADH/NADPH dependency. Multiple activity bands were found in several strains indicating presence of more than one isozyme unlike single isozyme reported for *Clostridium* spp. (Rafii et al., 1990). *Enterococcus* sp. showed high NAD(P)H azoreductase activities compared to other gram negative strains.

Role of redox mediators (RMs) in azo bond reduction by bacteria has been reported by Dos Santos (2003) and van der Zee (2009).Different groups of eubacteria possess specific signature of quinone reductases which in turn define a substrate spectra of quinones that can be reduced and thus act as redox mediators. RMs speed up the reaction rate by shuttling electrons from the biological oxidation of primary electron donors or from bulk electron donors to the electron-accepting azo dyes (van der Zee et al., 2003).Flavin enzyme cofactors, such as Flavin adenine dinucleotide, Flavin

adenine mononucleotide, and Riboflavin, as well as several quinone compounds, such as Anthraquinone-2,6-disulfonate (AQDS), Anthraquinone-2-sulfonate (AQS), and Lawsone, have been found to act as RMs. Quinones can freely mediate extracellular reductions of azo dyes. The acceleration mechanism of RMs has been elucidated byZee and Villaverde(2005). In present study AQS and AQDS were found to be the most effective RMs, enhancing the rate of azo dye decolorization. Particularly, positive effect was observed at optimum concentrations, at higher concentration quinones addition showed negative effect on decolorization. Similar effect was also found in the experiment carried out by Rau el al. (2002) wherein deleterious effect of quinone lead to decrease in the azo dye decolorization and growth. Menadione might have shown oxidative stress on *Citrobacter* sp. A3, *Enterococcus* sp. L2 and *Enterococcus* sp.ME1 which at high concentrations led to negative effect decolorization. Significant results were obtained in presence of AQS and AQDS showing ~10 to 20% increase in decolorization at optimum concentration. These results support the hypothesis that based on type of quinone reductase system available in each bacteria, effect of RMs on dye decolorization differs.

FTIR profiles of the end products of RV5R decolorization/degradation by pure cultures of bacterial isolates suggest that they were capable of removing the sulphonate groups from the dye structure and reducing its polarity, which enables them to pass through the membrane barrier.

Enterococcus sp. L2 was further characterized for azo dye decolorization since it was the most efficient among all the bacterial isolates obtained in this study. *Enterococcus*spp. have been reported for decolorization of azo dyes (Bafana et al., 2008d; Handayani et al. 2007; Mate & Pathade, 2012). In most instances, dye decolorizing isolates of *Enterococcus* spp. have been obtained from intestinal flora, which is generally rich in azo dye decolorizers as they are exposed to azo dyes from environmental contamination as well as food, drugs and cosmetics (Chen et al., 2004). In this study, *Enterococcus* sp. L2 was obtained from Dalc consortium enriched from the petroleum industry effluent from Vadodara, India and *Enterococcus* sp. ME1 was obtained from effluent of a dye manufacturing industry. The *Enterococcus* sp. L2 displayed efficient RV5R decolorization with complete decolorization in 5-6 h (100mg/L) and could decolorize up to 500mg/L. This correlated well with its high

azoreductase activity and the demonstration of two isoforms of azoreductases. The broad spectrum of azo dyes by this organism reflects the ability of the azoreductases to utilize multiple substrate. Previously *Enterococcus* spp. have been reported to decolorize azo dyes such as Acid red 27, Reactive red 195 and Direct Black 38 (Bafana et al., 2008d; Handayani et al. 2007; Mate & Pathade, 2012). With contribution of this work the repertoire of dyes decolorized by enterococcal strains has been further expanded. The characteristics of dye decolorization kinetics, dye spectrum, effect of pH, temperature and NaCl suggest the wide applicability of this strain in azo dye decolorization.

Summarizing, the salient findings of this Chapter, samples from both pristine and contaminatedniches lead to development ofacclimatised RV5R decolorizing microbial consortia. Total 12 efficient RV5R decolorizingacclimatised consortia were enriched having different RV5R decolorization kinetics, incubation conditions and media used for enrichment. Culture independent community profiling of the dye decolorizing consortia usingARDRA and DGGE analysis showed their population diversity and species richness. Acclimatised microbial consortium Gly wasfound to efficiently degrade RV5R.*Enterococcus* spp. L2 and ME1 were found to be the most effective RV5R decolorizing bacterial isolateswith high azoreductase activity and decolorization abilities under various conditions as compared to the gram negative isolates. Growth associated RV5R decolorization by *Enterococcus* sp. L2 was found to be optimum up to 40°C, pH 8 and 2% NaCl salt conditions which makes it interesting for further studies. Various isolates could be used for further enhancement studies for azo dye decolorization as host system for synthetic biology approach. *Enterococcus* spp. having high azoreductase activities could be a potential source for azoreductase gene which was used for overexpression studies in the following Chapters.

4 Azoreductase (*azoA*) from *Enterococcus*sp. L2: cloning, heterologous expression and physiological role

4.1. Introduction

Azoreductases are enzymes involved in the azo dye decolorization and catalyse the reductive cleavage of the azo bond. These enzymes find their presence in difference class of enzyme such as E.C. 1.7.1.6, E.C. 1.5.1.30 and E.C. 1.6.5.2 based on selective enzymes able to act on azo substrates. They may be flavin independent or flavin-dependent reductases and belong to quinone reductase family (Rau et al., 2000; Deller et al., 2008). Flavin independent azoreductases are found to be monomeric while the flavin dependent enzymes are found in polymeric forms as homodimer or homo-tetramer. The flavin-dependent azoreductases are further organized into three groups depending on the co-enzymes that serve as electron donors; those preferring NADH only (Nakanishi et al., 2001; Chen et al., 2004), NADPH only (Chen et al., 2005) or both NADH and NADPH(Ghosh et al., 1992b; Wang et al., 2007).Azoreductases have been reported from diverse biological systems from prokaryotes to mammals(Bafana and Chakrabarti, 2008). Among eubacteria azoreductase have been well characterized from *Escherichia coli*(Nakanishi et al., 2001) , *Pseudomonas*sp. (Ryan et al. 2010) , *Citrobacter*sp. strain KCTC 18061P (Jang et al., 2007), *Xanthomonas campestris* MTCC10108 (Sharma et al., 2011), *Pigmentiphaga kullae* K24 (Stolz, 2003) and *Enterococcus*spp.(Chen et al., 2004; Punj and John, 2008, 2009). Thermostable azoreductase from *Geobacillus stearothermophilus*(Matsumoto et al., 2010) and alkali-thermostable azoreductase from *Bacillus*sp. strain SF (Maier et al., 2004a) have shown to justify need of the industrial dye decolorization process. Azoreductase are found to be oxygen sensitive and insensitive from different microorganisms. Under anaerobic or oxygen depletion conditions resting cells of bacteria such as *Bacteroides* spp., *Eubacterium*sp., *Clostridium* and facultative anaerobes *Proteus*sp. and *Streptococcus*sp. due to fermentative metabolism cytosolic NAD(P)H concentration increases and alternative electron acceptors are recognized, one of the reductase supported under this physiological state are anaerobic azoreductases (e.g. AzoC) for azo dye decolorization. Under aerobic azo dye decolorization is mainly considered to be enzymatic mode by aerobic azoreductase (*azoA*, AzoB, AZR and AzoR) which are basically oxygen tolerant, thus able to show in vitro activity in presence of

atmospheric oxygen. Crystal structure of aerobic FMN-dependent azoreductases AzoA and AzoR from *Enterococcus faecalis* and *E.coli* have been elucidated at 2.07A˚ and 1.8 A˚ resolutions respectively with bound FMN ligand (Ito et al., 2006; Liu et al., 2007). Ligand-bound structure of an azoreductase from *Pseudomonas aeruginosa* has shown the hydrophobic interaction between FMN and the active site in the protein. The structure of the ligand-bound protein also highlights the π-stacking interactions between FMN and the azo substrate(Wang et al., 2007). This group of enzymes catalyse the reduction using bi-bi ping-pong mechanism for electron transfer (Liu et al., 2008; Bürger and Stolz, 2010).

Major studies involved a overexpression, purification and biochemical characterization for enzyme kinetics of azoreductases from different microorganisms such as *E. coli*, *Enterococcus*sp., *Enterobacter*sp., *Shigella*sp. and *Bacillus*sp.; however in vivo studies of azoreductase heterologous expression are limited. The genes of NADH-dependent azoreductase (GenBank AY422207) and NADPH-dependent azoreductase (GenBank AY545994) were overexpressed in *E.coli* cells lead to growth perturbation in presence of 200 and 250 mM Methyl red, respectively(Kim et al., 2009), apparently efficient dye decolorization from *E. coli* strain BL21-Gold (DE3)pLysS harboring pAzoA required external source of NADH as coenzyme (Feng et al., 2010).

The requisite to isolate, identify and characterize newer genes from different environment sources and microorganisms by various methodsis the need of the synthetic biology based bioremediation strategy (Shah and Madamwar, 2013). *Enterococcus*sp. L2 and ME1 are our novel isolates obtained from Dalc and ME consortia which were enriched from petroleum and dye manufacturing industry effluents respectively (Chapter 1). These strains were found to be most efficient among all the isolates obtained in this study for Reactive violet 5R (RV5R) and Methyl red (MR) decolorization as well as they are better than the most of the reported strains (Chen, 2004, Saratale et al., 2011). Thus *Enterococcus* spp. are of interest as azoreductase gene source. So far physiological role of azoreductase (*azoR*) have been demonstrated in oxidative stress management in *E. coli*, thus physiological role of this enzyme has been an enigma.

This chapter deals with cloning and overexpression of *azo*A gene from *Enterococcus*sp. L2 and its contribution to the decolorization properties of the host strains. Further physiological role of AzoA was studied by constructing a knockout strain for *azoA* and by overexpression of *azoA* in *Enterococcus*sp. L2.

4.2. Results

4.2.1. Cloning of azoreductase gene from *Enterococcus* sp. L2 and ME1

Isolates L2 and ME1 were identified as *Enterococcus*spp. based on 16S rRNA gene sequence. Isolate *Enterococcus* spp. L2 and ME1 were found to be positive for NADH as well as NADPH dependent azoreductase activities, with strain L2 showing higher activities of 18.7 and 29.9 µmole/min/mg, respectively (Table 3.4,Chapter 3). Using nucleotide primers (*azoA*F and *azoA*R, Table 2.5, Chapter 2) complementary to the azoreductase of *Enterococcus faecalis*ATCC 19433 deposited at NCBI, regionsencoding *azoA* in *Enterococcus*sp. L2 and ME1 were amplified as approximately 650 bp fragment (Fig. 4.1). Sequencing of the PCR amplicons from both the strains showed that the sequences had 99% (Strain L2, (GenBank accession no. KC254724) and 98% (Strain ME1) similaritywith the reported *azoA* gene sequence from *Enterococcus faecalis* ATCC 19433. Figure 4.2 shows the multiple sequence alignment of *azoA* gene sequences from *Enterococcus faecalis* ATCC19433, *Enterococcus* sp.L2and *Enterococcus* sp. ME1. Since the sequences from two strains were very similar further work was continued with *azoA* gene of *Enterococcus*sp. L2. Gene *azo*A from *Enterococcus* sp. L2 was cloned in pBBR1MCS2 under plac promoter of the vector. pBBR1MCS2 is a broad host range gram negative mobilizable expression vector having origin of replication of *Bordetella* sp. (Kovach et al. 1995). These series of vectors have been reported to drivethe expression of the cloned gene under p*lac*in various gram negative hosts (Patel et al., 2010b). The PCR amplified *azoA*product from strain L2 was designed to carry gram negative ribosome binding site (RBS) upstream of start codon for ideal translation (Ma et al., 2002).

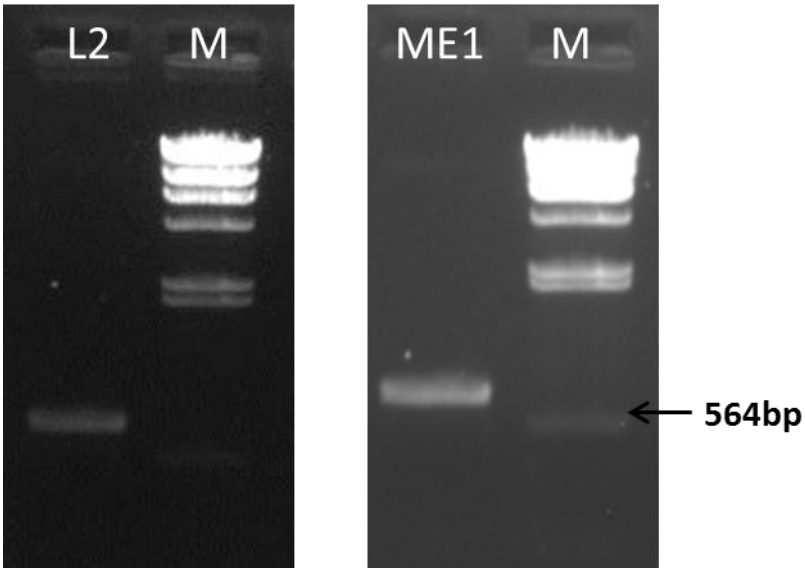

Figure 4.1 PCR amplification using *azoA* specific primers from *Enterococcus* spp. L2 and ME1

(M- λ/HindIII digest marker)

Sequence View: Similarity Format, Color areas of high matches at same base position

```
azoA ATCC194      1 atgtcaaaattattagttgttaaagcacatccattaacaaaagaagaatcacgctcagttcgtgcgttagaaacatttttagcttcataccgtgaaacaaatccatcagacgaaatcgaaatttttagatg
azoA L2           1 atgtcaaaattattagttgttaaagcacatccattaacaaaagaagaatcacgctcagttcgtgcgttagaaacatttttagcttcataccgtgaaacaaatccatcagacgaaatcgaaatttttagatg
azoA ME1          1 atgtc-aaattattagttgt-aaagcacatccattaacaaaagaagaatcacgctcagttcgtgcgttagaaacatttttagcttcataccgtgaaacaaatccatcagacgaaatcgaaatttttagatg

azoA ATCC194     131 tttatgcaccagaaacaaacatgccggaaatcgatgaagaattattatctgcttggggtgcacttcgagctggcgcagcatttgaaacattaagcgaa---aaccaacaacaaaaagtggctcgtttttaa
azoA L2         131 tttatgcaccagaaacaaacatgccggaaatcgatgaagaattattatctgcttggggtgcacttcgagctggtgcagcatttgaaacattaagcgaa---aaccaacaacaaaaagtggctcgtttttaa
azoA ME1        129 tttatgcaccagaaacaaacatgccggaaatcgatgaagaattattatctgcttggggtgcacttcgcgctggtgcagcatttgaaacattaagcgaagaaaaccaacaacaaaaagtggctcgtttttaa

azoA ATCC194     258 tgaattaactgatcaatttttatctgcagacaaagtagtaattgctaatccaatgtggaacttaaacgtaccgacacgcttaaaagcttgggtagatacaatcaacgttgctggaaaaacattccaatat
azoA L2         258 tgaattaactgatcaatttttatctgcagacaaagtagtaattgctaatccaatgtggaacttaaacgtaccgacgcgcttaaaagcttgggtagatacaatcaacgttgctggaaaaacattccaatat
azoA ME1        259 tgaattaactgatcaatttttatctgcagacaaagtagtaattgctaatccaatgtggaacttaaacgtaccgacgcgcttaaaagcttgggtagatacaatcaacgttgctggaaaaacattccaatat

azoA ATCC194     388 actgcagaaggaccaaaacctctaacaagtggtaaaaaagccttacacatccaatcaaatggcggcttctacgaaggaaaagattttgcttctcaatacattaaagcgattctaaactttattggcgttg
azoA L2         388 actgcagaaggaccaaaacctctaacaagtggtaaaaaagccttacacatccaatcaaatggcggcttctacgaaggaaaagattttgcttctcaatacattaaagcgattctaaactttattggtgttg
azoA ME1        389 actgcagaaggaccaaaacctctaacaagtggtaaaaaagccttacacatccaatcaaatggcggcttctacgaaggaaaag-ttttgcttctcaatacat-aaagcgattctaaactttattggtgttg

azoA ATCC194     518 atcaagtcgacggattattcatcgaaggaatcgatcatttccctgatcgcgcggaagaacttttaaatactgccatgaccaaagcaactgaatacggtaaaacattctaa
azoA L2         518 atcaagttgacggattattcatcgaaggaatcgatcatttccctgatcgcgcggaagaacttttaaatactgccatgaccaaagcaactgaatacggtaaaacattctaa
azoA ME1        517 atcaagtcgacggattattcatcgaaggaatcgatcatttccctgatcgtgcggaagaacttttaaatactgctatgaccaaagcaact----------
```

Figure 4.2Multiple sequence alignment of the *azoA*gene sequences from *Enterococcus* spp. L2 and ME1 with reference sequence of *E. feacalis* ATCC 19433

For the cloning of the *azoA* gene from *Enterococcus*sp. L2, it was PCR amplified using PR polymerase having high fidelity (Fig. 4.3a) and purified for blunt end ligation with EcoRV digested pBBR1MCS2 linearized vector (5.1kb) (Fig. 4.3b).Ligation mixturewas subjected to EcoRV digestion to avoid the self-ligated

vector background. Subsequently it was transformed in to *E. coli* DH5αand putative clones were screenedby blue white selection. Plasmids from white colonies were subjected to SalI digestion and clones with correct orientation to plac promoter showed a release of ~550bp insert fragment (Fig. 4.4) and subsequently confirmed by PCR amplification with *azoA* specific primers (data not shown). One of the positive clones was denoted as pBBR1MCS2*azoA*and used for further studies.Map of the plasmid pBBR1MCS2*azoA* is depicted in Fig. 4.5.

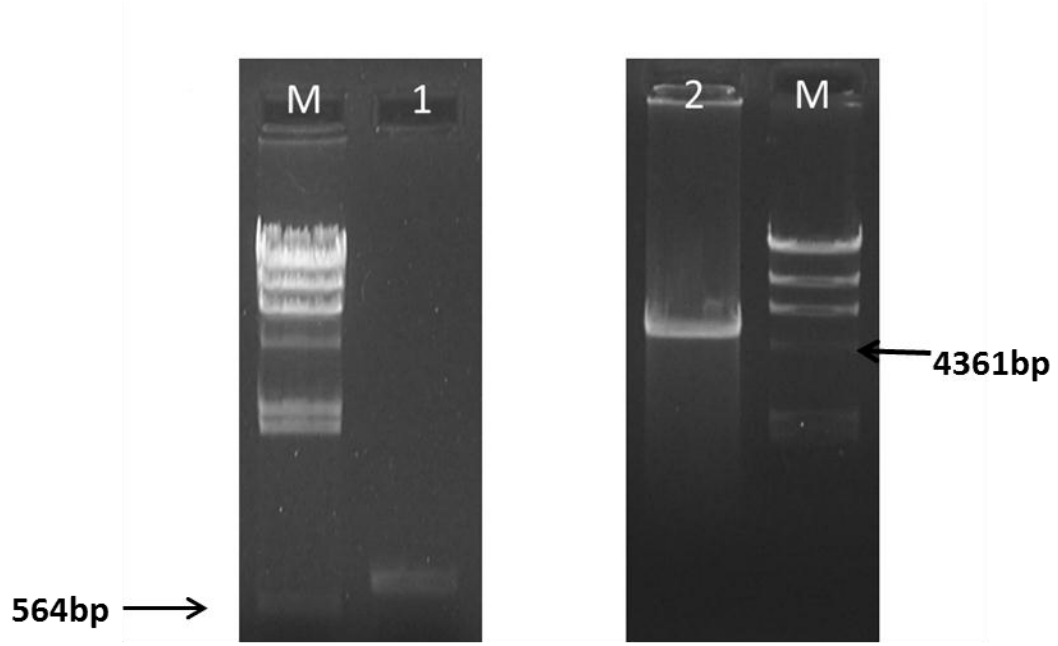

Figure 4.3 PCR amplification of *azoA* by PR polymerase and EcoRV digested pBBR1MCS2.

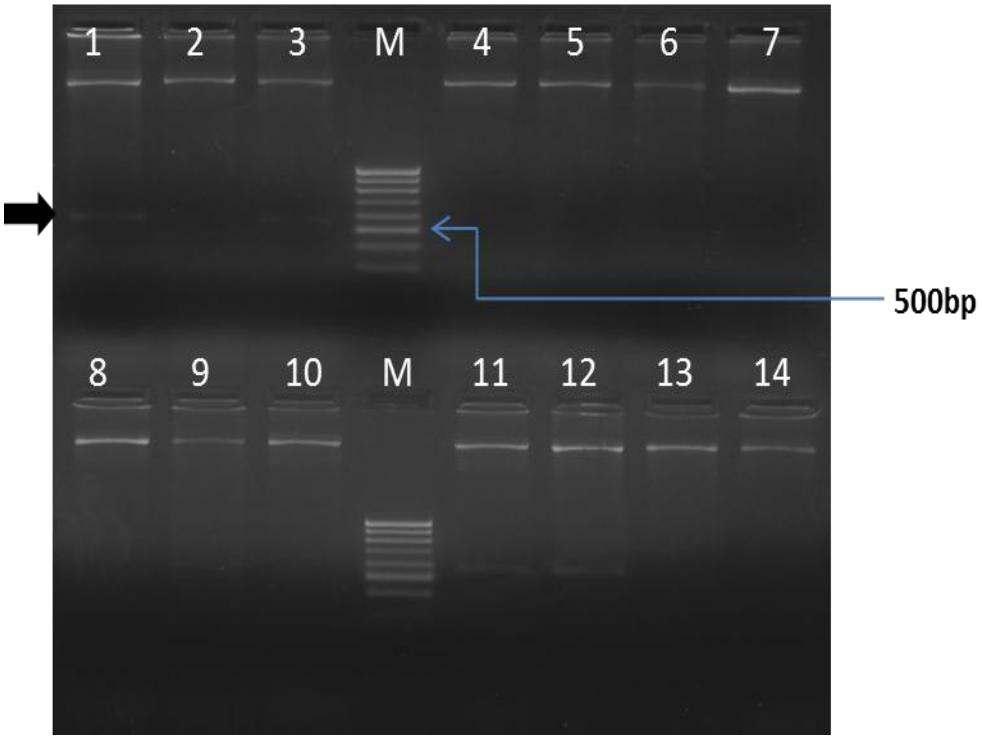

Figure 4.4 SalI digestion of putative clones of pBBR1MCS2*azoA*.

(M- 100bp ladder; Dark black arrow shows the 550bp insert release in clones with correct orientation to p*lac*)

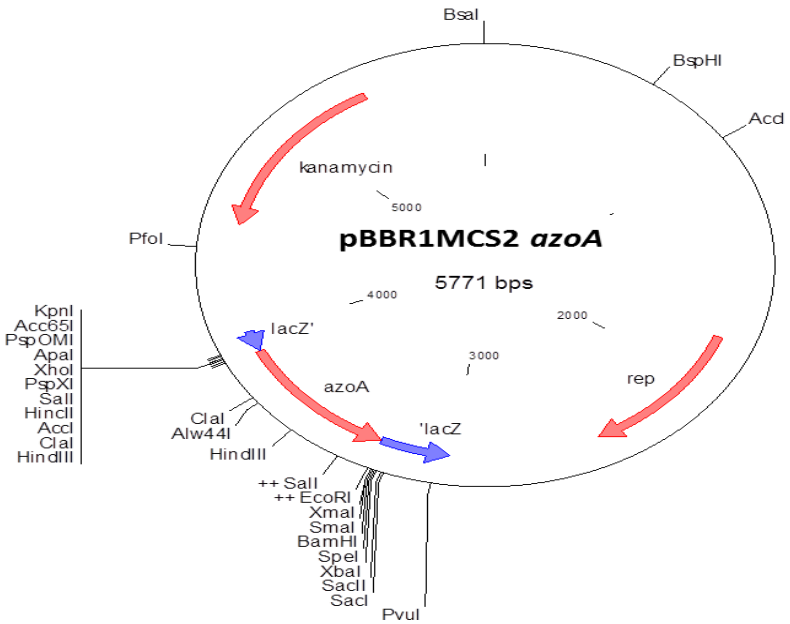

Figure 4.5 Map of pBBR1MCS2*azoA*

4.2.2. Heterologous expression of *azoA* from *Enterococcus* sp. L2 in various gram negative hosts

pBBR1MCS2*azoA* was transformed in to various gram negative standard strains(*E. coli* DH5α and *Pseudomonasfluorescens* PfO-1) and bacterial isolates (*Citrobacter*sp. A3, *Providencia*sp. C1, *Klebsiella*sp. E2, *Providencia*sp. G1, *Klebsiella*sp. K1 and *Acinetobacter*sp. L1; Table 3.3 Chapter 3) by chemical transformation. All the transformants of isolates were confirmed for host identity using ARDRA shown in chapter 5 with other transformants confirmation. These RV5R decolorizing bacterial isolates were transformed with pBBR1MCS2*azoA* for heterologous expression to analyze for enhancement of azo dye decolorizing phenotype. Each of these strains was also transformed with empty pBBR1MCS2 plasmid and considered as vector control.

4.2.2.1. *Azoreductase activity of azoA transformants*

Azoreductase specific activity was analyzed using RV5R and NADH as substrate and cofactor respectively. As compared to the corresponding vector controls (VC) azoreductase activity was increased by 7 fold in *E. coli* DH5α and approximately 4 fold in *P. fluorescens* PfO-I (Table 4.1). The other isolates showed an increase in azoreductase activity ranging from 2 to 4.68 fold except for *Providencia*sp. G1 which did not show any significant increase in the azoreductase activity compared to the vector control.

4.2.2.1.1. Azo dye decolorization by pBBR1MCS2*azoA* transformants

RV5R decolorization by pBBR1MCS2*azoA* transformants of various standard strains and isolates was checked. *E. coli* DH5α cells overexpressing *azoA* showed significant 2 fold increase in the RV5R decolorization with IPTG induction (1mM), however high decolorization was also noticed under uninduced condition (Fig. 4.6). *P. fluorescens* PfO-1 and *Providencia* spp. C1 and G1 do not possess lac repressor, thus IPTG induction was not given to these strains. Two fold increase in RV5R decolorization was found in *P. fluorescensazoA* transformant, however *Providencia* spp. C1 and G1 *azoA* transformants did not show increase over vector control.

Table 4.1 Azoreductase activity of pBBR1MCS2*azoA* transformants

Isolate /Strain	Organism		Azoreductase specific activity*	Fold increase
DH5α	*Escherichia coli*	VC	0.1±0.02	7.0 (p<0.01)
		azoA	0.7±0.08	
PfO-I	*Pseudomonas fluorescens*	VC	0.43±0.05	3.65 (p<0.01)
		azoA	1.57±0.23	
A3	*Citrobacter* sp.	VC	4.34±0.25	3.88 (p<0.01)
		azoA	16.87±1.50	
C1	*Providencia* sp.	VC	5.36±0.11	2 fold (p<0.01)
		azoA	10.70±1.27	
E2	*Klebsiella* sp.	VC	4.12±0.29	3.40 (p<0.01)
		azoA	14.04±1.83	
G1	*Providencia sp*	VC	4.36±0.62	1.17
		azoA	5.13±0.79	
K1	*Klebsiella* sp.	VC	7.24±0.8	2.73 (p<0.01)
		azoA	19.77±1.6	
L1	*Acinetobacter* sp.	VC	4.73±0.46	4.68 (p<0.01)
		azoA	22.14±2.01	

(VC- Vector control and *azoA* denote the pBBR1MCS2*azoA* harboring transformants, * activity measured with 1mM IPTG)

Surprisingly, *Providencia* sp.C1 harboring*azoA*construct decolorized RV5R slower as compared to the vector control. The *azoA* expression in lab isolates such as *Citrobacter* sp. A3, *Acinetobacter* sp.L1 and *Klebsiella* sp. E2 resulted in faster decolorization as compared to the control strains with empty vector. Rate of decolorization remains unchanged for K1 (*Klebsiella* sp.) clone with and without induction. *Citrobacter* sp.A3 and*Klebsiella* sp. E2 *azoA* transformantinduced by 1mM IPTG did not yield any significant change in RV5R decolorization compare to uninduced cells.At the same time, there is a noticeable increase in decolorization in case of *E. coli*DH5α and *Acinetobacter* sp.L1 after induction with 1mM IPTG. Overall heterologous expression of *azoA* in *E. coli*DH5α, *P. fluorescens*PfO1

,*Citrobacter* sp. A3 ,*Acinetobacter* sp.L1 and*Klebsiella* sp. E2 has resulted in increase in decolorization rate as well as percentage decolorization in 30h. *Providencia*spp. C1 and G1,*Klebsiella* sp. K1 did not show any significant change in RV5R decolorization upon *azoA* expression (Fig. 4.6).The RV5R decolorization results are in accordance with the fold increase inazoreductase activities of C1, K1 and G1 (Table 4.1).

4.2.2.1.1.1. Effect of glucose on RV5R decolorization by *azoA* transformants

Since azo dye decolorization rate depends on reducing equivalents, it was of interest to study RV5R decolorization by *azoA* transformants in the presence of glucose as electron donor. In presence of additional glucose (0.5% w/v), overall RV5R decolorization was enhanced in all the transformants except *Klebsiella* sp. K1 (Fig. 4.7). *Providencia* sp. G1 overexpressing *azoA*shows significant increase in RV5R decolorization only in presence of glucose. Additionally presence of glucose as the carbon source and electron donor has resulted in faster decolorization for vector controls as well as *azoA* transformants, for all the strains except *Providencia* sp. C1.Hence, these resultsshow that glucose shows increasesthe rate of RV5R decolorization in gram negative strains.

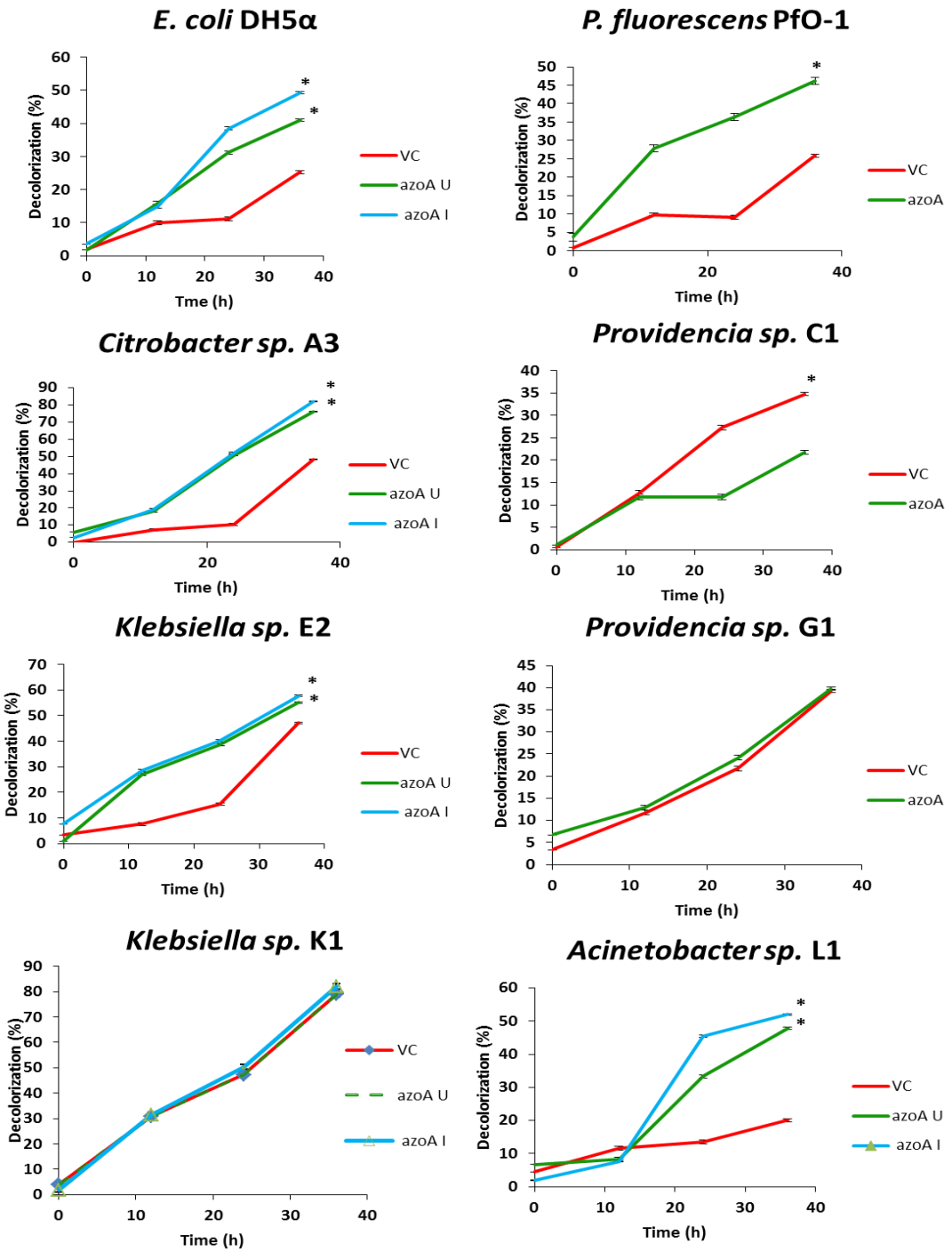

Figure 4.6RV5R decolorization by pBBR1MSC2*azoA*transformants.

(U-uninduced, I- Induced) (* data was found significantly different compared to corresponding vector control at p < 0.05)

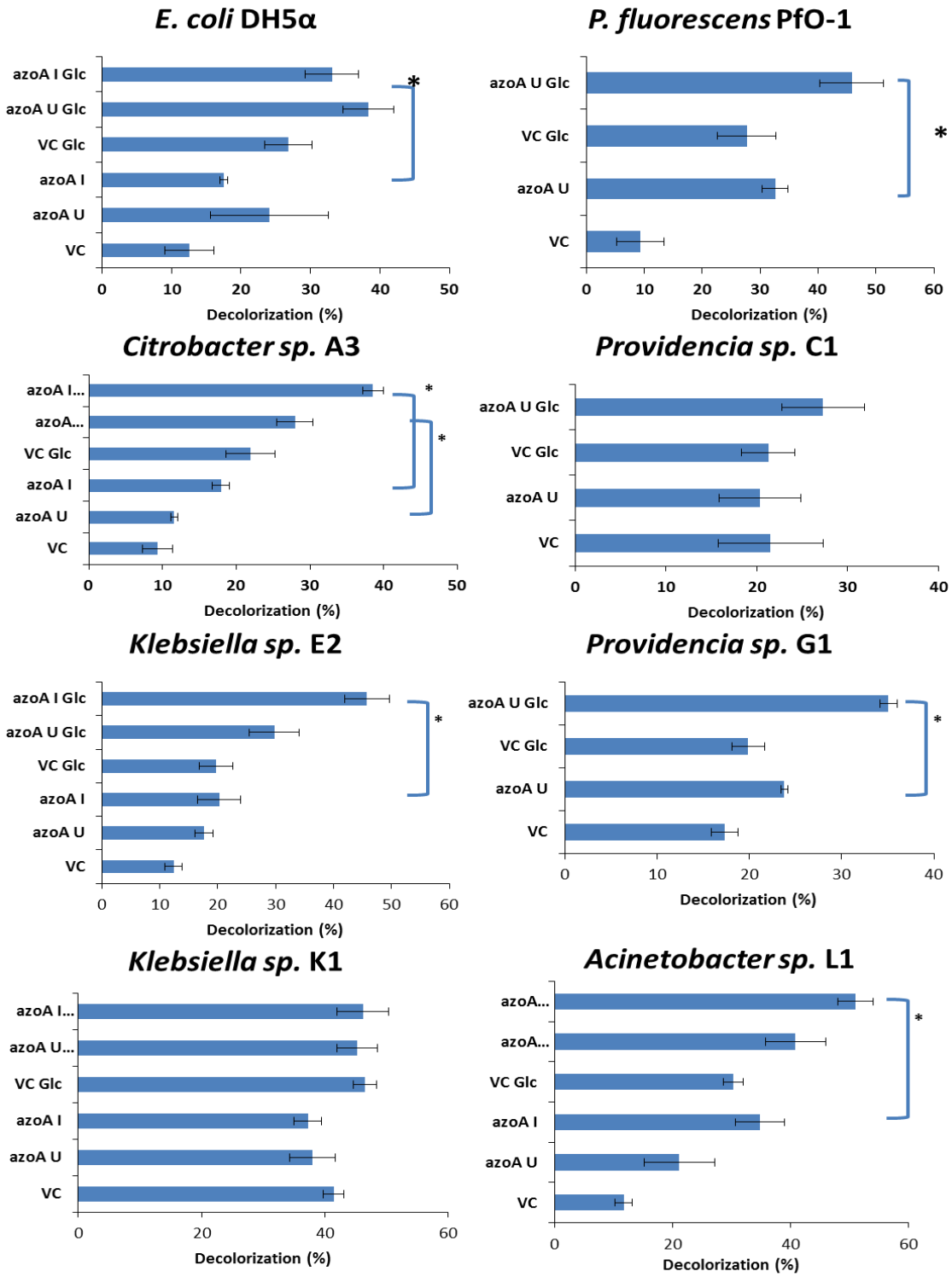

Figure 4.7 Effect of glucose on decolorization patterns by pBBR1MCS2 *azoA* transformants

4.2.3. *azoA* knockout of *Enterococcus* sp. L2

To elucidate the physiological role of *azoA* in *Enterococcus* sp. L2, reverse genetics approach was used to construct an *azoA* knockout of *Enterococcus* sp. L2.

4.2.3.1. Construction of disruption plasmid

*AzoA*knockout was created using pTEX5501ts system. This plasmid contains (i) *E. coli oriR* of pUC18; (ii) a Gram-positive *repAts,a* temperature sensitive replicon from pTV1-OK which is functional in *E. faecium* at a permissive temperature of 28°C; (iii) two distinct multiple cloning sites (MCSs) on either side of the *cat* (chloramphenicol acetyl transferase) gene to provide several alternative sites for cloning of flanking regions of the target gene for double-crossover mutagenesis; (iv) a synthetic functional promoter region (with two extended -35 and -10 boxes) to overcome relatively low expression levels of the pC194-based *cat* gene in gram positive; (v) a gentamicin resistance gene *aph*(*2"*)-*Id* from *Enterococcus casseliflavus*for the counter selection of the disruptants;(vi) transcriptional terminator sites (tts) to terminate undesired read through and to prevent destabilizing effects of cloned inserts. The resistance markers are functional in *E. coli* and *Enterococcus* backgrounds (Nallapareddy et al. 2006). *Enterococcus*sp.L2 (WT)is sensitive to chloramphenicol and gentamycin.

PCR amplicons of the *upazoA* and *downazoA* regions which denote the flanking ~1.2 kb fragments both the sides of the*azoA*gene of *Enterococcus* sp. L2 (Fig. 2.13, Chapter 2) were obtained using primers mentioned in Table 2.5 (Chapter 2) (Fig. 4.8a). They were further confirmed by internal RE digestions, such as for up*azoA* region PCR product was digested with EcoRI& PvuII and down*azoA* region PCR product was digested withEcoRI. Fig. 4.8b shows the expected fragmentation patterns based on the sequence details of *E.faecalis* V583.

The *upazoA* was cloned into pJET1.2 vector at the blunt end site andpJETup*azoA*was confirmed by digestion with BglII (Fig. 4.9a) which flank the up*azoA* in pJETup*azoA* (Fig. 4.9b) and PCR using up*azo*A primers (Fig. 4.9c). Simultaneously cloning of down*azoA* into pBS KS(+) at the EcoRV site was done. pBS KSdown*azoA* was confirmed by RE digestion with EcoRI (Fig. 4.10a) which lies internally in down*azoA* (Fig. 4.10b) and down*azoA* PCR (Fig. 4.10c). The cloned up*azoA* region was released from pJETup*azoA* using BglII and subsequently ligated into pTEX5501ts at BglII in MCSI. pTEX5501tsup*azoA* was confirmed by EcoRI, BglII digestions (Fig. 4.11a) and PCR using *upazo*A primers (Fig. 4.11b). Subsequently, the pBS KSdown*azoA* was digested using PvuII which released blunt ended down*azoA*cassette. This

down*azoA* fragment was subsequently ligated into pTEX5501tsup*azoA* at SmaI. The final construct named pTEX5501tsupdown*azoA*was the disruption plasmid. The disruption plasmid was confirmed by EcoRI and HincII digestions (Fig. 4.12a). These restriction enzymes cut at three sites on the plasmid and the expected pattern of released fragments was obtained. PCR confirmation was done by three systems; up*azoA* primers, down*azoA* primers and upazo F & down*azoA* R primers. The expected bands of 1.2 kb (Fig. 4.12b) were obtained in the up*azoA* and down*azoA* systems while an approximately 3.4kb band (Fig. 4.12c) was obtained in the third system which corresponds to whole recombination cassettes regions. Map of the resulting plasmid pTEX5501tsupdown*azoA* is depicted in Fig. 4.13.

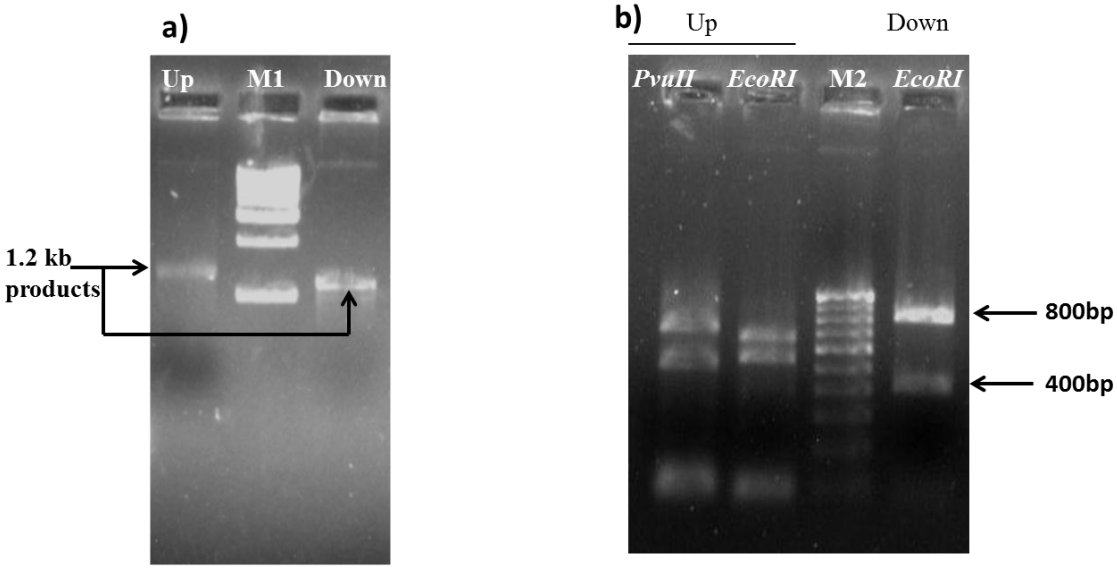

Figure 4.8 PCR amplificationand RE digestionof up*azoA* and down*azoA*flanking regions of *azoA* gene of *Enterococcus* sp. L2

(M1- 1kb ladder and M2- 100bp ladder)

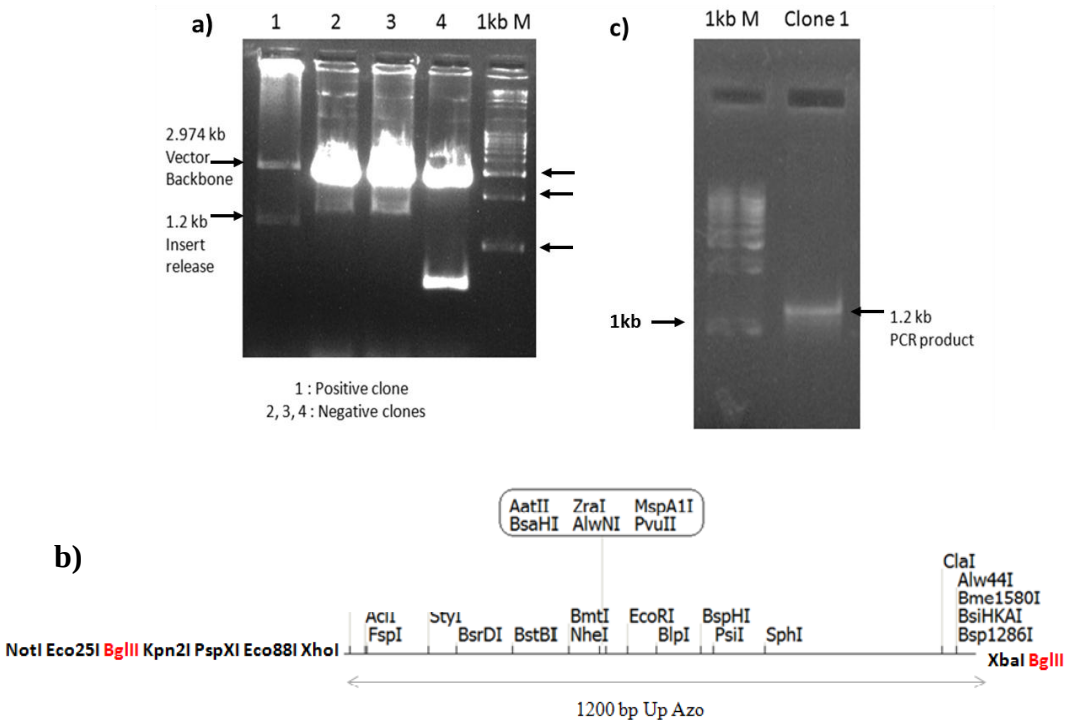

Figure 4.9Confirmation of pJETup*azoA* construct by RE digestion and PCR amplification.

a) BglII digestion b) up*azoA* RE map c) PCR amplification

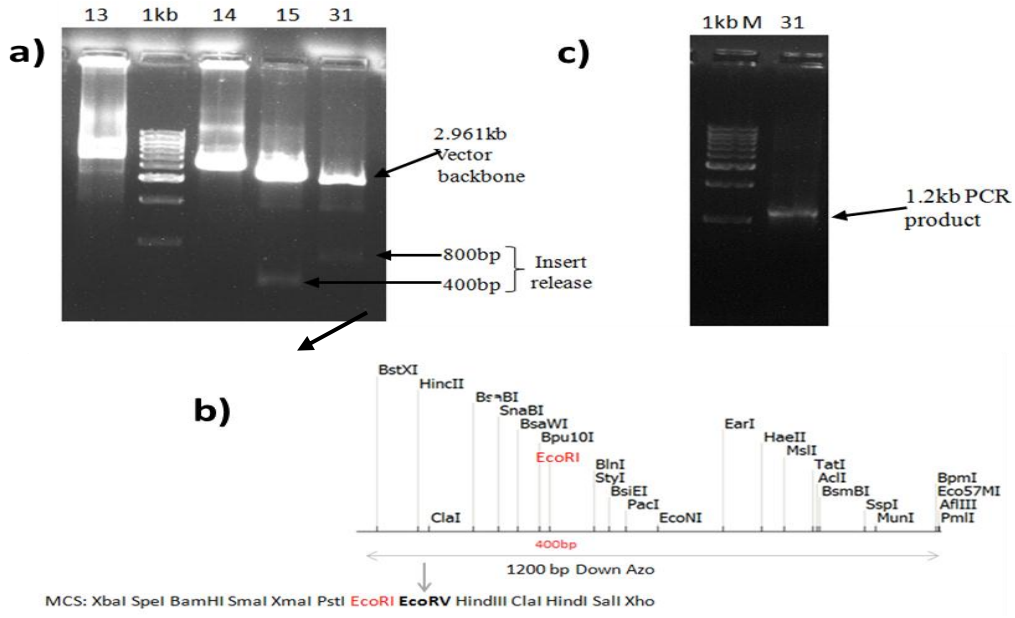

Figure 4.10pBS KSdown*azoA* confirmation by RE digestion and PCR amplification

a) EcoRI digestion b) RE map of dwon *azoA* c) PCR amplification

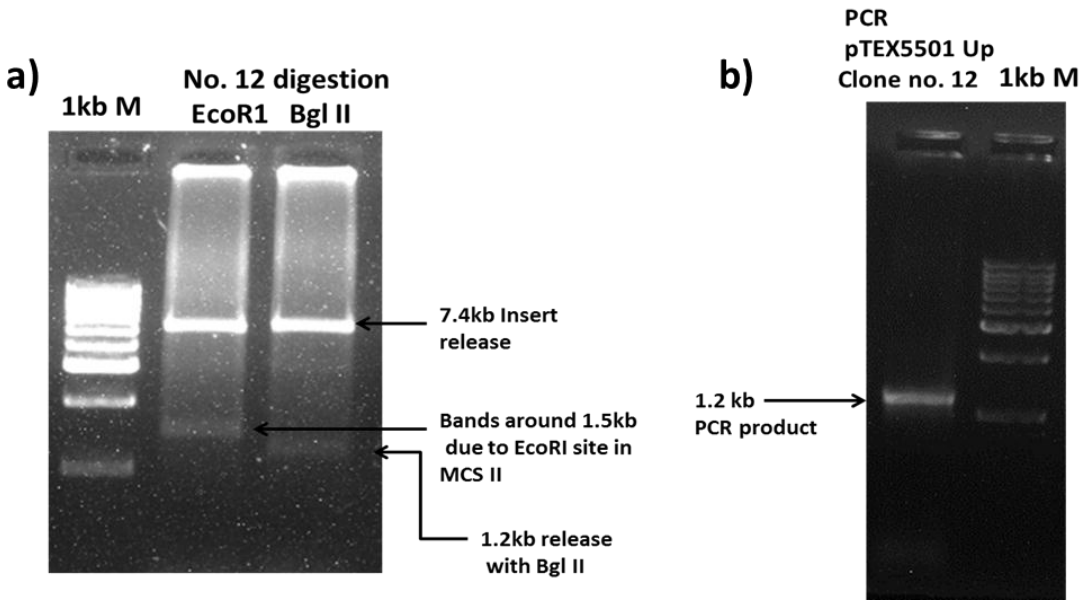

Figure 4.11 Clone confirmation for pTEX5501ts*upazoA*by RE digestion and PCR amplification.

a) EcoRI and BglII digestion b) PCR confirmation.

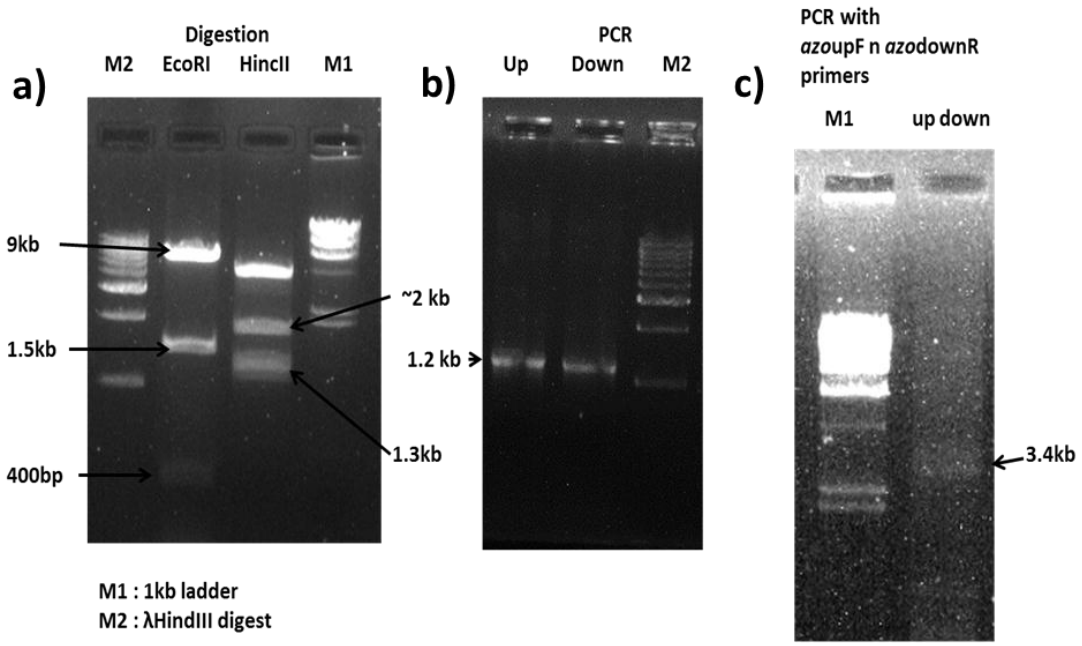

Figure 4.12 Confirmation of pTEX5501tsupdown*azoA* by RE digestion and PCR amplification.

a) EcoRI and HincII digestion b) individual PCR amplification and c) whole up cat down azo cassette PCR confirmation

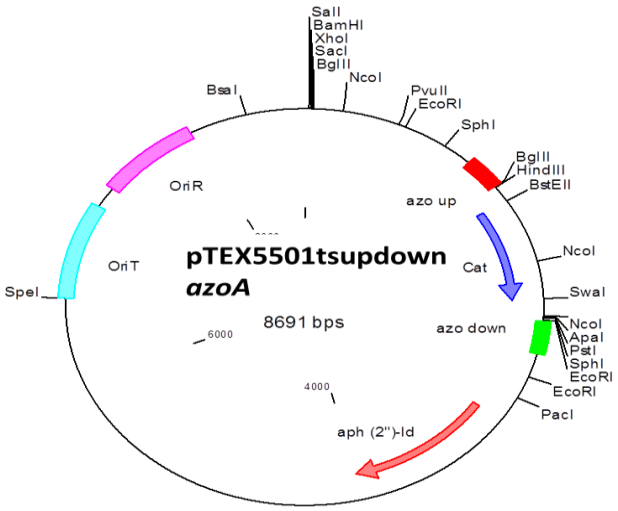

Figure 4.13 Map of pTEX5501tsupdown*azoA*

The disruption vector was electroporated into wild type *Enterococcus*sp.L2.ARDRA with HinfI of the transformant confirmed its similarity to wild type L2 (Fig. 4.14a). It was also checked by gram staining (Fig. 4.14b) and PCR amplification of Chloramphenicol resistance gene fragments using primers mentioned in Table 2.5 (Chapter 2).

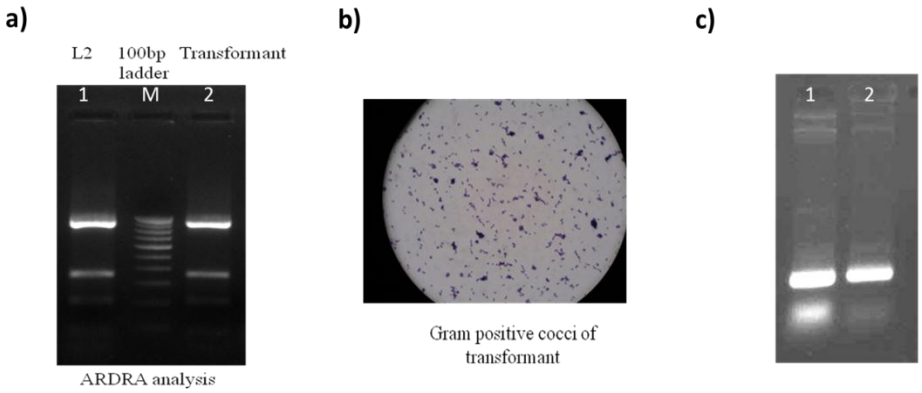

Figure 4.14Confirmation of *Enterococcus*sp. L2 carrying the disruption plasmid.

a) ARDRA with Hinf1 (Lane 1- Transformed strain, M- 100bp marker, Lane 2- Wild type strain; b) Gram staining c) Chloramphenicol resistance gene specific PCR

(Lane 1- Transformed strain, Lane 2- Constructed plasmid from *E.coli* as positive control)

4.2.3.2. Chromosomal integration of disruption plasmid and scoring for double recombinants

The chloramphenicol resistance gene can be used as a marker for selecting chromosomal integration of the pTEX5501tsupdown*azoA.* Subsequently loss of the gentamicin resistance marker located on the vector backboneis used to distinguish double-crossover recombinants.According to the schematic shown in Fig. 2.15 (Chapter 2) explaining the method of generating a knockout and its screening strategy, thepTEX5501tsupdown*azoA*transformant was grown first at permissive temperature (28^{o}C) to allow the replication of the disruption plasmid and then it was shifted to a restrictive temperature of 42^{o}C and grown for eight serial passages in presence of chloramphenicol to select for the integration as the episome. The culture was then serially diluted and plated on chloramphenicol containing plates and incubated at 37°C. These master plates were then replica plated on chloramphenicol plates and gentamicin plates (separately) to identify colonies that retained the chloramphenicol resistance but were gentamycin sensitive. Screening of approximately ~2000 colonies showed them to be gentamycin resistant. Thus no double recombinantwas obtained. This indicated that strain L2 possessed low native recombination frequency or the knockout strain might have survival problem suggesting that the target gene (*azoA*) is essential for growth.

There are occurrences of knockouts with no growth, slow growth and those with normal growth classified on the basis of essentialness of the gene involved (Joyce et al. 2006, Gerdes et al.2003). Liu et al. (2009) showed that AzoR is an NADH: quinone oxidoreductase with a role in protection against thiol specific stress. AzoR is active on a variety of electrophilic quinones. An *E. coli azoR::kan* mutant had impaired growth in the presence of 2-methylhydroquinone, catechol and menadione and showed decreased levels of glutathione. Externally added glutathione could partially restore impaired growth of the *azoR* mutant caused by 2-methylhydroquinone. Our results of screening of *ΔazoA*indicate that *azoA* may be contributing significantly to growth and survival even in normal stress free conditions, hence the distruptant might not be viable.

It was hypothesized that the glutathione supplementation might rescue the growth of the disruptant. Thus the screening of double recombinant was attempted by incorporating glutathione supplemented growth medium inthe screening strategy.

After screening ~1000 chloramphenicol resistant colonies, one colony having appropriate antibiotic profile (Cat^r Gen^s) was obtained. The disruption of the *azoA* in this colony was confirmed by PCR amplification of *azoA*gene and its flanking region (Fig. 4.15). In disruptant *azoA* specific PCR resulted in 1.5kb amplicon however the wild type size of intact *azoA*(650bp) was missing indicating double crossover has taken place. This was further confirmed by lack of the PCR amplification of gentamycin resistance gene fragment. The obtained disruptant of Δ*azoA* of *Enterococcus* sp. L2 could not survive during subsequent transfers on plates or growth in liquid medium (supplemented with 10mM glutathione). Therefore it may be concluded that *azoA* plays a vital role in survival of*Enterococcus* sp. L2.PCR confirmation of disruption by double crossoveris depicted in Fig. 4.15.

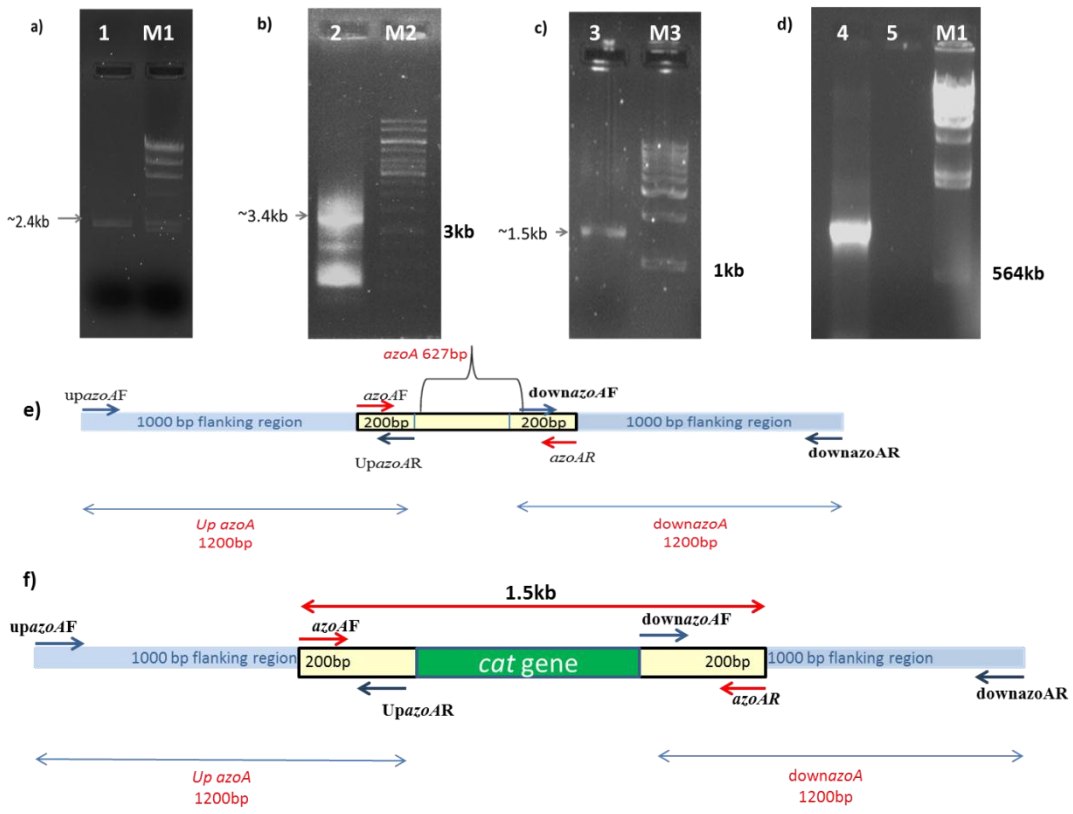

Figure 4.15 PCR confirmation of double crossover.

a) Wild type flanking regions PCR amplification b) Putative knockout strain flanking regions PCR amplification c) *azoA* specific PCR from Knockout strain d) Gentamycin resistance gene fragment PCR e) *Enterococcus* sp. L2 (WT) *azoA* and its flanking regions d) *azoA* disruption map of *ΔazoA* L2 strain.

(Lane-1 and Lane-2 PCR using up*azoA*F & down*azoA*R primers; Lane-3 *azoA* gene specific PCR by *azoA*F and *azoA*R primers; Gentamycin PCR, Lane-4 pTEX5501tsupdown*azoA* plasmid and Lane-5 knockout strain)

4.2.4. Homologous overexpression of *azoA* in *Enterococcus* sp. L2

Previous attempt to obtain the *azoA*knockout in *Enterococcus*sp. L2 did not result in successful development of Δ*azoA* strain, thus another reverse genetics approach was used by overexpressing *azoA* gene in *Enterococcus* sp. L2. In this study we cloned *azoA* ORF in pMGS100,an *E. coli- Enterococcal* shuttle vector having constitutive expression in *Enterococcus* under *pbacA* and ribosome binding site (RBS) of bacitracin resistance gene to drive *azoA* expression..

4.2.4.1. Construction of pMGS100*azoA*

azoA ORF region from start to stop codon was amplified using *Pfu*-polymerase using gene specific forward primers *azoA*ATGF (Table.2.5, Chapter 2) and *azoA*R. PCR amplified product was purified and ligated with NruI digested linearized pMGS100 vector. Ligation product was transformed in *E. coli* DH5α for screening of the pMGS100*azoA* construct. Plasmids from putative colonies obtained on chloramphenicol containing LB agar plateswere digested by SalI whichlies at an internal position in *azoA* ORF as well as on the plasmid backbone releasing 650bp fragment when in correct orientation with p*bacA.* Fig. 4.16 shows that transformants numbered 1, 8, 12 and 18 have the desired construct.Map for pMGS100*azoA* is shown in Fig. 4.17.

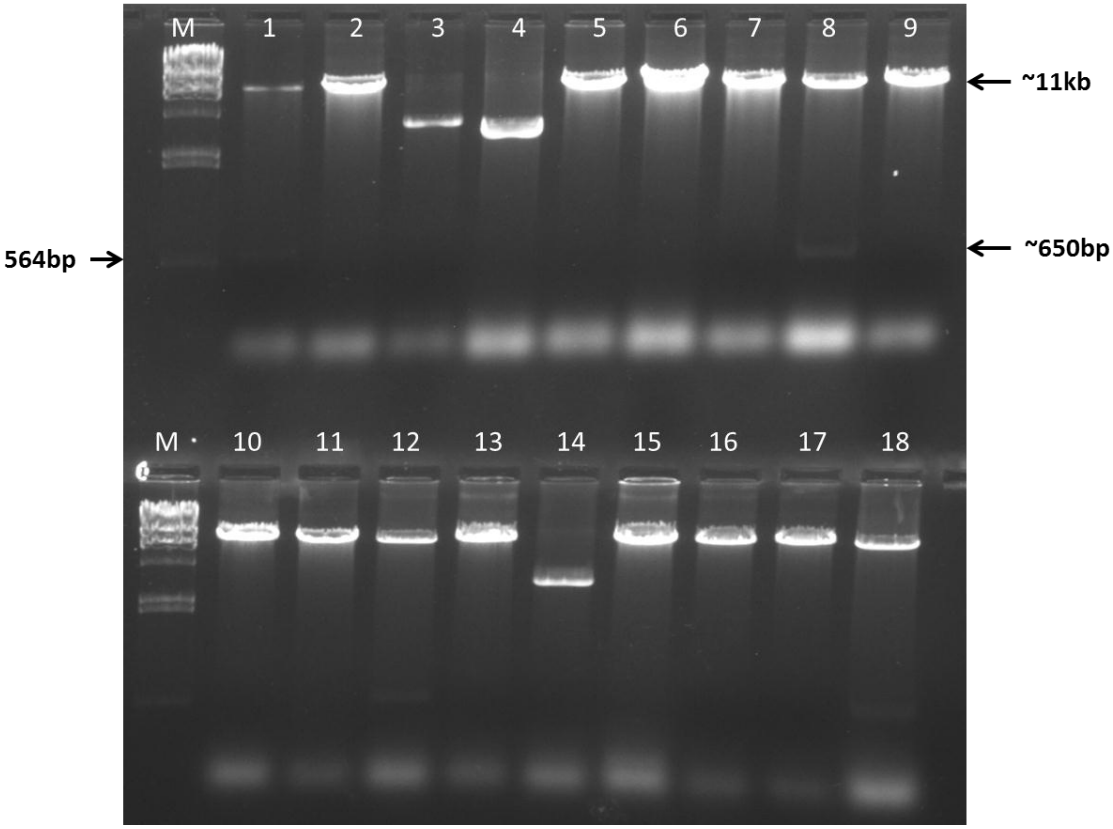

Figure 4.16 pMGS100*azoA* confirmation by insert fragment release using SalI digestion

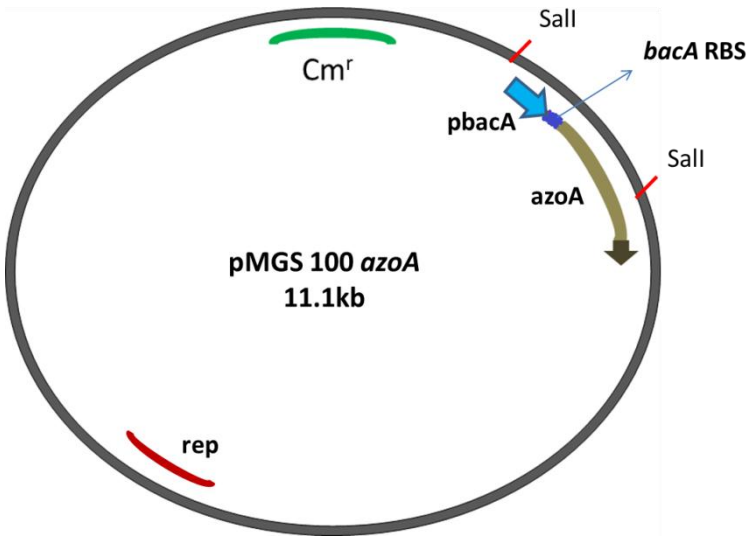

Figure 4.17 Map of pMGS100*azoA*.

4.2.4.2. Azoreductase activity and SDS-PAGE analysis of *Enterococcus* sp. L2 (pMGS100*azoA*)

Azoreductase specific activity was assayed for *Enterococcus*sp. L2 (WT), *Enterococcus*sp. L2 (VC, pMGS100) and *Enterococcus*sp. L2 (pMGS100*azoA*).*azoA* transformant showed 3.46 fold increase in the azoreductase activity compared to the VC (Table 4.3). SDS-PAGE analysis of *azoA*transformantof*Enterococcus* sp. L2 showed higher intensity 23kDa protein band of *azoA* expression compared to VC (Fig. 4.20).

Table 4.2Azoreductase specific activity of *Enterococcus*sp. L2 harboring pMGS100 *azoA*

Organism	Specific Activity µM/min/mg of protein	Fold increase
Enterococcus sp. L2 VC	18.1±2.37	
Enterococcus sp. L2 *azoA*	62.62±5.23	3.46

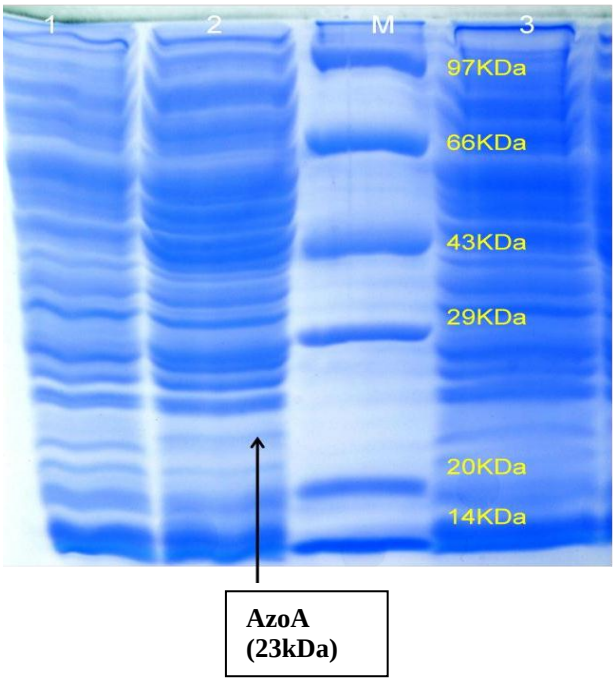

1-*Enterococcus sp*. L2 pMGS100 VC
2-*Enterococcus sp*. L2pMGS100*azoA*
M- Protein marker
3- *Enterococcus sp*. L2

Figure 4.18SDS-PAGE analysis of *Enterococcus*sp. L2 homologously over-expressing *azoA*

4.2.4.3. Morphological, growth and dye decolorization characteristics of*azoA* overexpressing*Enterococcus* sp. L2

It was observed that *Enterococcus* sp. L2 (pMGS100*azoA*) cells form tended to settle down in the liquid growth medium rapidly compared to the WT and VC and showed sediment like growth. Fig. 4.19 shows the gram stained morphology and cell arrangements of *Enterococcus* sp. L2 (pMGS100*azoA*)in comparison with the WT strain and VC. It was observed that *Enterococcus*sp. L2 (pMGS100*azoA)*formed cell aggregates. This was in contrast to the field captured in case of L2VC and L2WT where the cells are arranged in the diplococcic form which is the normal morphology of the organism.

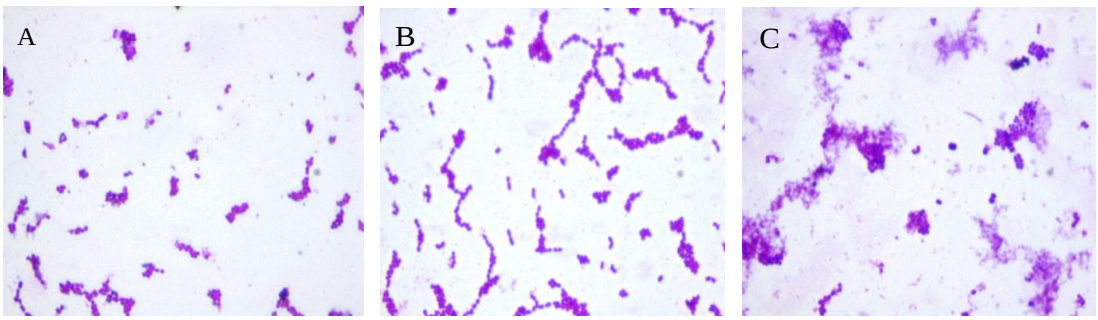

Figure 4.19Microscopicanalysis (Gram staining)of*Enterococcus* sp. L2 (pMGS100*azoA*).

a) WT b) VC c) *azoA* transformant

Over-expression of *azoA*resulted in delayed decolorization of RV5R and impaired growth as compared toVC (Fig. 4.20a and b). In spite of a significant fold increase in the enzyme activity in *azoA* expressing strain, due to retarded growth transformant showed delayed decolorization.

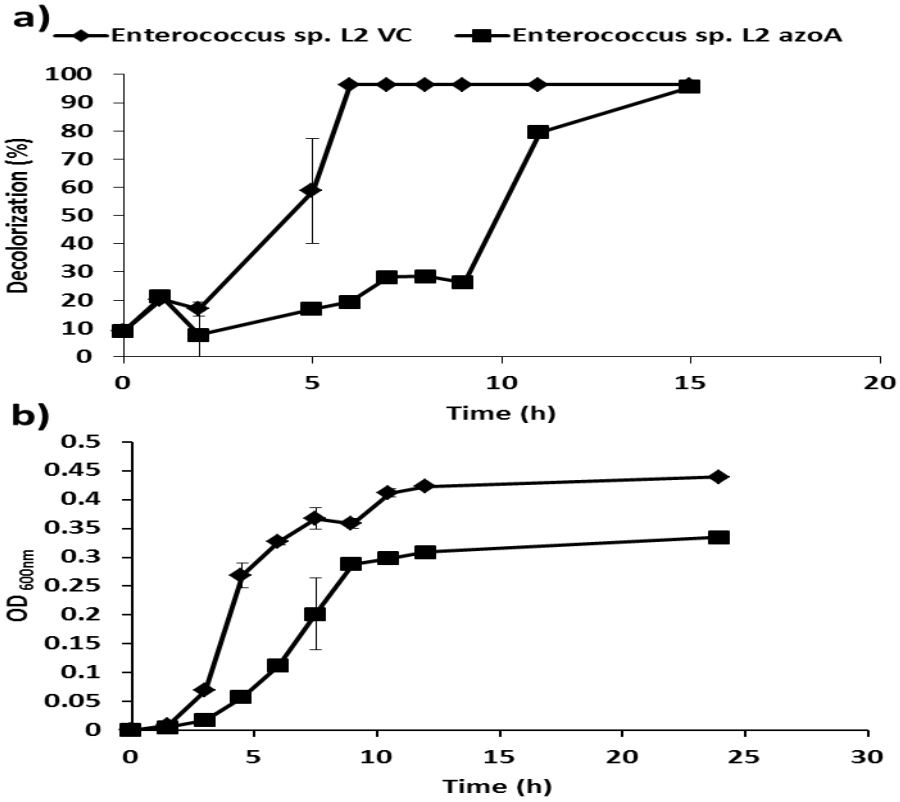

Figure 4.20RV5R decolorization and growth of*azoA* overexpressing transformant of*Enterococcus* sp. L2.

a) RV5R decolorization; b) growth (O.D. at 600nm).

4.2.4.4. Oxidative stress survival of *azoA* transformant of *Enterococcus* sp. L2

Azoreductase belong to the quinone reductase flavoenzymes catalyzing two electron transfer by Ping-Pong mechanism (Liu et al., 2008). Quinone reductasesplay a vital role in providing tolerance to oxidative stress by quenching reactive oxygen species (ROS) by not allowing semihydroquinone radicals to be generated.Thus it was of interest to study the effect of azoreductase over-expression on oxidative stress survival. With varying concentrations of H_2O_2, it was found out that *azoA*transformantsurvived up to 30mM H_2O_2while VC showed growth inhibition above 15mM H_2O_2(Fig. 4.21a) .These results were quantified by the % survival in terms of cfu at different H_2O_2concentrations.A higher % survival was observed in case of *azoA*transformantat all concentrations as when compared to VC and WT (Fig. 4.21b).

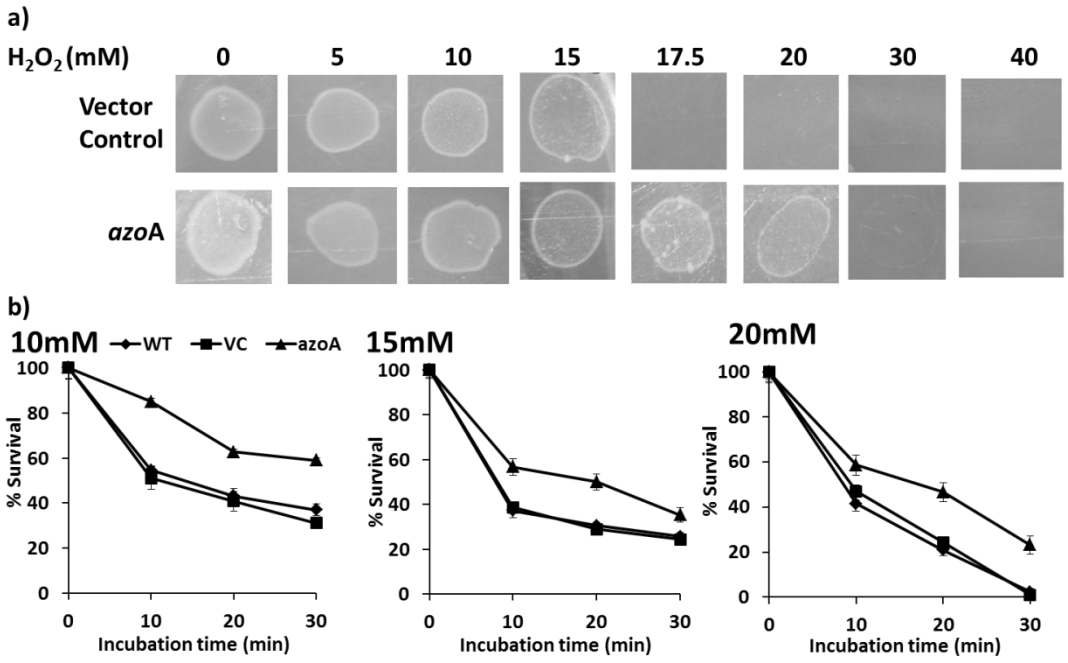

Figure 4.21 H_2O_2stress survival of*Enterococcus*sp. L2 *azoA* transformant.

a) Spot assay b) Percentage survival(WT- wild type, VC- vector control, *azoA*- overexpressing clone) (* data was found significant at p < 0.01)

Further, using fluorescence microscopy with ROS specific green probe 2',7'-dichlorodihydrofluorescein diacetate (H_2DCFDA)(Pérez et al., 2007), the accumulation of ROS in the cells was monitored. Cells exposed to varying concentrations of H_2O_2showed increase in fluorescence intensity. At all concentrations of H_2O_2 treatment,*Enterococcus* sp. L2*azoA*transformant was found to have reduced intensity of fluorescence as compared to WT and VC (Fig. 4.22a). Subsequently, fluorescence was quantified using fluorimeter which showed 2.4 and 2.1 fold lower fluorescence compared to wild type and VC, respectively (Fig. 4.22b). In conclusion over-expression of *azoA* resulted reduction of ROS like superoxide and hydroxyl radicals, thus enhancing the cell survival under oxidative stress. This finding indicates physiological role of azoreductase in oxidative stress management in catalase negative *Enterococcus* sp. L2.

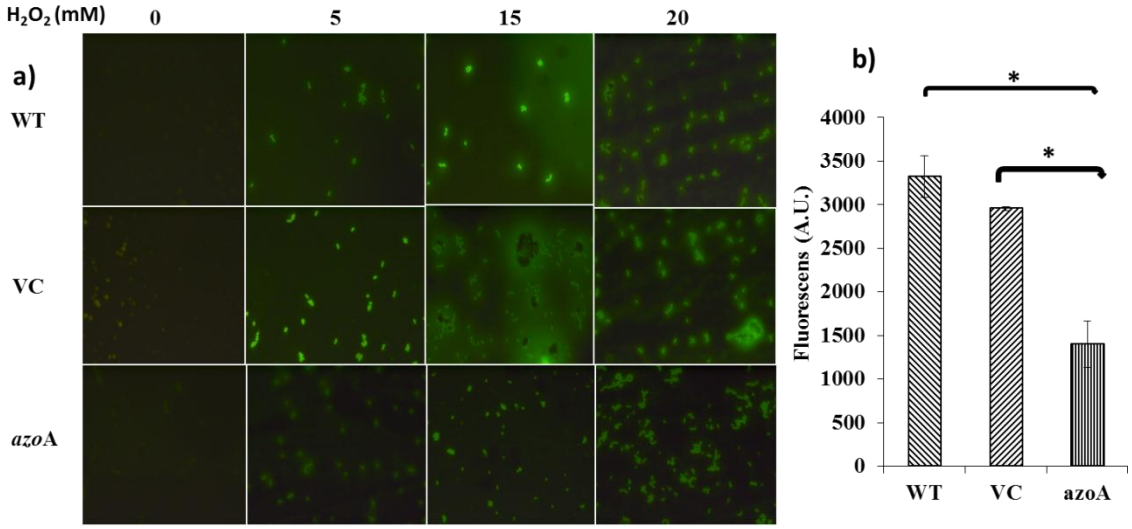

Figure 4.22 Intracellular ROS detection by H_2DCFDA in H_2O_2 treated *azoA* transformant.

a) Fluorescence microscopic image of cells exposed to H_2O_2; b) Fluorescence spectroscopy of lysate from cells exposed to 20mM H_2O_2.(Fluorescence A.U. expressed as normalized values using the protein content, * denotes the data found significantly different at p<0.01)

4.2.4.5. Heavy metal tolerance of *Enterococcus* sp. L2 *azoA* transformant

Heavy metals lead to toxicity at high concentrations and have the ability to cause oxidative damage to pro-eukaryotic cells. Specifically, heavy metals such as chromate and copper are present in high levels in dye effluents(Banat et al., 1997). Microbial systems gain heavy metal tolerance via diverse mechanisms such as metal efflux, reduction or adsorption. Role of AzoA in heavy metal tolerance was studied by monitoring the growth of *Enterococcus* sp. L2 *azoA*transformant in presence of toxic levels of Cu (II) and Cr (VI). Fig. 4.23 shows *azoA* transformant had a growth advantage over the WT and VC in presence of 0.3mM Cr (VI) and 3mM Cu (II) in spite of the fact that the *azoA* transformant was slow growing in absence of metal. Certain flavoenzymes from *Pseudomonas putida*(ChrR) homologous toazoreductases are characterized to reduce heavy metals such as chromium. ChrR reduces quinones by two-electron transfer, avoiding formation of highly reactive semiquinone intermediates and producing quinols that promote tolerance of H_2O_2 (Gonzalez et al., 2005).

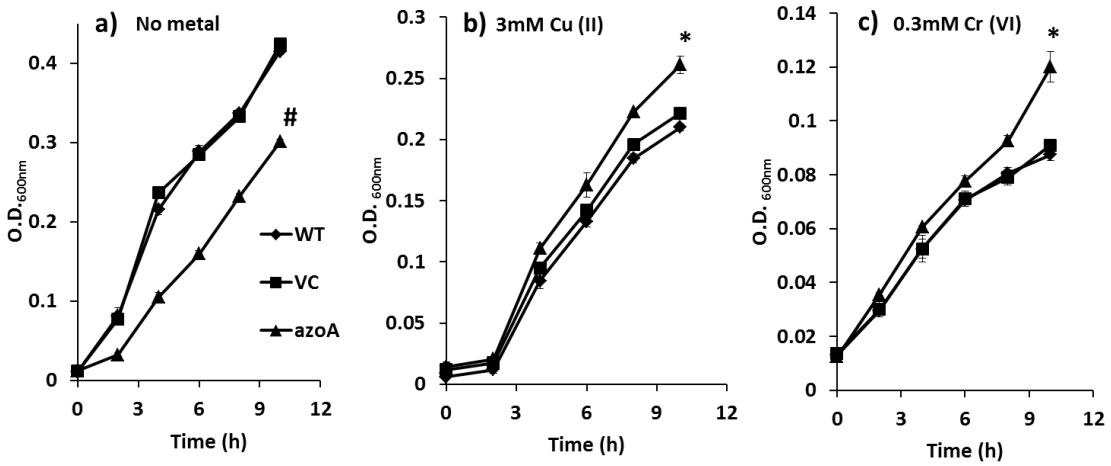

Figure 4.23Growth of *Enterococcus*sp. L2 overexpressing *azoA* under heavy metal stress.

a) no metal b) 3mM Cu(II) c) 0.3mM Cr (VI)

(WT- wild type, VC- vector control, *azoA*- overexpressing transformant; # significant decrease and * significant increase in growth at p < 0.01 as compared to WT and VC)

4.3. Discussion

Azo dyes are considered to be recalcitrant due to the electronegativity around azo bond. Different enzymes such as azoreductase, laccase, mono-di oxygenase are reported to play major role in biodegradation of azo dye. Number of potential genera like *Bacillus, Geobacillus, Enterococcus, Sphingomonas, Pseudomonas* are reported to express genes for azo dye decolorization/degradation (Chen, 2006). However, the requisite to isolate, identify and characterize new genes from different environmental sources isessential need as diverse structures of azo dyes are synthesized every year.

Based on the various characteristics of the dye decolorizing bacterial strains obtained in this study, *Enterococcus*sp. L2was considered appropriate for the cloning of azoreductase gene (*azoA*). The *azoA* gene was cloned in gram negative broad host range vector for heterologous expression studies. It was found that heterologous expression of *azoA*driven by p*lac* in gram negative strains resulted in enhanced RV5R decolorization in the *azoA* transformants of *E. coli* DH5α and *P. fluorescens* PfO-1 and the transformed isolate strains of *Citrobacter* sp. A3, *Klebsiella* sp. E2 and *Acinetobacter* sp. L1. Interestingly the transformant of *Klebsiella* (K1) did not show any difference in RV5R decolorization compared to VC, indicating strain to strain variation. Similarly the two strains of *Providencia* spp. (C1 and G1) behaved differently upon *azoA* transformation but both failed to show enhanced decolorization.

In correlation with this *azoA* transformants of strains C1, G1 and K1 did not show an increase in azoreductase activity. The differences in the physiological response to *azoA* overexpression in different strain background could be because of codon bias or the effectiveness of the *plac* promoter. However the *azoA* of *Enterococcus* is considered to be derived from *E. coli azoA* by lateral gene transfer (Bafana and Chakrabarti, 2008a). Azoreductase from *Enterococcus faecalis* has been shown to be overexpressed in *E. coli* indicating codon bias is not a problem in *E. coli* host (Chen, 2004). Azoreductase gene from *Rhodococcus sphaeroides*another gram positive firmicute was also expressed in *E. coli*.This genetically modified *E. coli*strain showed higher decolorization rate of Acid Red GR (pigment in plastic and acrylamide) (Bin, 2004). Feng et al. (2010) demonstrated of entereorcoccal (*azoA*) heterologously overexpressed in *E. coli* showed 2- 4 fold increase in decolorization compared to non-induced cells. So far no study of RV5R a textile azo dye decolorization was demonstrated using enterococcal AzoA.This is being the first study demonstrating enhancement of decolorization ability by its heterologous expression in various non-conventional host systems.

Enterococcus sp. L2 was found to decolorize 100mg/L RV5R completely in 5-6h. *azoA* gene cloning from this isolate demonstrated the role of this enzyme in RV5R decolorization. Although heterologous expression of *azoA*from this strain into different gram negative bacteria resulted in improved RV5R decolorization, none of the transformants were found to be as efficient as native *Enterococcus* sp. L2. To pin point the role of *azoA* in *Enterococcus* sp. L2 and its precise contribution in azo decolorization *azoA* knockout and homologous expression was carried out.

AzoA knock out strain of *Enterococcus* sp. L2 was constructed using pTEX5501ts temperature sensitive suicidal vector. However it was found that the knockout was not stable. In *E.coli azoR* mutant was reported to besensitive to the electrophilic quinones showing retarded growth which could be normalized by addition of reduced glutathione (Liu et al., 2009). Enterococcal Δ*azoA* could not be rescued even when growth was carried out in medium containing reduced glutathione. In contrast with the *E. coli*Δ*azoA,* which showed growth defects only when exposed to quinones, the enterococcal Δ*azoA* showed survival problem in normal growth medium. This could be expleained on the basis of physiological differences *E. coli* and *Enterococcus* spp.

Enterococcus spp.aregenerally catalase negative and possesses a single Mn-SOD characterized at the biochemical level (Gregory &Fridovich, 1973; Britton et al., 1978) and limitedorthologs of thioredoxin and NADPH-thioredoxinreductase system (single copy of both trx and trxreductase in *E. faecalis* V583 genome). Genome of *E. faecalis* V583 also contains single set of glutathione reductase and glutathione synthesis genes. *Enterococcus* spp. areknown to produce substantial extracellular superoxide (O_2^-) and H_2O_2via auto-oxidation of membrane associated quinones(Huycke et al., 2002). Azoreductases are known to carry out two electron transfer to various quinones which renders them incapable of generating ROS (Deller et al., 2008). Taking in to consideration that enterococci possess limited oxidative stress scavenging enzyme machinery and prolific endogenous ROS generation system, azoreductases could play an active role in combating ROS in this organism. Present work on Δ*azoA* of *Enterococcus* sp. L2 corroborates this view. Further, the observation that exposure of *Enterococcus*sp. L2 to H_2O_2, menadione, AQDS and RV5Rinduced the AzoA enzyme activivty level (Table 4.2, Chapter 4)supports its role in oxidative stress.The induction of AzoA by different quinones and pseudo substrates (RV5R, azo dye) suggest that the native substrate for the AzoA in normal physiological condition should be different endogenous quinones. Thus it may be surmised that enterococcal *azoA*belonging to flavin dependent quinonereductases plays a crucial role in reduction of oxidative stress. In future, a conditional knockdown approach of *azoA* couldlead to more in depth details about its role in facultative anaerobic life style and stress responses in *Enterococcus* spp.

To further investigate the role of *azoA* in *Enterococcus* sp. L2, overexpression of *azoA*using pMGS100 *E. coli-Enterococcus* shuttle vector in which *azoA* expression was driven by strong constitutive p*bacA* promoter. This resulted in growth perturbation under static condition in LB containing appropriate antibiotics and showed delayed azo dye (RV5R) decolorization. Kim et al. (2009) demonstrated that overexpression of NADH-dependent azoreductase *azoA* from *Enterococcus faecalis* KCTC 3206 in *E. coli* negatively affected the growth in presence of azo dye (Methyl red) and decrease its dye decolorizing ability. They attributed these effects of *azoA* overexpression to depletion of NADH pool. In this work, the heterologous expression of NADH-*azoA* of *Enterococcus* sp. L2 driven by p*lac* promoter in *E.*

*coli*DH5α showed enhanced RV5R decolorization. However homologous expression of *azoA* in *Enterococcus* sp. L2 showed decrease in RV5R decolorization.

Interestingly homologous expression of *azoA* in *Enterococcus* sp. L2 imparted oxidative stress resistance to the *azoA* transformant at 20mM H_2O_2wherein WT and VC were found to experience oxidative burst and later lysis as shown by H_2DCFA staining. At same time*azoA*transformant of L2 strain was found to be intact and showed decreased fluorescens showing low ROS production. In addition to H_2O_2stress, *azoA* transformant of *Enterococcus* sp. L2 also showed higher tolerance to toxic concentration of heavy metals such as copper and chromate. Azoreductase AZRfrom *Rhodobacter sphaeroides*when expressed in *E. coli*imparted H_2O_2 resistance (Liu et al. 2008). ChrR a chromate reductase from *Pseudomonasputida* was also implicated in H_2O_2 resistance.Like azoreductases this enzyme has higher activity for quinone reduction compared to chromate reduction and homologous overexpression reduced the ROSwhile knock out showed retarted growth in presence of H_2O_2(Gonzalez et al. 2005). Our results suggest role of *azoA* in oxidative stress management in catalase negative, facultative anaerobe, fermentative*Enterococcus* spp.

Azoreductase have been considered for the azo dye bioremediation in decolorization process as catalyst, to reductively cleave the azo bond releasing aromatic amines. Heavy metals such as chromate and copper are present in high concentrations in effluents from dyeing industry(Kulkarni and Chaudhari, 2007). Our findings demonstrate that although *azoA* overexpression in *Enterococcus* sp. L2 led to compromised growth and decolorization rate, however *azoA* transformant of L2 strain gained additional advantage of enhanced tolerance to oxidative and heavy metals stress thus it can be utlized for bioremediation of textile effluents.

Summarizing this Chapter, *azoA* gene from *Enterococcus* sp. L2 was isolated using PCR approach and further cloned in pBBR1MCS2 and pMGS100 expression systems. Several gram negative host strains transformed with pBBR1MCS2*azoA* lead to enhanced the RV5R decolorization compared to respective control strains. To elucidate the physiological function of *azoA* in *Enterococcus* sp. L2, knockout construction of *azoA* was done. However it was found that the Δ*azoA* mutant of strain

L2 could not survive even when growth medium was supplemented with glutathione. Thus concluding that *azoA* gene might be essential element for growth even under normal non-stressed conditions. Overexpression of *azoA* in *Enterococcus* sp. L2 showed 3.4 fold increase in azoreductase activity but did not result in increase in the RV5R decolorization and showed impaired growth. *AzoA*transformant of *Enterococcus* sp. L2 was found resistant to H_2O_2 stress and showed reduced level of ROS formation as compared to WT and VC. At the same time *azoA*transformant of *Enterococcus* sp. L2 showed enhanced ability to grow in presence of heavy metals such as copper and chromium which are reported to cause oxidative damage to cells suggesting adventitious roles of AzoA in oxidative stress tolerance and growth in presence of heavy metal in addition to azo dye decolorization.

5 Metabolic engineering for efficient azo dye decolorization by NADH regeneration system.

5.1. Introduction

Metabolic engineering is defined as the "directed improvement of cellular properties through the modification of specific biochemical reaction(s) or the introduction of new ones, with the use of recombinant DNA technology"(Stephanopoulos et al., 1998). It can be considered as the targeted and purposeful alteration of metabolic pathways in an organism in order to thoroughly understand and effectively utilize cellular pathways for chemical transformation, energy transduction, and supramolecular assembly (Lessard, 1996).The process involves introducing a specific genetic modification to overcome these rate limiting step(s) of a bioprocess(Vemuri & Aristidou, 2005). Metabolic engineering is also redefined as the approach that alters not only the metabolism itself but also the regulatory and gene expression networks of the target organism. It should be directed at optimizing both the production flux and the functioning of the organism itself, such that most of the unfavorable homeostatic responses and malfunctioning of the metabolism are prevented.

Nicotinamide adenine dinucleotide (reduced, NADH; oxidized,NAD^+) is a major cofactor for electron transfer in metabolism of living systems.During aerobic respiration, the resulting NADH isreoxidized by oxygen via an electron transport chain (ETC),and the released free energy is captured in the form of anelectrochemical proton gradient, which is subsequentlyused to drive ATP synthesis.Thecontinued availability of NAD^+ for substrate oxidationrelies on concomitant NADH reoxidation, and hence on acontinuous supply of oxygen. SinceNADH levels become elevated when oxygen is limited orthe electron transport chain (ETC) is inhibited (Williamson et al., 1967), the intracellular NADH/NAD+ ratio acts as a one of the sensitive indicatorof the redox state. Addition to their well-establishedmetabolic functions, pyridine dinucleotides contributerefined allosteric signals in the regulation of redox-responsivegene transcription(Lamb et al., 2008; Pan et al., 2009).

Nicotinamide adenine dinucleotide (NAD) functions as a cofactor in over 300 oxidation–reduction reactions and regulates various enzymes and genetic processes (San et al., 2002). From the total number of known redox enzymes about 80% require

NAD(H), and about 10(%) require NAD(P)H. Fewer enzymes require flavines like Flavin mononucleotide (FMN), Flavin adenine dinucleotide (FAD) or Pyrroloquinoline quinone (PQQ).Bacterial metabolism (fermentative, substrate level or oxidative phosphorylation) plays direct role in maintaining the reductive pool.Since the NADH/NAD+ pool is relatively small compared with its turnover, oxidation of the redox molecules are also equally important to keep them available for the glycolysis and TCA cycles. Supplying specific carbon sources such as pyruvate or lactate can directly oscillates the cellular NADH/NAD+ ratio (Hung et al., 2011).

Importance of NADH-NAD^+ redox has been implicated in the industrial fermentation or bio-transformation (Bäumchen & Bringer-Meyer, 2007; Parales et al., 2002). Dye decolorization by azoreductases, which carry two electron transfers at a time collectively across the azo bond in azo dyes require reduction power from redox equivalents (NAD(P)H or $FADH_2$). These enzymes compete with other cellular enzymes for NAD(P)H in cytosolic soup based on their Km values for NAD(P)H. Biocatalytic reduction of the dye molecule is initiated by electron transfer from NADH to the dye via azoreductase. However, it was found that azoreductases have high K_m values for NADH(K_m^{NADH} for AzoA is 0.14mM). So affinity values would limit the overall rate of dye decolorization. To overcome this problem, two strategies can be used.The first strategy is to perform site directed mutagenesis in the genes encoding azoreductase enzyme, and hence to achieve lower km valuesfor NADHwhereas second strategy deals with increase in the overall NADH pool inside the cell by NADH regeneration system. This chapter deals with the metabolic engineering for efficient azo dye decolorization by incorporation of NADH regeneration system in dye decolorizing bacteria. In the chapter introduction different NADH regeneration systems are discussed.

5.1.1. NADH/NAD^+ manipulation strategies

A simple approach to alter the NADH pool or NADH/NAD^+ ratio is based on the use of carbon sources with different oxidation statessuch as glucose (0), sorbitol(-1)and gluconate (+1). When these carbon sources enter the glycolytic pathway, they produce different levels of reducing equivalents in the order sorbitol>glucose>gluconate(San et al., 2002).

Genetic manipulation offers an alternative approach for manipulation of NADH pool. Overexpressing NAPRTase (encoded by the pncB gene), an enzyme in the NAD salvage pathway under its native or p*lac* promoter has been shown to increase in total levels of NAD resulting in an increase in NADH/NAD^+ ratio in batch cultures of *E. coli*(San et al., 2002). This approach was used to enhance succinate production in *E. coli*(Ma et al., 2013). Berrios-Rivera et al. (2003) used the approach of reducing the metabolic reaction competing for NADH such as lactate dehydrogenase to increase the NADH availability to enzyme of interest. A similar approach has be used wherein aldehyde dehydrogenase was inactivated to increase the availability if NADH for 1,3 propanediol production (Mu et al., 2006) and lactate/ succinate production (Yun et al., 2005).

5.1.2. NAD(P)H regeneration systems

NAD(P)H regeneration can be done by non-enzymatic (direct method) and enzymatic methods. The enzymatic approach is particularly preferred for industrial processes due to its high selectivity and efficiency. The following section describes briefly various enzymatic NAD(P)H regeneration systems.

In substrate coupled method, a single enzyme uses both the reduced and oxidized forms of a co-factor to catalyse both the desired synthesis of the product from one substrate and the cofactor regeneration reaction with a second substrate (Fig.5.1).

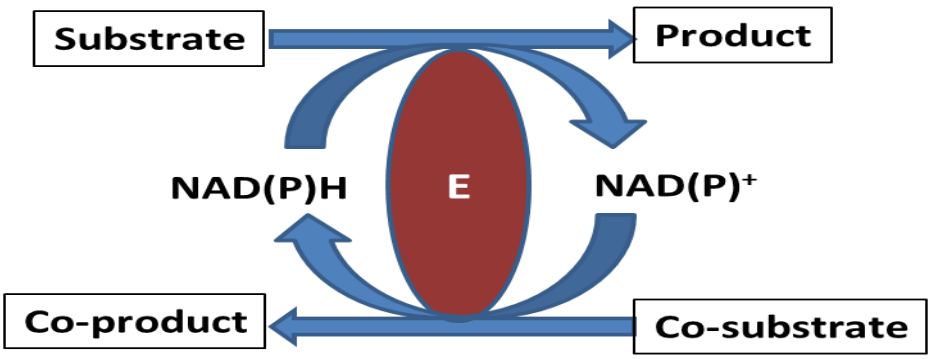

Figure 5.1 Substrate coupled method for cofactor NADH regeneration.

(E is the enzyme)

In case of the enzyme coupled method, two parallel redox reactions i.e. conversion of the main substrate and cofactor-recycling- are catalysed by two different enzymes. To achieve optimal results, both of the enzymes should have sufficiently different specifications for their receptive substrates whereupon the two enzymatic reactions

can proceed independently from each other and, as a consequence, both the substrate and the auxiliary substrate do not have to compete for the active site of a single enzyme, but are efficiently converted by the two biocatalysts independently (Figure 5.2). As a result, the enzyme-coupled approach is more advantageous. Various oxidoreductases catalyzing oxidation of particular substrates (e.g. formate, phosphite or glucose) and in turn reducing $NAD(P)^+$ have been used for NAD(P)H regeneration (Table 5.1).

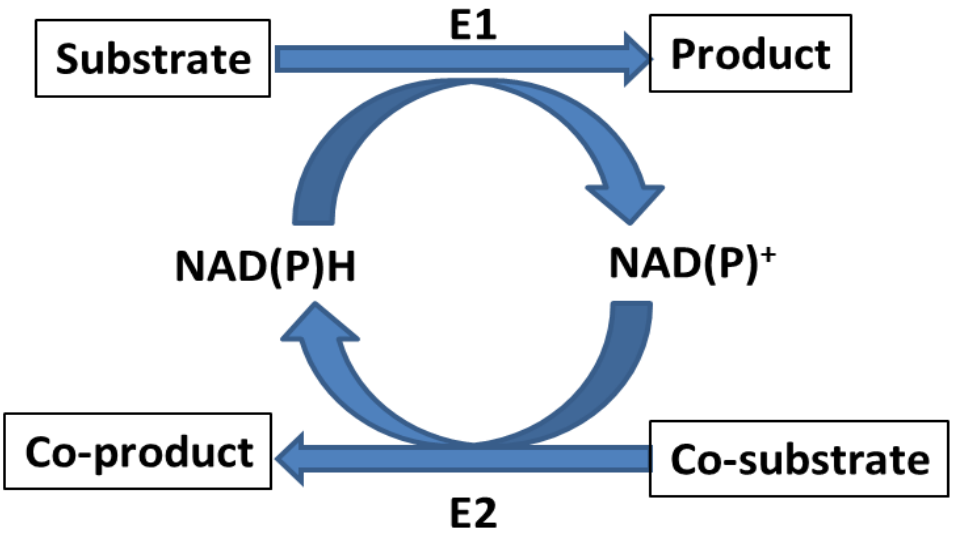

Figure 5.2Enzyme coupled method for NAD(P)H regeneration.

(E1= enzyme catalyzing desired reaction, E2 =the enzyme catalyzing regeneration reaction)

5.1.3. Formate dehydrogenase as NADH regeneration system

There is no single cofactor regeneration method which is ideal and a combination of factors determines the best method for a certain application. From the point of view of the cost, the efficiency of such a procedure may be estimated by the molar amount of synthesized product per molar amount of consumed cofactor during the course of the complete reaction. Among the various enzymes mentioned for NADH regeneration systems formate dehydrogenase is considered best for several reasons (Tishkov and Popov, 2006). The name formate dehydrogenase (FDH) combines several groups of enzymes belonging to the superfamily of D-specific 2- hydroxy acid

dehydrogenasesand are strongly varied in quaternary structure, presence and type of prosthetic group, and also in substrate specificity.

One of such groups is represented by NAD^+-dependent formate dehydrogenases (EC1.2.1.2), which catalyze oxidation of formate ion to carbon dioxide in the coupled reduction of NAD+ to NADH:

$$\mathbf{HCOO^- + NAD^+ \rightarrow NADH + CO_2.}$$

FDHs of this group consist of two identical subunits, contain no metal ions or prosthetic groups, are unable to use one-electron carriers as oxidizers, and are highly specific to both formate and NAD^+.As NADH regenerations systems, FDHs from several sources such as the methylotropic yeast *Candida boidinni*, *Pseudomonas* sp. 101 and *Paracoccus* sp. 12-A and*Mycobacterium vaccae*(Popov & Vladimir, 2000). Differently localized FDHs have been shown to accept various electron acceptors such as methyl viologen, NAD^+ and ferricytochrome b1; for NADH regeneration NAD^+ dependent formate dehydrogenase specifically utilized.Thereaction catalyzed by FDH fits all the criteria for NAD(P)H regeneration such as: the reaction is irreversible under normal conditionsresulting in a 99–100% yield of the finalproduct; formate-ion is a cheap substrate, and the reaction product,CO2, can be easily removed from the reaction mixture anddoes not interfere in the main reaction; FDH exhibits a wide pH-optimum of catalytic activity (6.0–9.0);bacterial and yeast FDHs are sufficiently stable for continuous reactors.

Azoreductases catalyze two electron transfer across the azo bond in azo dyes using NAD(P)H as cofactor. Azoreductases have high Km values for NADH as compared to the NADH peroxidase and other NADH:quinone reductase systems, thus cofactor levels directly affect the overall rate of dye decolorization. This chapter deals withthe metabolic engineering approach by incorporationof NADH regeneration system using NAD^+ formate dehydrogenase for enhancing the availability of reducing equivalents (NADH) for *in vivo* for dye decolorization. Further, overexpression systems were developed for gram negative and gram positive bacteria for NADH regeneration and their effect on azo dye decolorization studied. Subsequently, a transcription fusion of

azoA and *fdh*was constructed as a dual enzyme based azo dye decolorizing machinery for the efficient bio-decolorization.

Table 5.1 Enzymes used for NAD(P)H regeneration system

Enzyme	**Coenzyme require**	**Reaction catalyzed**	**Source**	**Reference**
Formate dehydrogenase	NAD^+	Formate+NAD^+→ NADH+ H^+ +CO_2	*Candida boidinii*	San (2002)
Soluble pyridine nucleotide transhydrogenase (STH)	NAD^+	NAD^++NADPH↔ NADH +$NADP^+$	*Pseudomonas fluorescens*	Boonstra et al. (2000)
Phosphite dehydrogenase	NAD^+	Phosphite + NAD^+→ Phosphate+ NADH + H^+	*Pseudomonas stutzeri*	Johannes et al. (2006)
Alcohol dehydrogenase	NAD^+	Alcohol+ NAD^+→ Acetone+ NADH + H^+	*Pseudomonas* sp.	Bradshaw, et al (1992)
Alcohol dehydrogenase	$NADP^+$	Alcohol+ $NADP^+$→ Acetone+ NADPH + H^+	*Thermoanaerobacter brockii*	Lamed et al. (1981)
Glucose 6-phosphate dehydrogenase	$NADP^+$	Glucose 6-phosphate + $NADP^+$→ 6-phospho glucono lactone + NADPH +H^+	*Leuconostocme senteroides*	C.Wong et al. (1981)
Glucose dehydrogenase	NAD^+ or $NADP^+$	β-DGlucose+$NAD(P)^+$→ D-glucono 1,5 lactone +NAD(P)H + H^+	*Bacillus subtilis*	Weckbecker & Hummel (2005)
Hydrogenase	NAD^+ or $NADP^+$	H_2+ $NAD(P)^+$→ NAD(P)H+H^+	*Methanothermobacter thermoautotrophicum*	Wong et al. (1981)

5.2. Results

5.2.1. Cloning of *M. vaccaefdh* and *fdh-azoA* in expression vectors

The source of *fdh* gene for this study was *Mycobacterium vaccae* N10. With a specific activity of approximately 10 U/mg and pH range between 5.5-11.0, the FDH from *Mycobacterium vaccae* N10 (MycFDH) is among the most stable and active FDH enzymes known. The *azoA* gene was from efficient RV5R decolorizing isolate *Enterococcus* sp. L2 obtained in this work (Table 2.1, Chapter 2).

5.2.1.1. *Construction of pBBR1MCS2fdh*

The p*T7fdh* gene cassette (1.5kb) was PCR amplified using Myc*fdh*F and Myc*fdh*R primers and it was ligated at EcoRV site of pBBR1MCS2. The ligation product was then transformed into competent *E.coli* DH5α. Based on blue-white screening strategy total 9 white putative colonies were screened for the clone confirmation. Presence of p*T7-fdh* gene cassette in correct orientation with p*lac* promoter was checked by the XbaI digestion of plasmids extracted from the selected colonies. The size of the recombinant plasmid is around 6.3kb which is expected to release of 1.2kb insert fragment and 5.1kb vector backbone upon XbaI digestion (Fig. 5.3a). Subsequently pBBR1MCS2*fdh*was confirmed by PCR amplification using Myc*fdh*F and Myc*fdh*R primers amplifying 1.5kb cassette (Fig. 5.3b). Map of pBBR1MCS2*fdh* is show in Fig. 5.4.

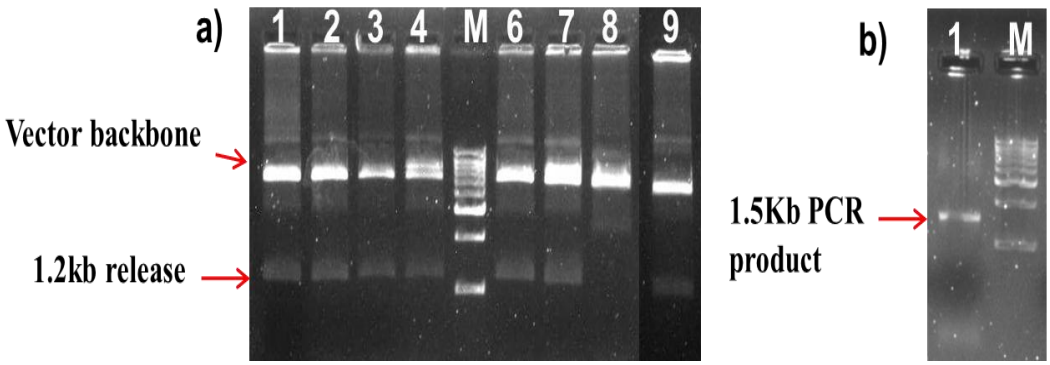

Figure 5.3 Clone confirmation of pBBR1MCS2*fdh* by RE digeston and PCR amplification.

a) XbaI digestion b) PCR confirmation(Lane-1 to 9 XbaI digestions of transformants)

5.2.1.2. *Construction of pBBR1MCS2fdh-azoA*

To construct pBBR1MCS2*fdh-azoA*, the p*T7fdh* cassette was first cloned in pBS KS(+) and subsequently ligated in to pBBR1MCS2*azoA*(Fig. 4.5, Chapter 4). Insertion of p*T7-fdh* cassette at EcoRV site of pBS KS(+) was determined by restriction digestion of the recombinant plasmid with SalI in which the expected release of 1.2kb *fdh* insert along with 2.9kb vector backbone was obtained as shown in Fig.5.5a.The presence of *fdh* cassette in the putative clone was confirmed by PCR using Myc*fdh*F and Myc*fdh*R primers and the expected 1.5kb amplicon of p*T7fdh* cassette was obtainedin three transformants (Fig.5.5b). This plasmid was denoted as pBS KS(+)*fdh*(Fig 5.6).

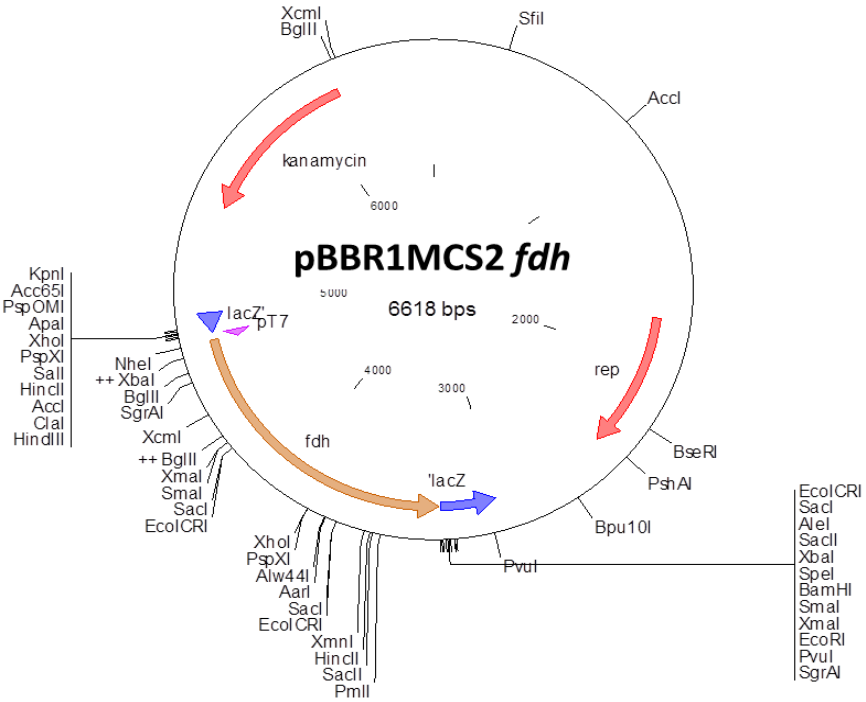

Figure 5.4 Map of pBBR1MCS2*fdh*

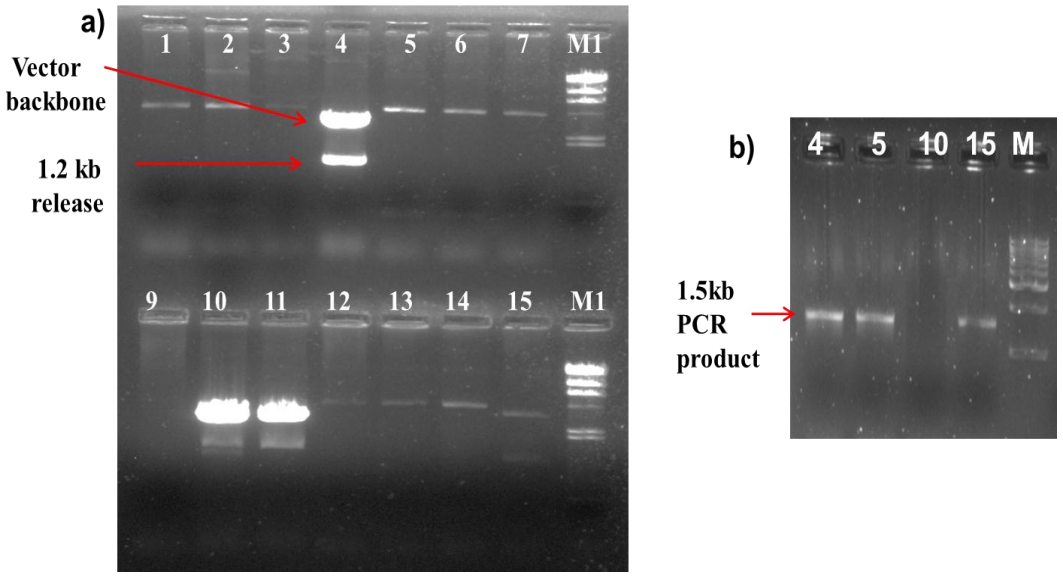

Figure 5.5 Clone confirmation of pBS KS(+)*fdh*by RE digestion and PCR confirmantion

a) SalI digestion (Lane1 to 15 SalI digestion of transformants)b) PCR confirmation(4,5,10,15 are transformants *fdh* gene PCR amplicons)

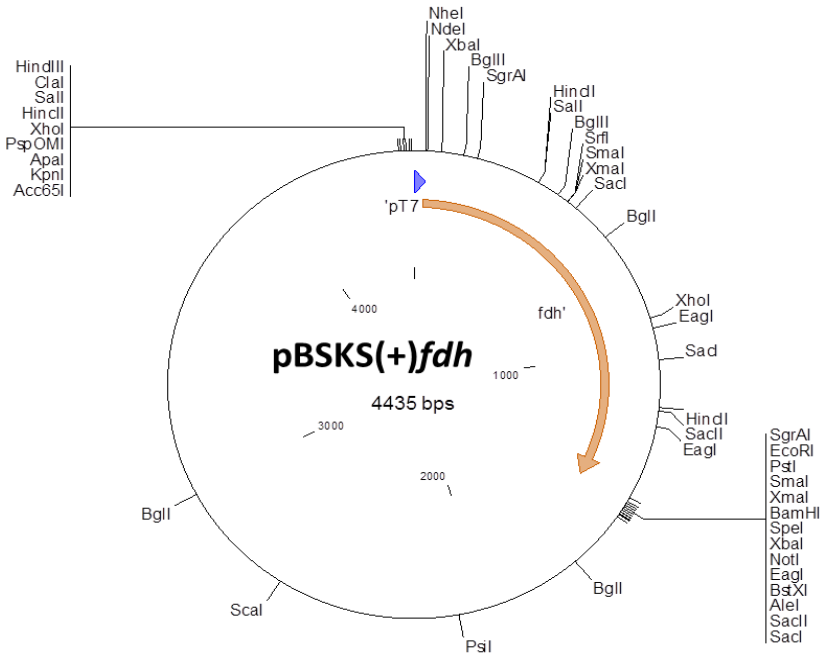

Figure 5.6 Map of pBS KS(+)*fdh*

Coexpression construct of *fdh* and *azoA* (pBBR1MCS2*fdh-azoA)* was synthesizedby firsteluting the p*T7-fdh* cassette released by KpnI digestion of pBS KS(+)*fdh* (Fig. 5.6) and subsequently ligating with KpnI lineralized

pBBR1MCS2*azoA*.The ligation product was transformed into *E.coli* DH5α and atotal 6 kanamycin resistantputative clones were obtained and screened for positive construct. The direction of the *fdh* relative to *plac* was determined by restriction digestion with SalI and XbaI. There are three restriction sites for SalI in the recombinant plasmid which releases approximately 0.5kb, 1.1kb and 5.6kbfragments as seen in Fig.5.7a (Lane 2).Further confirmation was done by XbaI digestion. Two restriction sites for XbaIis expected to release two bands of approximately2.1kb and 5.1kb were obtained (Fig.5.7a, lane3) confirming the pBBR1MCS2*fdh-azoA.* The presence of *azoA*and *fdh* in the putative clones was confirmed by PCR amplification,resulting in band of 0.6kb (Fig.5.7b) and 1.5kb (Fig.5.7c) using *azoA* and *fdh* specific primers respectively. Map of the pBBR1MCS2*fdh-azoA*is depicted in Fig. 5.8.

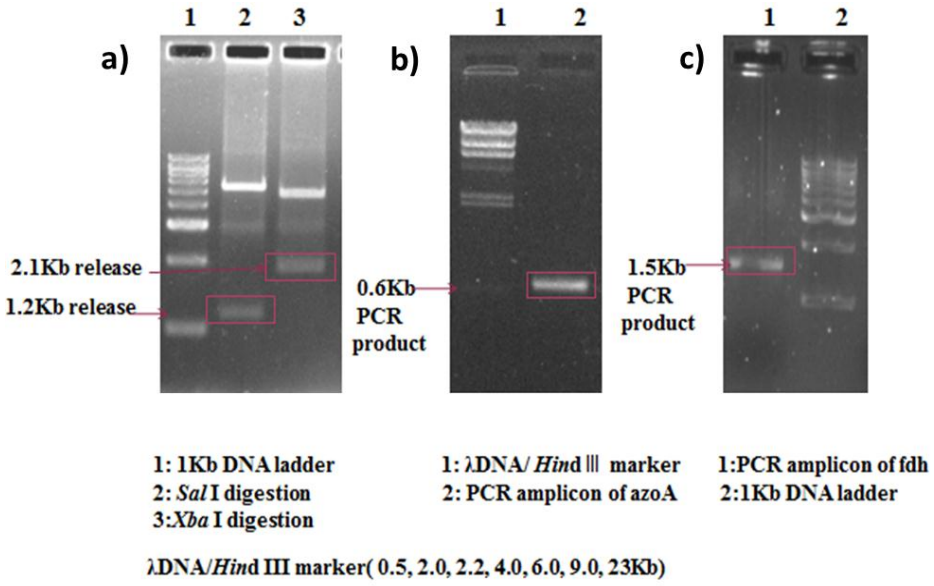

Figure 5.7 Clone confirmation of pBBR1MCS2*fdh-azoA* RE digestion and PCR confirmation.

a) RE digestions; b) *azoA* PCR confirmation; c) *fdh* PCR confirmation

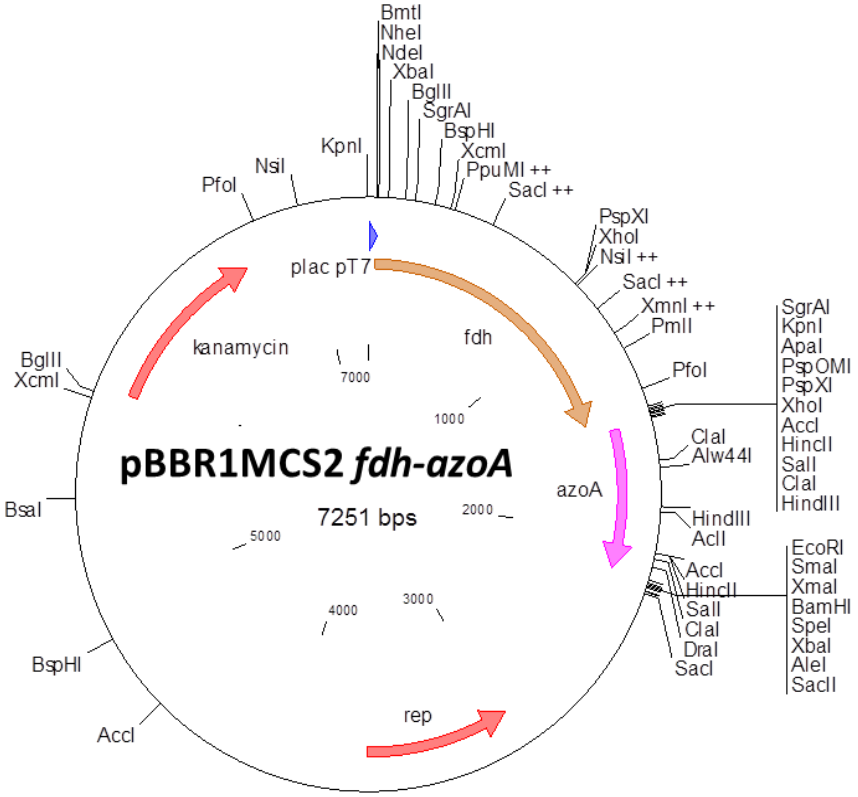

Figure 5.8 Map of pBBR1MCS-2*fdh-azoA*

5.2.1.3. *Construction of pMGS100fdh*

pMGS100*fdh*was constructed for heterologous expression of *fdh* in *Enterococcus* sp. L2 (gram positive host system). Plasmid pMGS100is an *E. coli-Enterococcus*shuttle expression vector containing constitutive bacitracin promoter and its corresponding ribosome binding site. The coding region of *fdh*(start to stop codon) was PCR amplified using MGS100*fdh*F and Myc*fdh*R primers and the blunt ended product was ligated with NruI digested pMGS100.The ligated product obtained was then transformed into *E.coli* DH5α. Total 90 chloramphenicol resistant colonies were screenedfor clone confirmation using BamHI digestion since this RE is expected to give rise to bands of 1.2kb (*fdh*) and 10.4kb (vector backbone) when in the correct orientation (of *fdh*ORF relative to constitutive bacitracin promoter). The resulted for RE digestion is shown in Fig.5.9a showing positive band pattern in two transformants. PCR amplification of *fdh* from recombinant plasmid was done, resulting in 1.2kb band corresponding to *fdh* (Fig.5.9b). Map for pMGS100*fdh* is shown in Fig. 5.10.

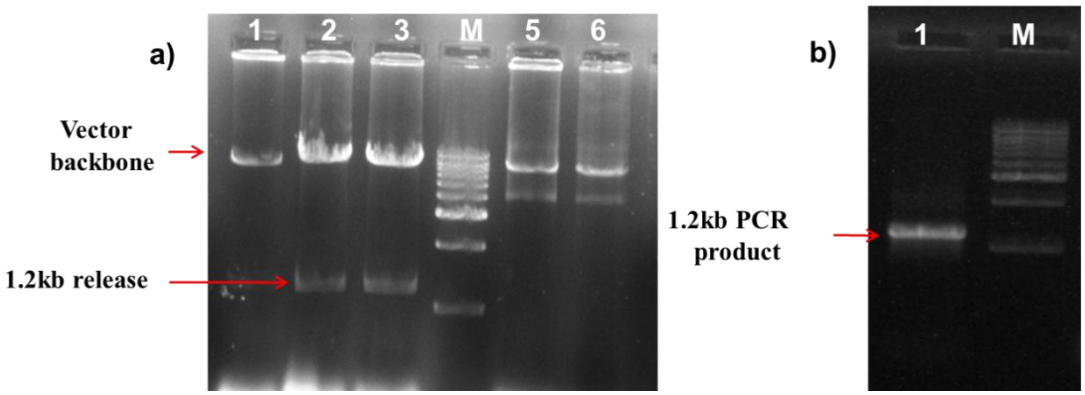

Figure 5.9Clone confirmation of pMGS100*fdh* by RE digestion and PCR confirmation.

a) BamHI digestion b) *fdh* (coding ORF)PCR confirmation(a)Lane-1 to 6 BamHI digestion of transformants)

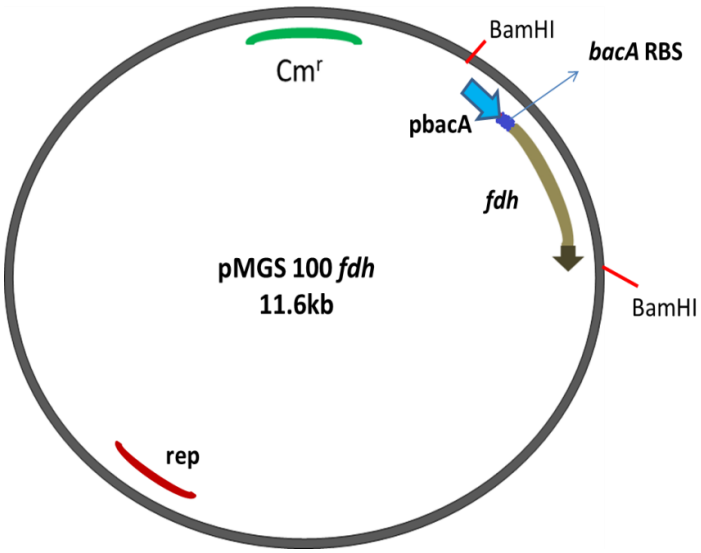

Figure 5.10Map of pMGS100*fdh*

5.2.1.4. *Transformation of fdh and fdh-azo constructs in to various bacterial strains*

The plasmids pBBR1MCS2*fdh* and pBBR1MCS2*fdh-azoA* were transformed into gram negative strains such as *E. coli* DH5α, *E.coli*BL21 (DE3),*P.fluorescens* PfO-1 (standard strains) and RV5R decolorizing isolates A3, C1, E2, G1, K1, L1 obtained in this study (Table 2.1, Chapter 2). pMGS100*fdh* was electroporated in to *Enterococcus* sp. L2.

5.2.1.4.1. PCR confirmation of pBBR1MCS2 *fdh*, pBBR1MCS2 *fdh-azoA* and pMGS100*fdh* transformants

The presence of appropriateplasmids (pBBR1MCS2*fdh* and pBBR1MCS2*fdh-azoA*)from all the gram negative transformantswere confirmed by PCR using corresponding gene specific primers. Figs. 5.11 and 5.12 show PCR confirmation of *fdh* transformants of bacterial isolates and standard strains respectively. Fig. 5.13 depicts PCR confirmation of *fdh-azoA* transformants. The *fdh* transformant of *Enterococcus* sp. L2 was confirmed by PCR using the *fdh*specific primers (data not shown).

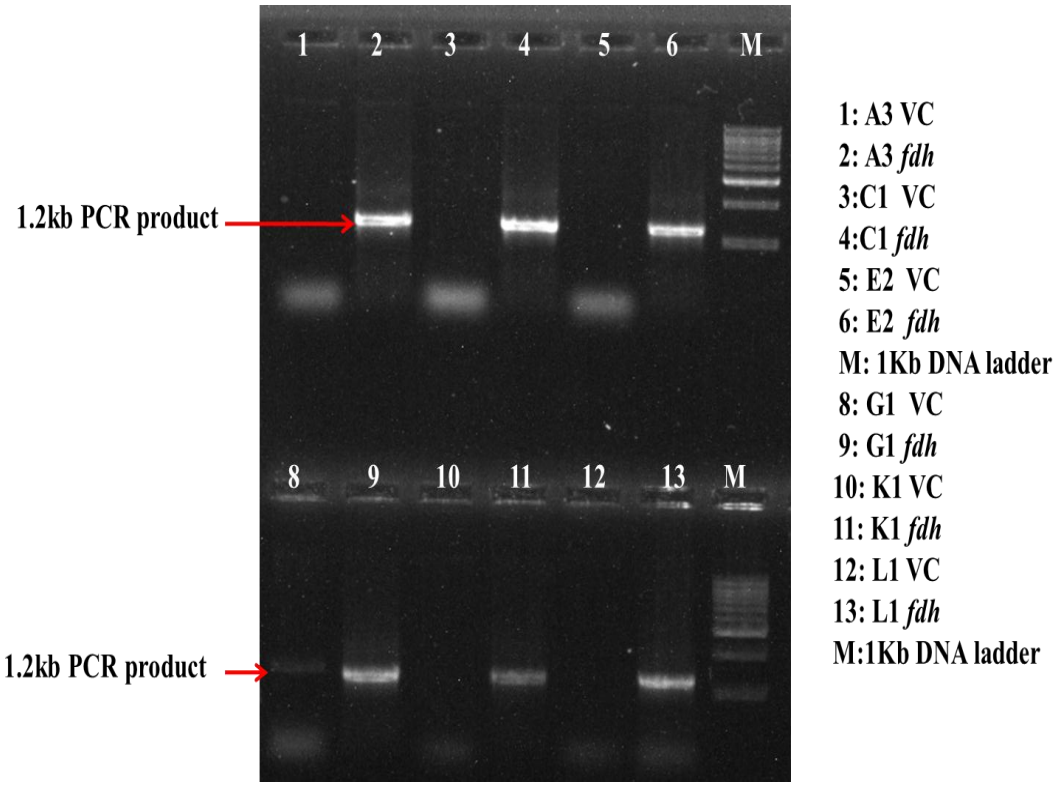

Figure 5.11PCR confirmation of pBBR1MCS2*fdh* transformants by *fdh* specific PCR.

VC: Vector control and *fdh* denotes the pBBR1MCS2*fdh* transformants.

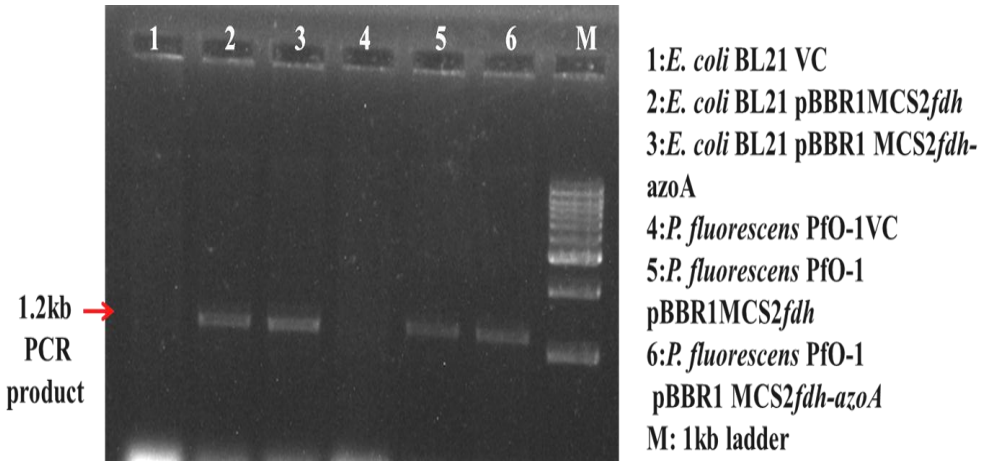

Figure 5.12PCR confirmation of pBBR1MCS2*fdh* and pBBR1MCS2*fdh-azoA* transoformants of*E.coli* BL21(DE3) and *P.fluorescens* PfO-1 with *fdh* specific primers.

VC: Vector control.

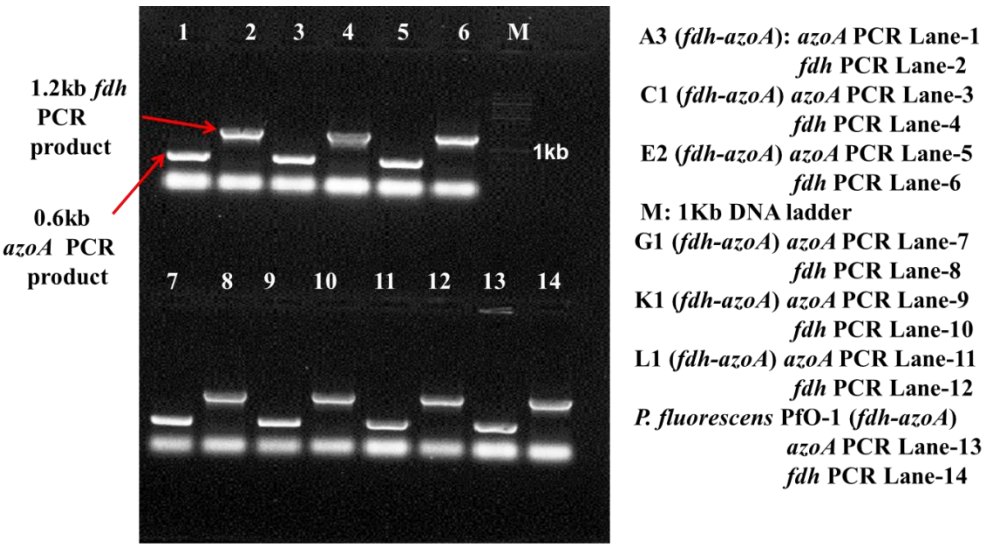

Figure 5.13PCR confirmation of pBBR1MCS2*fdh-azoA* transformants by *fdh* and *azoA* specific primers.

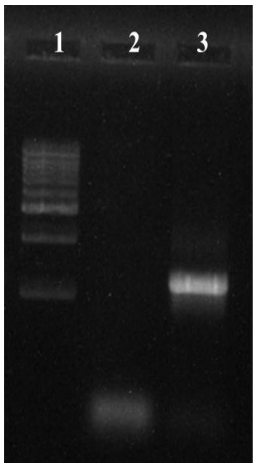

Figure 5.14PCR confirmation of Enterococccus sp. L2 harboring pMGS100*fdh* (transformant) by corresponding *fdh* specific primers

5.2.1.4.2. Strain confirmation of *fdh* and *fdh-azoA* transformants

Various transformants harbouring different plasmids for *fdh* and *fdh-azoA* expression were confirmed for strain identity using 16S rRNA genotyping (ARDRA) comparison with corresponding untransformed bacterial isolate or standard strains. The ARDRA patterns obtained using HinfI for all transformants werefound to be same as their corresponding wild type strains confirming the host strains (Fig.5.15).

5.2.1.4.3. Whole cell protein profile of *fdh* and *fdh-azoA* transformants

Presence of overexpressed proteins were analysed in the transformants using SDS-PAGE. The overexpression of FDH protein of 44kDa was clearly seen in the whole cell lysate of *E.coli* BL21 (DE3) (pBBR1MCS2*fdh)* with 1mM IPTG induction as seen in Fig.5.16 (lane 2). The corresponding band was also seen in uninduced condition at much lesser intensity indicating basal level expression via p*lac* promoter. *E.coli* BL21(DE3) harbouring pBBR1MCS2*fdh-azoA*showed a23kDa corresponding to the AzoA in addition to the 44kDa (FDH) under induced as well as uninduced conditions (Fig.5.16). *Enterococcus*sp.L2 harboringpMGS100*fdh* showed the expected overexpressed band of 44kDa(Fig.5.17).

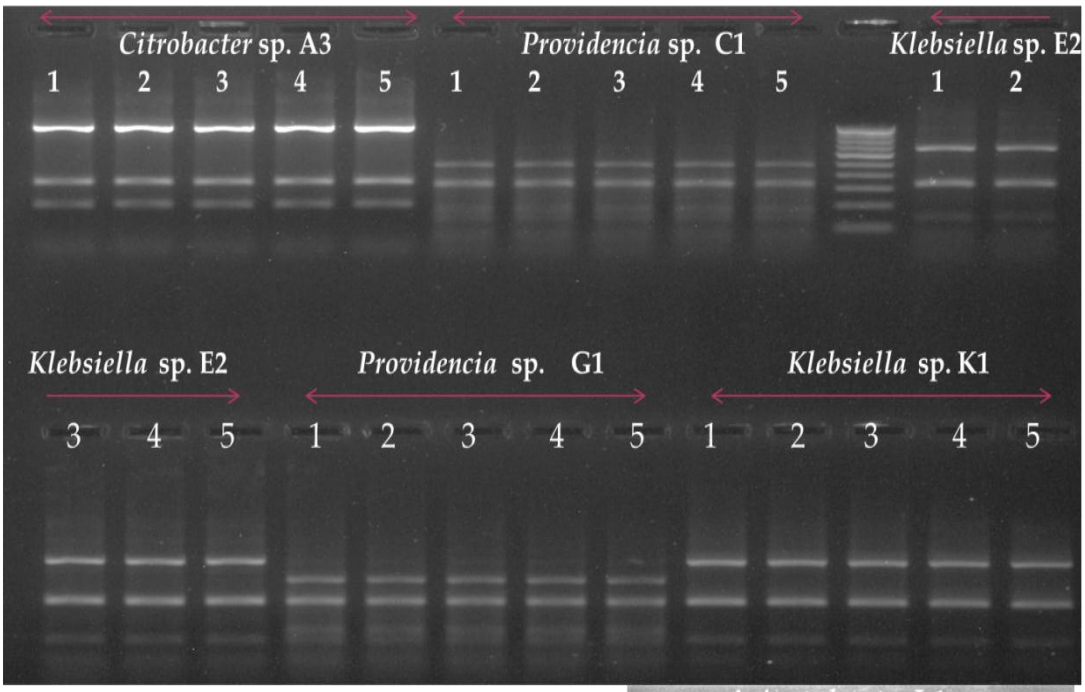

1. Isolate
2. pBBR1MCS2 (VC)
3. pBBR1MCS2*azoA*
4. pBBR1MCS2*fdh*
5. pBBR1MCS2*fdh-azoA*

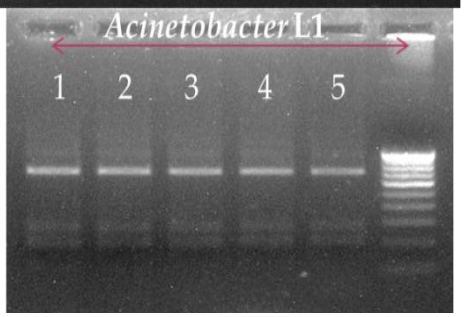

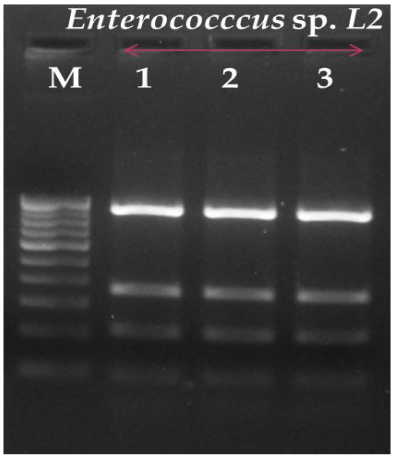

1. L2 strain (WT)
2. pMGS100 (VC)
3. pMGS100fdh

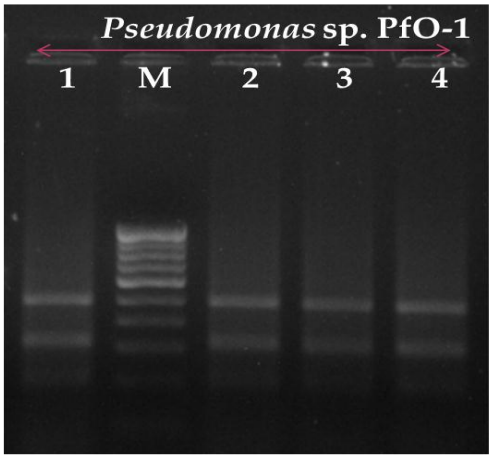

1. pBBR1MCS2 (VC)
2. pBBR1MCS2*azoA*
3. pBBR1MCS2*fdh*
4. pBBR1MCS2*fdh-azoA*

Figure 5.15ARDRA profiles of*azoA*, *fdh* and *fdh-azoA* transformant strains.

(M-100bp ladder; VC: Vector control)

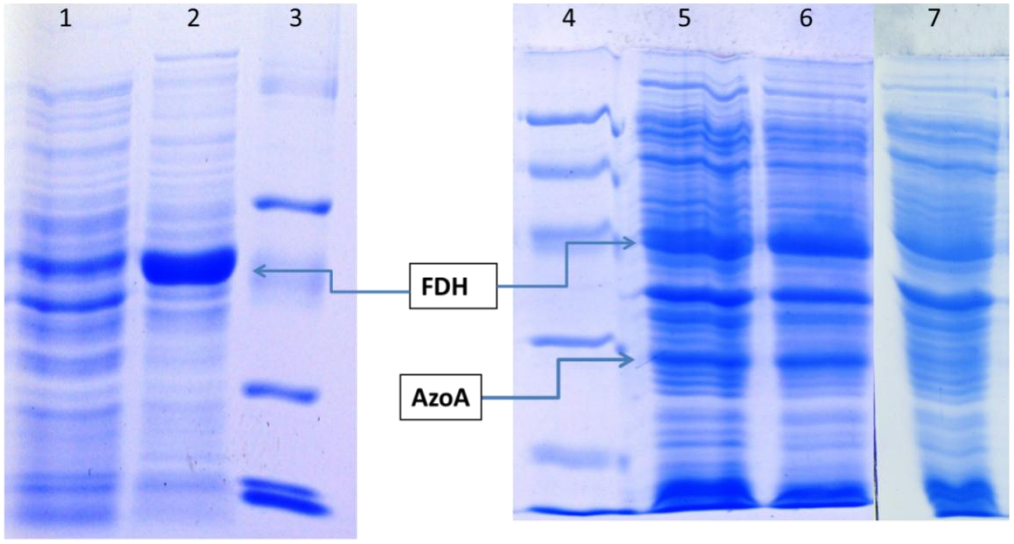

1: pBBR1MCS2*fdh* uninduced; 2: pBBR1 MCS2*fdh* induced; 3 and 4: Marker;
5: pBBR1MCS2*fdh*-azoA uninduced; 6:pBBR1MCS2*fdh-azoA* induced; 7: : pBBR1MCS2 (VC)
Marker = 97,66,43,29,20,14KDa

Figure 5.16SDS-PAGE analysis of *E.coli* BL21 pBBR1MCS2*fdh* and *fdh-azoA*transformants.

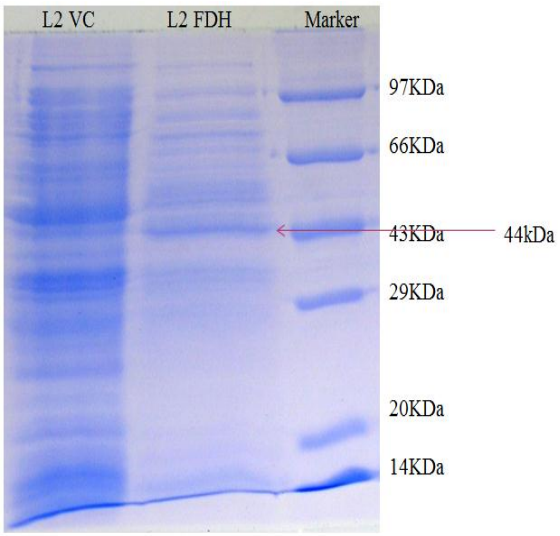

Figure 5.17SDS-PAGE analysis of *Enterococcus*sp. L2 (pMGS100*fdh*) transformant.

(VC-vector control)

5.2.2. Effect of heterologous expression of pBBR1MCS2*fdh*and pMGS100*fdh*

Azoreductase dependent azo dye decolorization demands high supply of reducing equivalents in form of NAD(P)H. To increase the supply of this cofactor *in vivo*,

various NADH regeneration systems could be used. In this study, formate dehydrogenase (FDH) was used as NADH regeneration system to assess its contribution to azo dye decolorization in different bacterial strains. A collection of diverse RV5R decolorizing bacteria and standard strains were engineered for *fdh* overexpression and their physiological characterization was done.

5.2.2.1. *FDH activity of fdh transformants*

FDH activity was assayed in bacterial strains expressing *Mycobacterium vaccae* NAD^+ dependent formate dehydrogenase. As seen in Fig. 5.18, various host strains exhibited different levels of inherent FDH activity (as seen in untransformed and VC strains) with *Klebsiella* spp. E2 and K1 showing maximum FDH activity and *E. coli* strains showing lowest. Approximately 2 fold higher NAD^+FDH specific activity was obtained in *E. coli* DH5α and *P. fluorescens* PfO-1 strains harboring pBBR1MCS2*fdh* wherein expression was driven by p*lac* promoter (Fig. 5.18).*E. coli* BL21 (DE3) harbouring pBBR1MCS2*fdh* showed 6 fold increase in FDH specific activity compared to the VC presumably due to collective transcription from p*lac* and p*T7*promoters. For *Pseudomonas* sp. and *Enterococcus* sp. IPTG induction was not carried out since the expression was expected to be constitutive. *P.fluorescens* PfO-1 *fdh*transformant showed 9.58U/mg with fold increase of 2.35 as compared to VC which has specific activity of 4.08U/mg.*Enterococcus*sp. L2 *fdh*transformant showed specific activity of 12.56U/mg with a fold increase of 6.05.

Among all the other gram negative transformants, *Klebsiella*sp. E2 transformant (IPTG induced) showed maximum specific activity of 70.87U/mg as compared to VC (34.12U/mg) with only 2.07 fold increase. This is due to higher native FDH activity in E2 as compared to other organisms. Similar results were obtained for other transformant of *Klebsiella* sp. K1, which showed higher specific activity of 49.45U/mg with fold increase of only 1.5. The specific activity for*Acinetobacter* sp. L1 *fdh* transformant was found to be 45.88U/mg under IPTG induction which appears to be constitutively expressed since uninduced activity was equally high. Overall it can be seen that the FDH activity of all the transformants was significantly due to plasmid borne heterologous overexpression of mycobacterial NAD^+*fdh.*

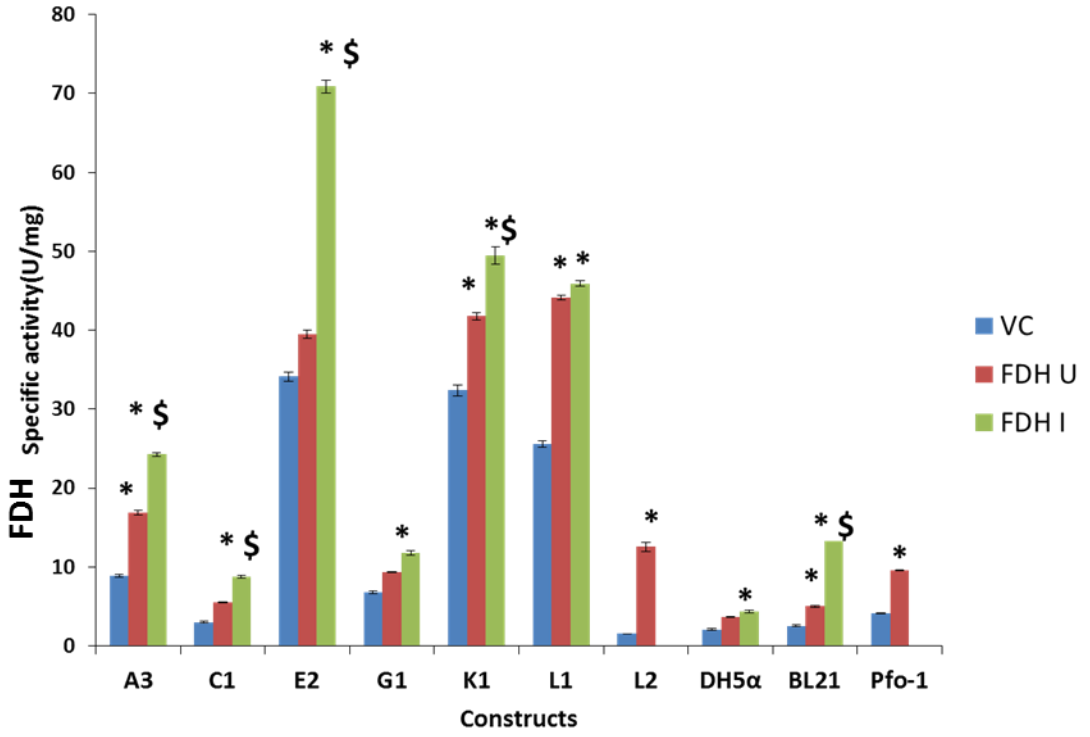

Figure 5.18FDH activity of *fdh* transformants

VC: Vector control; FDH U:*fdh* transformants uninduced ; FDH I:*fdh* transformants induced with IPTG (1mM) (* indicates significant p<0.01 increase in FDH activity in *fdh* transformant compared to the VC, $ indicates significant p<0.01 increase in FDH activity in induced compared to uninduced conditions)

5.2.2.2. *NADH estimation in fdh transformants*

The absorbance ration of $A_{340/280nm}$ was used as a measure of intracellular NADH concentration relative to the total protein concentration. Table 5.2 shows the average absorbance reading for 340nm, 280 nm and $A_{340/280nm}$ ratio and fold increase for all the transformants when grown in LB amended with formate (300mM). There was a significant increase in NADH/ total intracellular protein seen for *fdh* transformants of *E. coli* strains, *Citrobacter* sp. A3 (uninduced), *Providencia* sp. C1, *Klebsiella* spp. E2 and K1 (uninduced) and *Enterococcus* sp. L2. In other cases, induced cells of *fdh* transformants showed a decrease or no significant increase in $A_{340/280nm}$ ratio. However the NADH levels did not correlate with the FDH activity and in general increase in NADH levels were much less than the increase in FDH activity.

Table 5.2 $A_{340/280nm}$ ratio and fold increase for *fdh*transformants.

Transformants	A_{340nm}	A_{280nm}	$A_{340/280\ nm}$	Fold increase
***E. coli* DH5α VC**	0.100	1.015	0.099 ± 0.007	
***E. coli* DH5α FDH U**	0.127	1.122	0.114 ± 0.004	**1.15**
***E. coli* DH5α FDH I**	0.144	1.317	0.110 ± 0.004	**1.11**
***E. coli* BL21 (DE3) VC**	0.096	0.864	0.111 ± 0.005	
***E. coli* BL21 (DE3) FDH U**	0.177	1.244	0.143 ± 0.004	**1.28**
***E. coli* BL21 FDH I**	0.162	1.213	0.134 ± 0.007	**1.20**
***P. fluorescens* Pfo-1 VC**	0.250	1.778	0.141 ± 0.004	
***P. fluorescens* Pfo-1 FDH**	0.286	1.914	0.149 ± 0.004	**1.06**
***Citrobacter* sp. A3 VC**	0.094	1.201	0.079 ± 0.004	
***Citrobacter* sp.A3 FDH U**	0.118	1.242	0.095 ± 0.004	**1.21**
***Citrobacter* sp.A3 FDH I**	0.115	1.396	0.082 ± 0.005	**1.05**
***Providencia* sp. C1 VC**	0.115	1.151	0.100 ±0.004	
***Providencia* sp.C1 FDH U**	0.127	0.398	0.319 ± 0.004	**3.19**
***Providencia* sp.C1 FDH I**	0.149	1.259	0.118 ± 0.001	**1.18**
***Klebsiella* sp. E2 VC**	0.115	1.205	0.095 ± 0.004	
***Klebsiella* sp.E2 FDH U**	0.181	1.220	0.148 ± 0.007	**1.56**
***Klebsiella* sp. E2 FDH I**	0.109	1.026	0.106 ± 0.001	**1.11**
***Providencia* sp.G1 VC**	0.211	1.293	0.163 ± 0.005	
***Providencia* sp.G1 FDH U**	0.231	1.338	0.172 ± 0.027	**1.06**
***Providencia* sp.C1 FDH I**	0.204	1.350	0.151 ± 0.005	**0.92**
***Klebsiella* sp.K1 VC**	0.091	0.890	0.102 ± 0.008	
***Klebsiella* sp.K1 FDH U**	0.134	0.976	0.137 ±0.006	**1.34**

***Klebsiella* sp.K1 FDH I**	0.105	1.145	0.091 ± 0.005	**0.89**
***Acinetobacter* sp. L1 VC**	0.106	1.120	0.095 ± 0.006	
***Acinetobacter* sp.L1 FDH U**	0.103	1.001	0.103 ± 0.005	**1.08**
***Acinetobacter* sp.L1 FDH I**	0.112	1.288	0.087 ± 0.006	**0.92**
***Enterococcus* sp.L2 VC**	0.205	0.519	0.395 ± 0.009	
***Enterococcus* sp.L2 FDH U**	0.247	0.543	0.455 ± 0.012	**1.15**

VC: Vector control; FDH U: *fdh* transformant uninduced; FDH I: *fdh* transformant induced with 1mM IPTG.

5.2.2.3. *Effect of fdh overexpression on growth*

To understand the effect of heterologous expression of *fdh*, growth curve analysis was performed with standard strains (*E.coli*DH5α,*E. coli*BL21 (DE3), *P. fluorescens* PfO1) and one lab isolate *Enterococcus* sp. L2. Eachofthesesystemswaskeptunder shakingas wellas static condition of incubation except strain L2 which wasanalyzed onlyunder static conditions,growth in Luria broth (LB)as wellas Bushnell-Haas medium (BHM) amended with 0.5% yeast extract (YE) and with and withoutformate.

Under static conditions, *E. coli* DH5α*fdh*transformantgrew equally well with and without formate as compared to VC (Fig. 5.19). However the growth of the transformant exceeds that of VC when formatewas amended in BHM+YE. InBHM+YE, formate addition provides significant growthadvantageto the*fdh* transformant. Under shakingconditions, initially the*fdh* transformantgrows slowlyas compared to its controlin all media,except BHM +YE, however after 12 hofincubation the *fdh* transformant outgrows the VC. In*E. coli* BL21 (DE3), *fdh* expression resulted in significant growth advantage in LB amended with formate as compared to VC (Fig. 5.20). *P. fluorescens* PfO-1 expressing *fdh*, showed significant increase in growth under shaking conditions regardless of formate amendment (Fig. 5.21). *Enterococcus* sp. L2 *fdh* transformantgrowsenormouslyfaster with and without formate supplement in both media under static condition (Fig. 5.22). This indicates that expression of*fdh* in*Enterococcus* sp.L2 hasprovided a growth advantage as *Enterococcus*spp.lack formate metabolizing machinery and additionally secrete formate in medium.

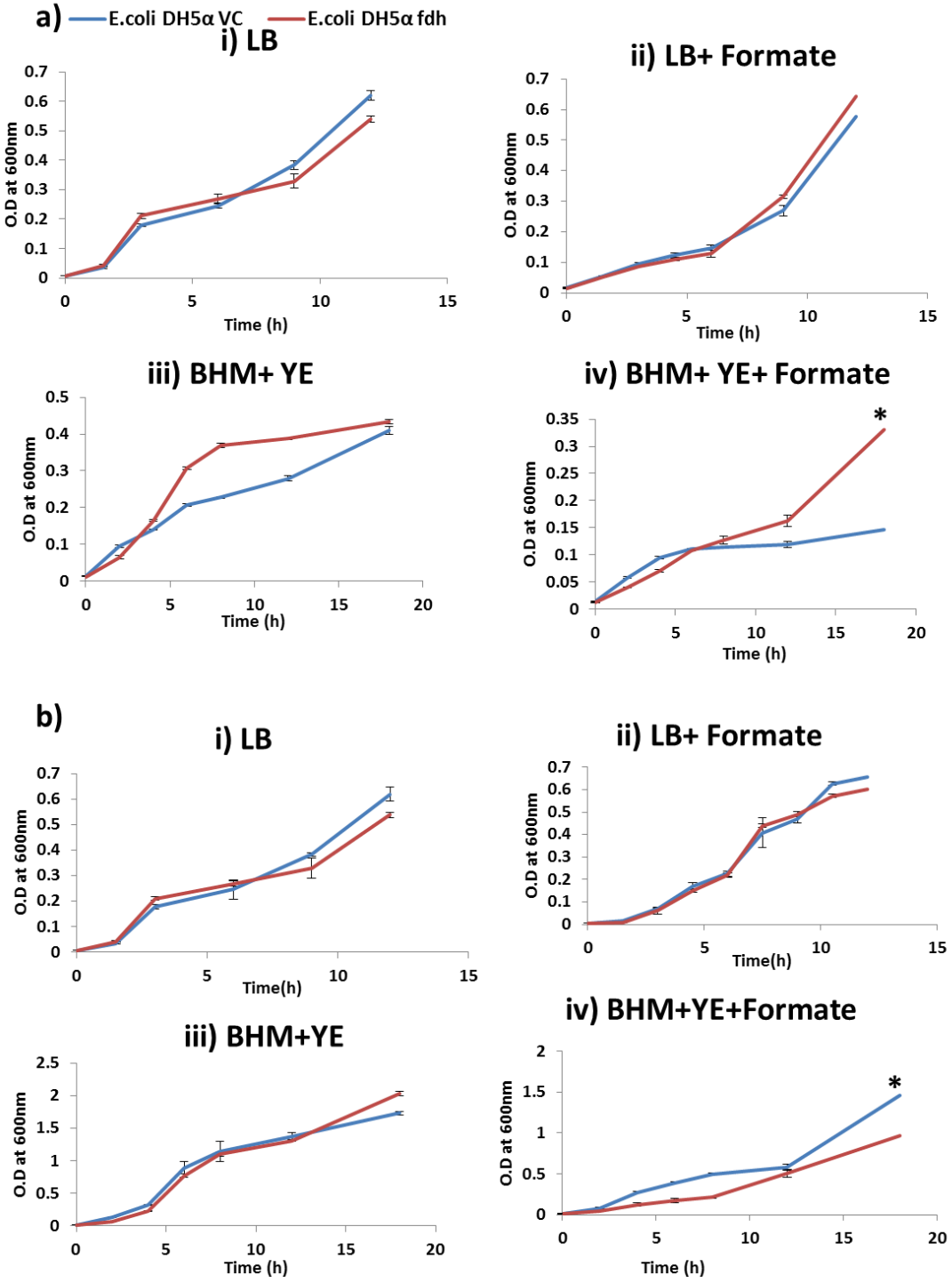

Figure 5.19 Effect of heterologous expression of *fdh* on growth of *E. coli* DH5α.

a) static and b) shaking conditions(* indicates significant difference compared to VC at p<0.01)

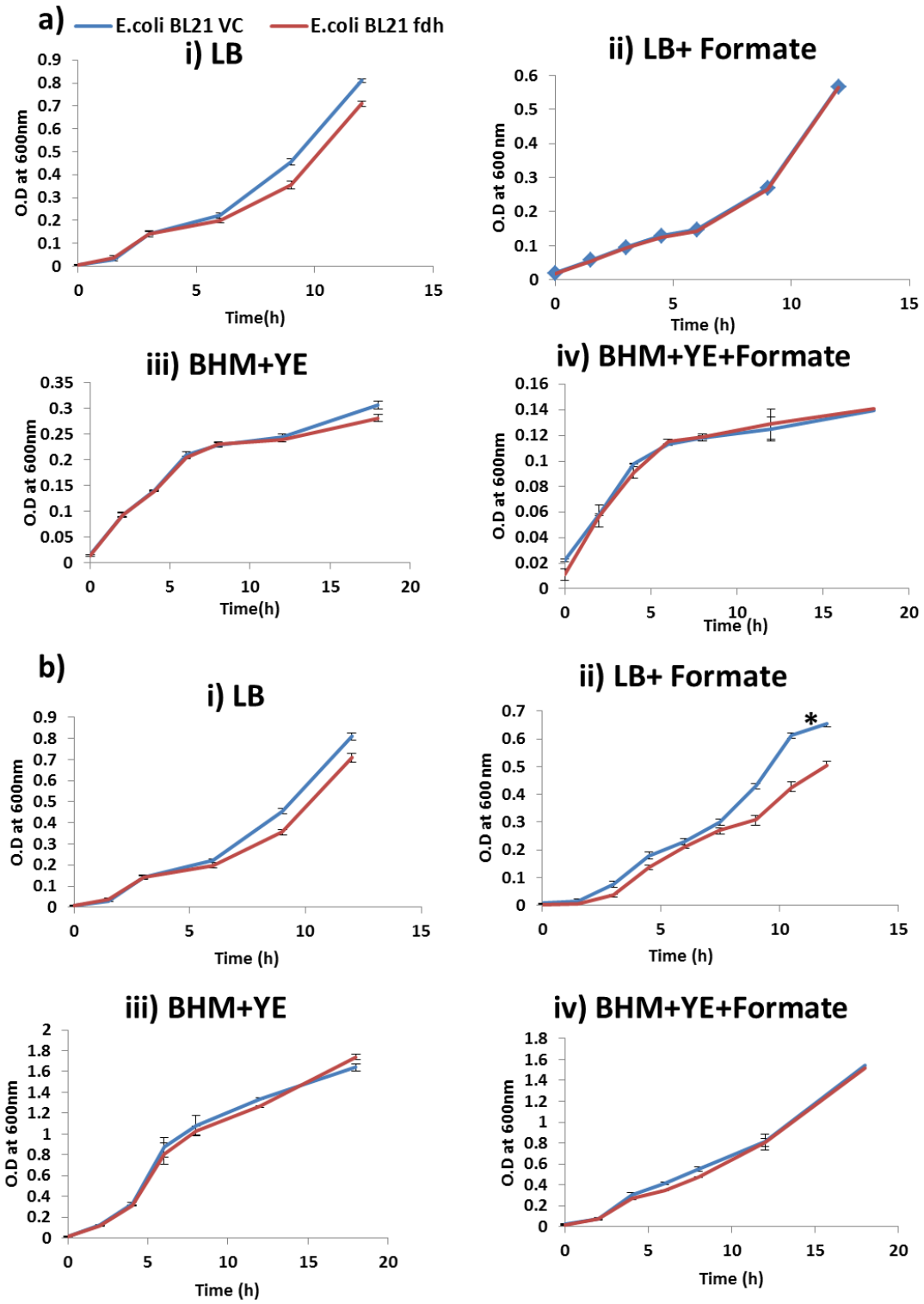

Figure 5.20 Effect of heterologous expression of *fdh* on growth of *E. coli* BL21 (DE3).

(Under a) static and b) shaking conditions)(* indicates significant difference compared to VC at $p<0.01$)

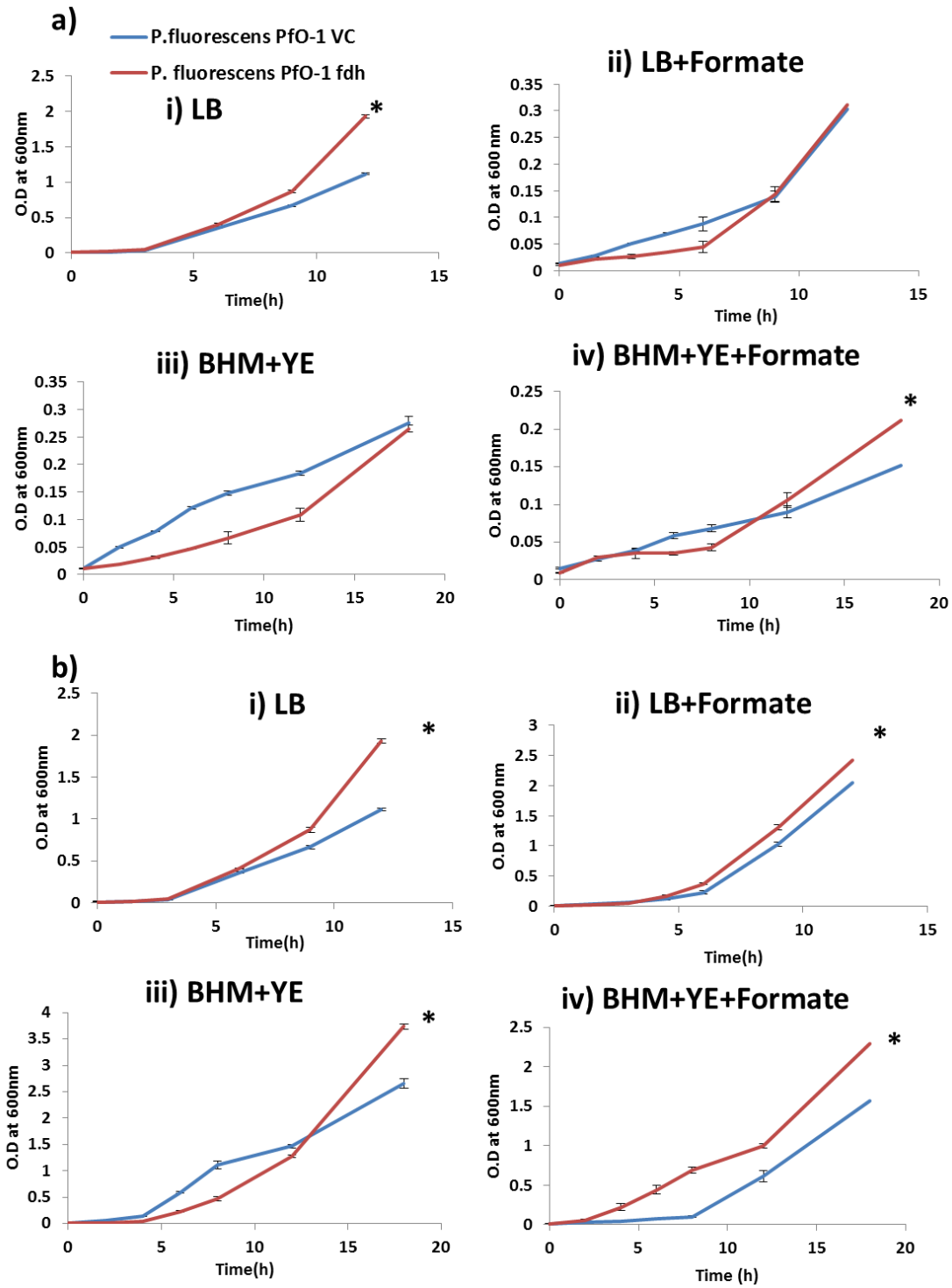

Figure 5.21 Effect of heterologous expression of *fdh* on growth of *P. fluorescens* PfO-1.

(Under a) static and b) shaking conditions)(* indicates significant difference compared to VC at $p<0.01$)

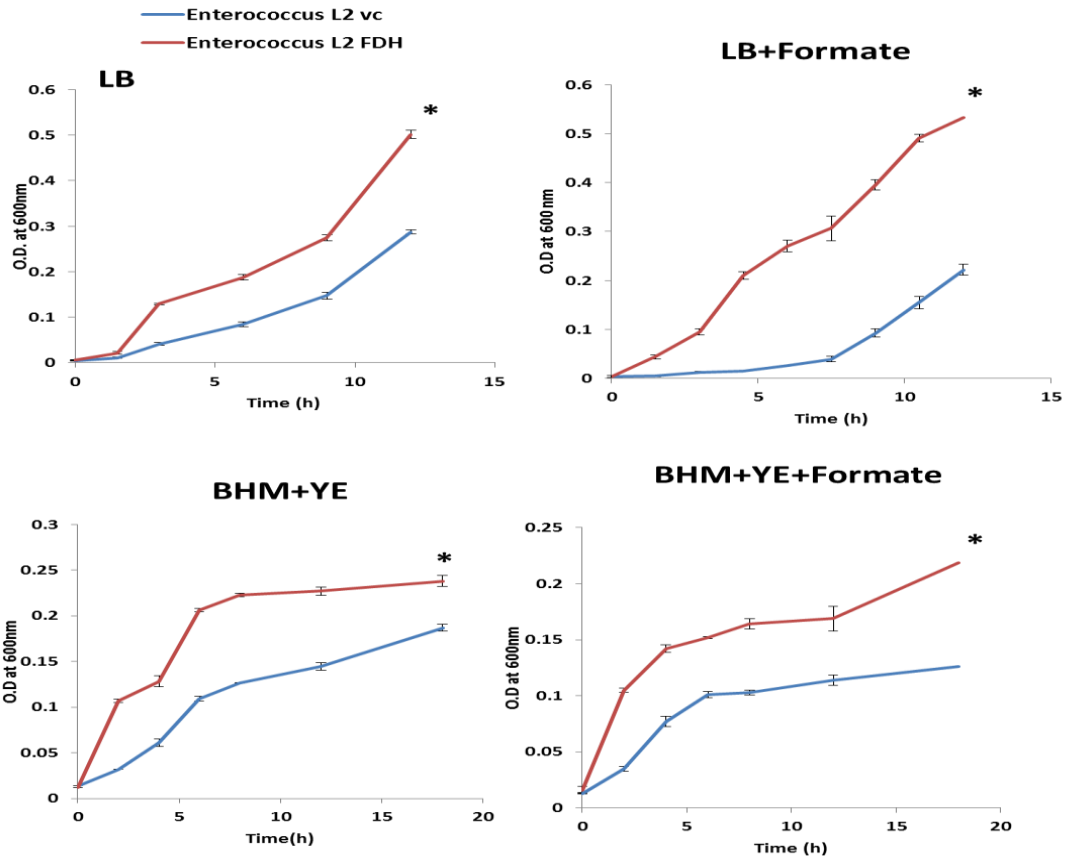

Figure 5.22Effect of *fdh* expression on growth of *Enterococcus* sp. L2 under static condition.

(* indicates significant difference compared to VC at p<0.01)

5.2.2.4. *Reactive violet 5R (RV5R) decolorization by fdh transformants*

The effect of NADH regeneration system on RV5R decolorization was analysed in various *fdh* transformants. Among the standard strains used, highest RV5R decolorizationof 92.16% was observed within 36h in case of *P.fluorescens* PfO-1 *fdh*transformant as compared to VC (Fig. 5.23c). Surprisingly, higher RV5R decolorization was obtained with *E.coli* DH5α *fdh*transformantwithout IPTG induction (Fig. 5.23a) and *E.coli* BL21 (DE3) *fdh*(Fig. 5.23b) with IPTG induction (with fold increase of 3.57 and 1.51 respectively) but for IPTG induced *E.coli* DH5α *fdh*transformant did not showed significant increase in RV5R decolorization. Among all the gram negative laboratory transformants, *Acinetobacter* sp. L1 showed highest decolorization of 93.32% at 36h with fold increase of 4.64 as compared to VC as shown in Fig.5.18j.However A3, C1, K1 and G1*fdh* transformants strainsshowed no significant increase in RV5R decolorization at the end of 36h.*Enterococcus* sp. L2 *fdh*

transformant, at 6h showed 73.45%decolorization with a fold increase of 3.2 as compared to VC which showed only 22.97% RV5R decolorization (Fig. 5.23d). With further incubation (12h) both VC and *fdh* transformant showed approximately 100% decolorization indicating that the rate of RV5R decolorization was increased by *fdh*overexpression in spite of the strain being highly efficient RV5R decolorizer.

There is a significant co-relation between the FDH activity and dye decolorization for organisms i.e. *E. coli* strains,*Pseudomonasfluorescens* PfO-1, *Klebsiella* sp. E2, *Acinetobacter* sp. L1 and *Enterococcus* sp. L2 these organisms showed higher fold increase in FDH specific activities and higher decolorization. It is marked from these results that dye decolorization process by these organisms might have been restricted by NADH availability and introduction of NADH regeneration system could increase in overall dye decolorization.

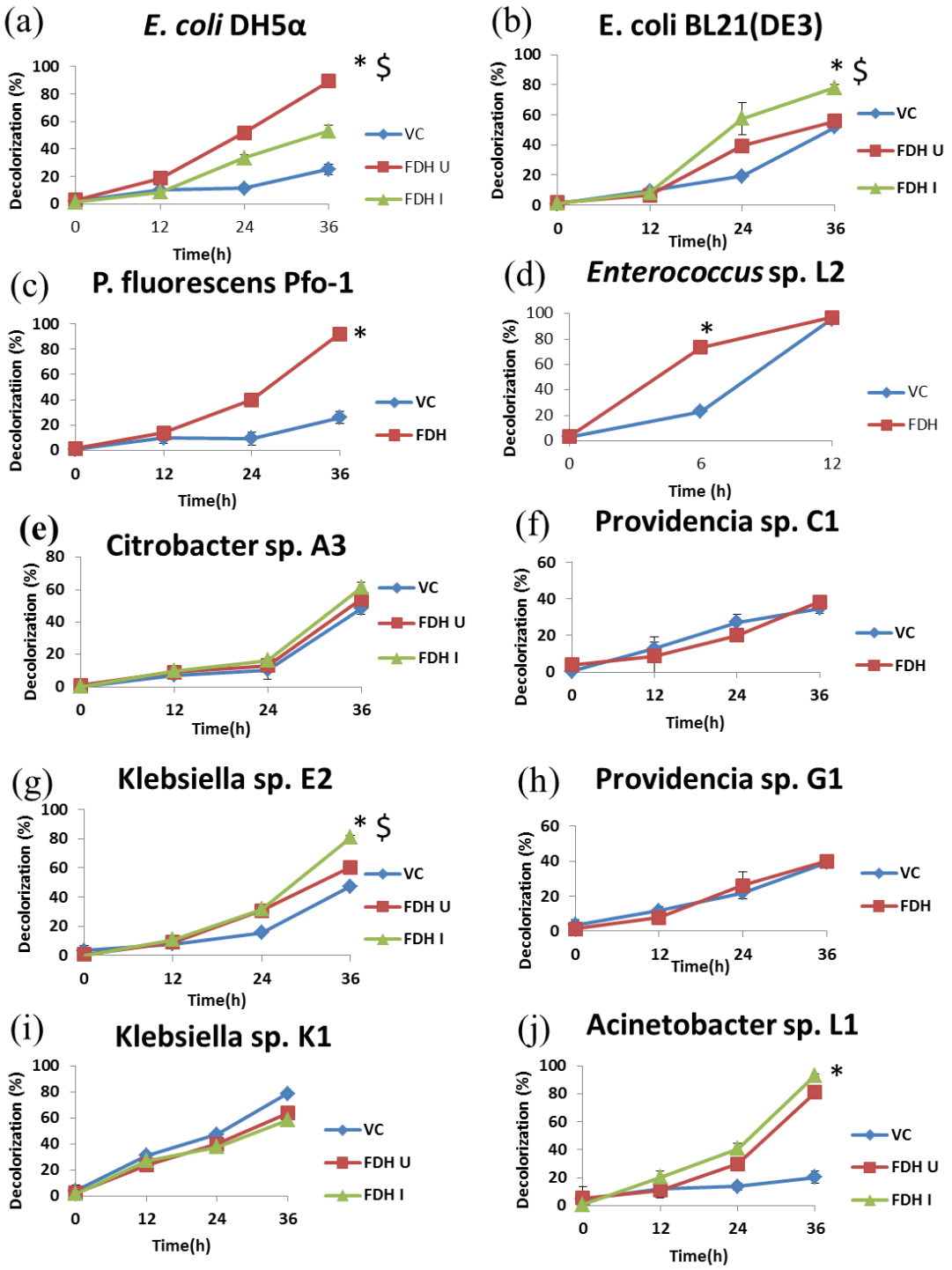

Figure 5.23Effect of heterologous expression of *fdh* on RV5R decolorization.

VC: Vector control; FDH U: *fdh* transformant uninduced; FDH I: *fdh* transformant induced with 1mM IPTG ($p<0.01$, * *fdh*transformant found significant compared to VC, $ *fdh*transformant induced found significant compared to VC and uninduced *fdh* transformant)

5.2.2.5. *Comparison of azo dye decolorization by individual transformants of azoA and fdh*

In Chapter 4, *azoA* overexpression was shown to increase RV5R decolorization by different bacterial strains. In this chapter, *fdh* overexpression was seen to enhance RV5R decolorization in several bacterial strains. Azo dye decolorization was therefore compared for RV5R and various other azo dyes used in textile applications for *E. coli* DH5α and *P. fluorescens* PfO-1 *fdh* and *azoA*transformants.Overall azo dye decolorization was higher(~1.5-2.0 fold increase) in *azoA*transformants of both strains compared to the VC. In case of *fdh*transformantsazo dye decolorization was found to be even better (~2.5-3.0 fold increase) than the corresponding VC (Fig. 5.24).Reactive yellow 186 was found to be most resistant dye for this biodecolorization studies. These results demonstrate that for *E. coli* and *P. fluorescens* PfO-1 strains, *fdh* overexpression resulted in the enhancement of azo bond reduction due to higher NADH regeneration which might have supported the native azoreductases in these strains. High azo dye decolorization in *azoA* transformants indicates that the azoreductases levels also determine decolorization efficiency.Thus, it could be hypothesized that simultaneous overexpression of *azoA* and *fdh* would result in a highly efficient dye decolorizing strain.

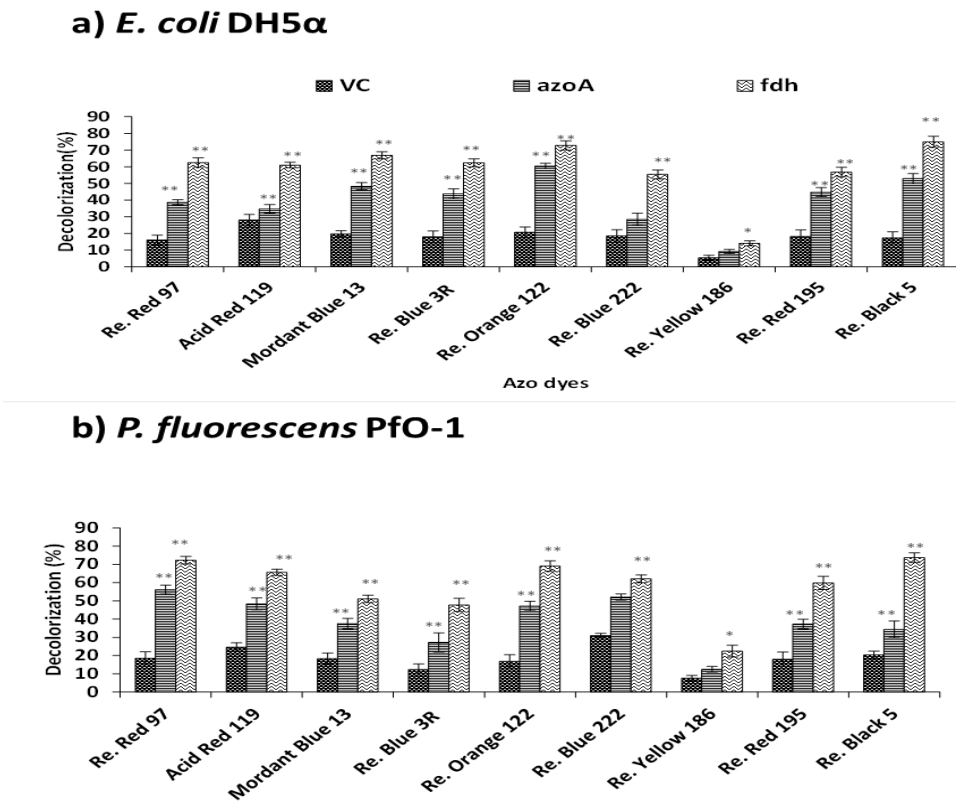

Figure 5.24Comparison of azo dye decolorization by *azoA* and *fdh* overexpressing transformants of standard strains.

a) *E. coli* DH5α and; b) *P. fluorescens* PfO-1(VC-Vector control; Significant difference at p<0.05* and p<0.01) [Re. – Reactive group of azo dye]**

5.2.3. Effect of heterologous expression of pBBR1MCS2*fdh-azoA*

To study the effect of coexpression of *fdh*and *azoA*on azo dye decolorization, a dual gene construct pBBR1MCS2*fdh-azoA* was developed in which both the genes are under p*lac* and p*T7* promoters in gram negative hosts. This construct was transformed into standard strains and bacterial isolates obtained in this study to investigate its effect on azo dye decolorization. Plasmid and strain confirmation for pBBR1MCS2*fdh-azoA* transformants have been shown in Fig. 5.15.

5.2.3.1. *FDH assay of pBBR1MCS2 fdh-azoA transformants*

The FDH activityfrom *fdh-azoA* transformants is shown in Fig. 5.25. *P.fluorescens* PfO-1 *fdh-azoA*transformant showed specific activity of 9.364U/mg with fold increase of 2.29 as compared to VC (4.08U/mg). *Acinetobacter* sp.L1 transformant showed specific activity of 37.28 U/mg as compared to VC(21.02 U/mg). *Klebsiella* sp. E2 and K1 transformants showed high specific activity of 58.47

U/mg and 48.07 U/mg respectively as compared to other transformants. But FDH activity for E2*fdh-azoA* transformant was found low compared to E2 *fdh*transformant which showed specific activity of 70.87 U/mg. Overall the FDH levels of the dual gene *(fdh-azoA)* transformants were similar to the levels in single (*fdh*) transformants (Fig. 5.18).

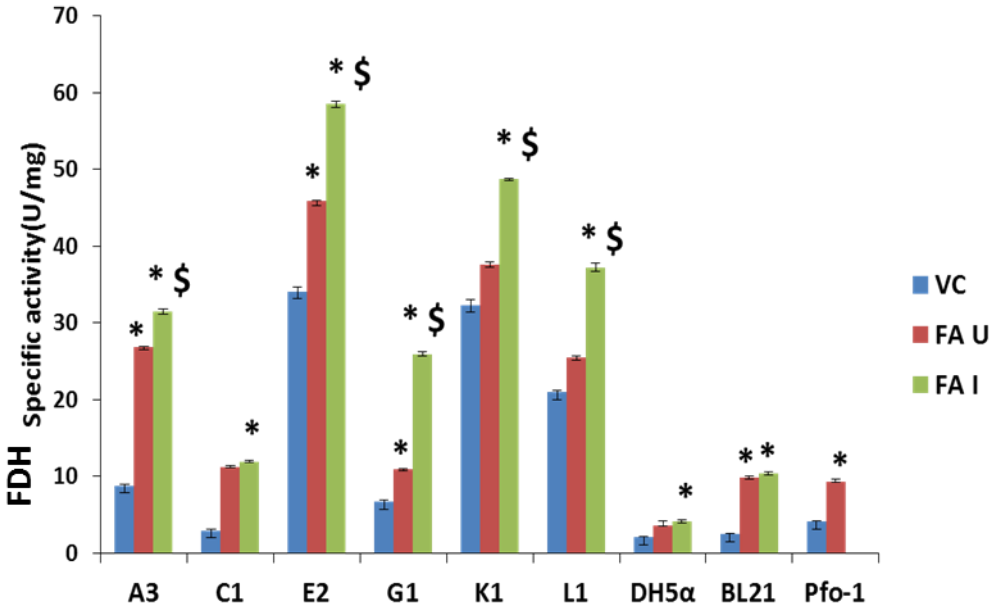

Figure 5.25FDH activity of pBBR1-MCS2*fdh-azoA* transformants.

VC: Vector control; FA U: pBBR1MCS2*fdh-azoA* transformants uninduced; FA I: pBBR1MCS2*fdh-azoA* transformants induced with IPTG (1mM) (* indicates significant p<0.01 increase in FDH activity in *fdh-azoA* transformant compared to the VC, $ indicates significant p<0.01 increase in FDH activity in induced compared to uninduced conditions)

5.2.3.2. *Azoreductase activity of pBBR1MCS2fdh-azoA transformants*

Azoreductase activity of pBBR1MCS2*fdh-azoA*transformants measured using RV5R as substrate is shown in Fig.5.26. *E.coli* BL21(DE3) *fdh-azoA*transformant showed AzoA specific activity of 2.82U/mg with a fold increase of 34.38 as compared to its VC which showed an activity of 0.082U/mg. *E.coli* DH5α transformant showed 10.84 fold increase in AzoA specific activity.*Acinetobacter* sp. L1 *fdh-azoA*transformant showed higher specific activity of 3.14 with fold increase of 4.49 U/mg. *Klebsiella* sp. E2 *fdh-azoA*transformant showed highest specific activity of 4.09U/mg with 6.66 fold increase as compared to all the other organisms used in current study. The azoreductase activity in the *fdh-azoA* transformants was 3 to 34 fold higher than the corresponding VC and strains A3, E2, K1, L1, DH5α and BL21

showed significant increase upon IPTG induction. However, in general the AzoA activity of the dual gene transformants (*fdh-azoA*) were much less than the corresponding activity in the single transformant (*azoA*) (Table 4.1).

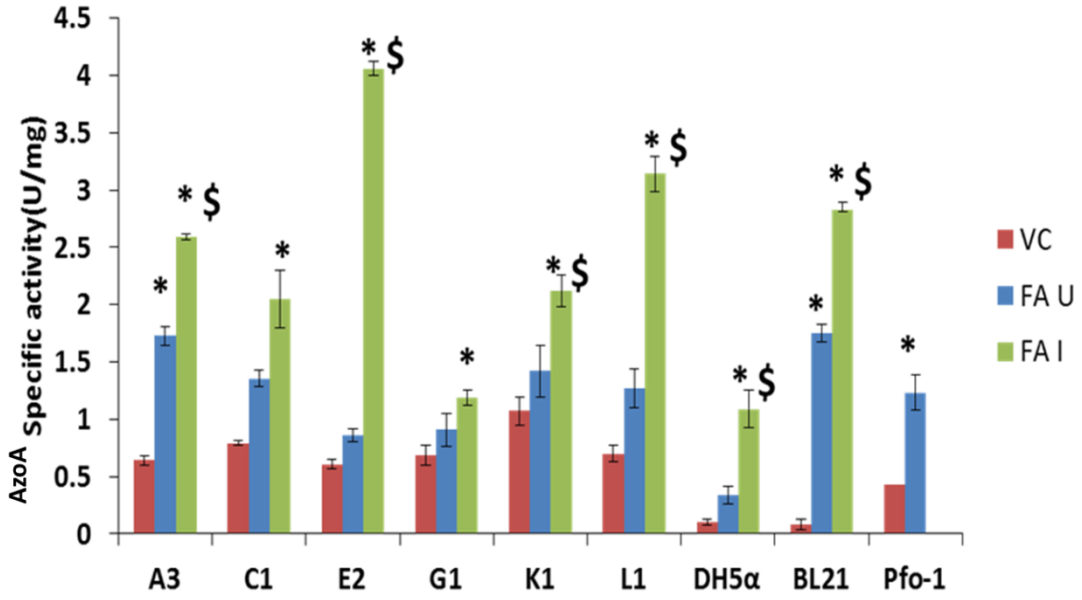

Figure 5.26Azoreductase activity of pBBR1MCS2*fdh-azoA* transformants.

VC: Vector control; FA U: pBBR1MCS2*fdh-azoA* transformants uninduced; FA I: pBBR1MCS2*fdh-azoA* transformants induced with IPTG (1mM) (* indicates significant p<0.01 increase in azoreductase activity in *fdh-azoA* transformant compared to the VC, $ indicates significant p<0.01 increase in azoreductase activity in induced compared to uninduced conditions)

5.2.3.3. *Formate dehydrogenase dependent Azoreductase coupled activity*

In order to study the combined effect ofNADH regeneration system and azoreductases overexpression, an *in vitro* Formate dehydrogenase dependent azoreductase coupled assay was done. In this assay, RV5R decolorization by cell free extracts was monitored without external supplementation of NADH,but instead providing NAD^+ and formate which would result in regeneration of NADH internally by the FDH present in cell free extracts. *E.coli* DH5α *fdh-azoA*transformant showed higher specific activity of 0.69U/mg with a fold increase of 2.44 as compared to VC (0.283U/mg). Significantly, *E.coli* BL21 *fdh-azoA* transformant showed highest specific activity of 7.09 U/mg with maximum fold increase of 23.85 as compared to

VC which showed specific activity of 0.3U/mg. These results clearly demonstrate that FDH-NADH regeneration system is efficiently working and NADH availability can be increased by providing formate. Surprisingly the specific activity of azoreductase obtained in uncoupled azoreductase assay of*E.coli* BL21(DE3)*fdh-azoA*transformantwas 2.82 U/mg (Fig. 5.26) which was lower than that in coupled assay (7.09U/mg).*E. coli* DH5α and *P. fluorescens* PfO-1 showed no significant coupled azoreductase activity.

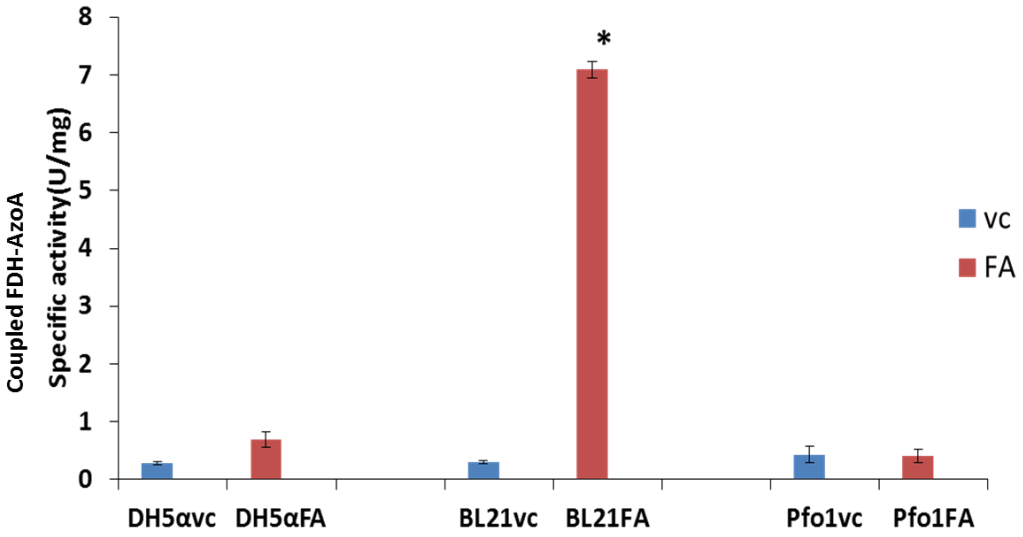

Figure 5.27Formate dehydrogenase dependent azoreductase coupled assay

VC : Vector control ; FA: *fdh-azoA* transformant

5.2.3.4. *Reactive violet 5R decolorization by pBBR1MCS2fdh-azoA transformants*

The *P.fluorescens* PfO-1 *fdh-azoA*transformant showed significant enhancement in RV5R decolorization as compared to VC. At 36h the decolorization was 54.72% with fold increase of 2.12 as compared to VC (Fig.5.28). Other strains in which the *fdh-azoA* dual gene construct showed significant effect on RV5R decolorization were *E. coli* DH5α and *Acinetobacter* sp. L1. In some strains such as *E. coli* BL21(DE3), *Citrobacter* sp. A3, *Klebiella* sp. E2 and *Providencia* sp. G1 enhanced RV5R decolorization was observed in early stages of growth which subsequently became comparable to VC. Even though co-expression of both *fdh* and *azoA* genes resulted in better RV5R decolorization than VC (Fig. 5.28) but it was less than when *fdh* was expressed alone (Fig. 5.23).

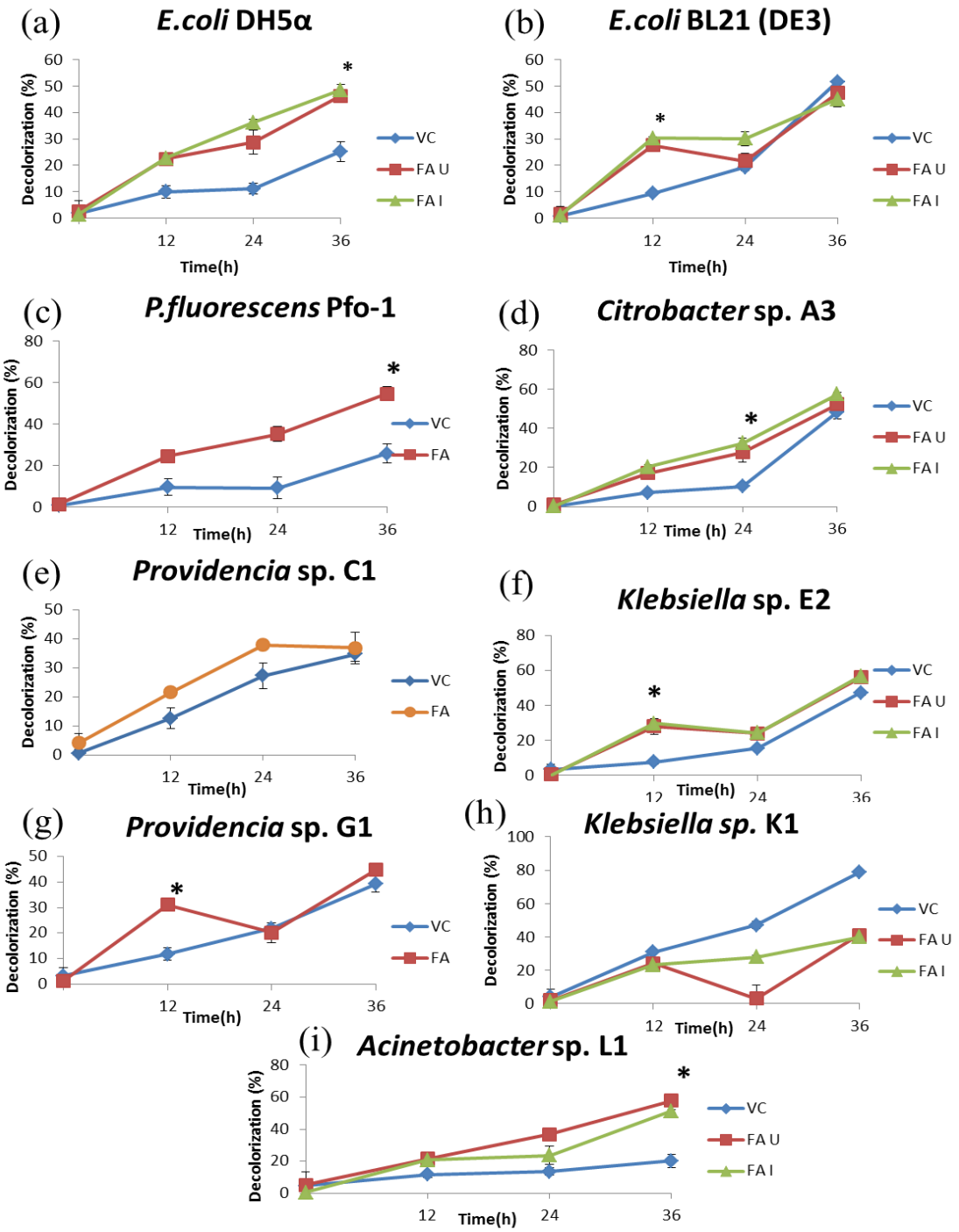

Figure 5.28RV5Rdecolorization by pBBR1MCS2*fdh-azoA* transformants.

VC: Vector control; FA U: pBBR1MCS2*fdh-azoA* transformants uninduced; FA I: pBBR1MCS2*fdh-azoA* transformants induced with IPTG (1mM) (* indicates significant p<0.01 increase in azoreductase activity in *fdh-azoA* transformant compared to the VC)

5.2.3.5. *Reactive violet 5R decolorization by non-growing cells of azoA, fdh and fdh-azoA transformants*

In the previous experiments RV5R decolorization by the transformants of single and dual expression systems was monitored in growing conditions. It is likely that during the active growth NADH requirements for the metabolic activities might limit the azo dye decolorization. Hence RV5R decolorization was monitored in non-growing condition in formate containing buffered conditions. In this experiment, pre-grown IPTG induced cells (for *E. coli* DH5α) were checked for their ability to decolorize RV5R. In case of both *E. coli*DH5α and *P.fluorescens* PfO-1 transformants RV5R decolorization was in the order of *azoA*<*fdh*<*fdh-azoA*(Fig. 5.29). There was a 10% incremental increase in RV5R decolorization in each case with overall ~30-40% increase in dual gene construct as compared to VC.

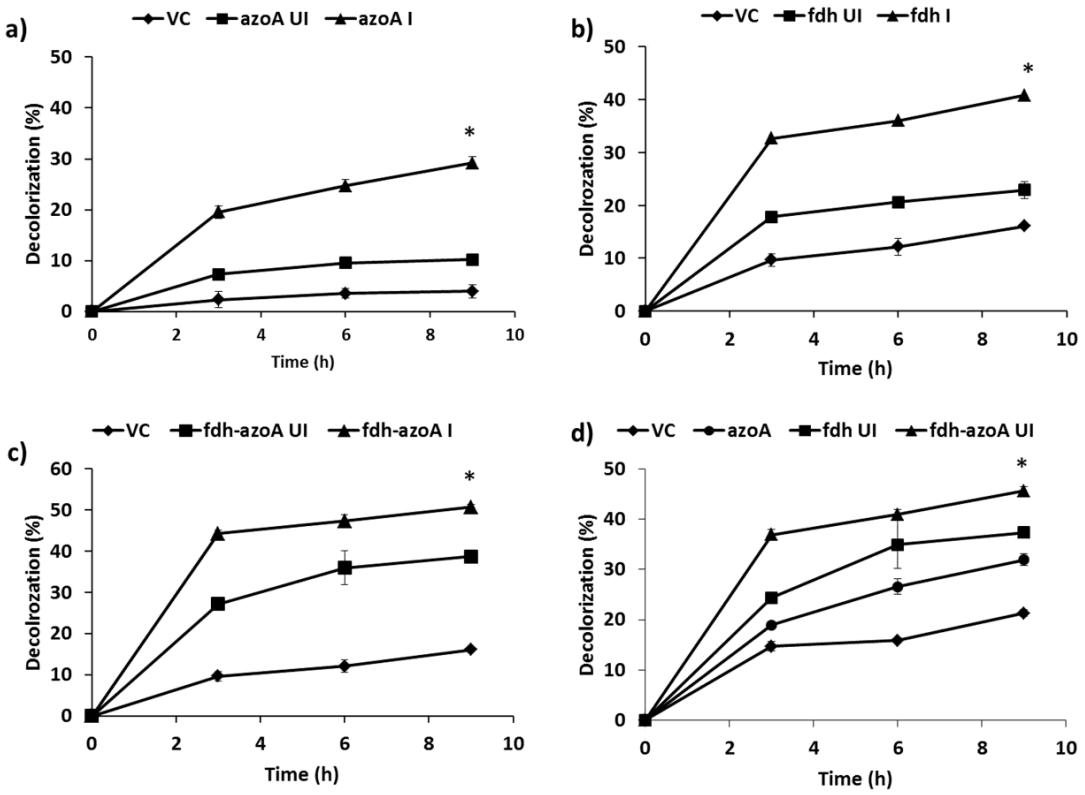

Figure 5.29 RV5R decolorization by pre-grown cells of transformants.

Singlegene transformants (*azoA* or *fdh*) and dual gene (*fdh-azoA*) transformants of *E. coli* DH5α (a,b and c) and *P. fluorescens* PfO-1 (d). (VC: vector control;UI- uninduced and I-induced with 1mM IPTG; * data was found significant at p < 0.01)

5.3. Discussion

Azoreductase catalytic chemistry requires prosthetic groups (FMN) as well as cofactor (NAD(P)H). For efficient functioning of azoreductases *in vivo* or *invitro,* the cofactor pool available to the enzyme needs to be optimum. In normal physiological conditions NAD(P)H pool goes through continuous oscillations based on the balance of catabolic and anabolic metabolism ($_{DE}$Graef et al., 1999). Most of the azoreductases from bacteria are NADH preferring flavin dependent quinone reductases. As azoreductases have high K_m value for NADH relative to other oxidoreductases involved in electron transport chain, this might limit the overall rate of dye decolorization. Thus, constant high availability of NADH in the cell would be expected to maintain high rate of dye reduction. To address the problem of NADH limitation, an NADH regeneration system was engineered through overexpression of *Mycobacteriumvaccae* N10 encoded NAD^+- dependent formate dehydrogenase (*fdh*). FDH based NADH regeneration system was selected from among several NADH regeneration systems (van der Donk and Zhao, 2003) available since it has distinct advantages for industrial application (Tishkov and Popov, 2004). The effect of NADH regeneration system was studied in various bacterial strains including model organisms (*E. coli* DH5α and BL21(DE3) as well as *Pseudomonas fluorescens* PfO-1) and RV5R decolorizing bacterial isolates obtained in this study.

ThepBBR1MCS2*fdh*construct was used for *fdh* overexpression in gram negative hosts and pMGS100*fdh* was used for gram positive hosts. In the former construct *fdh* gene is expressed under the inducible p*lac* promoterprovided by the vector (Kovach et al., 1995) and p*T7* promoter co-amplified with *fdh*cassette (functional only in *E. coli* BL21(DE3)). In the latter construct *fdh* expression is driven under the constitutive p*bacA* promoter (Fujimoto, 2001). Also pBBR1MCS2*fdh-azoA* dual geneconstruct which overexpressed the *fdh* along with *azoA*from *Enterococcus* sp. L2 as a transcription fusion was analyzed. Thus three constructs, pBBR1MCS2*fdh,* pBBR1MCS2*fdh-azoA* for gram negative host system and pMGS100*fdh* for gram positive host system were transformed into A3, C1, E2, G1, K1, L1, *E. coli* DH5α, *E .coli* BL21(DE3), *P. fluorescens* PfO-1 and *Enterococcus* sp. L2, respectively. Many of the*fdh*transformants were able to decolorize the RV5R more efficiently as compared to respective VC, except for *Providencia* spp. C1 and G1 as well as*Klebsiella* sp. K1.It is not clear why these transformants failed to show

enhanced decolorization since they showed increase in FDH activity. Notably, the *azoA* transformants of these three strains also failed to show enhanced decolorization (Fig.4.6, Chapter 4) in spite of increase in AzoA activity (Table 4.1, Chapter 4). *Acinetobacter* sp. L1 *fdh* showed highest RV5R decolorization of 93.33% with fold increase of 4.63 as compared to corresponding VC, 20.17%. This result is co-related with specific activity of 45.88U/mg for L1*fdh* transformant.The gram positive *Enterococcus* sp. L2 *fdh* transformant showed faster RV5R decolorization of 73.45% with fold increase of 3.20 at 6h as compared to VC. It is reported that *Enterococcus* spp. accumulate formate during micro-aerophilic growth conditions (Sarantinopoulos et al., 2001), thus by providing subsequent metabolic ability to oxidize formate and regenerate NADHcould enhanceazo dye decolorization as seenfrom this study.

It is evident from these results that dye decolorization process inseveralbacteria is limited by NADH availability and introduction of NADH regeneration system could lead to increase in overall dye decolorization. The reducing equivalent in the cell are important determinants of cellular physiology and adaptation to environments (Foster et al., 1990; $_{DE}$Graef et al., 1999). Accordingly, NAD^+ dependent *fdh* expression altered the intracellular NAD^+/NADH ratio andalso modified the normal physiology and growth of bacterial strain according to the host metabolism. In present study, *fdh* transformants of *E. coli* DH5α. *E. coli* BL21(DE3) and *P. fluorescens* PfO-1showed significant growth advantages under certain media and growth conditions. In case of *Enterococcus* sp. L2 *fdh*overexpression resulted in highly significant growth benefit regardless of addition of formate in rich as well as minimal medium. Berrı´os-Rivera et al.(2002) reported several metabolic changes in *E. coli* over-expressing NAD^+ dependent *fdh* from *Candida boidinii.* The *fdh* transformant displayed double yield of NADH when glucose was provided as C-source and interestingly showed that during aerobic growth the increased availability of NADH induced shift to fermentative pathways. NADH regeneration systems have been shown to increase NADH levels in rich as well as minimal medium supplemented with various carbon sources (Berríos-Rivera, 2002; San et al., 2002).

In case of the dual gene construct pBBR1MCS2*fdh-azoA*transformants significantlyhigher RV5R decolorization was obtained as compared to corresponding VC in *E. coli* DH5α, *P. fluorescens* PfO-1 and *Acinetobacter* sp. L1 transformants.

Other transformants showed marginally increased RV5R decolorization at specific time point. On the whole the dual gene (*fdh-azoA*) transformants showed reduced RV5R decolorization compared to the corresponding pBBR1MCS2*fdh*transformants. Among all the three standard strains *P. fluorescens* PfO-1 *fdh*transformant showed highest RV5R decolorization of 92.16% at 36h with fold increase of 3.57 which is in good co-relation with specific activity of FDH, 9.58U/mg from the same organism. On the other hand dual gene transformant showed ~60% RV5R decolorization in 36h. This might be due to plasmid load and simultaneous expression of two heterologous proteins.

In order to eliminate the growth constraint of the transformants, pre-grown and induced cells were characterized for RV5R decolorization under non-growing formate containing buffered conditions. Under these conditions *E. coli* DH5α and *P. fluorescens* PfO-1 demonstrated higher decolorization in all the transformants as compared to VC. The *fdh-azoA* dual gene transformant showed highest as compared to individual gene transformants indicating that increase in both *azoA* and NADH have additive effects on azo dye decolorization. This result clearly demonstrates that NADH regeneration system is efficiently working in the organism and NADH availability inside the cell is a limiting factor for azo dye decolorization.

So far azo dye decolorization by microorganisms has been improved by genetic manipulation (overexpression) of azoreductase genes (Chang and Lin, 2001; Chen et al., 2004; Sandhya et al., 2008; Jin et al., 2009). Feng et al. (2010) demonstrated that extrinsic addition of NADH to *E. coli* transformant overexpressing entereorcoccal (*azoA*) increased azo dye decolorization. Recently, Yang et al. (2013b) developed an *in vitro*immobilized enzymesystem with purified azoreductase from *Shewanella oneidensis* MR-1 and purified glucose1-dehydrogenase from *Lysinibacillus sphaericus* G10, wherein glucose oxidation provided NADH to azoreductase. The novelty of this work is the improvement of azo dye decolorization by increasing the cofactor level (NADH) *in vivo* by an NADH regeneration system. Merely the increase in intracellular levelsof NADH was shown to enhance the azo dye decolorization but simultaneously increasing azoreductase and NADH levels resulted in maximum decolorization.

Summarizing, in this Chapter the cloning and heterologous expression of mycobacterial *fdh* in various standard bacterial strains and azo dye decolorizing

bacterial isolates is reported to function as an efficient NADH regeneration system bringing about enhanced azo dye decolorization. The combined effect of heterologously expressed azoreductase and *fdh* resulted in further improvement of azo dye decolorization in several strains.

APPENDICES

Appendix APCR program for 16S rRNA gene from community DNA

Step	Temperature(^{0}C)	Duration
Initial denaturation	94	5min
Step down PCR (10 cycles) (-0.5^{0}C)		
Cycle denaturation	94	30s
Cycle annealing	62.5-57.5	45s
Cycle extension	72	1.5min
Normal PCR(20 cycles)		
Cycle denaturation	94	30s
Cycle annealing	58	45s
Cycle extension	72	1.5min
Final extension	72	15min
Cooling	4	α

Appendix B DGGE-PCR program for amplification of V3 regions of 16S rRNA gene from community DNA

Step	Temperature(^{0}C)	Duration
Initial denaturation	94	5min
Step down PCR (10 cycles) (-1^{0}C)		
Cycle denaturation	94	30s
Cycle annealing	65-55	45s
Cycle extension	72	1min
Normal PCR(20 cycles)		
Cycle denaturation	94	40s
Cycle annealing	55	45s
Cycle extension	72	1min
Final extension	72	10min
Cooling	4	α

Appendix C PCR program for 16S rRNA gene fragment amplification from pure cultures

Step	Temperature (^{0}C)	Duration
Initial denaturation	94	5min
Cycle denaturation	94	30s
Cycle annealing	58	45s
Cycle extension	72	1.0min
Final extension	72	10.0min
Cooling	4	α

Appendix DPCR program for full length 16s rDNA amplification

Step	Temperature(^{0}C)	Duration
Initial denaturation	94	5min
Normal PCR (30 cycles)		
Cycle denaturation	94	30s
Cycle annealing	58	45s
Cycle extension	72	1.5 min
Final extension	72	10.0 min
Cooling	4	α

Appendix EPCR program for *azoA*

Step	Temperature(^{0}C)	Duration
Initial denaturation	94	5min
Step down PCR (10 cycles) (-0.5^{0}C)		
Cycle denaturation	94	30s
Cycle annealing	62.5-57.5	45s
Cycle extension	72	1min
Normal PCR(20 cycles)		
Cycle denaturation	94	30s
Cycle annealing	57	45s
Cycle extension	72	1min
Final extension	72	10min
Cooling	4	α

Appendix F PCR program for *fdh* gene

Step	**Temperature(^{0}C)**	**Time duration**
Initial denaturation	94	4min
Step down PCR(10 cycles)(- 0.5^{0}C)		
Cycle denaturation	94	40s
Cycle annealing	62-58	45s
Cycle extension	72	1min10 sec
Normal PCR(20 cycles)		
Cycle denaturation	94	40s
Cycle annealing	58	45s
Cycle extension	72	1min10 sec
Final extension	72	10min
Cooling	4	α

Appendix G PCR program using up azo and down azo primers

Step	**Temperature**	**Time Duration**	**Description**
	94^{O}C	5 minutes	Initial Denaturation
Step down PCR			
1.	94^{O}C	40 seconds	Cycle Denaturation
2.	60-53^{O}C	45 seconds	Step Down Annealing
3.	72^{O}C	1 minute 10 seconds	Elongation
			Return to step 1 for 14 cycles
NORMAL PCR			
1.	94^{O}C	40 seconds	Cycle Denaturation
2.	52^{O}C	45 seconds	Annealing
3.	72^{O}C	1 minute 10 seconds	Elongation
			Return to step 1 for 16 cycles
	72^{O}C	12 minutes	Final Extension
	4^{O}C	α	Cooling

Appendix HPCR program for Chloramphenicol cassette amplification

Step	Temperature	Time duration
Initial Denaturation	94^0C	5mins
Normal PCR(30 cycles)		
Cycle Denaturation	94^0C	30secs
Cycle annealing	45^0C	45secs
Cycle extension	72^0C	1min 30 sec
Final extension	72^0C	10mins
Cooling	4^0C	α

Appendix IPCR program for *azoA* flanking region amplification

Step	Temperature	Time duration
Initial Denaturation	94^0C	5mins
Normal PCR (25 cycles)		
Cycle Denaturation	94^0C	30secs
Cycle annealing	58^0C	45secs
Cycle extension	72^0C	3min 30 sec
Final extension	72^0C	20mins
Cooling	4^0C	α

Appendix JPCR program for Gentamycin cassette amplification

Step	Temperature	Time duration
Initial Denaturation	94^0C	5mins
Normal PCR(30 cycles)		
Cycle Denaturation	94^0C	30secs
Cycle annealing	48^0C	45secs
Cycle extension	72^0C	1min 30 sec
Final extension	72^0C	10mins
Cooling	4^0C	α

REFERENCES

Abraham, K., John, G. 2007. Development of a classification scheme using a secondary and tertiary amino acid analysis of azoreductase gene. J. Med. Biol. sci. 1(1).

Albuquerque, M.G.E., Lopes, A. T., Serralheiro, M.L., Novais, J.M., Pinheiro, H.M., 2005. Biological sulphate reduction and redox mediator effects on azo dye decolourisation in anaerobic–aerobic sequencing batch reactors. Enzyme Microbial Technol. 36, 790–799.

An, S., Min, S., Cha, I., Choi, Y., Cho, Y., Lee, Y., 2002. Decolorization of triphenylmethane and azo dyes by Citrobacter sp. Biotechnol. Lett. 24, 1037–1040.

An, Y., Jiang, L., Cao, J., Geng, C., Zhong, L., 2007. Sudan I induces genotoxic effects and oxidative DNA damage in HepG2 cells. Mutat. Res. 627, 164–70.

Aranganathan, V., Kanimozhi, A.M., Palvannan, T., 2013. Statistical optimization of synthetic azo dye (orange II) degradation by azoreductase from Pseudomonas oleovorans PAMD_1. Prep. Biochem. Biotechnol. 43, 649–67.

Asad, S., Amoozegar, M.A, Pourbabaee, A. A., Sarbolouki, M.N., Dastgheib, S.M., 2007. Decolorization of textile azo dyes by newly isolated halophilic and halotolerant bacteria. Bioresour. Technol. 98, 2082–8.

Bafana, A., & Chakrabarti, T. 2008., Lateral gene transfer in phylogeny of azoreductase enzyme. Comput. Biol. Chem. 32, 191-197.

Bafana, A., Chakrabarti, T., Devi, S.S., 2008. Azoreductase and dye detoxification activities of Bacillus velezensis strain AB. Appl. Microbiol. Biotechnol. 77, 1139–44.

Bafana, A., Chakrabarti, T., Krishnamurthi, K., Devi, S.S., 2008. Biodiversity and dye decolourization ability of an acclimatized textile sludge. Bioresour. Technol., 99, 5094-5098.

Bafana, A., Chakrabarti, T., Muthal, P., Kanade, G. 2009. Detoxification of benzidine-based azo dye by E. gallinarum: Time-course study. Ecotoxicol. Environ. Safety, 72, 960-964.

Bafana, A., Krishnamurthi, K., Devi, S. S., & Chakrabarti, T., 2008. Biological decolourization of CI Direct Black 38 by E. gallinarum. J. Hazard. Mater. 157, 187-193.

Banat, I. M., Nigam, P., Singh, D., & Marchant, R. 1996. Microbial decolorization of textile-dyecontaining effluents: A review. Bioresour. Technol. 58, 217-227

Bäumchen, C., Bringer-Meyer, S. 2007. Expression of glf Zm increases D-mannitol formation in whole cell biotransformation with resting cells of Corynebacterium glutamicum. Appl. Microbiol.Biotechnol. 76, 545-552.

Berrios-Rivera, S. J., Bennett, G. N., & San, K.-Y. 2002. The effect of increasing NADH availability on the redistribution of metabolic fluxes in Escherichia coli chemostat cultures. Metab. Eng. 4, 230-237.

Berríos-Rivera, S., 2002. The Effect of NAPRTase Overexpression on the Total Levels of NAD, The NADH/NAD+ Ratio, and the Distribution of Metabolites in Escherichia coli. Metab. Eng. 4, 238–247.

Beydilli, M.I., Pavlostathis, S.G., 2005. Decolorization kinetics of the azo dye Reactive Red 2 under methanogenic conditions: effect of long-term culture acclimation. Biodegradation 16, 135–146.

Bhatt, N., Patel, K.C., Keharia, H., Madamwar, D., 2005. Decolorization of diazo-dye Reactive Blue 172 by Pseudomonas aeruginosa NBAR12. J. Basic Microbiol. 45, 407-418.

Bin, Y., 2004. Expression and characteristics of the gene encoding azoreductase from Rhodobacter sphaeroides AS1 . 1737. FEMS Microbiol Lett. 236, 129–136.

Blümel, S., & Stolz, A., 2003. Cloning and characterization of the gene coding for the aerobic azoreductase from Pigmentiphaga kullae K24. Appl. Microbiol. Biotechnol. 62, 186-190.

Blumel, S., Knackmuss, H.-J., Stolz, A., 2002. Molecular cloning and characterization of the gene coding for the aerobic azoreductase from Xenophilus azovorans KF46F. Appl. Environ. Microbiol. 68, 3948-3955

Boonstra, B., Rathbone, D. A., French, C. E., Walker, E. H., & Bruce, N. C., 2000. Cofactor regeneration by a soluble pyridine nucleotide transhydrogenase for biological production of hydromorphone. Appl. Environ. Microbiol. 66, 5161-5166.

Bradford M.M., 1976. A rapid and sensitive method for quantification of microgram quantities of protein utilizing the principle of protein dye binding. Anal. Biochem. 72, 278-254

Bradshaw, C. W., Fu, H., Shen, G. J., & Wong, C. H., 1992. A Pseudomonas sp. alcohol dehydrogenase with broad substrate specificity and unusual stereospecificity for organic synthesis. J. Org. Chem. 57, 1526-1532.

Bragger, J.L., Lloyd, A.W., Soozandehfar, S.H., Bloomfield, S.F., Marriott, C., Martin, G.P. 1997. Investigations into the azo reducing activity of a common colonic microorganism. Int. J. Pharm. 157, 61-71.

Bürger, S., Stolz, A., 2010. Characterisation of the flavin-free oxygen-tolerant azoreductase from Xenophilus azovorans KF46F in comparison to flavin-containing azoreductases. Appl. Microbiol. Biotechnol. 87, 2067–76.

Chacko, J. T., & Subramaniam, K. 2011. Enzymatic degradation of azo dyes–A Review. Int. J. Environ. Sci. 1, 1250-1260.

Chan, G.F., Gan, H.M., Rashid, N.A.A., 2012a. Genome sequence of Citrobacter sp. strain A1, a dye-degrading bacterium. J. Bacteriol. 194, 5485–6.

Chan, G.F., Gan, H.M., Rashid, N.A.A., 2012b. Genome Sequence of Enterococcus sp. Strain C1, an Azo Dye Decolorizer. J. Bacteriol. 194, 5716–7.

Chang, J., Chou, C., Lin, Y., Lin, P., Ho, J., Hu, T.L., 2001. Kinetic characteristics of bacterial azo-dye decolorization by Pseudomonas luteola. Water Res. 35, 2841–2850.

Chang, J.-S., Kuo, T.-S., 2000. Kinetics of bacterial decolorization of azo dye with Escherichia coli NO3. Bioresour. Technol. 75, 107–111.

Chang, J. S., & Lin, C. Y., 2001. Decolorization kinetics of a recombinant Escherichia coli strain harboring azo-dye-decolorizing determinants from Rhodococcus sp. Biotechnol. Lett. 23, 631-636.

Chaturvedi, R., Archana, G., 2012. Novel 16S rRNA based PCR method targeting Deinococcus spp. and its application to assess the diversity of deinococcal populations in environmental samples. J. Microbiol. Methods 90, 197–205.

Chen, B.Y., Lin, K.W., Wang, Y.M., Yen, C.Y. 2009a. Revealing interactive toxicity of aromatic amines to azo dye decolorizer Aeromonas hydrophila. J.Hazard. Mater. 166, 187-194.

Chen, H., 2006. Recent advances in azo dye degrading enzyme research. Curr. Protein Pept. Sci. 7, 101–111

Chen, H., Feng, J., Kweon, O., Xu, H., Cerniglia, C.E., 2010. Identification and molecular characterization of a novel flavin-free NADPH preferred azoreductase encoded by azoB in Pigmentiphaga kullae K24. BMC Biochemistry 11, 13.

Chen, H., Hopper, S. L., & Cerniglia, C. E. 2005. Biochemical and molecular characterization of an azoreductase from Staphylococcus aureus, a tetrameric NADPH-dependent flavoprotein. Microbiology. 151, 1433-1441.

Chen, H., Shaw, N., Hopper, S.L., Chen, L., Chen, S., Cerniglia, C.E., Wang, B., 2007. Crystal structure of an aerobic FMN-dependent azoreductase (AzoA) from Enterococcus faecalis. Arch Biochem Biophys. 463, 68–77.

Chen, H., Wang, R.F., & Cerniglia, C.E. 2004. Molecular cloning, overexpression, purification, and characterization of an aerobic FMN-dependent azoreductase from Enterococcus faecalis. Protein Expression Purif. 34, 302-310.

Chen, H., Xu, H., Heinze, T. M., & Cerniglia, C. E. 2009b. Decolorization of water and oil-soluble azo dyes by Lactobacillus acidophilus and Lactobacillus fermentum. J. Ind. Microbiol. Biotechnol. 36, 1459-1466.

Chen, K.C., Huang, W.T., Wu, J.Y., Houng, J.Y. 1999. Microbial decolorization of azo dyes by Proteus mirabilis. J. Ind. Microbiol. Biotechnol., 23, 686-690.

Chen, K.C., Wu, J.Y., Liou, D.J., Hwang, S.C.J., 2003. Decolorization of the textile dyes by newly isolated bacterial strains. J. Biotech. 101, 57–68.

Chen, X., Xu, M., Wei, J., & Sun, G. 2010. Two different electron transfer pathways may involve in azoreduction in Shewanella decolorationis S12. Appl. Environ. Microbiol. 86, 743-751.

Chengalroyen, M.D., Dabbs, E.R., 2013. The microbial degradation of azo dyes: minireview. World J. Microbiol. Biotechnol. 29, 389–99.

Chivukula, M., Renganathan, V., 1995. Phenolic azo dye oxidation by laccase from Pyricularia oryzae. Appl. Environ. Microbiol. 61, 4374–4377.

Christie, R.M. 2001. Colour chemistry. Royal Society of Chemistry.

Claus, H., Faber, G., König, H., 2002. Redox-mediated decolorization of synthetic dyes by fungal laccases. Appl. Microbiol. Biotechnol. 59, 672–8.

Dafale, N., Rao, N.N., 2008. Decolorization of azo dyes and simulated dye bath wastewater using acclimatized microbial consortium – Biostimulation and halo tolerance. Bioresour. Technol. 99, 2552-2558.

Dave, S. R., & Dave, R. H. 2009. Isolation and characterization of Bacillus thuringiensis for Acid red 119 dye decolourisation. Bioresour. Technol., 100, 249–253.

Dawkar, V. V, Jadhav, U.U., Ghodake, G.S., Govindwar, S.P., 2009. Effect of inducers on the decolorization and biodegradation of textile azo dye Navy blue 2GL by Bacillus sp. VUS. Biodegradation 20, 777–87.

Deller, S., Macheroux, P., Sollner, S., 2008. Review Flavin-dependent quinone reductases. Cell. Mol. Life Sci. 65, 141–160.

Desai, C., Jain, K., Patel, B., Madamwar, D., 2009. Efficacy of bacterial consortium-AIE2 for contemporaneous Cr (VI) and azo dye bioremediation in batch and continuous bioreactor systems, monitoring steady-state bacterial dynamics using qPCR assays. Biodegradation 20, 813–826.

Dhanve, R.S., Shedbalkar, U.U., Jadhav, J.P. 2008. Biodegradation of diazo reactive dye Navy blue HE2R (Reactive blue 172) by an isolated Exiguobacterium sp. RD3. Biotechnol. Bioprocess Eng. 13, 53-60.

Dias, A. A., Lucas, M. S., Sampaio, A., Peres, J. A., & Bezerra, R. M., 2010. Decolorization of azo dyes by yeasts. In Biodegradation of Azo Dyes (pp. 183-193). Springer Berlin Heidelberg.

Dos Santos, A., Cervantes, F., Yaya-Beas, R., Van Lier, J., 2003. Effect of redox mediator, AQDS, on the decolourisation of a reactive azo dye containing triazine group in a thermophilic anaerobic EGSB reactor. Enzyme Microb. Technol. 33, 942–951.

Dos Santos, A. B., Cervantes, F. J., & Van Lier, J. B. 2007. Review paper on current technologies for decolourisation of textile wastewaters: perspectives for anaerobic biotechnology. Bioresour. Technol. 98, 2369-2385.

Dunny, G.M., Lee, L.N., Leblanct, D.J., 1991. Improved electroporation and cloning vector system for gram-positive bacteria. Appl. Environ. Microbiol. 57, 1194–1201.

Dykes, G. A, Timm, R.G., Von Holy, A., 1994. Azoreductase activity in bacteria associated with the greening of instant chocolate puddings. Appl. Environ. Microbiol. 60, 3027–9.

Elisangela, F., Andrea, Z., Fabio, D.G., DeMenezes Cristiano, R., Regina, D.L., Artur, C.-P., 2009. Biodegradation of textile azo dyes by a facultative Staphylococcus arlettae strain VN-11 using a sequential microaerophilic/aerobic process. Int. Biodeter. Biodegr. 63, 280–288.

Elliott, B.M., 1984. Azoreductase activity of Sprague Dawley and Wistar-derived rats towards both carcinogenic and non-carcinogenic analogues of 4-dimethyl aminophenyl azobenzene (DAB). Carcinogenesis 5, 1051–1055.

Ernst, M., Kaup, B., Müller, M., Bringer-Meyer, S., & Sahm, H. 2005. Enantioselective reduction of carbonyl compounds by whole-cell biotransformation, combining a formate dehydrogenase and a (R)-specific alcohol dehydrogenase. Appl. Environ. Microbiol. 66, 629-634.

Evangelista-Barreto, N.S., Albuquerque, C.D., Vieira, R.H.S.F., Campos-Takaki, G.M., 2009. Cometabolic decolorization of the reactive azo dye orange II by Geobacillus stearothermophilus UCP 986. Text. Res. J. 79, 1266-1273.

Feng, J., M. Heinze, T., Xu, H., & Cerniglia, C. 2010. Evidence for significantly enhancing reduction of azo dyes in Escherichia coli by expressed cytoplasmic Azoreductase (AzoA) of Enterococcus faecalis. Protein Pept. Lett. 17, 578-584.

Ferguson, G.P., Battista, J.R., Lee, A.T., Booth, I.R., 2000. Protection of the DNA during the exposure of Escherichia coli cells to a toxic metabolite : the role of the KefB and KefC potassium channels 35, 113–122.

Fernandez, C., Larrechi, M.S., Callao, M.P., 2010. An analytical overview of processes for removing organic dyes from wastewater effluents. Trends Anal Chem. 29, 1202–1211.

Fisher, K., & Phillips, C., 2009. The ecology, epidemiology and virulence of Enterococcus. Microbiology 155, 1749-1757.

Flahaut, S., Hartke, A., Giard, J. C., Benachour, A., Boutibonnes, P., & Auffray, Y., 1996. Relationship between stress response towards bile salts, acid and heat treatment in Enterococcus faecalis. FEMS Microbiol. Lett. 138, 49-54.

Flores E.R., Luijten, M., Donlon, B.A., Lettinga, G., Field, J.A., 1997. Complete biodegradation of the azo dye azodisalicylate under anaerobic conditions. Environ. Sci. Technol. 31, 2098-2103.

Franciscon, E., Zille, A., Fantinatti-garboggini, F., Serrano, I., Cavaco-paulo, A., Regina, L., 2009. Microaerophilic – aerobic sequential decolourization and biodegradation of textile azo dyes by a facultative Klebsiella sp. strain VN-31. Process Biochem. 44, 446–452.

Fujimoto, S., & Ike, Y., 2001. pAM401-based shuttle vectors that enable overexpression of promoterless genes and one-step purification of tag fusion proteins directly from Enterococcus faecalis. Appl. Environ. Microbiol. 67, 1262-1267.

Gerdes, S., Scholle, M. D., Campbell, J. W., Balazsi, G., Ravasz, E., Daugherty, M. D., & Osterman, A. L., 2003. Experimental determination and system level analysis of essential genes in Escherichia coli MG1655. J. Bacteriol. 185(19), 5673-5684.

Ghodake, G., Jadhav, S., Dawkar, V., Govindwar, S., 2009. Biodegradation of diazo dye Direct brown MR by Acinetobacter calcoaceticus NCIM 2890. Int. Biodeter. Biodegr. 63, 433-439.

Ghosh, D.K., Mandal, A., Chaudhuri, J. 1992. Purification and partial characterization of two azoreductases from Shigella dysenteriae Type 1. FEMS Microbiol. Lett. 98, 229-234.

Gomare, S.S., Govindwar, S.P., 2009. Brevibacillus laterosporus MTCC 2298: a potential azo dye degrader. J. Appl. Microbiol. 106, 993–1004.

Gonza, L. V, Gonza, G., Escamilla-silva, E.M., 2009. Proposed pathways for the reduction of a reactive azo dye in an anaerobic fixed bed reactor. World J. Microbiol. Biotechnol. 25,415–426.

Gonzalez, C.F., Ackerley, D.F., Lynch, S. V, Matin, A., 2005. ChrR, a soluble quinone reductase of Pseudomonas putida that defends against H2O2. J. Biol. Chem. 280, 22590–22595.

Gopinath, K.P., Asan Meera Sahib, H., Muthukumar, K., Velan, M., 2009. Improved biodegradation of Congored by using Bacillus sp. Bioresour. Technol. 100, 670–5.

Graef, M.R., Alexeeva, S., Snoep, J.L., 1999. The steady-state internal redox state (NADH / NAD) reflects the external redox state and is correlated with catabolic adaptation in Escherichia coli. J. Bacteriol. 181, 2351–2357.

Han, J., Ng, I., Wang, Y., Zheng, X., Chen, W., Hsueh, C., Liu, S., Chen, B., 2012. Exploring new strains of dye-decolorizing bacteria. J. Biosci. Bioeng. 113, 508–514.

Handayani, W., Meitiniarti, V. I., & Timotius, K. H., 2007. Decolorization of Acid Red 27 and Reactive Red 2 by Enterococcus faecalis under a batch system. World J. Microbiol. Biotechnol. 23, 1239-1244.

Hans-Joachim Knackmuss 1996. Basic knowledge and perspectives of bioelimination xenobiotic compounds. J. Biotechnol. 51, 287–295.

Hill, T.C.J., Walsh, K.A., Harris, J.A., Moffett, B.F., 2006. Using ecological diversity measures with bacterial communities. FEMS Microbiol. Ecol. 43, 1-11.

Holt J.G., Krieg N.R., Sneath P.H.A., Staley J.T., 1994. .Bergey‘s manual of determinative bacteriology, 9th edition. Williams and Wilkins, Baltimore, 559-562

Hong, Y.G., Gu, J.D., 2010. Physiology and biochemistry of reduction of azo compounds by Shewanella strains relevant to electron transport chain. Appl. Environ. Microbiol. 88, 637-643.

Hsueh, C.C., Chen, B.Y., Yen, C.Y. 2009. Understanding effects of chemical structure on azo dye decolorization characteristics by Aeromonas hydrophila. J.Hazard. Mater. 167, 995-1001.

Hu, T.L., 1994. Decolourization of reactive azo dyes by transformation with Pseudomonas luteola. Bioresour. Technol. 49, 47-51.

Huang, W. E., Hopper, D., Goodacre, R., Beckmann, M., Singer, A., & Draper, J., 2006. Rapid characterization of microbial biodegradation pathways by FT-IR spectroscopy. J. Microbiol. Methods. 67, 273-280.

Huber, P., Carre, B., 2012. Decolorization of process waters in deinking mills and similar applications: A review. Bioresource 7, 1366–1382.

Hung, P., Albeck, JohnÂ G., Tantama, M., Yellen, G. 2011. Imaging Cytosolic NADH-NAD+ Redox State with a Genetically Encoded Fluorescent Biosensor. Cell Metabolism, 14, 545-554.

Huycke, M.M., Abrams, V., Moore, D.R., 2002. Enterococcus faecalis produces extracellular superoxide and hydrogen peroxide that damages colonic epithelial cell DNA the human intestinal tract that produces substantial extra-. Carcinogenesis 23, 529–536.

Idaka, E., Ogawa, T., Horitsu, H., Tomoyeda, M. 1978. Degradation of azo compounds by Aeromonas hydrophila var. 24B. Journal of the Society of Dyers and Colourists, 94, 91-94.

Ito, K., Nakanishi, M., Lee, W. C., Sasaki, H., Zenno, S., Saigo, K. & Tanokura, M., 2006. Three-dimensional Structure of AzoR from Escherichia coli. J. Biol. Chem. 281, 20567–20576.

Jadhav, J.P., Parshetti, G.K., Kalme, S.D., Govindwar, S.P., 2007. Decolourization of azo dye methyl red by Saccharomyces cerevisiae MTCC 463. Chemosphere 68, 394–400.

Jadhav, U.U., Dawkar, V.V., Ghodake, G.S., Govindwar, S.P., 2008. Biodegradation of Direct Red 5B, a textile dye by newly isolated Comamonas sp. UVS. J. Hazard. Mater. 158, 507-516.

Jain, K., Shah, V., Chapla, D., Madamwar, D., 2012. Decolorization and degradation of azo dye – Reactive Violet 5R by an acclimatized indigenous bacterial mixed cultures-SB4 isolated from anthropogenic dye contaminated soil. J. Hazard. Mater. 213–214, 378–386.

Jang, M.S., Kang, N.-Y., Kim, K.-S., Kim, C.-H., Lee, J.H., Lee, C., Lee, Y.C., 2007. Mutational analysis of NADH-binding residues in triphenylmethane reductase from Citrobacter sp. strain KCTC 18061P. FEMS microbial. Lett. 271, 78–82.

Jin, R., Yang, H., Zhang, A., Wang, J., Liu, G., 2009. Bioaugmentation on decolorization of C.I. Direct Blue 71 by using genetically engineered strain Escherichia coli JM109 (pGEX-AZR). J. Hazard. Mater. 163, 1123-1128.

Jin, X.-C., Liu, G.-Q., Xu, Z.-H., Tao, W.-Y., 2007. Decolorization of a dye industry effluent by Aspergillus fumigatus XC6. Appl. Microbiol. Biotechnol. 74, 239–43.

Johannes, T.W., Woodyer, R.D., Zhao, H., 2007. Efficient regeneration of NADPH using an engineered phosphite dehydrogenase Biotechnol. Bioeng. 96, 18–26

Joshi, T., Iyengar, L., Singh, K., Garg, S., 2008. Isolation, identification and application of novel bacterial consortium TJ-1 for the decolourization of structurally different azo dyes. Bioresour. Technol. 99, 7115–21.

Joyce, A. R., Reed, J. L., White, A., Edwards, R., Osterman, A., Baba, T., & Agarwalla, S., 2006. Experimental and computational assessment of conditionally essential genes in Escherichia coli. J. Bacteriol. 188, 8259-8271.

Kagalkar, A.N., Jagtap, U.B., Jadhav, J.P., Bapat, V. a, Govindwar, S.P., 2009. Biotechnological strategies for phytoremediation of the sulfonated azo dye Direct Red 5B using Blumea malcolmii Hook. Bioresour. Technol. 100, 4104–10.

Kalyani, D.C., Telke, A.A., Dhanve, R.S., Jadhav, J.P. 2009. Ecofriendly biodegradation and detoxification of Reactive Red 2 textile dye by newly isolated Pseudomonas sp. SUK1. J. Hazard. Mater. 163, 735-742.

Kandelbauer, A., Erlacher, A., Cavaco-paulo, A., Gu, G.M., 2004. A New Alkali-Thermostable Azoreductase from Bacillus sp. Strain SF. Appl. Environ. Microbiol. 70, 837–844.

Keck, A., Klein, J., Kudlich, M., Stolz, A., Knackmuss, H., Mattes, R., 1997. Localization of the Enzyme System Involved in Anaerobic Reduction of Azo Dyes by Sphingomonas sp. Strain BN6 and effect of artificial redox mediators on the rate of azo dye reduction. Microbiology 63, 3691–3694.

Keck, A., Reemtsma, T., Mattes, R., Stolz, A., Klein, J., 2002. Identification of Quinoide Redox Mediators That Are Formed during the Degradation of Naphthalene-2-Sulfonate by Sphingomonas xenophaga BN6. Society 68, 4341–4349.

Khehra, M.S., Saini, H.S., Sharma, D.K., Chadha, B.S., Chimni, S.S., 2005. Comparative studies on potential of consortium and constituent pure bacterial isolates to decolorize azo dyes. Water Res. 39, 5135–5141.

Kim, S., Moon, D. B., Lee, C. H., Nam, S. W., & Kim, P., 2009. Comparison of the Effects of NADH-and NADPH-perturbation stresses on the growth of Escherichia coli. Curr. Microbiol. 58, 159-163.

Kim, W., Silby, M.W., Purvine, S.O., Nicoll, J.S., Hixson, K.K., Monroe, M., Nicora, C.D., Lipton, M.S., Levy, S.B., 2009. Proteomic detection of non-annotated protein-coding genes in Pseudomonas fluorescens Pf0-1. PloS one 4, e8455. DOI: 10.1371/journal.pone.0008455

Kirk, J. L., Beaudette, L. A., Hart, M., Moutoglis, P., Klironomos, J. N., Lee, H., & Trevors, J. T., 2004. Methods of studying soil microbial diversity. J. Microbiol. Methods. 58, 169-188.

Knackmuss, H., Stolz, A., 2002. Molecular Cloning and Characterization of the Gene Coding for the Aerobic Azoreductase from Xenophilus azovorans KF46F. Appl. Environ. Microbiol. 68, 3948–3955.

Knapp, J.S., Zhang, Z., Gray, C., Hetheridge, M.J., Evans, M.R., 2000. Decolorization of an azo dye by unacclimated activated sludge under anaerobic conditions. Water Res. 34, 4410–4418.

Kolekar, Y.M., Konde, P.D., Markad, V.L., Kulkarni, S. V, Chaudhari, A.U., Kodam, K.M., 2013. Effective bioremoval and detoxification of textile dye mixture by Alishewanella sp. KMK6. Appl. Microbiol. Biotechnol. 97, 881–9.

Kolekar, Y.M., Nemade, H.N., Markad, V.L., Adav, S.S., Patole, M.S., Kodam, K.M., 2012. Decolorization and biodegradation of azo dye, reactive blue 59 by aerobic granules. Bioresour. Technol. 104, 818–22.

Kolekar, Y.M., Pawar, S.P., Gawai, K.R., Lokhande, P.D., Shouche, Y.S., Kodam, K.M., 2008. Decolorization and degradation of Disperse Blue 79 and Acid Orange 10, by Bacillus fusiformis KMK5 isolated from the textile dye contaminated soil. Bioresour. technol. 99, 8999–9003.

Kovach, M. E., Elzer, P. H., Steven Hill, D., Robertson, G. T., Farris, M. A., Roop, R. M., & Peterson, K. M., 1995. Four new derivatives of the broad-host-range cloning vector pBBR1MCS, carrying different antibiotic-resistance cassettes. Gene 166, 175-176.

Kulkarni, M., Chaudhary, A., 2007. Microbial remediation of nitro-aromatic compounds : An overview. J. Environ. Manag. 85, 496–512.

Laemmli, U.K., 1970. Cleavage of structural proteins during the assembly of the head of bacteriophage T4. Nature 227, 680–685.

Lamb, H.K., Stammers, D.K., Hawkins, A.R. 2008. Dinucleotide-sensing proteins: linking signaling networks and regulating transcription. Sci. Signal. 1, pe38. DOI: 10.1126/scisignal.133pe38

Lamed, R. J., Keinan, E. J. G. Z., & Zeikus, J. G. 1981. Potential applications of an alcohol-aldehyde/ketone oxidoreductase from thermophilic bacteria. Enzyme Microbial Technol. 3, 144-148.

Lessard, P. 1996. Metabolic engineering: the concept coalesces. Nature Biotechnol. 14, 1654-1655.

Li, J., Lin, J.C., Wang, H., Peterson, J.W., Furie, B.C., Furie, B., Booth, S.L., Volpe, J.J., Rosenberg, P.A., 2003. Novel Role of Vitamin K in Preventing Oxidative Injury to Developing Oligodendrocytes and Neurons. J Neurosci. 23, 5816–5826.

Liebeke, M., Pöther, D.-C., van Duy, N., Albrecht, D., Becher, D., Hochgräfe, F., Lalk, M., Hecker, M., Antelmann, H., 2008. Depletion of thiol-containing proteins in response to quinones in Bacillus subtilis. Mol. Microbiol. 69, 1513–29.

Liger, D., Graille, M., Zhou, C.Z., Leulliot, N., Quevillon-Cheruel, S., Blondeau, K., Janin, J., van Tilbeurgh, H., 2004. Crystal structure and functional characterization of yeast YLR011wp, an enzyme with NAD(P)H-FMN and ferric iron reductase activities. J. Biol. Chem. 279, 34890–34897.

Lin, J., Zhang, X., Li, Z., Lei, L., 2010. Biodegradation of Reactive blue 13 in a two-stage anaerobic/aerobic fluidized beds system with a Pseudomonas sp. isolate. Bioresour. Technol. 101, 34–40.

Liu, G., Zhou, J., Fu, Q.S., Wang, J., 2009. The Escherichia coli azoreductase AzoR Is involved in resistance to thiol-specific stress caused by electrophilic quinones. J. Bacteriol. 191, 6394–400.

Liu, G., Zhou, J., Jin, R., Zhou, M., Wang, J., Lu, H., Qu, Y., 2008. Enhancing survival of Escherichia coli by expression of azoreductase AZR possessing quinone reductase activity. Appl. Microbiol. Biotechnol. 80, 409–16.

Liu, G., Zhou, J., Lv, H., Xiang, X., Wang, J., Zhou, M., & Qv, Y., 2007. Azoreductase from Rhodobacter sphaeroides AS1. 1737 is a flavodoxin that also functions as nitroreductase and flavin mononucleotide reductase. Appl. Microbiol. Biotechnol. 76, 1271-1279.

Liu, G., Zhou, J., Wang, J., Song, Z., Qv, Y. 2006. Bacterial decolorization of azo dyes by Rhodopseudomonas palustris. World J. Microbiol. Biotechnol., 22, 1069-1074.

Liu, Z.-J., Chen, H., Shaw, N., Hopper, S.L., Chen, L., Chen, S., Cerniglia, C.E., Wang, B.-C., 2007. Crystal structure of an aerobic FMN-dependent azoreductase (AzoA) from Enterococcus faecalis. Arch. Biochem. Biophys. 463, 68–77.

Lowry, O.H., Roberts, N.R., Kapphahn, J.I., 1957. The fluorometric measurement of pyridine nucleotides. J. Biol. Chem. 224, 1047-1064.

Ma, J., Campbell, A., & Karlin, S. 2002. Correlations between shine-dalgarno sequences and gene features such as predicted expression levels and operon structures, J. Bacteriol. 184, 5733-5745.

Ma, J., Gou, D., Liang, L., Liu, R., Chen, X., Zhang, C., & Jiang, M., 2013. Enhancement of succinate production by metabolically engineered Escherichia coli with co-expression of nicotinic acid phosphoribosyltransferase and pyruvate carboxylase. Appl. Microbiol. Biotechnol. 97, 6739-6747.

Madigan, M.T., Martinko, J.M., Parker, J., 2003. Brock Biology of Microorganisms, 10th ed. ed, Brock Biology of Microorganisms. Prentice-Hall Inc., Simon & Schuster-A Viacom Company, Upper Saddle River, New Jersey, USA.

Maier, J., Kandelbauer, A., Erlacher, A., Cavaco-paulo, A., Gübitz, G.M., Gu, G.M., 2004. A New Alkali-Thermostable Azoreductase from Bacillus sp. Strain SF. Appl. Environ. Microbiol. 70, 837–844.

Malik, S., Beer, M., Megharaj, M., Naidu, R., 2008. The use of molecular techniques to characterize the microbial communities in contaminated soil and water. Environ. Int. 34, 265-276.

Mate, M. S., & Pathade, G., 2012. Biodegradation of CI Reactive Red 195 by Enterococcus faecalis strain YZ66. World J. Microbiol. Biotechnol. 28, 815-826.

Matsumoto, K., Mukai, Y., Ogata, D., 2010. Characterization of thermostable FMN-dependent NADH azoreductase from the moderate thermophile Geobacillus stearothermophilus. Appl. Microbiol. Biotechnol. 29, 1431–1438.

McMullan, G., Meehan, C., Conneely, a., Kirby, N., Robinson, T., Nigam, P., Banat, I.M., Marchant, R., Smyth, W.F., 2001. Microbial decolourisation and degradation of textile dyes. Appl. Microbiol. Biotechnol. 56, 81–87.

Mechsner, K., Wuhrmann, K., 1982. Cell permeability as a rate limiting factor in the microbial reduction of sulfonated azo dyes. Appl. Microbiol. Biotechnol. 15, 123–126.

Meehan, C., Bjourson, A.J., McMullan, G. 2001. Paenibacillus azoreducens sp. nov., a synthetic azo dye decolorizing bacterium from industrial wastewater. Int. J. Syst. Evol. Microbiol. 51, 1681-1685.

Mendes, S., Pereira, L., Batista, C., 2011. Molecular determinants of azo reduction activity in the strain Pseudomonas putida MET94. Applied Microbiol. Biotechnol. 92, 393–405.

Mercier, C., Chalansonnet, V., Orenga, S., Gilbert, C., 2013. Characteristics of major Escherichia coli reductases involved in aerobic nitro and azo reduction. J. Appl. Microbiol.

Mikesková, H., Novotný, Č., Svobodová, K., 2012. Interspecific interactions in mixed microbial cultures in a biodegradation perspective. Appl Microbiol Biotechnol. 95, 861–870.

Mohana, S., Desai, C., Madamwar, D., 2007. Biodegradation and decolourization of anaerobically treated distillery spent wash by a novel bacterial consortium. Bioresour. Technol. 98, 333–339.

Moosvi, S., Keharia, H., Madamwar, D., 2005. Decolourization of textile dye Reactive Violet 5 by a newly isolated bacterial consortium RVM 11.1. World J. Microbiol. Biotechnol. 21, 667–672.

Morrison, J.M., Wright, C.M., John, G.H., 2012. Identification, Isolation and characterization of a novel azoreductase from Clostridium perfringens. Anaerobe 18, 229–34.

Moutaouakkil, A., Zeroual, Y., Dzayri, F.Z., Talbi, M., Lee, K., 2003. Bacterial decolorization of the azo dye methyl red by Enterobacter agglomerans. Ann. Microbiol. 53, 161–170.

Mu, Y., Teng, H., Zhang, D. J., Wang, W., & Xiu, Z. L., 2000. Microbial production of 1, 3-propanediol by Klebsiella pneumoniae using crude glycerol from biodiesel preparations. Biotechnol. Lett. 28, 1755-1759.

Mugerfeld, I., Law, B. a, Wickham, G.S., Thompson, D.K., 2009. A putative azoreductase gene is involved in the Shewanella oneidensis response to heavy metal stress. Appl. Microbiol. Biotechnol. 82, 1131–41.

Muyzer, G., de Waal, E.C., Uitterlinden, A.G., 1993. Profiling of complex microbial populations by denaturing gradient gel electrophoresis analysis of polymerase chain reaction-amplified genes coding for 16S rRNA. Appl. Environ. Microbiol. 59, 695-700.

Nachiyar, C.V., Rajakumar, G.S., 2005. Purification and characterization of an oxygen insensitive azoreductase from Pseudomonas aeruginosa. Enzyme Microbial Technol. 36, 503–509.

Nakanishi, M., Yatome, C., Ishida, N., Kitade, Y., Esche-, A.F.N., 2001. Putative ACP Phosphodiesterase Gene (acpD) encodes an azoreductase. Biochemistry 276, 46394–46399.

Nallapareddy, S. R., Singh, K. V., & Murray, B. E., 2006. Construction of improved temperature-sensitive and mobilizable vectors and their use for constructing mutations in the adhesin-encoding acm gene of poorly transformable clinical Enterococcus faecium strains. Appl. Environ. Microbiol. 72, 334-345.

Naumann, D., Helm, D., & Labischinski, H., 1991. Microbiological characterizations by FT-IR spectroscopy. Nature, 351, 81-82.

Ndasi, N. P., Augustin, M., & Bosco, T. J., 2011. Biodecolourisation of textile dyes by local microbial consortia isolated from dye polluted soils in ngaoundere (Cameroon). Int. J. Environ. Sci. 1, 1403-1419.

Olukanni, O.D., 2006. Textile effluent biodegradation potentials of textile effluent-adapted and non-adapted bacteria. Afr. J. Biotechnol. 5, 1980–1984.

Olukanni, O.D., Osuntoki, A. a, Awotula, A.O., Kalyani, D.C., Gbenle, G.O., Govindwar, S.P., 2013. Decolorization of dyehouse effluent and biodegradation of Congo red by Bacillus thuringiensis RUN1. J. Microbiol. Biotechnol. 23, 843–9.

Pan, J.S., Hong, M.Z., Ren, J.L., 2009. Reactive oxygen species: a double-edged sword in oncogenesis. World journal of gastroenterology: WJG, 15, 1702.

Pandey, A., Singh, P., Iyengar, L., 2007. Bacterial decolorization and degradation of azo dyes. Int. Biodeter. Biodegr. 59, 73–84.

Parales, R.E., Bruce, N.C., Schmid, A., Wackett, L.P. 2002. Biodegradation, biotransformation, and biocatalysis (B3). Appl. Environ. Microbiol. 68, 4699-4709.

Parikh, A., Madamwar, D., 2005. Textile dye decolorization using cyanobacteria. Biotechnol. Lett. 27, 323–326.

Patel, K.J., Singh, A.K., Nareshkumar, G., Archana, G., 2010a. Organic-acid-producing, phytate-mineralizing rhizobacteria and their effect on growth of pigeon pea (Cajanus cajan). Appl. Soil Ecol. 44, 252–261.

Patel, K.J., Vig, S., Nareshkumar, G., Archana, G., 2010b. Effect of transgenic rhizobacteria overexpressing Citrobacter braakii appA on phytate-P availability to mung bean plants. J. Microbiol. Biotechnol. 20, 1491-1499.

Patridge, E. V., & Ferry, J. G., 2006. WrbA from Escherichia coli and Archaeoglobus fulgidus is an NAD(P)H:quinone oxidoreductase. J. Bacteriol. 188, 3498-3506.

Pérez, J.M., Calderón, I.L., Arenas, F. a, Fuentes, D.E., Pradenas, G. A, Fuentes, E.L., Sandoval, J.M., Castro, M.E., Elías, A.O., Vásquez, C.C., 2007. Bacterial toxicity of potassium tellurite: unveiling an ancient enigma. PloS one 2, e211. 10.1371/journal.pone.0000211

Phugare, S.S., Kagalkar, A.N., Govindwar, S.P., Jadhav, J.P., 2011. A study on significant microbial interaction leading to decolorization and degradation of textile dye Rubine 3GP. J. Basic Microbiol. 51, 499–514.

Pillai, P., Archana, G., 2008. Hide depilation and feather disintegration studies with keratinolytic serine protease from a novel Bacillus subtilisisolate. Appl. Environ. Microbiol. 78, 643-650.

Popov,V.O. & Lamzin, V. S. (1994). NAD (+)-dependent formate dehydrogenase. Biochemical J. 301, 625-643

Punj, S., & John, G. H. 2008. Physiological characterization of Enterococcus faecalis during azoreductase activity. Microb. Ecol. Health. D. 20, 65-73.

Punj, S., John, G.H., 2009. Purification and identification of an FMN-dependent NAD(P)H azoreductase from Enterococcus faecalis. Curr. Issues Mol. Biol. 11, 59–65.

Puvaneswari, N., Muthukrishnan, J., & Gunasekaran, P. 2006. Toxicity assessment and microbial degradation of azo dyes. Indian J. Exp. Biol. 44, 618-626.

Rafii, F., Franklin, W., & Cerniglia, C. E., 1990. Azoreductase activity of anaerobic bacteria isolated from human intestinal microflora. Appl. Environ. Microbiol. 56, 2146-2151.

Rafii, F., Hall, J.D., Cerniglia, C.E., 1997. Mutagenicity of azo dyes used in foods, drugs and cosmetics before and after reduction by Clostridium species from the human intestinal tract. Food Chem. Toxicol. 35, 897-901.

Rai, H.S., Bhattacharyya, M.S., Singh, J., Bansal, T.K., Vats, P., Banerjee, U.C., 2005. Removal of Dyes from the Effluent of Textile and dyestuff manufacturing industry: A review of emerging techniques with reference to biological treatment. Crit. Rev. Env. Sci. Tec. 35, 219–238.

Ramalho, P. c. A., Paiva, S., Cavaco-Paulo, A., Casal, M., Cardoso, M. H., & Ramalho, M. T. 2005. Azo reductase activity of intact Saccharomyces cerevisiae cells is dependent on the Fre1p component of plasma membrane ferric reductase. Appl. Environ. Microbiol. 71, 3882-3888.

Rau, J., Knackmuss, H.J., Stolz, A., 2002. Effects of different quinoid redox mediators on the anaerobic reduction of azo dyes by bacteria. Environ. Sci. Technol. 36, 1497–504.

Russ, R., Rau, J., & Stolz, A., 2000. The function of cytoplasmic flavin reductases in the reduction of azo dyes by bacteria. Appl. Environ. Microbiol. 66, 1429-1434.

Ryan, A., Laurieri, N., Westwood, I., Wang, C.-J., Lowe, E., Sim, E., 2010. A novel mechanism for azoreduction. J. Mol. Biol. 400, 24–37.

Salame, T.M., Yarden, O., Hadar, Y., 2010. Pleurotus ostreatus manganese-dependent peroxidase silencing impairs decolourization of Orange II. Microbial biotechnol. 3, 93–106.

Sambrook, J. and D. W. Russell. 2001. Molecular Cloning: A Laboratory Manual. Cold Spring Harbor Laboratory Press, Cold Spring Harbor, New York.

San, K. Y., Bennett, G. N., Berrios-Rivera, S. J., Vadali, R. V., Yang, Y. T., Horton, E., Rudolph, F. B., Sariyar, B. & Blackwood, K. 2002. Metabolic engineering through cofactor manipulation and its Effects on metabolic flux redistribution in Escherichia coli. Metab. Eng. 4, 182-192.

Sandhya, S., Sarayu, K., Uma, B., & Swaminathan, K., 2008. Decolorizing kinetics of a recombinant Escherichia coli SS125 strain harboring azoreductase gene from Bacillus latrosporus RRK1. Bioresour. Technol. 99, 2187-2191.

Santos, B., Cervantes, F.J., Lier, J.B. Van., 2007. Review paper on current technologies for decolourisation of textile wastewaters : Perspectives for anaerobic biotechnology. Bioresour. Technol. 98, 2369–2385.

Sarantinopoulos, P., Kalantzopoulos, G., & Tsakalidou, E. 2001. Citrate Metabolism by Enterococcus faecalis FAIR-E 229. Appl. Environ. Microbiol. 67, 5482-5487.

Saratale, R.G., Saratale, G.D., Chang, J.S., Govindwar, S.P., 2009a. Ecofriendly degradation of sulfonated diazo dye C.I. Reactive Green 19A using Micrococcus glutamicus NCIM-2168. Bioresour. Technol. 100, 3897–905.

Saratale, R.G., Saratale, G.D., Chang, J.S., Govindwar, S.P., 2011. Bacterial decolorization and degradation of azo dyes: A review. J. Taiwan Inst. Chem. Eng. 42, 138-157.

Saratale, R.G., Saratale, G.D., Kalyani, D.C., Chang, J.S., Govindwar, S.P., 2009b. Enhanced decolorization and biodegradation of textile azo dye Scarlet R by using developed microbial consortium-GR. Bioresour. Technol. 100, 2493-2500.

Sarayu, K., Sandhya, S., 2010. Aerobic biodegradation pathway for Remazol Orange by Pseudomonas aeruginosa. Appl. Biochem. Biotechnol. 160, 1241-1253.

Seesuriyachan, P., Takenaka, S., Kuntiya, A., Klayraung, S., 2007. Metabolism of azo dyes by Lactobacillus casei TISTR 1500 and effects of various factors on decolorization. Water Res. 41, 985-992.

Senan, R.C., Abraham, T.E., 2004. Bioremediation of textile azo dyes by aerobic bacterial consortium aerobic degradation of selected azo dyes by bacterial consortium. Biodegradation 15, 275-280.

Shah, V., Madamwar, D., 2013. International Biodeterioration & Biodegradation Community genomics : Isolation , characterization and expression of gene coding for azoreductase. Int. Biodeter. Biodegr. 79, 1–8.

Sharma, S., Munjal, A., Gupta, S., Khan, A., 2011. Kinetic Characterization of Azoreductase Enzyme Isolated from Xanthomonas campestris MTCC 10, 108 J. Pharm. Res. 4, 2648–2650.

Shaul, G.M., Holdsworth, T.J., Dempsey, C.R., Dostal, K.A., 1991. Fate of water soluble azo dyes in the activated sludge process. Chemosphere 22, 107–119.

Shenai, V.A. 1995. Azo Dyes on Textiles Vs. German Ban-An Objective Assessment. Chemical- Weekly- Bombay, 41, 137-144.

Solís, M., Solís, A., Pérez, H.I., Manjarrez, N., Flores, M., 2012. Microbial decolouration of azo dyes: A review. Process Biochem. 47, 1723–1748.

Soojhawon, I., Lokhande, P.D., Kodam, K.M., Gawai, K.R., 2005. Biotransformation of nitroaromatics and their effects on mixed function oxidase system. Enzyme Microbial Technol. 37, 527–533.

Spadaro, J. T., Gold, M. H., & Renganathan, V., 1992. Degradation of azo dyes by the lignin-degrading fungus Phanerochaete chrysosporium. Appl.Environ. Microbiol. 58, 2397-2401.

Stephanopoulos, G., Aristidou, A.A., Nielsen, J.H., Nielsen, J. 1998. Metabolic engineering: principles and methodologies. Academic Press.

Stingley, R.L., Zou, W., Heinze, T.M., Chen, H., Cerniglia, C.E., 2010. Metabolism of azo dyes by human skin microbiota. J. Med. Microbiol. 59, 108–14.

Stolz, A. 2001. Basic and applied aspects in the microbial degradation of azo dyes, Appl. Environ. Microbiol. 56, 69-80.

Sugiura, W., Yoda, T., Matsuba, T., Tanaka, Y., Suzuki, Y., 2006. Expression and Characterization of the Genes Encoding Azoreductases from Bacillus subtilis and Geobacillus stearothermophilus. Biosci. Biotechnol. Biochem. 70, 1655–1665.

Suzuki, Y., Yoda, T., Ruhul, a, Sugiura, W., 2001. Molecular cloning and characterization of the gene coding for azoreductase from Bacillus sp. OY1-2 isolated from soil. J. Biol. Chem. 276, 9059–65.

Swamy, J., Ramsay, J.A., 1999. Effects of glucose and NH4+ concentrations on sequential dye decoloration by Trametes versicolor. Enzyme Microbial Technol. 25, 278–284.

Tamura, K., Dudley, J., Nei, M., Kumar, S. 2007. MEGA4: molecular evolutionary genetics analysis (MEGA) software version 4.0. Mol. Biol. Evol. 24, 1596-1599.

Tan, N. C., van Leeuwen, A., van Voorthuizen, E. M., Slenders, P., Prenafeta-Boldu, F. X., Temmink, H., ... & Field, J. A., 2005. Fate and biodegradability of sulfonated aromatic amines. Biodegradation 16, 527-537.

Telke, A., Kalyani, D., Jadhav, J., Govindwar, S., 2008. Kinetics and mechanism of Reactive Red 141 degradation by a bacterial isolate Rhizobium radiobacter MTCC 8161. Acta. Chimica. Slovenica, 55, 320.

Telke, A.A., Kalyani, D.C., Dawkar, V.V., Govindwar, S.P., 2009. Influence of organic and inorganic compounds on oxidoreductive decolorization of sulfonated azo dye CI Reactive Orange 16. J. Hazard. Mater. 172, 298-309.

Tishkov, V.I., Popov, V.O., 2004. Catalytic Mechanism and Application of Formate Dehydrogenase. Biochemistry, 69. (Moscow)

Tishkov, V.I., Popov, V.O., 2006. Protein engineering of formate dehydrogenase. Biomol. Eng. 23, 89–110.

Van der Donk, W. a, Zhao, H., 2003. Recent developments in pyridine nucleotide regeneration. Curr. Opin. Biotechnol. 14, 421–426.

Van der Zee, F.P., Bisschops, I. a E., Lettinga, G., Field, J. A., 2003. Activated carbon as an electron acceptor and redox mediator during the anaerobic biotransformation of azo dyes. Environ. Sci. Technol. 37, 402–8.

Van der Zee, F.P., Cervantes, F.J., 2009. Impact and application of electron shuttles on the redox (bio)transformation of contaminants: a review. Biotechnol. Adv. 27, 256–77.

Vemuri, G.N., Aristidou, A.A. 2005. Metabolic Engineering in the -omics Era: Elucidating and Modulating Regulatory Networks. Microbiol. Mol. Biol. Rev., 69, 197-216.

Wang, C.-J., Hagemeier, C., Rahman, N., Lowe, E., Noble, M., Coughtrie, M., Sim, E., Westwood, I., 2007. Molecular cloning, characterisation and ligand-bound structure of an azoreductase from Pseudomonas aeruginosa. J. Mol. Biol. 373, 1213–28.

Wang, H., Su, J.Q., Zheng, X.W., Tian, Y., Xiong, X.J., Zheng, T.L. 2009a. Bacterial decolorization and degradation of the reactive dye Reactive Red 180 by Citrobacter sp. CK3. Int. Biodeter. Biodegr. 63, 395-399.

Wang, H., Zheng, X.W., Su, J.Q., Tian, Y., Xiong, X.J., Zheng, T.L. 2009b. Biological decolorization of the reactive dyes Reactive Black 5 by a novel isolated bacterial strain Enterobacter sp. EC3. J. Hazard. Mater. 171, 654-659.

Wang, R.C., Fan, K.S., Chang, J.S. 2009c. Removal of acid dye by ZnFe2O4- TiO2-immobilized granular activated carbon under visible light irradiation in a recycle liquid-solid fluidized bed. J. Taiwan Inst. Chem. Eng. 40, 533-540.

Weckbecker, A., Hummel, W. 2005. Glucose Dehydrogenase for the Regeneration of NADPH and NADH. in: Microbial Enzymes and Biotransformations, (Ed.) J. Barredo, Vol. 17, Humana Press, pp. 225-238.

Wichmann, R., Vasic-Racki, D. 2005. Cofactor Regeneration at the Lab Scale. in: Technology Transfer in Biotechnology, (Ed.) U. Kragl, Vol. 92, Springer Berlin Heidelberg, pp. 225-260.

Williamson, D.H., Lund, P., Krebs, H.A. 1967. The redox state of free nicotinamide-adenine dinucleotide in the cytoplasm and mitochondria of rat liver. Biochem. J. 103, 514.

Wong, C. H., & Whitesides, G. M., 1981. Enzyme-catalyzed organic synthesis: NAD (P) H cofactor regeneration by using glucose-6-phosphate and the glucose-5-phosphate dehydrogenase from Leuconostoc mesenteroides. J. Am. Chem. Soc. 103, 4890-4899.

Wong, P.K., Yuen, P.Y., 1996. Decolorization and biodegradation of methyl red by Klebsiella pneumoniae RS-13. Water Res. 30, 1736-1744.

Xu, M., Guo, J., Sun, G., 2007. Biodegradation of textile azo dye by Shewanella decolorationis S12 under microaerophilic conditions. Appl.Microbiol. Biotechnol. 76, 719-726.

Yang, Y., Lu, L., Gao, F., Zhao, Y., 2013a. Characterization of an efficient catalytic and organic solvent-tolerant azoreductase toward methyl red from Shewanella oneidensis MR-1. Environ. Sci. Pollut. Res. 20, 3232–9.

Yang, Y., Wei, B., Zhao, Y., Wang, J., 2013b. Construction of an integrated enzyme system consisting azoreductase and glucose 1-dehydrogenase for dye removal. Bioresour. Technol. 130, 517–21.

Yeh, R.Y.-L., Thomas, A., 1995. Color removal from dye wastewaters by adsorption using powdered activated carbon: Mass transfer studies. J. Chem. Technol. Biotechnol. 63, 48-54.

Yoo, E.S., Libra, J., Adrian, L., 2001. Mechanism of decolorization of azo dyes in anaerobic mixed culture. J. Environ. Eng. 127, 844-849.

Zee, F.P. Van Der, Villaverde, S., 2005. Combined anaerobic – aerobic treatment of azo dyes — A short review of bioreactor studies. Water Res. 39, 1425–1440.

Zhang, J., Zhang, Y., Quan, X., Chen, S., Afzal, S., 2013. Enhanced anaerobic digestion of organic contaminants containing diverse microbial population by combined microbial electrolysis cell (MEC) and anaerobic reactor under Fe(III) reducing conditions. Bioresour. Technol. 136, 273–80.

Zhao, X., Hardin, I.R., 2007. HPLC and spectrophotometric analysis of biodegradation of azo dyes by Pleurotus ostreatus. Dyes Pigm. 73, 322–325.

Zhou, J., Bruns, M.A., Tiedje, J.M., 1996. DNA recovery from soils of diverse composition. Appl. Environ. Microbiol. 62, 316-22.

Zhou, J., Xu, Y., Qu, Y., Tan, L., 2010. Decolorization of Brilliant Scarlet GR enhanced by bioaugmentation and redox mediators under high-salt conditions. Bioresour. Technol. 101, 586–91.

Zille, A., Go, B., Rehorek, A., Cavaco-paulo, A., 2005. Degradation of azo dyes by Trametes villosa laccase over long periods of oxidative conditions. Appl. Environ. Microbiol. 71, 6711–6718.

Zimmermann, T., Gasser, F., Kulla, H.G., Leisinger, T., 1984. Comparison of two bacterial azoreductases acquired during adaptation to growth on azo dyes. Arch. Microbiol. 138, 37–43.

Zollinger, H. 2004. Color chemistry: syntheses, properties, and applications of organic dyes and pigments. Wiley-VCH.

SUMMARY

Azo dyes make up approximately 70% of all dyestuffs, making them the largest group of synthetic colorants and the most common synthetic dyes released into the environment. In India, dyestuff industry produces around 60,000 t of dyes, which is approximately 6.6% of total world output. Effluents containing dyes have the ability to impart colour in to large volume of natural aquatic sources and create a serious environmental problem and public health concern due to their toxic and recalcitrant nature. Efficient colour removal and degradation process, specifically from textile industry effluents, has become great concern over the last few decades. Most of the synthetic dyes resist biodegradation in conventional sewage-treatment plants and require specialised biological systems to metabolize azo compounds into less toxic nature. An important aspect of azo dye degradation is the reductive cleavage of the azo bond which results in dye decolorization and is considered as the bottle neck step in the degradation pathway. This work deals with the study of azo bond reduction by bacterial enzyme systems known as azoreductases.Azoreductases are cytoplasmic enzymes that catalyze the reductive cleavage of azo bonds to produce colorless aromatic amine products. They are categorized into three groups; NADH-preferring flavin reductases, NADPH-preferring flavin reductases, and general flavin reductases. Azoreductases belonging to all three groups have been found in various bacteria. Voluminous literature is available on azo dye decolorization by microbes; however, knowledge on dye decolorization and degradation vis-à-vis microbial physiology and diversity is poorly understood. The physiological role of azoreductases is unclear although they are categorized as quinone reductases. Azoreductases have been frequently overexpressed in heterologous systems but do no result in effective dye decolorization. One plausible reason could be the limitation of cofactor levels available for azoreductase *in vivo.* Taking in to account some of these lacunae in microbial azo dye decolorization this work was aimed at,

- **The enrichment of azo-dye decolorizing microbial consortia from various dye contaminated and pristine environment and their community fingerprinting**
- **Cloning of *azoA* gene from an efficient azo dye decolorizing strain in to various hosts and *s*tudying role of azoreductase in bacterial physiology**

- **Understanding the importance of reducing equivalents for efficient dye decolorization by constructing an *in vivo* NADH regeneration system with formate dehydrogenase.**

The efficacy of azo dye decolorization/degradation is highly dependent on the development of an effective microbial strain, mixed cultures or consortium. In this work Reactive Violet 5R (RV5R), a monoazo, sulfonated and metal stabilized dye, was used. RV5R decolorizing acclimatized bacterial consortia were enriched from industrial effluents, contaminated and pristine samples from Gujarat, India on several different media. Both pristine and dye contaminated environmental samples resulted in enriched acclimatized bacterial consortia for RV5R decolorization. For the 12acclimatized consortia able to decolorize 100 mg/L RV5R in 30 h under shaking or static conditions, eubacterial diversity was studied by 16S rRNA gene based culture-independent methods such as ARDRA and DGGE analysis. Acclimatized consortia formed6 clusters based on the DGGE and ARDRA patterns. Both the techniques showed the community differences in 12 consortia, indicating that sample site and the enrichment conditions can result in the development of different members in the dye decolorizing consortia. Acclimatized consortia enriched from highly contaminated niche were found to possess low H' index demonstrating reduced population diversity, indicating natural selection of resistant strains. Highest H' index was obtained for consortium MITZ which is from intertidal zone sample from a pristine marine environment while lowest H' index was found in AKW consortium obtained from highly contaminated waste water canal. The most efficient consortia were PBC and ME under static and PBR under shaking conditions as they were able to decolorize RV5R with a $t_{1/2}$ of 3-3.5h. Seven acclimatized consortia were found to decolorize higher concentrations up to 1000mg/L of RV5R, thus these consortia could be utilized for highly concentrated dye effluent under aerobic conditions.

Decolorized end products of all the consortia were analysed by FTIR showing cleavage of the azo bond and other group modifications. The phylogenetic diversity in the consortia was correlated with different dye decolorization/degradation end products as revealed by FTIR. GC–MS data of dye decolorized end products of Gly consortium obtained from hydrocarbon contaminated soil demonstrated benzene ring cleavage activity. This study suggests that enrichment of acclimatized consortia under different conditions can result in diverse microbial communities that differentially

degrade RV5R.It may be concluded that the composition of the consortia is governed by nature of the sample, enrichment media composition and incubation conditions. These consortia were found to be constituted of efficient decolorizing isolates as well as non-decolorizing members. Eight efficient RV5R decolorizing bacterial isolates were obtained and found to belong to ɣ - *Proteobacteria*(6 strains) and *Firmicutes*(2 strains) which were identified based on16S rRNA gene sequencing as *Enterococcus, Citrobacter, Acinetobacter, Providencia* and *Klebsiella* sp. Effect of different sugars on RV5R decolorization showed unique preferences in each isolate. These dye decolorizing isolates preferred different redox mediators at various concentrations, which accelerate the RV5R decolorization. AQS and AQDS found to be most suitable. FTIR analysis of the decolorized end products by isolates showed the azo bond (–N=N-) cleavage and $–SO_3H$ group removal. Each isolate possessed unique azoreductase profile of different molecular size and charges. *Enterococcus* sp. L2 was found to be most effective in RV5R and MR decolorization it could decolorize >90% of 100mg/L dye in 5-6h of incubation. Specifically, *Enterococcus* sp. L2showed high NADH and NADPH dependent azoreductase activity of 18.73 ± 1.91 and29.87 ± 2.14, respectively. *Enterococcus* sp. L2, a novel bacterial isolate obtained fromRV5R decolorizing consortium (Dalc), was found to decolorize a broad spectrum of azo dyes under optimum conditions.

PCR amplification and sequencing of the azoreductase gene from *Enterococcus* sp. L2 showed it to be canonical FMN dependent aerobic azoreductase constituted as homodimer of 23kDa polypeptide. Cloning and heterologous expression of *azo*A gene from *Enterococcus* sp.L2 was done using the broad host range gram negative expression vector pBBR1MCS2 under the inducible p*lac* promoter. About 2-7 fold increase in azoreductase activity was observed in *azoA* transformants of standard strains (*E. coli*DH5α and *P. fluorescens* PfO-1) and RV5R decolorizing isolates. The increase in AzoA activity improved RV5R decolorization ~2fold as compared to the vector control in several strains such as *E. coli* DH5α,*P. fluorescens* PfO-1, *Citrobacter* sp. A3, *Klebsiella* sp. E2 and *Acinetobacter* sp. L1. Addition of glucose as carbon source and electron donor resulted in a further increase in RV5R decolorization.

Flavin dependent azoreductases belong to broad group of quinone reductases which catalyze two electron transfers to quinones forming hydro-quinone without semi-quninone intermediate. To elucidate the physiological role of *azoA* in RV5R decolorization by *Enterococcus* sp. L2, two approaches were considered; generation of *azoA* knockout and homologous overexpression of *azoA.* Δ*azoA* of *Enterococcus* sp. L2 was constructed using pTEX5501ts temperature sensitive suicidal vector which would result in disruption of *azoA* chromosomal gene. However, it was found that the knockout was not able to survive under normal growth conditions in rich medium as well as when supplemented with reduced glutathione. Taking in to consideration that enterococci possess limited oxidative stress scavenging enzyme machinery and prolific endogenous ROS generation system, *azoA* could play an active role in combating ROS in this organism. Present work on Δ*azoA* of *Enterococcus* sp. L2 corroborates this view. Further, the observation that exposure of *Enterococcus*sp. L2 to H_2O_2, menadione, AQDS and RV5Rinduced the AzoA enzyme activivty level supports its role in oxidative stress.*AzoA* constitutive homologous overexpression resulted in 3.5 fold increase in azoreductase activity in the strain L2 and it manifested reduced growth and azo dye decolorization. However, *azoA* transformant of L2 strain was found to have gained H_2O_2resistance. Additionally, *azo* transformant of L2 strain showed improved growth in presence of toxic levels of Cu (II) and Cr (VI). Thus present study provides an insight into the vital role of azoreductases in the oxidative and metal stress condition survival of *Enterococcus* L2 sp.

To increase the efficiency of decolorization process in RV5R decolorizing bacteria, the intracellular NADH pool was enhanced by the overexpression of *Mycobacterium vaccae* N10 NAD^+ dependent formate dehydrogenase (*fdh*) gene. *Fdh* overexpression in *E. coli* and *P. fluorescens* PfO-1 resulted ~3.5-4 fold increase dye decolorization. Heterologous expression of *fdh* in *Klebsiella* sp. E2, *Acinetobacter* sp. L1 and *Enterococcus* sp. L2 also showed increased RV5R decolorization. Growth advantage was found via NAD^+- *fdh* expression in various host strains under specific conditions. Thus it may be concluded that reductive cleavage of azo bond resulting in dyed colorization could be enhanced by increasing the reducing equivalents pool intracellularly. *In vitro* FDH coupled azoreductase activity of *E. coli* BL21 (DE3) was demonstrated to show RV5R decolorization in presence of formate and NAD^+. Dual gene construct of *azoA*(transcription fusion) transformants showed enhanced azo dye

decolorization compared to individual gene constructs under non growing formate containing buffered conditions. This could be used to develop an effective bioremediation process for azo dye decolorization.

To conclude, salient findings/achievements of the present work are listed below,

- Efficient RV5R decolorizing microbial consortia having distinct eubacterial community profiles have been obtained.
- Novel effective RV5R decolorizing bacterial strains belonging to various genera have been isolated.
- *Enterococcus* sp. L2 was characterized as most proficient broad spectrum azo dye decolorizing strain.
- Δ*azoA* of *Enterococcus* sp. L2 could not survive under normal growth conditions even when growth medium was supplemented with reducing agent such as reduced glutathione suggesting its essential role in cell survival.
- Homologous expression of *azoA* in *Enterococcus* sp. L2 compromised its growth and RV5R decolorizing ability; however it showed enhanced H_2O_2 survival due to reduction in ROS production and increased growth in presence of toxic heavy metals such as copper and chromium suggesting role of *azoA* in oxidative stress management.
- Heterologous expression *azoA* gene of *Enterococcus* sp. L2 showed enhanced RV5R decolorization for several bacterial strains.
- Azo dye decolorization process in several bacteria is limited by NADH availability and introduction of NADH regeneration system based on *fdh* overexpression could lead to increase in overall dye decolorization.
- Overexpression of *fdh* and *azoA* can result in increased decolorization(depending on the strain background)as compared to *azoA* or *fdh* alone under non-growing conditions.
- RV5R decolorization can be genetically improved by *azoA* and *fdh* over-expression in following order *fdh-azoA*>*fdh*>*azoA*.

PUBLICATIONS AND PRESENTATIONS

PUBLICATIONS

Rathod, J., & Archana, G. Molecular fingerprinting of bacterial communities in enriched azo dye (Reactive violet 5R) decolorizing native acclimatized bacterial consortia. Bioresource Technology 2013; 142, 436-444. (http://dx.doi.org/10.1016/j.biortech.2013.05.057)

Manuscripts communicated/ in preparation:

1. Enhancement of azo dye decolorization by overexpression of *Enterococcus* sp. L2 azoreductase (*azo*A) and *Mycobacterium vaccae* formate dehydrogenase (*fdh*) in heterologous bacterial systems.

2. Characterization of efficient azo dye decolorizing intrinsic members from acclimatized consortia and assessment of factors influencing decolorization.

3. Enhancement of oxidative stress resistance by homologous over-expression of *azo*A in *Enterococcus* sp. L2

ORAL PRESENTATIONS

1) **5th International Symposium on Biosorption and Bioremediation, Prague, Czech Republic.**

   Title: Metabolic engineering for efficient azo dye decolorization by NADH regeneration system. Date: June, 2012.

2) **XXVI Gujarat Science Congress 2012**

   Title: Involvement of an aerobic FMN dependent azoreductase in Reactive violet 5 decolorization by *Enterococcus* sp. L2. Date: February, 2012.

POSTER PRESENTATIONS

1) "Cloning of aerobic FMN-dependent azoreductase genes of *Enterococcus* isolates from Reactive violet 5 decolorizing consortia" at 49th Annual conference of Association of Microbiologist of India (AMI) held at University of Delhi, Delhi from 18-20th November, 2008.

2) "Diversity of microbial consortia capable of decolorizing Reactive Violet 5" at 48th Annual Conference of Association of Microbiologist of India (AMI) held at IIT Chennai from 18-21st December, 2007.